

**DECLARATION**

This work has not been accepted in substance for any degree and is not being concurrently submitted in candidature for any degree.

Signed.....

Date .....

## **ACKNOWLEDGEMENTS**

I would like to thank my supervisor, Professor Michael Pillay, for his patience, advice and mentorship in the area of molecular genetics. He has greatly assisted me in executing this project timeously. He spent several hours reviewing this dissertation in its several stages, for which I am eternally grateful.

I would also like to express my gratitude to my co-supervisor, Doctor Peter Stegmann for his practical assistance and valuable advice in the microbiological work carried out in this dissertation.

Thanks also to my peers Steven Manzi, Sam Laereng and Gabriel Thathana for their ideas and advice throughout the course of this study.

A warm appreciation goes out to the Laboratory Technicians Nnana Moelefe and Doreen Busane whose advice and assistance is much valued.

Thanks to Tawanda and his wife, Gina Shumbayaonda, for their emotional and financial assistance during the course of my studies. I would also like to acknowledge Doctor Abraham Mwadiwa for his advice and support.

I would also like to express my gratitude to my employer Vaal University of Technology, in particular Ms Terblanche for her assistance and support during the tutorship programme. I would also like to acknowledge the VUT Research Award for funding my studies.

A big recognition goes out to Regis and Collina Nyamukoho, Dynes and Faides Ngoma for the financial assistance, laughs and the friendship. Last but not least, I greatly appreciate my family for their on-going support and financial assistance.

## **DEDICATION**

This dissertation is dedicated to my family; my Dad Simon Chihomvu, who has always believed in me and helped me become the best that I can be. My mother Jane Shumbayaonda, whose constant love and affection has moulded me to become the woman I am today; my sisters Memory, Meroline and Sandra and my only brother Tendai for their advice and support.

Most of all I want to say “Thank you” to God Almighty (Jehovah) whose mercies, love and provision have taken me thus far and I know the best is yet to come.

## **PUBLICATIONS**

CHIHOMVU, P., STEGMANN, P. & PILLAY, M. 2014. Identification and Characterization of Heavy Metal Resistant Bacteria from the Klip River. *International Conference on Ecological, Environmental and Biological Sciences, WASET*, Cape Town **8**(11):166-174.

## ABSTRACT

The Klip River has suffered severe anthropogenic effects from industrial, agricultural, mining and domestic activities. As a result harmful contaminants such as heavy metals have accumulated in the river, causing microorganisms inhabiting the environment to develop mechanisms to protect them from the harmful effects of the contaminants. The current study deals with the isolation and characterization of heavy metal resistant bacteria isolated from the Klip River Catchment. Water and sediment samples were collected from 6 sites of the Klip River, and the Vaal Barrage (control). In-situ parameters, such as pH, turbidity, salinity, conductivity, temperature and dissolved oxygen were determined. Lead, iron, cadmium, nickel, zinc and copper concentrations of water were determined by atomic absorption spectroscopy. For bacterial analysis sediment and water samples were collected in sterile glass jars and bottles respectively. Heavy metal resistant bacterial isolates were screened on heavy metal constituted Luria Bertani (LB) agar. Biochemical profiles of the isolates were constructed using the API 20E® strips, antibiotic susceptibility tests were done and growth studies were carried out using spectrophotometric methods. The isolates were identified using 16SrDNA sequencing and alignment.

A partial sequence of the copper resistance gene *pcoA* was amplified from strains *Lysinibacillus* sp. KR25 [KJ935917], and *Escherichia coli* KR29 [KJ935918]. The *pcoR* gene was amplified from *E. coli* (KR29) and the partial sequence for the chromate resistance gene *chrB*, was amplified from *Pseudomonas* sp. KR23 [KJ935916]. The gene fragments were then sequenced and translated into protein sequences. The partial protein sequences were aligned with existing copper and chromate resistance proteins in the Genbank and phylogenetic analysis was carried out. The physico-chemical properties of the translated proteins were predicted using the bioinformatics tool ExPASy ProtParam Program. A homology modelling method was used for the prediction of secondary structures using SOPMA software, 3D-protein modelling was carried out using I-TASSER. Validation of the 3D structures produced was performed using Ramachandran plot analysis using MolProbity, C-score and TM-scores. Plasmid isolation was also carried out for both the wild type strains and cured derivatives and their plasmid profiles were analysed using gel electrophoresis to ascertain the presence of plasmids in the isolates. The cured derivatives were also plated on heavy metal constituted media. Antibiotic disc diffusion tests were also carried out to ascertain whether the antibiotic resistance determinants were present on the plasmid or the chromosome.

The uppermost part of the Klip River had the lowest pH and thus the highest levels of heavy metal concentrations were recorded in the water samples. Turbidity, salinity and specific conductivity

increased measurably at Site 4 (Henley on Klip Weir). Sixteen isolates exhibiting high iron and lead resistance (4 mM) were selected for further studies. Antibiotic susceptibility tests revealed that the isolates exhibited multi-tolerances to drugs such as Ampicillin (10 µg/ml), Amoxycillin (10 µg/ml), Cephalothin acid (30 µg/ml), Cotrimoxazole (25 µg/ml), Neomycin (30 µg/ml), Streptomycin (10 µg/ml), Tetracycline (30 µg/ml), Tobramycin (10 µg/ml) and Vancomycin (30 µg/ml). Growth studies illustrated the effect of heavy metals on the isolates growth patterns. Cadmium and chromium inhibited the growth of most of the microorganisms. The following strains had high mean specific growth rates; KR01, KR17, and KR25, therefore these isolates have great potential for bioremediative applications.

Using 16SrDNA sequencing the isolates were identified as KR01 (*Aeromonas hydrophila*), KR02 (*Bacillus* sp.), KR04 (*Bacillus megaterium*), KR06 (*Bacillus subtilis*), KR07 (*Pseudomonas* sp), KR17 (*Proteus penneri*), KR18 (*Shewanella*), KR19 (*Aeromonas* sp.), KR22 (*Proteus* sp.), KR23 (*Pseudomonas* sp.), KR25 (*Lysinibacillus* sp.), KR29 (*Escherichia coli*), KR44 (*Bacillus licheniformis*) and KR48 (*Arthrobacter* sp.).

Three heavy metal resistance genes were detected from three isolates. The *pcoA* gene was amplified from strains *Lysinibacillus* sp KR25, and *Escherichia coli* KR29; *pcoR* gene from *E. coli* KR29 and the *chrB* gene, from *Pseudomonas* sp. KR23. The genes encoding for heavy metal resistance and antibiotic resistance were found to be located on the chromosome for both *Pseudomonas* sp. (KR23) and *E.coli* (KR29). For *Lysinibacillus* (KR25) the heavy metal resistance determinants are suspected to be located on a mobile genetic element which was not detected using gel electrophoresis. The translated protein sequence for *pcoA*\_25 showed 82% homology with the copper resistant protein from *Cronobacter turicensis* [YP003212800.1]. Sequence comparisons between the *pcoR* partial protein sequence found in *E. coli* KR29 showed 100% homology with 36 amino acids (which was 20% of the query cover) from a transcriptional regulatory protein *pcoR* found in *E. coli* [WP014641166.1]. For the *chrB* partial protein sequence detected in *Pseudomonas* sp. (KR23), 97% of the query sequence showed 99% homology to a vitamin B12 transporter *btuB* in *Stenotrophus* sp. RIT309.

## ABBREVIATIONS

ADS	Antibiotic Disc Susceptibility
AMD	Acid Mine Drainage
API	Analytical Profile Index
AST	Antibiotic Susceptibility Test
BLAST	Basic Local Alignment Search Tool
CDF	Cation Diffusion Facilitator
CFU	Colony Forming Units
DNA	Deoxyribonucleic acid
DO	Dissolved oxygen
DOC	Dissolved organic carbon
EC	Electrical Conductivity
EDTA	Ethylenediaminetetraacetic acid
EPS	Exopolysaccharides
ERPM	East Rand Property Mine
ESTs	Expressed sequence tags
GRAVY	Grand Average of Hydropathicity Value
HDPE	High density polyethylene
HSPs	Heat shock proteins
HPC	Heterotrophic plate counts
LB	Luria Bertani
MCO	Multi-copper oxidase
MGE	Mobile Genetic Elements

MH	Mueller Hinton
MIC	Minimum Inhibitory Concentration
MRB	Metal resistant bacteria
MS	Mass spectrophotometry
MTCC	Microbiology type culture collection
NA	Nutrient Agar
NADP	Nicotinamide adenine dinucleotide phosphate
NCBI	National Center for Biotechnology Information
PCA	Principal Component Analysis
PCR	Polymerase Chain Reaction
PVC	Polyvinyl chlorides
RMSD	Root-mean-square deviation
ROI	Reactive Oxygen Intermediates
ROS	Reactive Oxygen Species
rRNA	Ribosomal ribonucleic acid
SDS	Sodium Dodecyl Sulphate
SOPMA	Self Optimized Prediction Method with Alignment
TDS	Total dissolved oxygen
UV	Ultra violet
WWTW	Waste water treatment works



# Table of Contents

DECLARATION .....	ii
ACKNOWLEDGEMENTS .....	iii
DEDICATION.....	iv
PUBLICATIONS.....	v
ABSTRACT.....	vi
ABBREVIATIONS .....	viii
LIST OF FIGURES .....	xv
LIST OF TABLES.....	xxi
LIST OF EQUATIONS .....	xxii
1. INTRODUCTION .....	1
1.1 Background.....	1
1.2 Significance of the Project.....	3
1.3 Problem statement.....	3
1.4 Aim .....	3
1.5 Objectives .....	4
1.6 The scope and limitations of the study .....	4
2. LITERATURE REVIEW.....	5
2.1 The Klip River Catchment .....	5
2.2 Water pollution sources .....	5
2.2.1 Mining Impacts.....	7
2.2.2 Industrial Impacts.....	8
2.2.3 Domestic Impacts.....	8
2.3 Physical characteristics.....	9
2.4 Chemistry, uses and toxicity of heavy metals.....	13
2.4.1 Lead .....	13
2.4.2 Cadmium .....	14
2.4.3 Copper.....	14
2.4.4 Chromium.....	15
2.4.5 Zinc.....	16
2.4.6 Iron .....	16
2.4.7 Nickel.....	17
2.5 Biochemical profiling using the API20E® Biochemical Test Strips .....	17

2.6	Antibiotic resistance .....	18
2.6.1	Antibiotic Susceptibility Tests .....	21
2.7	Heavy metal resistance mechanisms of microorganisms .....	23
2.7.1	Lead resistance .....	23
2.7.2	Chromium resistance .....	25
2.7.3	Zinc resistance.....	27
2.7.4	Iron resistance .....	31
2.7.5	Copper resistance.....	31
2.7.6	Nickel resistance.....	32
2.8	Plasmid curing .....	32
2.9	Protein homology modeling.....	33
3	RESEARCH DESIGN AND METHODOLOGY .....	35
3.1	Research design .....	35
3.2	Materials .....	36
3.2.1	Field data sheets .....	36
3.2.2	Kits, reagents, and chemicals .....	36
3.2.3	Buffers and stock solutions .....	36
3.2.4	Microbiological Media and Components.....	36
3.2.5	Sterilization of microbiological media, reagents, glassware, consumables and heavy metal stocks .....	36
3.2.6	Pre-conditioning of plastic bottles.....	36
3.2.7	Samples and sampling sites .....	37
3.3	Sample Collection .....	40
3.4	Heavy Metal Analysis of water samples .....	40
3.5	Preparation of heavy metal supplemented media .....	40
3.6	Enumeration and Isolation of bacteria .....	41
3.7	Study of colonial morphology .....	41
3.8	Study of cellular morphology.....	41
3.9	Determination of Minimum Inhibitory Concentration (MIC) .....	41
3.10	Determination of antibiotic resistance.....	42
3.11	Biochemical characterization .....	42
3.12	Catalase test.....	43
3.13	Oxidase test.....	43

3.13.1	Determination of optimal growth conditions.....	43
3.14	Growth studies.....	43
3.15	MOLECULAR TECHNIQUES .....	44
3.16	DNA extraction.....	44
3.17	Polymerase Chain Reaction (PCR).....	45
3.17.1	16SrDNA Amplification .....	45
3.17.2	Amplification of Heavy Metal resistant genes .....	45
3.18	Gel Electrophoresis.....	50
3.19	PCR product purification and sequencing of 16SrDNA and heavy metal resistance genes .....	50
3.20	Isolation of plasmid DNA.....	50
3.21	Plasmid curing .....	52
3.22	Homologous analysis of amplified genes .....	52
4.	RESULTS .....	54
4.1	Diversity of bacterial isolates from study sites .....	54
4.2	Physico-chemical results.....	54
4.3	Heavy metal analysis of water samples .....	56
4.4	Statistical analysis of physicochemical parameters .....	57
4.5	Enumeration of heavy metal resistant bacteria in sediment and water samples .....	60
4.6	Colony Morphology of isolates .....	61
4.7	Cellular Morphology of isolates .....	63
4.8	Minimum Inhibitory Concentrations .....	66
4.9	Biochemical Tests.....	67
4.10	Antibiotic susceptibility tests.....	70
4.11	Optimal growth studies .....	72
4.12	Influence of heavy metals on growth patterns of isolates .....	73
4.13	16SrDNA Sequencing and Phylogentic analysis .....	82
4.14	PCR amplification of heavy metal resistance genes .....	85
4.15	Homology analysis of amplified genes .....	89
4.16	Predictions of secondary structures using SOPMA .....	95
4.17	I-TASSER structural prediction results .....	97
4.18	Ramachandran Plot Analysis .....	98
4.19	Plasmid profiles of wild type and cured strains.....	100

4.20	Plasmid curing .....	101
5.	DISCUSSION .....	105
5.1	Physico-chemical properties of water.....	105
5.2	Interpretation of the principal components .....	106
5.3	Enumeration of bacteria.....	106
5.4	Morphological and physiological characteristics of isolates .....	107
5.5	Minimum Inhibitory Concentrations .....	107
5.6	Phenotypic profiles.....	108
5.7	Antibiotic susceptibility .....	108
5.10	Heavy metal resistance genes .....	111
5.10.1	Chromate resistance genes .....	111
5.10.2	Copper resistance genes .....	112
5.11	Physico-chemical properties .....	113
5.12	Protein structures.....	114
5.13	Plasmid isolation and curing .....	115
5.14	CONCLUSION.....	116
5.15	RECOMMENDATIONS.....	117
	REFERENCES .....	119
	APPENDICES.....	136
	APPENDIX I: FIELD SHEETS .....	136
	APPENDIX II: KITS, REAGENTS AND CHEMICALS .....	139
	APPENDIX III: BUFFERS AND STOCK SOLUTIONS.....	140
	APPENDIX IV: MICROBIOLOGICAL MEDIA AND COMPONENTS.....	141
	APPENDIX V: PRECONDITIONING OF PLASTIC BOTTLES.....	141
	APPENDIX VI: RAW DATA FOR WATER QUALITY PARAMETERS.....	142
	APPENDIX VII: RAW DATA FOR HEAVY METAL CONCENTRATIONS OF WATER SAMPLES .....	143
	APPENDIX VIII: RAW DATA FOR PLATE COUNTS.....	144
	APPENDIX IX: MINIMUM INHIBITORY CONCENTRATION ASSAY .....	147
	APPENDIX X: RAW DATA FOR OPTIMAL GROWTH STUDIES DATA.....	148
	APPENDIX XI: RAW DATA FOR ANTIBIOTIC SUSCEPTIBILITY TESTS (WILD TYPE STRAINS) .....	152
	APPENDIX XII: RAW GROWTH CURVE DATA (MEAN VALUES) .....	155

APPENDIX XIII: 16SRDNA NUCLEOTIDE SEQUENCES AND ACCESSION NUMBERS OF  
HEAVY METAL RESISTANT ISOLATES ..... 158

APPENDIX XIV: NUCLEOTIDE SEQUENCES AND TRANSLATED AMINO ACID  
SEQUENCES..... 163

APPENDIX XV TRANSLATED PROTEIN SEQUENCES OF HEAVY METAL RESISTANCE  
GENES..... 164

APPENDIX XVI: PUTATIVE CONSERVED DOMAINS OF PCOA\_25 PARTIAL PROTEIN  
SEQUENCE ..... 165

## LIST OF FIGURES

Figure 1:	Location of the Klip River System and water resources around the Klip River Wetland (Davidson 2003).....	1
Figure 2:	Location of the Klip River wetland in relation to industrial urban and mining development (Vermaak 2009).....	7
Figure 3:	Informal settlements in Lenasia and surface runoff being discharged into the Klip River .....	9
Figure 4:	Klip River Catchment showing distribution of a) pH and b) Conductivity (Davidson 2003) .....	12
Figure 5:	Klip River Catchment showing distribution of iron (Davidson 2003).....	12
Figure 6:	Chronic copper poisoning (Ashish <i>et al.</i> 2013) .....	15
Figure 7:	Negative and positive test results on API 20E® test strips (Zaree <i>et al.</i> 2014) ...	18
Figure 8:	Main mechanisms of gene transfer in bacterium (a) plasmid transfer, (b) transfer by viral delivery (c) transfer of free DNA (Levy 1998) .....	19
Figure 9:	(a) Bacterial efflux mechanism pumping antibiotics out of the cell, (b) antibiotic interfering with ribosomes in protein biosynthesis (Levy 1998).....	20
Figure 10:	Four genetic reactors in antibiotic resistance, where genetic exchange and recombination shapes the future evolution of resistance determinants. Particularly in the lowest reactors, bacteria from human or animal-associated microbiota (in black) mix with environmental bacteria (in white), increasing the power of genetic variation and possible emergence of novel mechanisms of resistance that are re-introduced in human or animal environments (back arrows) (Baquero <i>et al.</i> 2008). .....	21
Figure 11:	Lead resistance mechanisms by bacteria (Naik & Dubey 2013).....	24
Figure 12:	The <i>pbr</i> operon model in <i>C. metallidurans</i> CH34 and the connection between plasmid and chromosomal located functions. The <i>pbr</i> <i>UTRABCD</i> operon is located on the pMOL30 plasmid, <i>pbrR2</i> , <i>cadA</i> , <i>pbrC2</i> and <i>pbrR3</i> on chromosome 1 and <i>zntA</i> on chromosome 2. The asterisk symbol after <i>pbrU</i> * indicates the inactivation of the gene due to the insertion of <i>TnCme2</i> at the 3' end of the gene (Taghavi <i>et al.</i> 2009).....	25
Figure 13:	Mechanisms of chromate transport, toxicity and resistance in bacterial cells (Ahemad 2014) .....	26
Figure 14:	Cellular response to either limited (left) or toxic (right) (Braymer & Giedroc 2014) .....	29
Figure 15:	Czc efflux model (Choudhury & Srivastava 2001b) .....	30
Figure 16:	Diagram illustrating Fur mediated gene repression (Andrews <i>et al.</i> 2003).....	31

Figure 17:	Intercalation of the anti-plasmid compound into the plasmid DNA (Waring 1966) .....	33
Figure 18:	Research Design used in this study. ....	35
Figure 19:	Map showing sampling sites along the Klip River (Map adapted from Vermaak 2009) .....	37
Figure 20:	Site 1- Located in Roodekrans, close to the source of the Klip River .....	37
Figure 21:	Site 2- Klip River before it enters Lenasia Residential Area .....	38
Figure 22:	Site 3- Located in Lenasia: this site is characterized by the presence of several informal settlements close to the Klip River .....	38
Figure 23:	Site 4- Henley on Klip Weir: this site is mainly a recreational area .....	38
Figure 24:	Site 5- Klip River just upstream before the confluence of the Vaal River .....	39
Figure 25:	Site 6- Vaal Barrage (Reference Site) .....	39
Figure 26:	Location of primers designed to amplify the genes of the <i>pbr</i> operon. This figure indicates the location of and expected size of amplified products for each primer pair. These primers were designed based on the <i>pbr</i> operon of <i>C. metallidurans</i> CH34 (X71400) (Davis 2011) .....	49
Figure 27:	Location of primers designed to amplify the <i>cad</i> operon. This figure indicates the location of and expected size of amplified products for each primer pair. These primers were designed based on the <i>cadCA</i> genes of pI258 (PI25CADA) (Davis 2011) .....	49
Figure 28:	Diversity of isolates from study sites along the Klip River .....	54
Figure 29:	In situ measurements of temperature, pH and dissolved oxygen at various sites along the Klip River .....	55
Figure 30:	In situ measurements of conductivity and total dissolved solids at different sites along the Klip River .....	55
Figure 31:	Salinity trends at the different sites along the Klip River .....	56
Figure 32:	Histograms showing concentrations of the heavy metals zinc, nickel, copper and cadmium at different sites along the Klip River .....	56
Figure 33:	Histogram of concentrations for lead and iron at various sites along the Klip River. ....	57
Figure 34:	Scree plot of the eigenvalues versus factor components along with % cumulative variance .....	59
Figure 35:	Correlations between variables and factors .....	60
Figure 36:	Bi plots for principal component analysis 1 + 2 of water quality parameters .....	60
Figure 37:	Enumeration of heavy metal resistant bacteria in water samples .....	61
Figure 38:	Enumeration of heavy metal resistant bacteria in sediment samples .....	61

Figure 39:	Light microscope images (oil immersionx100) of bacterial strains a) KR01 b) KR02 c) KR03 d) KR04 e) KR29 f) KR44.....	65
Figure 40:	Minimum Inhibitory Concentrations of heavy metal resistant isolates from the Klip River .....	66
Figure 41:	Biochemical test results for KR29 and KR22.....	67
Figure 42:	Similarity dendrogram of cultured microorganisms isolated from the Klip River based on phenotypic profiles. A total of 23 different biochemical reactions were assayed using the API 20E@strips, catalase and McConkey Agar reactions (oxidase tests were excluded). Based on the number of positive tests, a phenotype profile was constructed and compared to the profile of all other isolates. The similarity coefficient is shown at the bottom.....	69
Figure 43:	Antibiotic resistance profiles of a) KR04, b) KR17 and c) KR25 .....	70
Figure 44:	Optimum pH determination of isolates. Experiments were performed in triplicate as described in Section 3.13.1. Cultures were inoculated with 100µl of parent culture and absorbance measured at an OD600.....	72
Figure 45:	Optimum temperature determination of isolates. Experiments were performed in triplicate as described in Section 3.13.1. Cultures were inoculated with 100µl of parent culture and absorbance measured at an OD600.....	73
Figure 46:	Growth curves of KR01 in the absence and presence of heavy metals .....	74
Figure 47:	Growth curves of KR02 in the absence and presence of heavy metals .....	74
Figure 48:	Growth curves of KR04 in the absence and presence of heavy metals .....	75
Figure 49:	Growth curves of KR06 in the absence and presence of heavy metals .....	75
Figure 50:	Growth curves of KR07 in the absence and presence of heavy metals .....	76
Figure 51:	Growth curves of KR08 in the absence and presence of heavy metals .....	76
Figure 52:	Growth curves of KR17 in the absence and presence of heavy metals .....	77
Figure 53:	Growth curves of KR19 in the absence and presence of heavy metals .....	77
Figure 54:	Growth curves of KR22 in the absence and presence of heavy metals .....	78
Figure 55:	Growth curves of KR23 in the absence and presence of heavy metals .....	78
Figure 56:	Growth curves of KR25 in the absence and presence of heavy metals .....	79
Figure 57:	Growth curves of KR29 in the absence and presence of heavy metals .....	79
Figure 58:	Growth curves of KR44 in the absence and presence of heavy metals .....	80
Figure 59:	Growth curves of KR48 in the absence and presence of heavy metals .....	80
Figure 60:	PCR amplification products of the <i>16SrDNA</i> gene from the isolates separated on a 1% agarose gel and stained with ethidium bromide. Lanes represent the following: M. KAPA Universal Ladder, 1. KR44, 2. KR48, 3. KR33, 4. KR06, 5.	



	KR08, 6. KR18, 7. KR25, 8. KR07, 9. KR01, 10. KR29 and 11. Negative control. .....82
Figure 61:	PCR amplification products of the <i>16SrDNA</i> gene from the isolates separated on a 1% agarose gel and stained with ethidium bromide. Lanes represent the following: M. KAPA Universal Ladder, 1. KR19, 2. KR19, 3. KR22, 4. KR22, 5. KR23, 6. KR23, 7. KR04, 8. KR04, 9. KR17, 10. KR17 and 11. Negative control. .....82
Figure 62:	The evolutionary history was inferred using the Neighbour Joining Method (Saitou & Nei 1987). The optimal tree with the sum branch length 0.82472703 is shown. The percentage of the replicate trees in which the associated taxa clustered together in the bootstrap test (1000 replicates) are shown next to the branches (Felsenstein 1985). The evolutionary distances were computed using the Kimura 2-parameter model (Kimura 1980) and are in the units of the number of base substitutions per site. The analysis involved 63 nucleotide sequences. Evolutionary analysis was conducted using MEGA 6 (Tamura <i>et al.</i> 2013). The red markers indicate the bacterial strains identified in this study. ....84
Figure 63:	PCR amplification products of the <i>pbrT</i> gene from isolates using pbr8-9 primers. PCR fragments were visualized on a 1% agarose gel stained with ethidium bromide. Lanes represent the following: M. KAPA Universal Ladder, 1. Negative control, 2. KR01, 3. KR02, 4. KR03, 5. KR06, 6. KR07, 7. KR08, 8. KR17, 9. KR18, 10. KR19, 11. KR23, 12. KR25, 13. KR44 and 14. KR48 .....85
Figure 64:	PCR amplification products of the <i>pbrT</i> gene from isolates using pbr10-11 primers. PCR fragments were visualized on a 1% agarose gel stained with ethidium bromide. Lanes represent the following: M. KAPA Universal Ladder, 1. Negative control, 2. KR01, 3. KR02, 4. KR03, 5. KR06, 6. KR07, 7. KR08, 8. KR17, 9. KR18, 10. KR19, 11. KR23, 12. KR25, 13. KR44 and 14. KR48 .....85
Figure 65:	PCR amplification of <i>pbrTR</i> gene from isolates using pbr14-15 primers. PCR fragments were visualized on a 1% agarose gel stained with ethidium bromide. Lanes represent the following: M. KAPA Universal Ladder, 1. Negative control, 2. KR48, 3. KR44, 4. KR25, 5. KR23, 6. KR19, 7. KR18, 8. KR17, 9. KR08, 10. KR07, 11. KR06, 12. KR03, 13. KR02 and 14. KR01.....86
Figure 66:	PCR amplification of <i>pbrRA</i> gene from isolates using pbr16-17 primers. PCR fragments were visualized on a 1% agarose gel stained with ethidium bromide. Lanes represent the following: M. KAPA Universal Ladder, 1. Negative control, 2. KR48, 3. KR44, 4. KR25, 5. KR23, 6. KR19, 7. KR18, 8. KR17, 9. KR08, 10. KR07, 11. KR06, 12. KR03, 13. KR02 and 14. KR01.....86
Figure 67:	PCR amplification of <i>pbrA</i> gene from isolates using pbr18-19 primers. PCR fragments were visualized on a 1% agarose gel stained with ethidium bromide. Lanes represent the following: M. KAPA Universal Ladder, 1. Negative control, 2. KR48, 3. KR44, 4. KR25, 5. KR23, 6. KR19, 7. KR18, 8. KR17, 9. KR08, 10. KR07, 11. KR06, 12. KR03, 13. KR02 and 14. KR01.....86

Figure 68:	PCR amplification of <i>pcoA</i> gene from the isolates. PCR fragments were visualized on a 1% agarose gel stained with ethidium bromide. Lanes represent the following: M. KAPA Universal Ladder, 1. Negative control, 2. KR44, 3. KR29, 4. KR25, 5. KR23, 6. KR19, 7. KR17, 8. KR06, 9. KR04, 10. KR03, 11. KR02 and 12. KR01	88
Figure 69:	PCR amplification of <i>pcoR</i> gene from isolates. PCR fragments were visualized on a 1% agarose gel stained with ethidium bromide. Lanes represent the following: M. KAPA Universal Ladder, 1. Negative control, 2. KR44, 3. KR29, 4. KR25, 5. KR23, 6. KR19, 7. KR17, 8. KR06, 9. KR04, 10. KR03, 11. KR02 and 12. KR01	88
Figure 70:	PCR amplification of <i>chrB</i> gene from isolates. PCR fragments were visualized on a 1% agarose gel stained with ethidium bromide. Lanes represent the following: M. KAPA Universal Ladder, 1. KR01, 2. KR02, 3. KR04, 4. KR06, 5. KR07, 6. KR08, 7. KR17, 8. KR18, 9. KR22, 10. KR23, 11. KR25, 12. KR29, 13. KR44 and 14. KR48	89
Figure 71:	PCR amplification of <i>chrB</i> , <i>pcoA</i> and <i>pcoR</i> genes from the isolates KR23, KR25 and KR29. The amplicons were visualized on a 1% agarose gel. Lanes represent the following: M 1. KAPA Universal Ladder, 2. Negative control for <i>chrB</i> primers, 2. Negative control for <i>pcoA</i> primers, 3. Negative control for <i>pcoR</i> primers, 4. <i>chrB</i> _23; 5. <i>chrB</i> _23, 6. <i>pcoA</i> _25, 7. <i>pcoA</i> _25, 8. <i>pcoA</i> _29, 9. <i>pcoA</i> _29, 10. <i>pcoR</i> _29 and 11. <i>pcoR</i> _29	89
Figure 72:	Translated partial protein sequences of (a) <i>chrB</i> _23 (b) <i>pcoA</i> _25, (c) <i>pcoA</i> _29 and (d) <i>pcoR</i> _29	92
Figure 73:	Phylogenetic tree representing related protein sequences found in the Genbank database using <i>chrB</i> _23 as the query. The tree was built using the Maximum Likelihood Method and the Approximate Likelihood –Ratio Test was used as statistical tests for branch support	93
Figure 74:	Phylogenetic tree representing <i>copA</i> protein sequences found in the Genbank database using <i>pcoA</i> _25 as the query. The tree was built using the Maximum Likelihood Method and the Approximate Likelihood –Ratio Test was used as statistical tests for branch support	94
Figure 75:	Phylogenetic tree representing related protein sequences found in the Genbank database using <i>pcoA</i> _29 as the query. The tree was built using the Maximum Likelihood Method and the Approximate Likelihood –Ratio Test was used as statistical tests for branch support	94
Figure 76:	Phylogenetic tree representing related protein sequences found in the Genbank database using <i>pcoR</i> _29 as the query. The tree was built using the Maximum Likelihood Method and the Approximate Likelihood –Ratio Test was used as statistical tests for branch support	95

Figure 77:	Shows the secondary structures of (a) chrB_23 (b) pcoA_25 (c) pcoA_29 and (d) pcoR_29 as predicted by SOPMA .....	96
Figure 78:	Shows the predicted structures of (a) chrB_23 (b) pcoA_25 (c) pcoA_29 and (d) pcoR_29 using I-TASSER.....	98
Figure 79:	Ramachandran Plot Analysis (Ramachandran of I-TASSER MODEL structures predicted for (a) chrB_23 (b) pcoA_25 (c) pcoA_29 and (d) pcoR_29 .....	100
Figure 80:	Plasmid profiles of wild strains of heavy metal resistant isolates and their cured derivatives. 1. Lambda DNA+HindIII/EcoRI Marker, 2. <i>Aeromonas hydrophila</i> (KR01) WT, 3. <i>Aeromonas hydrophila</i> (KR01) C, 4. <i>Bacillus</i> sp. (KR02) WT, 5. <i>Bacillus</i> sp (KR02). C, 6. <i>Bacillus megaterium</i> (KR04) WT, 7. <i>Bacillus megaterium</i> (KR04) C, 8. <i>Bacillus subtilis</i> (KR06) WT, 9. <i>Bacillus subtilis</i> (KR06) C, 10. <i>Pseudomonas</i> sp. (KR07) WT, 11. <i>Pseudomonas</i> sp. (KR07) C; 12. <i>Acinetobacter oleivorans</i> (KR08) WT, 13. <i>Acinetobacter oleivorans</i> (KR08) C, 14. <i>Proteus penneri</i> (KR17) WT and 15. <i>Proteus penneri</i> (KR17) C.....	100
Figure 81:	Plasmid profiles of wild strains of heavy metal resistant isolates and their cured derivatives. M. Lambda DNA+HindIII/EcoRI Marker; 1. <i>Aeromonas</i> sp. (KR19) WT, 2. <i>Aeromonas</i> sp. (KR19) C, 3. <i>Proteus</i> sp. (KR22) WT, 4 <i>Proteus</i> sp. (KR22) C, 5. <i>Pseudomonas</i> sp. (KR23) WT, 6. <i>Pseudomonas</i> sp. (KR23) C, 7. <i>Lyisnibacillus</i> sp. (KR25) WT, 8. <i>Lyisnibacillus</i> sp. (KR25) C, 9. <i>Escherichia coli</i> (KR29) WT, 10. <i>Escheriachia coli</i> (KR29) C, 11. <i>Arthrobacter</i> sp. (KR48) WT and 12. <i>Arthrobacter</i> sp. (KR48) C. ....	101
Figure 82:	Before and after curing antibiotic resistance profiles of isolates a) KR02-WT, b) KR02-C, c) KR04-WT, d) KR04- C, e) KR08- WT, f) KR08-C, g) KR22-WT and h) KR22-C.....	102

## LIST OF TABLES

Table 1:	Potential point and diffuse sources of pollution in different sections of the Klip River (DWAF 1999).....	6
Table 2:	Effects of some major physical and chemical attributes of water in aquatic systems (Dalls & Day 2004, Lawson 2011).....	10
Table 3:	Biochemical reagents on an API20E test strip with the corresponding reaction or enzyme under investigation .....	18
Table 4:	Geographical coordinates of sampling sites .....	39
Table 5:	Primers used to amplify heavy metal resistance gene in bacterial isolates.....	47
Table 6:	Summary of the average measured parameters from the different sites and percentages that fall within permissible limits from the Instream Klip River Guidelines (2003).....	58
Table 7:	Correlation coefficients among the physico-chemical parameters along the course of the Klip River (average values of all the sites).....	58
Table 8:	Explained total variance .....	59
Table 9:	Colony morphology of bacterial isolates .....	62
Table 10:	Cellular morphology of bacterial isolates .....	63
Table 11:	Biochemical characteristics of heavy metal resistant isolates from the Klip River .....	68
Table 12:	Antibiotic resistance profiles of heavy metal resistant isolates.....	71
Table 13:	Specific and average growth rates of the bacterial isolates in the presence and absence of heavy metals .....	81
Table 14:	Comparative and phylogenetic analysis of 16SrDNA sequences of heavy metal resistant isolates from the Klip River using highly matched species available in NCBI .....	83
Table 15:	Results obtained from the PCR analysis of the genomic DNA of the lead resistant isolates using pbr specific primers. ....	87
Table 16:	Results obtained from the PCR analysis of the genomic DNA from the PCR analysis of the genomic DNA from the copper resistant isolates using pcoA and pcoR specific primers.....	88
Table 17:	Physicochemical properties of partial protein sequences. ....	95
Table 18:	Secondary structure composition of chrB_23, pcoA_25, pcoA_29 and pcoR_29 partial proteins as derived using SOPMA (%). ....	97
Table 19:	Statistical analysis of predicted I-TASSER structures .....	98
Table 20:	Heavy metal resistance profiles after curing.....	103

Table 21:	Antibiotic resistance profiles of cured isolates .....	103
-----------	--	-----

## **LIST OF EQUATIONS**

Equation 1	Specific growth rate .....	44
------------	----------------------------	----

## 1. INTRODUCTION

### 1.1 Background

The Klip River Catchment is situated south of Johannesburg in the Gauteng Province of South Africa (Fig. 1). It lies between latitudes  $26^{\circ}10'$  and  $26^{\circ}25'$  south and longitudes  $27^{\circ}45'$  and  $28^{\circ}05'$  east at an altitude of approximately 1750m above sea level (Vermaak 2009). The tributaries of the Klip River include the Klipspruit, Bloubosspruit, Glenvistaspruit, Harringtonspruit, Rietspruit and Natalspruit, and located in the lower Klip sub-catchment is Foriespruit and Varkensfonteinspruit as described by Davidson (2003).

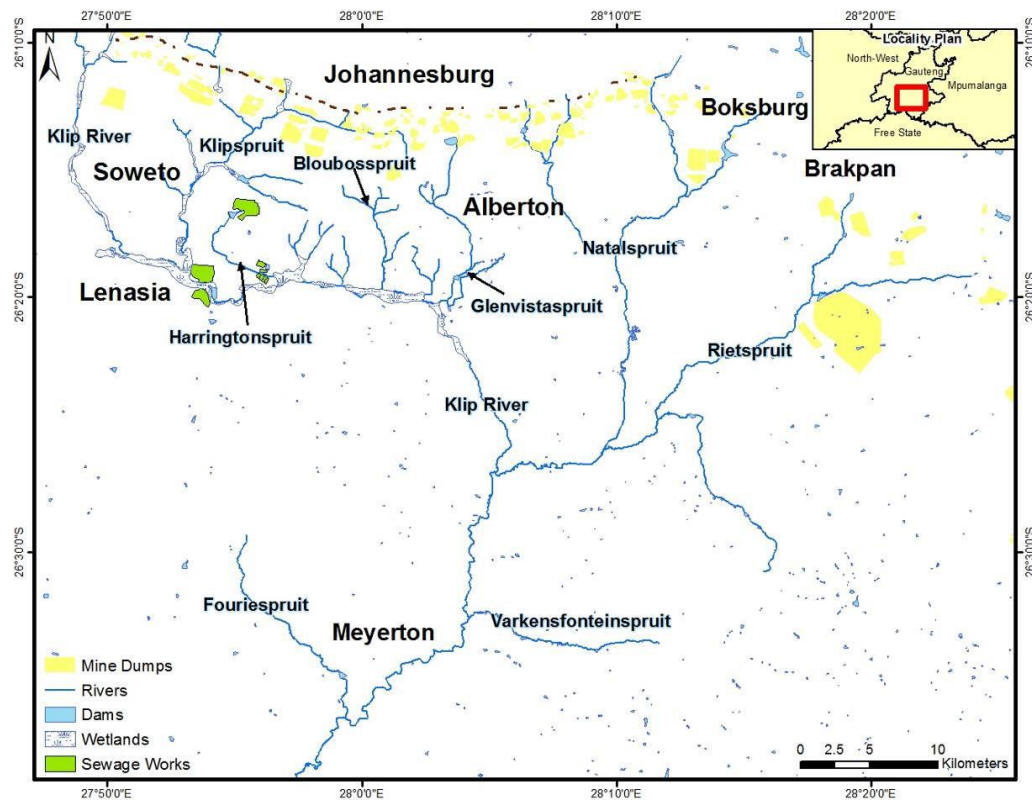


**Figure 1: Location of the Klip River System and water resources around the Klip River Wetland (Davidson 2003)**

As stated by Kotze (2008), the Klip River Catchment has been a major source of concern to human health due to the elevated concentrations of heavy metal pollutants. The point sources of pollution include gold mining activities, effluents from waste water treatment works (WWTW) while the diffuse pollution sources include, degraded sewage networks, industries, solid waste disposal sites, informal settlements and agricultural activities. Since the establishment of the

Witwatersrand metropolis, an increased concentration of heavy metals such as phosphorous, copper, uranium, mercury, cadmium, cobalt, zinc and lead have been reported to be trapped in the peat of the Klip River (McCarthy *et al.* 2007).

Due to the high concentrations of heavy metals in the river, the indigenous microorganisms develop heavy metal resistance mechanisms that enable efficient detoxification and transformation of heavy metals from their toxic to non-toxic forms (Srivasta & Kowshik 2013). Heavy metal resistance mechanisms include precipitation of metals as phosphates, carbonates and sulfides, enzymatic detoxification, physical exclusion by electronegative components in membranes, reduced influx or enhanced efflux and intracellular chelation with low molecular weight, cysteine-rich proteins (Gadd 1990, 1993; Blaudez *et al.* 2000). The adaptation of bacterial species to heavy metal contaminated environments reveals a potential source of biotechnological resources that deserve exploration. Knowledge of the genetic diversity of these microorganisms will be valuable in future bioremediation processes of the Klip and other river systems.

Metal resistance determinants are usually located on plasmids and transposons (which are most likely to carry the genes for antibiotic resistance). Bacterial plasmids encode resistance mechanisms for toxic metals including, zinc, copper, cadmium, chromium, arsenic, etc. (Silver & Phung 2009). However, when working with bacteria which contain plasmids, it is often advisable to compare the plasmid containing bacteria and the plasmid cured derivatives, to ascertain whether the genetic elements responsible for the phenotypic characteristic being observed, is located on the plasmid or on the chromosome. Some plasmids undergo spontaneous segregation and deletion; however, some are extremely stable and require the use of curing agents to increase the incidence of segregation (Trevors 1985).

The environment offers a rich source of novel genes, and these genes can be translated to protein sequences by using various bioinformatics tools. These protein sequences can be used in a variety of applications such as homology modeling. Homology modeling plays a crucial role in determining the protein structure. The importance of homology modeling has gradually increased because of the large gap that exists between the large numbers of available sequences and experimentally solved structures. A protein with over 30% similarity to a known structure can often be predicted with an accuracy equivalent to a low resolution X-ray structure. The incredible advances in homology modeling particularly in detecting distant homologs, sequence alignment with template structures, modeling of loops, detection of errors in a model has contributed to reliable prediction of protein structures which were impossible several years ago because several

protein modeling programs, such as I-TASSER had not yet been developed. Computational methods have managed to fill the gap and contributed to the understanding of the relationship between protein structure and function (Xiang 2006).

## **1.2 Significance of the project**

The enhanced scale of socio-economic activities such as mining, agricultural and industrial operations has increased the amount of heavy metal contaminants in the Klip River. Therefore, it is important to study the indigenous heavy metal resistant microorganisms present in this river since they have adapted to this harsh environment. The presence of heavy metal resistant bacteria, resistant to specific heavy metals is correlated with the increasing amounts of heavy metals being discharged in the Klip River; consequentially heavy metal resistant bacteria may be used as biological monitors or bio-indicators of heavy metal contamination in the environments. Bio-indicators are a sensitive and reliable tool in detecting the sub lethal toxicity of certain heavy metals. The isolates in this study have not been mentioned in previous literature. Research on heavy metal resistant microorganisms has resulted in the detection of several bacterial species with the ability to tolerate and immobilise metals in soil and water. Therefore, more information on metal resistant organisms is important and seems to be an important pathway to pursue. The species or strains in this study have the capacity to tolerate or accumulate metals and are potential candidates for bioremediation strategies. This study will also determine whether the isolates share common resistances to the heavy metals under study and if they do, it will be of interest to determine whether they share identical heavy metal resistant determinants or different ones. The genes obtained in this study would be useful in the design of biosensors. By understanding the physiological, biochemical and molecular characteristics of these isolates, useful information will be obtained that would be useful in the design of biosorption systems and on-site bioremediation experiments.

## **1.3 Problem statement**

Has the increased level of heavy metal pollution in the Klip River resulted in the indigenous microorganisms becoming heavy metal resistant and if they have, has this adaptation affected the genetic and biochemical diversity of the microorganisms. Moreover which heavy metals have they adapted to?

## **1.4 Aim**

The aim of this study is to isolate, identify and characterize the heavy metal resistant microorganisms isolated from the surface water and sediment in the Klip River using biochemical and molecular methods.



### **1.5 Objectives**

1. To collect water and sediment samples from five sites of the Klip River and a reference site (Vaal Barrage).
2. To determine the physico-chemical parameters of the water samples.
3. To isolate and identify microorganisms that are resistant to heavy metals from the soil and sediment samples.
4. To determine the biochemical, minimum inhibitory concentrations and antibiotic resistance characteristics of the isolates.
5. To determine the optimum conditions and growth curve characteristics of the isolates.
6. To identify the isolates by analysis of the gene encoding 16SrDNA.
7. To determine the presence and sequence of genes involved in copper, chromium, lead, cadmium, and zinc resistance. The sequences of all obtained genes will be analyzed and compared with other published heavy metal resistance genes.
8. To translate the nucleotide sequences to protein sequences of the amplified genes.
9. To predict the physico-chemical properties and 3D protein structures of the translated proteins
10. To isolate plasmids from the isolates and to determine their molecular weight
11. To determine whether the heavy metal resistant genes are encoded on the plasmids or chromosomal DNA of the isolates by curing methods.

### **1.6 The scope and limitations of the study**

The study was carried out at the Klip River Catchment Area, south of Johannesburg in South Africa. The study focused on assessing the extent of heavy metal contamination along the course of the Klip River and evaluating the heavy metal tolerance levels of the bacterial isolates obtained from the river with respect to the following heavy metals; zinc, copper, cadmium, lead, chromium, nickel and iron. The study also focused on the results obtained from physiological, biochemical and molecular tests to characterize the isolates.

The Klip River Catchment covers a very large area and a small sample was obtained for this particular study and therefore results obtained, may not be generalizable beyond the specific population studied in the Klip River.

## **2. LITERATURE REVIEW**

### **2.1 The Klip River Catchment**

The Klip River originates in the Witwatersrand range of Hills, which traverse the Witwatersrand Urban complex in an east-west position (Krugersdorp to Springs). The catchment lies between latitude 26°10' and 26°25' south and longitudes 27°45' and 28°05' east and is within the south central portion of a major urban and industrial economic region of South Africa (Vermaak 2009). The source of the Klip River is located proximate to Lewisham, in the West Rand District Municipality, South Africa. The source lies between latitude 26°7'33.06'' and longitude 27°48'50.22'' (Meissner 2010). The natural geography of the upper catchment is characterized by mine dumps and steep rock ridges, while the lower Klip area is fairly featureless as the flood plain widens and the catchment area narrows towards the confluence with the Vaal River (DWA1999). The river receives much of the industrial pollution from the Witwatersrand Escarpment. Most of the polluted water arising from the region therefore collects in the river via tributaries that enter the wetland on its northern bank (McCarthy *et al.* 2007). This wetland has proven to be one of Gauteng's most valuable natural resource assets due to its efficacy to remove pollutants e.g. heavy metals. Early economic development of the region took place south of the watershed within the Klip River Catchment, where the gold bearing corporations were established. Concentrations of heavy metals are higher in the uppermost sections of the wetland. For example in Lenasia, the nickel content in peat ash has been reported to reach 4500 ppm (McCarthy *et al.* 2007). Heavy metals that have been deposited in the river are not biodegradable, but accumulate in the environment and can be transferred to higher organisms of the food web as stated by Deforest *et al.* (2007). This can lead to serious ecological and health problems.

### **2.2 Water pollution sources**

The presence of heavy metals in the environment is due to either natural causes or anthropogenic activities. For instance, excessive heavy metals in nature may occur due to geographical phenomena such as volcanic activity, weathering of rocks and leaching of metals into water bodies. Heavy metals can be introduced into the environment due to anthropogenic activities such as mining, industrial effluent, domestic waste, agricultural runoff and pesticides containing compounds of heavy metals (Harisprasad & Dayanada 2013).

The Klip River has been severely affected by anthropogenic effects such as mining, industrial and farming activities and this is one of the main reasons why the Klip River was chosen for this particular study. The main anthropogenic factors affecting the River are summarized in Table 1.

**Table 1: Potential point and diffuse sources of pollution in different sections of the Klip River (DWAF 1999)**

Klip River Upstream of the Klipspruit confluences (Localities 1 to 3)	
Point sources	<ul style="list-style-type: none"> <li>• Durban Roodepoort Deep Gold Mine (ceased pumping end June 1998)</li> </ul>
Diffuse sources	<ul style="list-style-type: none"> <li>• Informal settlements near Kagiso, Durban Roodepoort Deep and western Soweto including Doornkop informal settlements.</li> <li>• Leaking sewers, especially in the Soweto area.</li> <li>• Industrial areas of Chamdor (Fig. 2)</li> <li>• Closed solid waste at Dobsonville</li> </ul>
Klipspruit Tributary	
Point sources	<ul style="list-style-type: none"> <li>• Orlando Power station (ceased operation in 1998)</li> </ul>
Diffuse sources	<ul style="list-style-type: none"> <li>• Slimes/ rock dumps and old waste sites on mine properties</li> <li>• Central gold recovery slimes dam reclamation</li> <li>• Informal settlement in Central Business District (CBD) Johannesburg and Soweto</li> <li>• Leaking sewers especially in the CBD and Soweto</li> <li>• Industrial areas of Main Reef Road, Industria, Newtown, Selby, Ophirton Area</li> <li>• Marie Louise and Robinson Deep Solid waste sites and the now closed waste site near Meredale</li> </ul>
Klip River between Klipspruit and Rietspruit confluences (Localities 4 and 5)	
Point sources	<ul style="list-style-type: none"> <li>• Goudkoppies, Olifantsvlei, Bush Koppies and water Vaal WWTWs</li> </ul>
Diffuse sources	<ul style="list-style-type: none"> <li>• Informal settlements near Eldorado Park, Lenasia and Eikenhof</li> <li>• Leaking sewers in the Eldorado Park Area</li> <li>• Industrial areas of the Kliprivier</li> <li>• Goodkoppies solid waste site</li> <li>• Agricultural runoff</li> </ul>

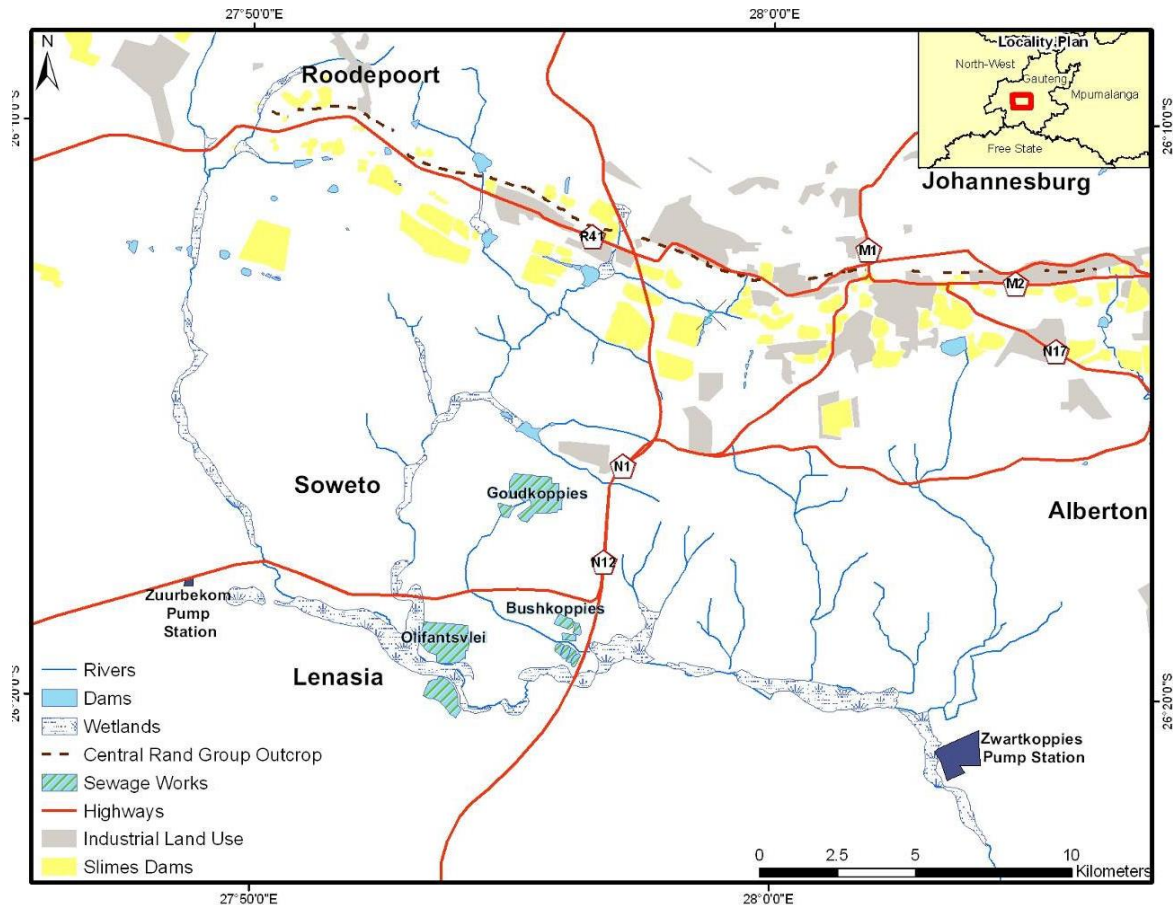


**Figure 2: Location of the Klip River wetland in relation to industrial urban and mining development (Vermaak 2009)**

### 2.2.1 Mining Impacts

Water is a vital requirement at a mine site for dust suppression, mineral processing, coal washing and hydrometallurgical extraction. Mine water is generated and eliminated at various stages during mining, mineral processing or metallurgical extraction. At the latter stages of the mining operations waste water is produced which has no value to the mine. The waste water requires remediation as its uncontrolled discharge from the mine site can impact the surrounding environment and maybe associated with the emission of heat, suspended solids, alkalis, acids and dissolved solids including process chemicals, metals, metalloids, and radioactive substances or salts (Lottermoster 2010).

The city of Johannesburg was founded in the 1880s when gold deposits were detected in the Witwatersrand area. It expanded and consequently towns developed. Most of the mining activities are south of the water shed falling within the upper sections of the Klip River Catchment. A decrease of mining activities has been noted over the past few decades and currently there are

only two operating underground mines in the Klip River Catchment (Durban Roodepoort Deep and East Rand Property Mines (ERPM) as described by Kotze (2008).

The Klip River System has also been affected greatly by Acid Mine Drainage (AMD). Gold tailings have been a major feature around gold mining towns. Gold mines have been discharging water for decades. The effect of this pollution has been pronounced in the Klip River Catchment (which drains the southern portion of the Witwatersrand Escarpment). Several mines in the Witwatersrand Escarpment closed over several years, and as each mine closed and ceased pumping, water accumulated in the voids and was then discharged into neighboring mines because of the close proximity of the mine workings. The neighbours then harboured the responsibility of pumping the waste water. The water had a very low pH and high iron content and therefore there was a need to lower the pH by adding limestone and precipitating the iron by blowing oxygen or air into the water. During the precipitation process several heavy metals apart from iron were precipitated. The iron was allowed to settle and was separated and disposed of in tailing dumps while the water was discharged into local rivers. The discharged water was generally clear; however, a high sulphate content of 1500 mg/l was observed. The effect of the diffuse and point source pollution arising from gold mines of the Central and Western basins is well illustrated by the elevated amounts of salinity levels of the Vaal River, which nearly doubles as a result of the inflow of water from the Klip River and Blespokspruit (via Suikerbos River) (McCarthy 2011).

### **2.2.2 Industrial Impacts**

The Vereeniging District in the lower reaches of the river close to its confluence with the Vaal River, was established due to coal mining and the steel industry. Industrial water users in the Klip River catchment are supplied with water by Rand Water either directly or via local authorities. A few industrial users abstract water directly from the River system (Hippo quarries in the upper Klip). Glen Douglas Dolomite Mine located in the lower Klip River utilizes ground water or purified sewage effluent. Several industries namely Nampak and Everite situated in the Upper Klip River used to abstract river water for industrial purposes. However, direct use of water from the Klip River has declined due to the deteriorating quality and increased accessibility to portable water (DWAF 1999).

### **2.2.3 Domestic Impacts**

Informal settlements of the Klip River Catchment are increasing. This user group uses water directly from the river for domestic purposes such as drinking, washing clothes *etc.* These informal settlements are generally supplied with potable water in tankers or stand pipes by Rand Water.

Community knowledge and awareness of the potential health risks associated with consumption of water from the Klip River seems to be relatively good, and has prevented the widespread use of the water for drinking purposes. However, if their water needs are not met, the direct use of the water from the Klip River is expected. The poor water quality of the river can therefore have detrimental effects on the health of these users (Muruvu 2011).



**Figure 3: Informal settlements in Lenasia and surface runoff being discharged into the Klip River**

### **2.3 Physical characteristics**

The mining, industrial and domestic activities pose a serious threat to the biota of the Klip River by altering the physico-chemical and biological concentration of the river system (Venkatesharaju *et al.* 2010). Therefore it was important to investigate the current physico-chemical state of the Klip River. Water quality variables can be grouped in several ways, the simplest is to divide the parameters into physical and chemical attributes. The physical parameters include temperature, turbidity, and concentration of suspended solids. The chemical attributes include total concentration of dissolved solids (TDS), and the concentration of solutes such as ions and dissolved gases. Although chemical substances may have a beneficial or detrimental effect on aquatic organisms, combinations of substances may be more or less toxic than each on its own. When two substances interact to produce a magnified effect, this is known as *synergism*. For example, nickel and zinc are synergistic in the sense that they are five times more toxic in combination than when either is alone. On the other hand the toxicity of some substances can be

decreased in the presence of other substances which are *antagonists*. For instance, calcium or high levels of alkalinity of TDS can reduce the toxicity of copper and other toxic heavy metals. Fluctuations in pH are particularly important in altering the toxicity of chemical constituents, including heavy metals. Organic compounds may lower both chronic and acute toxicity of metals by complexing with them (Dallas & Day 2004).

**Table 2: Effects of some major physical and chemical attributes of water in aquatic systems (Dalls & Day 2004, Lawson 2011).**

Water quality variables	Major effects
Physical Parameters	
Temperature	<ul style="list-style-type: none"> <li>• Determines metabolic rate of aquatic life</li> <li>• Determines availability of nutrients and toxins</li> <li>• Affects solubility of gases in water. Gas solubility decreases with increase in temperature (Lawson 2011)</li> <li>• Changes provide cues for breeding and migration patterns</li> </ul>
Turbidity and suspended solids	<ul style="list-style-type: none"> <li>• Turbidity determines degree of penetration of light, hence vision and photosynthesis are affected</li> <li>• Suspended solids reduce penetration of light, smother and clog surfaces (e.g. gills) and adsorb nutrients and toxins</li> </ul>
Chemical Factors	
pH	<ul style="list-style-type: none"> <li>• Determines ionic balance</li> <li>• Affects chemical species and therefore availability</li> <li>• Affects gill functioning</li> <li>• Decides the survival, metabolism and physiology of aquatic organisms (Lawson 2011)</li> </ul>
Conductivity, salinity, TDS, individual ions	<ul style="list-style-type: none"> <li>• Affect osmotic, ionic and water balance</li> <li>• TDS affects the physiology of fish and other aquatic organisms (Lawson 2011)</li> <li>• Dissolved solids also affects conductivity. The higher the TDS the higher the conductivity (Lawson 2011)</li> </ul>

---

	<ul style="list-style-type: none"> <li>• Salinity determines the distribution of organisms in an aquatic environment. There is a relation between dissolved oxygen and salinity. As salinity increases the solubility of oxygen decreases, however DO decreases more as temperature increases, regardless of salinity (Lawson 2011)</li> </ul>
Dissolved oxygen	<ul style="list-style-type: none"> <li>• Required for aerobic respiration</li> <li>• Affects the availability and solubility of nutrients (Lawson 2011)</li> <li>• Low DO can result in changes of oxidation states from oxidized to reduced therefore increasing toxicity of toxic metabolites.</li> </ul>
Trace metals	<ul style="list-style-type: none"> <li>• Many essential at low concentrations</li> <li>• Some mutagenic, teratogenic, carcinogenic</li> <li>• Some are metabolic inhibitors</li> </ul>

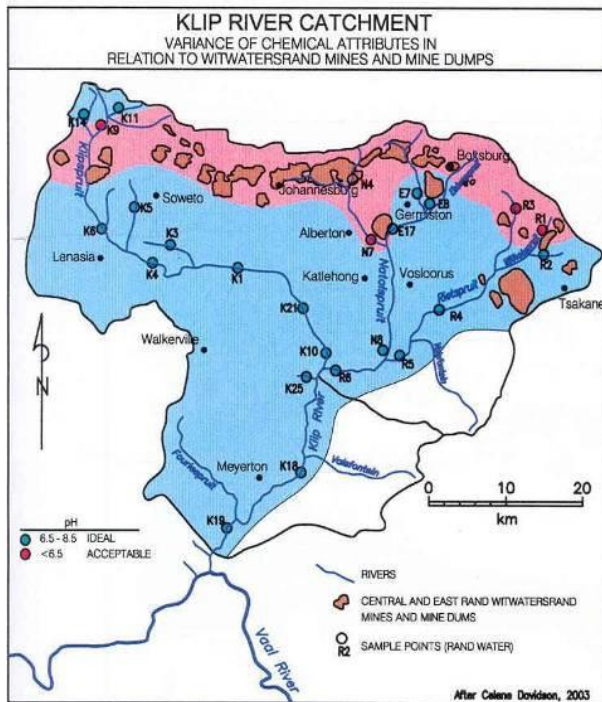
---

Previous studies have revealed that the Klip River's water quality has deteriorated over the years. Kotze (2008) carried out analysis on data collected by Rand Water between the periods of 1973 to 2001. A decline in the water quality with respect to the following parameters was noted; pH, turbidity, alkalinity, mercury, cyanide, lead, aluminium, manganese, iron, copper, cadmium, chromium and zinc. It was also reported by McCarthy and Venter (2006) that the establishment of the Witwatersrand conurbation has greatly contributed to the accumulation of heavy metals such as copper, uranium, magnesium, cadmium, nickel, cobalt, lead and zinc in the peat. They stated that seepage from mine tailings has been the major contributor to heavy metal pollution in the river. Moreover they postulated that the sequestration of metals by the peat has protected the Vaal River Drainage System from excessive pollution.

The Klip River Wetlands play a vital and important role in the removal of pollutants from mine water in the Central Rand. It has been previously observed that as water flows towards the Vaal River, heavy metal concentrations and physical attributes such as pH and conductivity improve to acceptable and ideal levels as compared to unacceptable levels of the river water near mine dumps (Fig. 4). Therefore in the current investigation the displayed trend is likely to be expected.



a. PH level



b. Conductivity

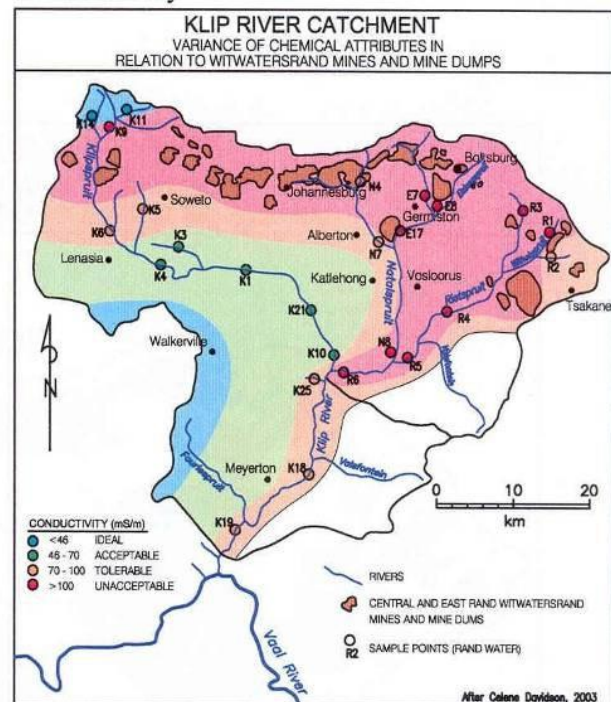


**Figure 4: Klip River Catchment showing distribution of a) pH and b) Conductivity (Davidson 2003)**

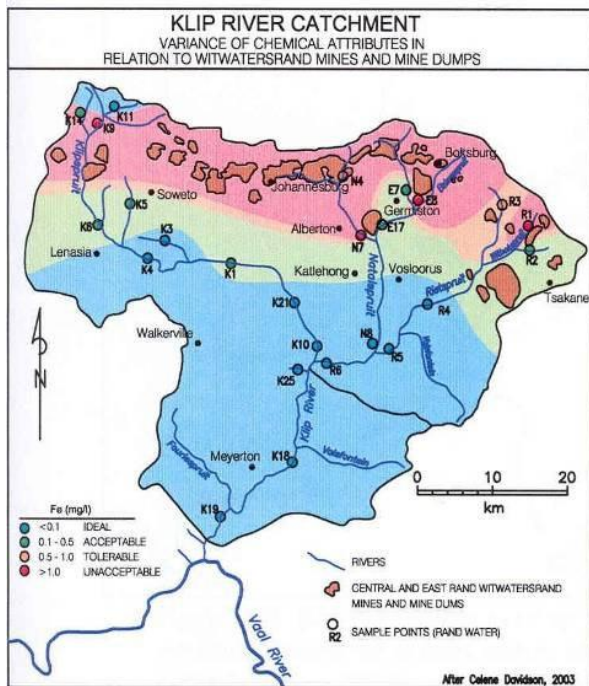


**Figure 5: Klip River Catchment showing distribution of iron (Davidson 2003)**

The improvement in the water quality has been greatly accredited to the presence of large tracts of Malmani dolomites as well as the wetlands in the catchment (Fig. 5). The alkaline nature of the dolomites cause a natural increase in the pH of the water and this enhances the precipitation of iron and other heavy metals which become insoluble in water at neutral pH (Davidson 2003). The wetlands trap heavy metals in its sediments and thus contribute to the overall improvement of the Klip River's water quality (McCarthy 2006).

## **2.4 Chemistry, uses and toxicity of heavy metals**

According to Barakat (2011), heavy metals possess a density of  $5g/cm^3$  or more. Several heavy metals are naturally occurring elements of the earth and some of them namely, zinc, nickel, copper, are regarded as essential elements which are vital to living microorganisms. However, in excessive amounts they have been proven to be toxic. Most heavy metals are transition elements with completely filled d-orbitals. The d-orbitals make it possible for the heavy metal action's to participate in vital redox reactions in metabolic processes which are necessary to sustain life. However, at elevated concentrations they form unspecific complex compounds in the cell with harmful effects. Some heavy metals such as mercury, lead, silver and cadmium are highly toxic even in minute amounts. Thus intracellular concentrations of heavy metal ions need to be tightly controlled and mechanisms are developed by the cell to regulate metals within the cells (Nies 1999).

With increased industrialization, enormous amounts of toxic waste including heavy metals have become a major source of concern. Wastes from mining, metal refining industries, sewage sludge, power plant and waste incineration plants often contain elevated amounts of heavy metals such as lead, mercury and cadmium. These heavy metals are a serious threat to environmental biota and urgent removal from polluted environmental sites is required (Naik & Dubey 2013).

### **2.4.1 Lead**

Lead is ubiquitous and one of the first and earliest metals to be discovered by humans. Lead possesses ideal properties such as softness, high malleability, ductility, low melting point and resistance to corrosion. Thus it has been used in various industrial applications such as, paint production, ceramics, automobile etc. These industrial activities has led to an increase in the occurrence of free lead in the biological systems and the inert environment (Flora *et al.* 2012)

Lead has no known function in the body and once it enters the body, it is known to cause severe health defects that might not be reversible. A variety of molecular, cellular and intracellular mechanisms have been proposed to explain the toxicological profile of lead that include generation of oxidative stress, ionic mechanisms and apoptosis. Oxidative stress is the major mechanism of lead toxicity. Lead causes generation of reactive oxygen species (ROS) which results in damage of biomolecules such as DNA, enzymes, proteins, and membranes while it simultaneously impairs the anti-oxidant defense system (Flora *et al.* 2012).

### **2.4.2 Cadmium**

Cadmium is a low melting point metal that has several uses in industry. Chemically it is a 4d transition element. Cadmium forms several alloys with a variety of metals. One of the crucial uses as an alloying agent is in the hardening and strengthening of copper used for electrical and thermal transfer applications. It is also a component of low melting point solders designed for use in electronics circuitry. Being similar to zinc in chemistry, cadmium is associated with zinc in ore deposits. It is produced mainly as a by-product of zinc processing. Cadmium is also used in the processing of NiCd batteries, coatings and platings. Cadmium provides exceptional corrosion resistance in most environments to products made from iron, aluminium, steel and titanium. It is very effective when used in electroplating especially on bolts, nuts and other types of fasteners. Cadmium coating has the advantage of predictable torque, which is a result of low coefficient of friction and its low specific volume. Cadmium can also be used in the production of polyvinyl chlorides (PVCs) which are subject to decomposition by heat or incident light. Cadmium salts such as cadmium carboxylate and cadmium laurate have been used extensively with barium as heat and light stabilizers for PVCs (Butterman & Plachy:1-18).

Cadmium has detrimental effects on biological processes such as gene expression, cell cycle, differentiation and proliferation. Cadmium causes oxidative damage and stress affecting DNA, proteins and membrane lipids. The induction of oxidative damage is associated with mitochondrial dysfunction, deregulation of intracellular antioxidants and apoptosis. Oxidative stress on proteins stimulates heat shock proteins (HSPs), coupled with an adaptive response, initiation of protein refolding and/or degradation by ubiquitine proteasome. Oxidative damage to DNA causes gene mutations and the induction of cancer (Bertin & Averbeck 2006).

### **2.4.3 Copper**

Copper has an atomic number of 29 and belongs to the group 1B of metals. It has a high electrical and thermal conductivity, high ductility and malleability and thus it is used widely in the production of wire. Copper is also corrosion resistant, although it is slowly oxidized in the presence of air. It has a very high melting point (1083°C) and a high boiling point of 2595°C, and has a low tendency to fume compared to other non-ferrous heavy metals such as arsenic, cadmium, zinc and lead. Copper has several valence states from 0 to +3. Copper is quite biologically active and has a tendency to form strong complexes with water, soil and with organic ligands containing nitrogen and sulfur. Copper primarily precipitates as hydroxides, and conditions of precipitation normally depend on oxygen level, pH and alkalinity. It also adsorbs on both inorganic particles (such as clays) and organic colloidal matter such as living or dead cells. Minute amounts of copper are

essential to all living organisms. However, copper is quite toxic at elevated levels. An important factor to consider is that only soluble copper is bio-available, and consequently, copper bound to matter is not available to living organisms. Therefore the total amount of copper in a water body is not an accurate measure of its potential hazard to biological organisms. Even the soluble fraction is only bio-available under specific conditions of pH, dissolved organic carbon (DOC), hardness and salinity (Ayres *et al.* 2002).

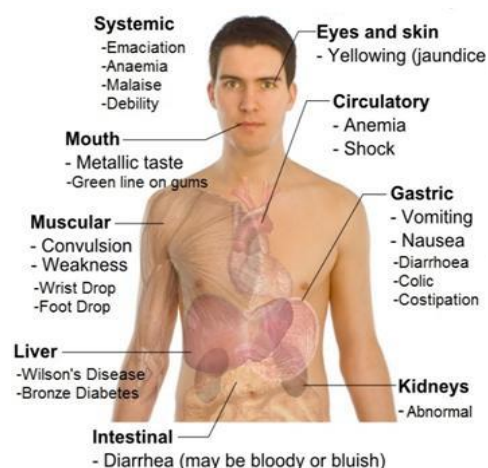


**Figure 6: Chronic copper poisoning (Ashish *et al.* 2013)**

Copper can contaminate the water and soil environments, posing risks to wildlife. On a more benign level, it can stain clothing and flesh. The general symptoms of copper toxicity include a metallic taste in the mouth, abdominal pains, vomiting, cramps of legs or spasm, diarrhoea, severe headaches, difficulty in breathing, jaundice, allergies, hair loss, anemia, anorexia, anxiety, attention deficit disorder, asthma, autism, candida, depression, male infertility, prostatitis, fibromyalgia and insomnia (Fig. 6) (Ashish *et al.* 2013).

#### 2.4.4 Chromium

Chromium is one of the most abundant elements present in the earth's crust and it exists naturally mostly in its trivalent state. It has an atomic weight of 52, and it is used in several chemical, industrial and metallurgical applications. One of the ideal properties that make chromium ideal in industrial uses is its natural existence in its trivalent state that makes the metal inert even in environments where it is not thermodynamically stable. Some of the industrial applications for chromium include electroplating, alloys, stainless steel production and leather tanning (Barnhart 1997).

The overall toxicity of chromium depends on the oxidation states. Chromium (IV) is the more poisonous toxin than its trivalent form chromium (III). Chromium (IV) is more easily ingested and

absorbed into the body. The respiratory tract is the main target for inhaled chromium after acute exposure. Swallowing high amounts of chromium can lead to acute, potentially fatal effects in the respiratory, gastrointestinal, cardiovascular, hepatic, renal and neurological systems. Chromium (IV) compounds have been shown to cause chromosomal aberrations and chromatid exchanges in humans (Assem & Zhu 2007).

#### **2.4.5 Zinc**

The most ideal characteristics of zinc include its durability and recyclability. It is used in a variety of applications in transportation, infrastructure, consumer products and food production. One of exceptional qualities of zinc is its ability to protect steel from corrosion. Zinc provides a physical barrier as well as cathodic protection for the underlying steel allowing its service life to be extended (Glinde & Johal 2011).

Generally zinc has been regarded as a relatively nontoxic element; however, recent studies have shown  $Zn^{2+}$ , to be a potential killer of neurons, glia and other cell types. The zinc concentrations in the brain are usually maintained within a very narrow range of 600-800 ng/l with deviations above or below this range being proconvulsive and cytolethal, respectively. Concentrations of zinc above 60 ng/l in eukaryotic cells can be toxic. The common effects related to long term excessive zinc intakes ranging from 150 mg/day to 1-2 g/day have included sideroblastic anaemia, hypochromic microcytic anaemia, leukopenia, lymphadenopathy, neutropenia, hyocupraemia and hypoferraemia. Usually patients recover to normal after cessation of zinc intake (Nriagu 2007).

#### **2.4.6 Iron**

Iron is the most commonly found element in the earth's crust. The metal is chemically active and occurs in nature combined with other elements in rocks and soils. In its natural state iron is combined with oxygen, carbon dioxide, water or sulfur in a number of minerals (BCS Incorporated 2002). Iron has quite a variety of uses; it is coupled with carbon to make steel, and steel can be coupled with other metals to make a wide variety of steel alloys which are durable and malleable to manufacture products such as cars, household appliances, buildings, bridges, railways, food cans, tools *etc.* Iron possesses several desirable properties which makes it ideal for several uses and applications. Iron has a high melting point of approximately (1535°C) and is quite soft; however, when made into steel it becomes very strong, malleable and ductile, it quickly corrodes and forms iron oxide when exposed to air.

Iron is an essential element to living organisms as it plays a crucial role in biochemical activities, such as oxygen sensing and transport, electron transfer and catalysis (Aisen *et al.* 2001). The biological functions of iron are based on its chemical properties, especially its favourable redox potential to switch between the ferrous, Fe (II) and ferric, Fe (III) states. However, this important property turns into a potential hazard because under aerobic conditions, iron catalyzes the production of noxious radicals. Iron toxicity is greatly based on the Fenton and Haber-Wess chemistry, where catalytic amounts of iron are able to produce hydroxyl radicals from superoxide and hydrogen peroxide, otherwise known as “reactive oxygen intermediates” (ROIs) (Halliwell & Gutteridge 1990). Below is a list of pathological situations associated with iron overload, such as hereditary hemochromatosis, Porphyrria cutanea tarda, Wilson’s disease, Menkes syndrome *etc.* as stated by Fraga & Oteiza (2002).

#### **2.4.7 Nickel**

Nickel is a metal with a high melting point and an atomic weight of 58.71. It has a variety of uses in industrial, military, transport, aerospace marine and architectural applications. The most important use is alloying, particularly with chromium and other metals to produce stainless steel and heat resistant steels (Nickel Institute 2011). In addition some major applications include electroplating, electroforming, battery production and catalysts (Henderson *et al.* 2012). Heavy metals such as nickel are mined and processed by the mining and ore smelting industries several of which occur in Gauteng. These are easily carried off together with runoff into rivers. Nickel in excess concentrations could have toxic effects to biological life including people who may have to drink from the river (Rand Water).

The main health related effects related to nickel poisoning include, skin allergies, lung fibrosis, kidney and vascular poisoning and stimulation of neoplastic formation (Denkhaus & Salnikow 2002).

#### **2.5 Biochemical profiling using the API20E® Biochemical Test Strips**

Biochemical or Phenotypic profiling can be performed using the Analytical Profile Index API 20E® test strips (BioMérieux Inc., Marcy l'Etoile, France) (Fig. 7). It is a fast and efficient way of creating biochemical profiles as compared to the conventional methods which are time consuming and involves the use of several reagents and materials. This method has been used in previous studies to analyse the biochemical profiles of environmental isolates (Philips *et al.* 2012; Espinoza *et al.* 2013, Zaree *et al.* 2014). It consist of 20 separate cupules, all containing dehydrated reagents (Table 3). A bacterial suspension is used to rehydrate each of the cupules. Some of the

wells will undergo color changes due to change in pH, whereas others will produce end-products that have to be identified by addition of reagents (Biomerieux).

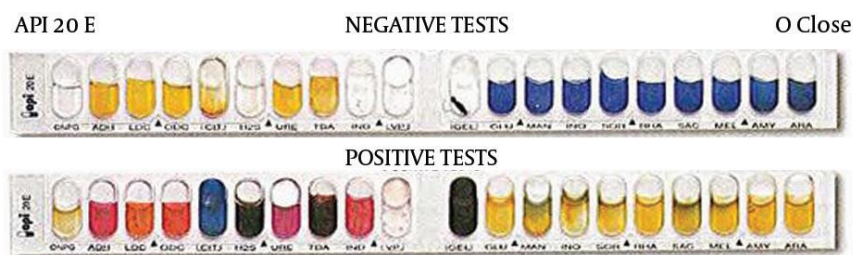


**Figure 7: Negative and positive test results on API 20E® test strips (Zaree *et al.* 2014)**

**Table 3: Biochemical reagents on an API20E® test strip with the corresponding reaction or enzyme under investigation**

Active component	Reaction/ enzyme
2-nitrophenyl-βD- galactopyranoside	B-galactosidase (ortho NitroPhenyl-βD-galactopyranosidase)
L-arginine	Arginine Dihydrolase
L-lysine	Lysine decarboxylase
L-ornithine	Ornithine decarboxylase
Trisodium citrate	Citrate utilization
Sodium thiosulphate	$H_2S$ production
Urea	Urease
L-tryptophane	Tryptophane deaminase
L-tryptophane	Indole production
Sodium pyruvate	Acetoin production
Gelatin	Gelatinase
D-glucose	Fermentation/ oxidation (Glucose)
D-mannitol	Fermentation/ oxidation (Mannitol)
Inositol	Fermentation/ oxidation (Inositol)
D-sorbitol	Fermentation/ oxidation (Sorbitol)
L- rhamnose	Fermentation/ oxidation (Rhamnose)
D-sucrose	Fermentation/ oxidation (Sucrose)
D-melibiose	Fermentation/ oxidation (Melibiose)
Amygdalin	Fermentation/ oxidation (Amygdalin)
L-arabinose	Fermentation/ oxidation (Arabinose)

## 2.6 Antibiotic resistance

Antibiotics are effective tools for controlling pathogenic bacteria. However, bacteria have evolved and have developed antibiotic resistance to several antibiotics and this poses a serious problem that diminishes the advantage of using antibiotics as chemotherapeutic agents. At present there is evidence that resistance to nearly all the clinically useful antibiotics. Some scientists have speculated that the situation might be pushed back to that resembling the pre-antibiotic era (Chattopadhyay & Grossart 2011).



Antibiotic resistant microorganisms are normally selected in environments contaminated with antibiotics and they are also found in natural environments in the presence of some non-antibiotic substances, especially heavy metals (mercury, arsenic, lead, cadmium *etc.*). The increased resistance to heavy metals has serious repercussions, since it may influence the evolution of antibiotic resistant genes due to increased selective pressure by the environment. The concurrent occurrence of resistance to antibiotics and heavy metals is a potential threat to human health and environmental balance (Sarma *et al.* 2010). Genes conferring antibiotic as well as heavy metal resistance are normally located on the same plasmid. This is the main reason why several bacteria that thrive in the presence of heavy metals, are also resistant to antibiotics (Chattopadhyay & Grossart 2011). Although antibiotic resistance can also develop as a result of chromosomal mutations, it is generally associated with mobile genetic elements (MGEs); such as plasmids, integrons and transposons acquired from other bacteria (Fig. 8) (Levy 1998).

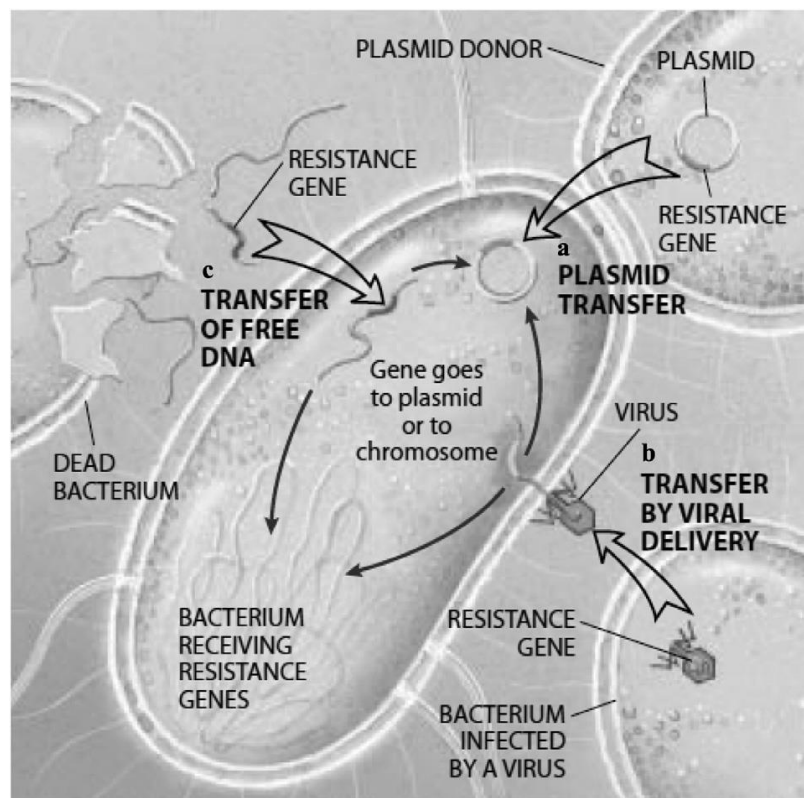


**Figure 8: Main mechanisms of gene transfer in bacterium (a) plasmid transfer, (b) transfer by viral delivery (c) transfer of free DNA (Levy 1998)**



Efflux mechanisms are recognized as the main multidrug mechanisms in bacteria (Fig. 9).

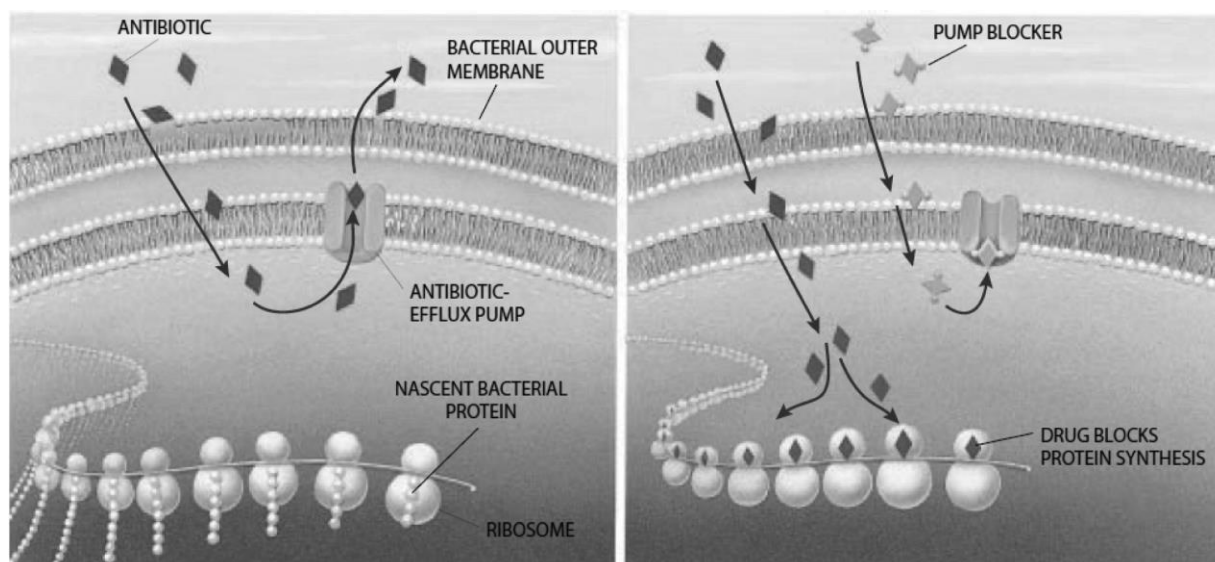


**Figure 9: (a) Bacterial efflux mechanism pumping antibiotics out of the cell, (b) antibiotic interfering with ribosomes in protein biosynthesis (Levy 1998)**

Genetic reactors are places in which genetic evolution takes place. This evolution is caused by high biological connectivity, generation of variation, and presence of specific selection factors such as antibiotics (Baquero *et al.* 2008).

The primary reactor is made up of human and animal microbiota that involve greater than 500 species on which therapeutic antibiotics exert their action. The secondary reactor includes the hospitals, long term care facilities, farms or any location in which susceptible individuals are crowded and exposed to bacterial exchange. The tertiary reactor includes wastewater and any type of biological residues that originated in the secondary reactor, e.g. lagoons, sewage treatment plants or compost toilets, in which bacterial microorganisms from several different individuals have the chance to interact. The fourth reactor is the soil and the ground water environments, where the bacteria that originated from the previous reactors mix and interact with environmental organisms. Water is a crucial agent in all four reactors especially the last one.

There are four main **genetic reactors** in antibiotic resistance (Fig. 10).

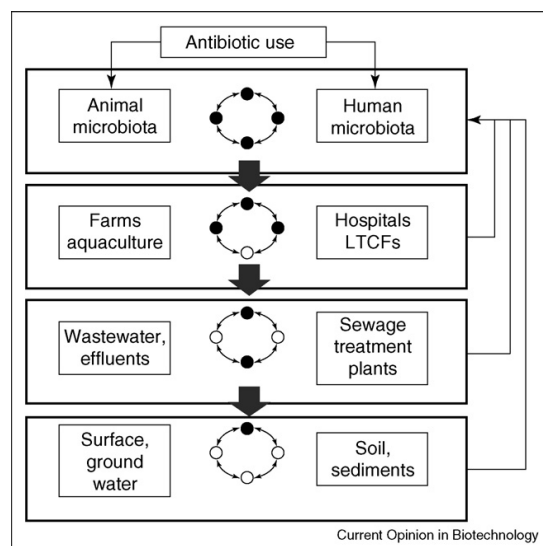


**Figure 10: Four genetic reactors in antibiotic resistance, where genetic exchange and recombination shapes the future evolution of resistance determinants. Particularly in the lowest reactors, bacteria from human or animal-associated microbiota (in black) mix with environmental bacteria (in white), increasing the power of genetic variation and possible emergence of novel mechanisms of resistance that are re-introduced in human or animal environments (back arrows) (Baquero *et al.* 2008).**

### 2.6.1 Antibiotic Susceptibility Tests

Antibiotic Disc Susceptibility (ADS) is an antibiotic susceptibility test (AST) which uses sterile paper discs containing a specific concentration of antibiotic. The antibiotic discs are placed on a lawn of bacteria which has been spread on an agar plate. The standard density for a bacterial suspension is normally compared to 0.5 McFarland standard (Andrews 2001a). Inoculums that are too heavy or too light do not produce reproducible results and can lead to errors. After a 24 hour incubation period, clear zones around the disc can be perceived indicating bacterial lysis. These zones can be analyzed to assess an isolate's susceptibility or resistance to a particular drug (Andrews 2001b). However, the zones of inhibition produced are not uniform due to variances in the testing methods adopted by different manufactures (Brown & Kothari 1975) and therefore it is important to use one type of discs for data to be comparable (Mistry 2013).

### Heavy metal resistant microorganisms

Heavy metal contamination of surface waters has a direct impact on the public health as well as the environment. For example, *P. aeruginosa* isolated from river water showed co-resistance to tetracycline and copper, supporting the concern that antibiotic resistance by the attainment of plasmids can be produced by the selective pressure of heavy metals in the environment (Martins *et al.* 2014). Microorganisms inhabiting contaminated surface water rapidly adapt and are sensitive to low concentrations of heavy metals and therefore they can be used as bio- indicators

to detect heavy metal pollution in the environment (Ozer *et al.* 2013). Microbial survival relies on the intrinsic biochemical, structural, and physiological properties and genetic adaptation (Aktan *et al.* 2013). As highlighted in the previous section there is evidence in previous studies (McCarthy & Venter 2006) that the Klip River System has been contaminated by heavy metals from various sources, especially mine tailings. Therefore, it is most likely that the river could be harbouring heavy metal resistant microorganisms which have developed coping mechanisms to survive harsh environments with toxic levels of drugs and metals. For instance, a heavy metal strain *Pseudomonas stutzeri* (MTCC101) from Microbial Type Culture Collection (MTCC), IMTECH, Chandigarh, India was found to tolerate high cadmium concentrations, up to 1200 µg/ml. The genes involved in such high resistance appear to be induced in the presence of cadmium. The genes are responsible for the synthesis of new proteins in the cell wall of the bacteria, and the highest levels of cadmium accumulation occurs in the cell wall fraction of the bacteria (Deb *et al.* 2013). A global proteome analysis carried out on the strain *Pseudomonas fluorescens* BA3SM1 showed the bacterial strain has developed several mechanisms against heavy metal toxicity. The organism's change in protein expression in the presence of cadmium (Cd), zinc (Zn) and copper (Cu) was assessed using two dimensional gel electrophoresis followed by mass spectroscopy. The analysis showed that the bacterial cell adapted to metals by inducing seven defense mechanisms i.e. cell aggregation, or biofilm formation, modification of envelope properties to increase the extracellular metal biosorption and/or uptake of metal; metal export; response to oxidative stress; intracellular metal sequestration; hydrolysis of abnormally folded proteins and the over-synthesis of proteins inhibited by the metal. *Pseudomonas fluorescens* is able to acquire a metal resistant phenotype making it ideal for bioremediation. *Proteus vulgaris* (BC1), *Pseudomonas aeruginosa* (BC2), *Acinetobacter radioresistens* (BC3) and *Pseudomonas aeruginosa* (BC5) were isolated from sewage water collected in and around Madurai District in South India. The isolates were resistant to cadmium (Cd), nickel (Ni), lead (Pd), arsenic (As), chromium (Cr) and mercury (Hg). These microorganisms exhibited optimum growth at 30°C and pH 7. The multiple metal resistances of these isolates were also associated with resistance to the following antibiotics: Ampicillin, Tetracycline, Cloramphenicol, Kanamycin, Erythromycin, Streptomycin and Nalidixic acid. These microorganisms could be regarded as ideal candidates for bioremediation of heavy metal contaminated sewage and wastewater (Raja *et al.* 2009). Çolak *et al.* (2011) isolated and identified *Bacillus cereus* and *B. pumilus* from heavy metal polluted soil in Turkey as potential bioremediation agents due to their heavy metal resistance and high adsorption capacities.

## **2.7 Heavy metal resistance mechanisms of microorganisms**

Some heavy metals such as zinc and copper are regarded as essential elements since they are required for important metabolic processes taking place in living microorganisms. However, all heavy metals are toxic in excess quantities. Therefore to avoid toxicity, cells have developed mechanisms to eliminate heavy metals from the cells quickly and efficiently. As postulated by Silver (1992) there are generally four basic mechanisms used in heavy metal resistance and these include:

- i. Exclusion of toxic heavy metal ions from the cell by the alteration of membrane transport systems involved in initial cellular accumulation.
- ii. Intracellular and extracellular sequestration of metal binding components similar to metallothioneins
- iii. Very specific cation/anion efflux systems that are encoded by resistance genes. These genes are usually present on the plasmids of most heavy metal resistant cells.
- iv. Enzymatic detoxification of toxic heavy metals from their toxic to less toxic forms. Mechanisms such as enzymatic transformations (methylation, demethylation, reduction and oxidation) can be incorporated by bacteria in their defense against metal toxicity (Hynninen 2010).

### **2.7.1 Lead resistance**

Very few natural microbial strains possess protective mechanisms to combat lead toxicity (Naik & Dubey 2013). However, lead resistance has been observed in both Gram negative and positive bacteria isolated from lead-contaminated environments. *Pseudomonas marginalis* and *Bacillus megaterium* were isolated from lead contaminated soils by Roane (1999) and *P. marginalis* exhibited higher lead resistance compared to *B. megaterium*. Transmission light microscopy, showed extracellular lead exclusions in *Pseudomonas marginalis* while the less resistant *B. megaterium* exhibited an intracellular cytoplasmic accumulation of lead (intracellular sequestration of lead). Bacteria possessing lead resistance have proven to be ideal for bioremediation of lead contaminated sites. Therefore understanding the mechanism of lead resistance in bacteria is very important, so that applications in the removal and recovery of lead can be developed (Naik & Dubey 2013).

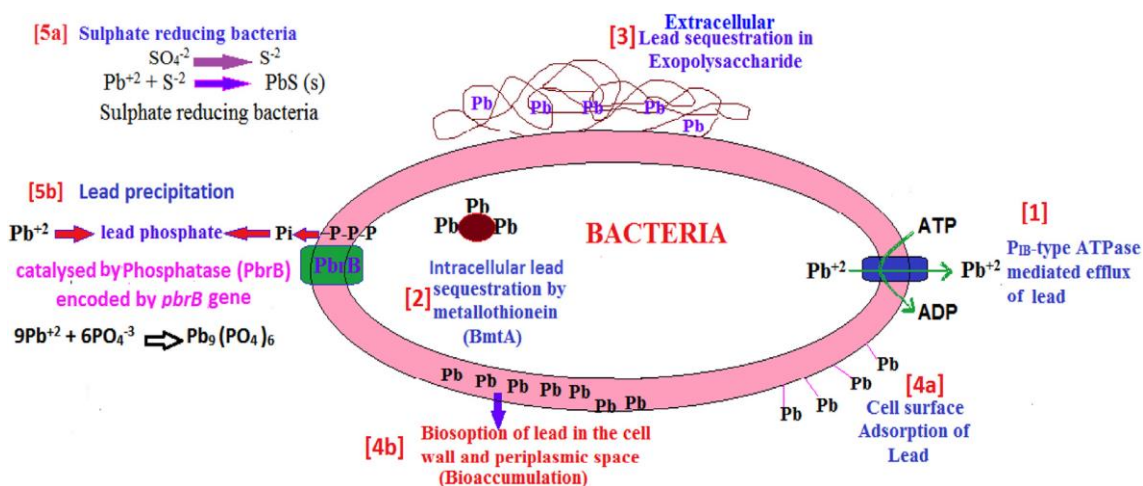


**Figure 11: Lead resistance mechanisms by bacteria (Naik & Dubey 2013)**

Lead resistant mechanisms operational in bacteria are illustrated in Fig. 11. At position **(1)** P -type ATPase mediated efflux of lead is shown. This mechanism involves the formation of a phosphorylated intermediate during their catalytic cycle and represents a collection of proteins involved in the transport of heavy metals outside the cell membrane controlling heavy metal resistance. These proteins prevent excessive accumulation of lead ions in the cell (Nies & Silver 1995). The gene *pbrA* is a gene encoding P-type ATPases in lead resistant microorganisms (Nies 2003). Position **(2)** represents lead sequestration by metallothionein (BmtA). Metallothioneins play a crucial role in the immobilization of lead within the cell thus shielding bacterial metabolic processes catalyzed by enzymes (Blindauer *et al.* 2002). There were several studies carried out to investigate this mechanism and *B. megaterium* was found to resist up to 0.6mM lead by sequestering lead nitrate by proteins which were almost similar to metallothioneins (Roane 1999). The gene *SmtA* in *Proteus penneri* GM10 encodes for the metal binding metallothioneins and is responsible for its lead resistance characteristics. **(3)** represents lead sequestration by exopolysaccharides (EPS). The EPS is composed of high molecular weight polymers secreted by bacterial cells and possess functional groups such as hydroxyl, carboxyl, and amides which creates a high affinity for heavy metals (Bramachari *et al.* 2007). **(4a)** illustrates the cell surface adsorption of lead. **(4b)** shows the biosorption of lead in the cell wall and periplasmic space (bioaccumulation). Surface biosorption is another method of extracellular sequestration of heavy metals which prevents their entry and maintains metal homeostasis. Biosorption involves ion exchange, adsorption and diffusion through cells and membranes (Chang *et al.* 1997). *Bacillus subtilis* has been shown to biosorb a high amount of lead ions, up to 97.68% under acidic conditions (Hossain & Anatharam 2006)

### 2.7.1.1 The *pbr* operon

The *pbr* operon of *Ralstonia metallidurans* CH34 (Fig. 12), formerly known as *Alcaligenes eutrophus* is unique in the sense that it combines functions involved in uptake, efflux and accumulation of  $Pb^{2+}$ . The *pbr* locus contains the following structural genes: *pbrT*, which encodes the *Pb* (II) uptake protein, *pbrA* the P-type *Pb*(II) efflux ATPase, *pbrB* encodes the undecaprenyl pyrophosphate phosphatase (Hynninen *et al.* 2009), *pbrC* encodes a predicted prolipoprotein signal peptidase, *pbrD* encodes *Pb*(II)-binding protein which is important in lead sequestration, and *pbrR* that belongs to the *MerR* family of metal ion-sensing regulatory proteins. This was the first report of a lead resistance mechanism in any bacterial genus (Borremans *et al.* 2001).

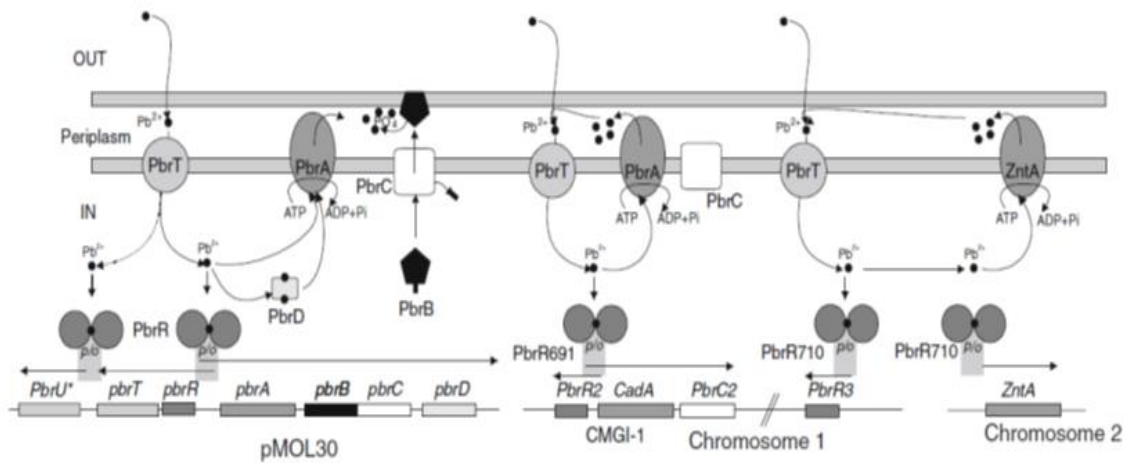


**Figure 12: The *pbr* operon model in *C. metallidurans* CH34 and the connection between plasmid and chromosomal located functions. The *pbr* *UTRABCD* operon is located on the pMOL30 plasmid, *pbrR*<sub>2</sub>, *cadA*, *pbrC*<sub>2</sub> and *pbrR*<sub>3</sub> on chromosome 1 and *zntA* on chromosome 2. The asterisk symbol after *pbrU*<sup>\*</sup> indicates the inactivation of the gene due to the insertion of *TnCme2* at the 3' end of the gene (Taghavi *et al.* 2009)**

### 2.7.2 Chromium resistance

Figure 13 illustrates the transport, toxicity and resistance mechanisms employed by chromium resistant microorganisms. Mechanisms of cell damage and resistance are indicated by thin and heavy arrows respectively. **(1)** illustrates the chromosome-encoded sulfate pathway which chromate ions use to gain access to the cell (Ramírez-Díaz *et al.* 2008). Chromate and sulphate are iso-structural ions, and this characteristic makes it difficult for cells to differentiate between these two ions resulting in the simultaneous uptake of chromium and sulphate by sulphate transporters (Zhirkovich 2005). At point **(2)** plasmid encoded efflux systems can be employed to expel toxic chromate ions from the cytoplasm of the cell thus protecting the cell from chromate toxicity. At point **(3)** intracellular enzymatic reduction of  $Cr^{6+}$  to  $Cr^{3+}$  by the reductase requires the presence of NADPH which is an electron donor, while anaerobic  $Cr^{6+}$  reduction occurs in the

electron transport pathway by cytochrome b or c along the respiratory chains in the inner membrane;  $Cr^{3+}$  ions are unable to pass through the membrane due to the insolubility of  $Cr^{3+}$  derivatives. At point (4) the membrane encoded reductase which is encoded by chromosomal DNA anaerobically reduces  $Cr^{6+}$  in the presence of electron donors such as NADPH. At point (5) reactive oxygen species (ROS) are produced during the redox cycle of  $Cr^{6+}$  and these ROS can cause oxidative stress to the bacteria. To protect the cell from ROS-generated oxidative stress, protective metabolic enzymes such as superoxide dismutase, catalase and glutathione are produced at point (6). At point (7) the presence  $Cr^{6+}$  and  $Cr^{3+}$  adversely affect DNA replication and RNA transcription by damaging DNA and altering gene expression. Moreover  $Cr^{3+}$  also damages proteins by impairing their functions. In order to combat these effects, a DNA repair system is activated by the cell at point (8) (Ahemad 2014).

The genes responsible for chromium resistance are either encoded on the plasmid or on the chromosome of bacteria. The genes located on plasmids normally encode membrane transporters which directly mediate efflux of chromate ions from the cell's cytoplasm (Fig. 13) and genes on the chromosomes are generally responsible for resistance strategies such as specific or unspecific Cr(VI) reduction, free-radical detoxifying activities, repairing of DNA damage and processes associated with sulfur or iron homeostasis (Fig. 13) (Ahemad 2014).

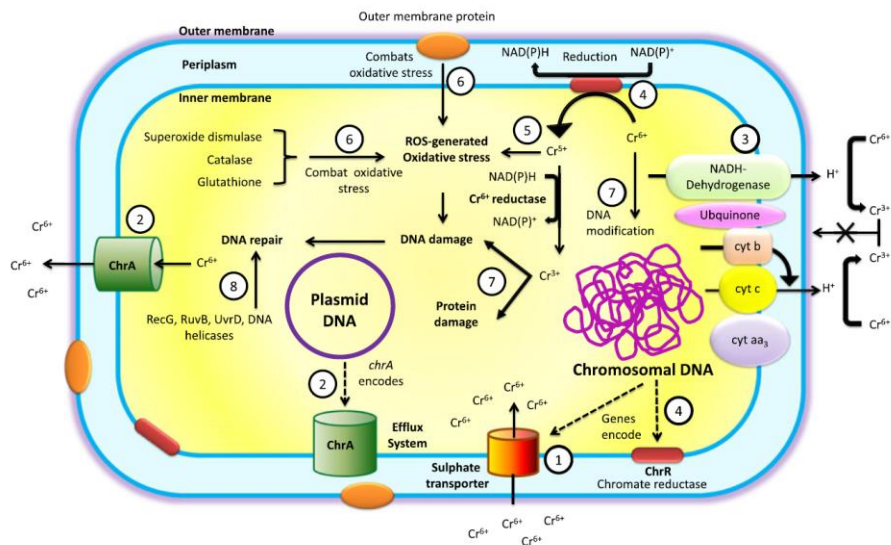


**Figure 13: Mechanisms of chromate transport, toxicity and resistance in bacterial cells (Ahemad 2014)**

### 2.7.2.1 The chr operon

Several bacterial species have developed resistance to chromate, and this phenotypic characteristic could be related to the presence of chromosomal or plasmid encoded genes (Ramírez-Díaz *et al.* 2008). The most common plasmid pMOL28 of *C. metallidurans* harbours the

*chrBAC* genes that are responsible for chromium resistance in the bacterium (Nies *et al.* 1990). *Shewanella* spp. have been shown to reduce Cr(VI) metals and therefore it has been used in the clean-up of terrestrial and aquatic environments (Hau & Gralnick 2007). Aguilar-Barajas *et al.* (2008) studied the expression of chromate resistance genes of *Shewanella*, and it was found that the expression of *chrA* gene alone conferred high chromate resistance, although the expression of the complete operon *chrBAC* did not result in a significant increase in resistance. The resistance of the strains was due to the chromate efflux system encoded by the *chrA* gene (Aguilar-Barajas *et al.* 2008). Cervantes *et al.* (1990) studied chromate resistance mechanisms encoded on the plasmid puM505 present in *Pseudomonas aeruginosa*. In this mechanism the role of the *chrA* protein in the extrusion of chromate ions from the cytoplasm of the bacteria was studied (Alvarez *et al.* 1999). The *chrA* protein belongs to the CHR superfamily of transporters (Di'az-Pe'rez *et al.* 2007). The *chrB* gene encodes a membrane bound protein necessary for the regulation of chromate resistance in the bacteria *C. metallidurans*. The *ChrC* gene *chrB* encodes a protein almost similar to iron-containing superoxide dismutase, the *chrE* gene encodes a gene product that is a rhodanese type enzyme and *chrF* most probably encodes a repressor for chromate-dependant induction (Di'az-Pe'rez *et al.* 2007)

The genes responsible for chromate resistance have been found in the following microorganisms: *C. metallidurans* (Nies *et al.* 1989), *Pseudomonas* spp. (Bopp *et al.* 1983.), *Streptococcus lactis* (Efsthathiou & McKay 1977), and *Arthrobacter* spp. (Henne *et al.* 2009). In another study carried out by Kamika and Momba (2013), the *chrB* gene was detected in several microorganisms, namely, *Pseudomonas putida*, *Bacillus licheniformis*, *Brevibacillus laterosporus*, *Trachelophylum* sp. *Peranema* and *Adispica* sp. *ChrIA1* and *chrA* genes which encode putative chromate transporters were identified in *Bacillus cereus* SJ1 which was isolated from contaminated wastewater by He *et al.* (2010). *Orthobacterium tritici* 5bvl1 was also found to be resistant to very high levels of chromate and the expression of an inducible chromate-resistant gene was detected on the mobile elements (TnOtChr which possesses the genes *chrB*, *chrA*, *chrC* and *chrF*) (Branco *et al.* 2008; Branco & Morais 2013).

### **2.7.3 Zinc resistance**

Zinc resistance is attributed to the following mechanisms: P-type ATPase based efflux mechanisms (Nies 1999), extracellular and intracellular sequestration by metallothioneins (Olafson *et al.* 1988).



#### **2.7.3.1 Efflux by P-type ATPase**

P-type ATPase-based resistance to zinc has been elucidated in *E. coli* (Beard *et al.* 1997) and *P. putida* (Choudhury & Srivastava 2001a). The genes *cadA* of *Staphylococcus aureus* found on plasmid p1258 (Nucifora *et al.* 1989) and *zntA* found in *E. coli* encodes for the ATPases that are responsible for zinc resistance (Rensing *et al.* 1997).

#### **2.7.3.2 Zinc binding proteins**

The presence of metallothioneins inside bacterial cells act as binding agents to zinc ions in a similar mechanism to that shown for lead (Fig. 9). The *Znu* proteins found in zinc resistant bacteria constitute a high affinity periplasmic binding protein that relies on the transport system of *E. coli* (Patzner & Hantke 1998).

#### **2.7.3.3 Post efflux binding**

This is a mechanism that consists of the precipitation or binding of zinc ions to a protein or cellular component. This mechanism was characterized in *C. metallidurans* CH34 in which heavy metal ions were precipitated as a post efflux management. The effluxed metals are precipitated in the form of bicarbonates and hydroxides and this prevents the re-entry of metals into the cell (Diels *et al.* 1995).

#### **2.7.3.4 Reduced uptake**

Zinc resistance inferred by reduced uptake was noted in *Azpospirillum brasiliense*. In a comparative study of zinc uptake between a zinc sensitive strain and the wild type, it was found that the former strain took up more zinc than the wild type. The morphology of the wild type also changed when it was exposed to zinc. The bacterial cells enlarged, and changed into non-motile melanized structures and these were termed encapsulated forms (Gowri & Srivastava 1996)

#### **2.7.3.5 Extracellular accumulation**

Zinc resistance is brought about by the accumulation of high amounts of zinc on the bacterial cells' outer membrane. This mechanism was noted in *P. stutzeri* RS34 isolated from industrially polluted soil in New Delhi (Bhagat & Srivastava 1993).

#### **2.7.3.6 Efflux by antiport system**

The most extensively studied zinc resistance mechanism is the Czc system (Fig. 13) which is expressed in *C. metallidurans* CH34. The Czc confers resistance to cadmium, zinc and cobalt in bacterial cells. The *czc* functions as a cation/ proton antiporter, by removing cations from the cells. The *czc* operon of the plasmid pMOL30 entails of three structural genes, namely *czcA*, *czcB* and *czcC* which encode for the proteins responsible for the complex cation pump (Choudhury & Srivastava 2001b).

### 2.7.3.7 Zinc homeostasis and host response

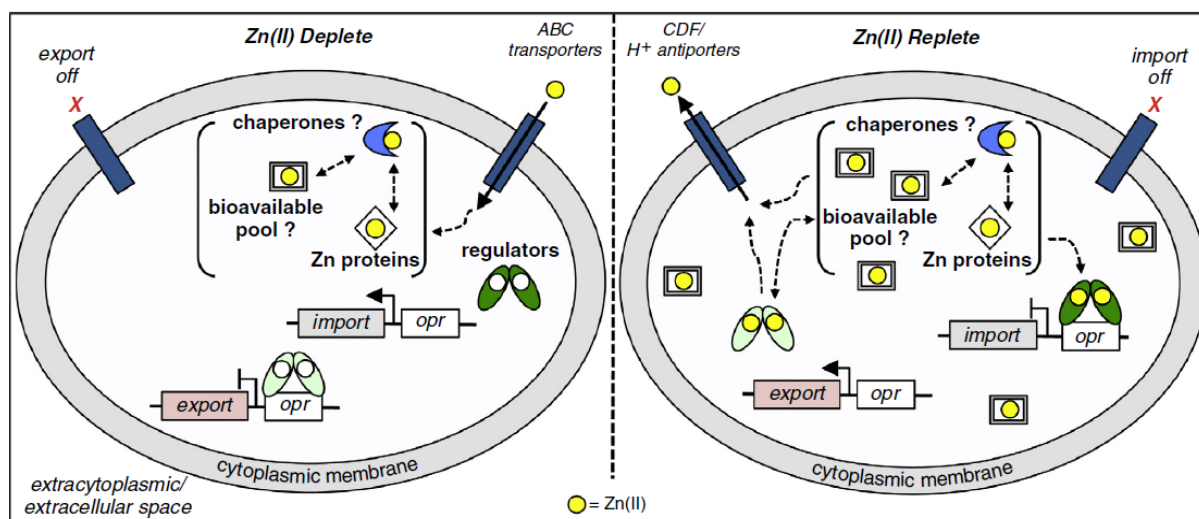


**Figure 14: Cellular response to either limited (left) or toxic (right) (Braymer & Giedroc 2014)**

Figure 14 shows cellular responses to either limited (left) or toxic (right) levels of  $Zn(II)$  concentrations. The efflux or influx of Zinc (II) is mediated by the coordinate action of zinc uptake (dark green calipers) and efflux (light green calipers) transcriptional regulators that control the expression of import (grey boxes) and efflux (pink boxes) genes, respectively, as a result of a  $Zn(II)$ -regulated binding (activation or inhibition, respectively) to their DNA operators (white boxes, opr). *Left panel*,  $Zn(II)$  uptake regulators have low affinity for their DNA operator sequence in the apo state in the presence of low concentrations of zinc conditions which allows for the expression of import genes.  $Zn(II)$  efflux regulators have high affinity for their DNA operator in the absence of  $Zn(II)$  and repress efflux. This response permits the cell to sustain a bioavailable concentration of  $Zn(II)$  that is adequate for cellular needs. Transferring of  $Zn(II)$  to designated proteins may involve the action of zinc chaperones, for which there is no conclusive evidence. *Right panel*, under conditions of toxic levels of zinc, the uptake regulators are metallated and attach to it for their DNA operator, thus suppressing import. In the presence of  $Zn(II)$ , efflux regulators separate from their operator sequence (Fig. 14), or become transcriptional activators, in the  $Zn(II)$ -bound state, causing the transcription of export genes. Zinc speciation in the cytoplasm is predicted to involve small molecules,  $Zn$ -requiring metalloproteins, and possibly zinc chaperones (Fig. 14). There is some proof that zinc-uptake and zinc-efflux regulation transpires at distinct zinc concentrations added to cells, with the suppression of uptake genes occurring at lower total zinc comparative to derepression/activation of export genes (Jacobsen *et al.* 2011).

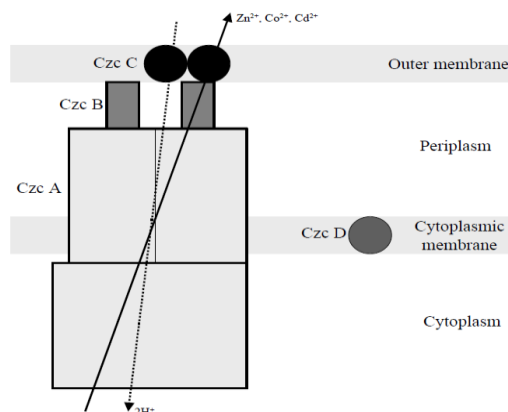


**Figure 15: Czc efflux model (Choudhury & Srivastava 2001b)**

The CzcA, is a cation diffusion facilitator (CDF) protein (Fig. 15), and it functions as a pump driven by an  $H^{+}$  gradient. The CzcB, is a membrane fusion protein, which probably acts as a link to the inner and outer membranes to facilitate the export of ions across both membranes without release in the periplasm. The CzcC is an outer membrane protein which enhances the efficiency of movement of ions across the outer membrane and the CzcD is a sensor (Choudhury & Srivastava 2001b).

### 2.7.3.8 The *czc* operon

The *czc* operon has been characterized in heavy metal resistant bacterium *Cupriavidus metallidurans* CH34. This operon encodes several resistances to cadmium, zinc and cobalt. The end product of these genes forms the above mentioned Czc efflux system (Nies 1992). The *czcA* gene encodes for the cation diffusion facilitator protein which acts as an anion/cation antiporter. The *czcB* gene encodes for the membrane fusion protein which acts as a connection to the inner and outer membranes and facilitates the transport of cations or anions without them being released into the periplasm. The *czcC* gene encodes for the outer membrane protein.

The CzcD protein present in the cytoplasmic membrane (Fig. 15) is not necessary for the cation reflux system; however the *czcD* gene together with the *czcR* gene has been postulated to play a regulatory role by controlling the gene expression of the *czc* resistance determinant (Nies 1999). In *Cupriavidus metallidurans* CH34, the expression of the operon relies on the regulation of *CzcR*, which binds to the *czcNp* promoter region, providing a regulatory path CzcS/CzcR/*czcNp* (Große *et al.* 2004).

The *czc* operon has been identified and characterized in several microorganisms. For example, in the plant-growth-promoting bacterium *Gluconacetobacter diazotrophicus* PAI 5 (Intorne *et al.* 2012) and in *Comamonas testosteroni* S44 (Xiong *et al.* 2011).

#### 2.7.4 Iron resistance

Bacteria possess a regulatory mechanism which controls their iron metabolism depending on iron availability. In *E. coli* and several other bacteria, this regulation is mediated by the ferric-uptake regulator protein (Fur) that regulates the expression of more than 90 genes in *E. coli* strains (Hantke & Braun 2000). Fur acts as a positive repressor, inhibiting the transcription of iron uptake genes upon contact with its co-repressor  $Fe^{2+}$  and inducing transcription of iron uptake genes in the absence of  $Fe^{2+}$  (Andrews *et al.* 2003)

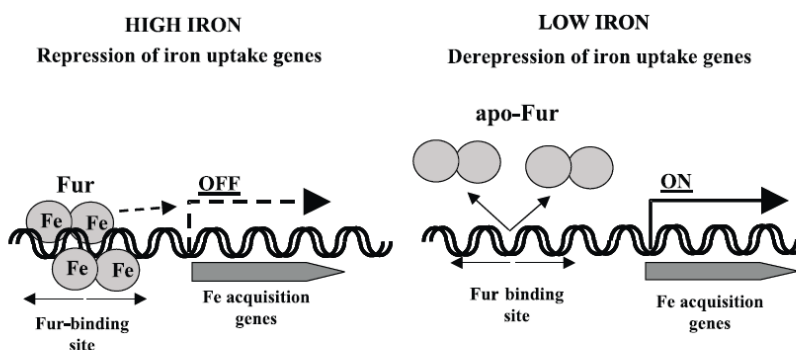


**Figure 16: Diagram illustrating Fur mediated gene repression (Andrews *et al.* 2003)**

#### 2.7.5 Copper resistance

Copper is an essential element for microorganisms. However, excess copper has proven to be toxic to microorganisms (Macomber & Imblay 2009), and this gives rise to copper resistance mechanisms. Bacterial copper resistance has been commonly found in plasmids in *E. coli* (Brown *et al.* 1992; Silver *et al.* 1993) and they have also been found in *Pseudomonas* sp. (Cooksey 1990). The copper resistance mechanisms present in *E. coli* are more or less similar to those that exist in *Pseudomonas*. There are basically four structured genes in *E. coli* known as *pcoA*, *pcoB*, *pcoC* and *pcoD* that are involved in copper resistance. While, *Pseudomonas* has the following: *copA*, *copB*, *copC* and *copD* (Silver *et al.* 1993). Moreover, the *E. coli* and *Pseudomonas* systems both have a pair of regulatory genes with an apparently membrane bound  $Cu^{2+}$  sensor which is a product of the *pcoS* and *copS* gene and these work together with the *pcoR* and *copR* gene which are DNA binding repressor proteins (Brown *et al.* 1992; Silver *et al.* 1993). The complete *pcoABCDRSE* operon was identified in *Enterobacter* sp. isolated from oil and petrol contaminated

sites (Badar *et al.* 2014). PcoA is a multicopper oxidase which is able to oxidise PcoC-bound copper (I) to its less toxic form copper (II) (Huffman *et al.* 2002; Djoko *et al.* 2008).

#### **2.7.6 Nickel resistance**

Nickel is toxic in excess amounts (Kasprzak *et al.* 2003). For most microorganisms nickel is a non-essential element and therefore microorganisms have developed mechanisms for nickel resistance. Several cell exporters have been studied and have been shown to pump nickel out of the cytoplasm and cause nickel resistance in microorganisms (Nies 2003). An example of a putative exporter is NreB from *Achromobacter xylosoxidans* 31A, which is induced by nickel and confers nickel resistance (Grass *et al.* 2001); CznABC is a cadmium, zinc, and nickel efflux pump (Stähler *et al.* 2006) ; RcnAB is a nickel and cobalt efflux system whose transcription is controlled by the metalloregulator RcnR; RcnB is a periplasmic protein that does not bind metals (Rodrigue *et al.* 2005); MrdH is a nickel, cadmium, and zinc efflux pump (Haritha *et al.* 2009); NrsD is a nickel efflux pump (Garcia-Domínguez *et al.* 2000) and NcrAC are membrane proteins that form a nickel efflux pump as well (Tian *et al.* 2007)

### **2.8 Plasmid curing**

The presence of plasmids in bacteria can have a major impact on their metabolism. For example, heavy metal and antibiotic resistance genes are normally encoded on the plasmids and confer resistance to particular microorganisms (Chattopadhyay & Grossart 2011). However, these genes could easily be removed by heterocyclic compounds that bind to the plasmid DNA during a process called plasmid curing. Therefore, plasmid curing can be defined as loss of plasmid from a bacterial cell which can lead to loss of a specific phenotype such as antibiotic resistance (Bouanchaud *et al.* 1969). These compounds can easily reverse the antibiotics and heavy metal resistance of some bacterial strains by eliminating the plasmids. Bacterial elimination of plasmids can be carried out on strains grown as pure cultures or mixed cultures in the presence of sub-inhibitory concentrations of non-mutagenic heterocyclic compounds. The anti-plasmid action of the substances' depends on the chemical structures of amphiphilic compounds that consist of a planar ring system with a substitution in the L-molecular region. A symmetrical  $\pi$ -electron conjugation at the highest occupied molecular orbitals greatly favours the antiplasmid effect (Spengler *et al.* 2006). There are several substances and methods that can be implemented to cure plasmids from bacteria. These include exposure of bacterial cultures to high temperatures, chemical agents such as intercalating dyes (acridine orange, ethidium bromide), treatment with sodium dodecyl sulfate (SDS), crystal violet and exposure to UV radiation (Clowers 1972). When studying the plasmid profiles of bacteria, it is often desirable to obtain a plasmid cured derivative

so as to compare its profiles. Some of the plasmids undergo spontaneous segregation and deletion, but the majority of the plasmids are fairly stable and require the use of curing agents to increase the frequency of spontaneous segregation. The application of agents is mainly carried out on a trial and error basis because different bacterial strains react differently to different curing agents, and there are no standard protocols for plasmid curing that is applicable to all strains (Trevors 1985). The DNA intercalating curing products such as ethidium bromide and acridine orange are the most commonly used curing agents because they have been found to be effective for a number of plasmids in a variety of bacterial genera (Grinsted & Bennet 1988). Zaman *et al.* (2010) carried out studies to investigate the effects of different curing agents on several drug resistant *E.coli* strains. Different concentrations of ethidium bromide, acridine orange and sodium dodecyl sulphate (SDS) were used, and curing was successful in the presence of ethidium bromide and SDS. However, acridine orange proved to be an unsuccessful curing agent. Raja & Selvam (2009) also managed to carry out plasmid curing studies on the strain *P. aeruginosa* which was isolated from a heavy metal polluted site. The curing was carried out using ethidium bromide, acridine orange, novobiocin, SDS and exposure to elevated temperatures (40°C). The sole purpose of the study was to determine whether the heavy metal resistance gene of *P. aeruginosa* strain was present on the plasmid or chromosome. The transformation and curing results confirmed the presence of the ampicillin gene on the plasmid, and the cadmium, lead and chromium resistant genes on chromosomal DNA as the cured and uncured cultures remained similar in heavy metal resistance characteristics.

It has been suggested by Waring (1966), that ethidium bromide interferes with plasmid replication as shown below (Fig. 17), and this is how plasmidless derivatives are produced.

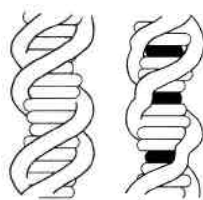


**Figure 17: Intercalation of the anti-plasmid compound into the plasmid DNA (Waring 1966)**

## **2.9 Protein homology modeling**

Computational tools have been used to aid in the elucidation of physico-chemical and structural properties of translated proteins. When experimentally determined structures have not been elucidated, computational methods can be used to accurately predict protein structures from the sequence (Zhang 2008). Protein structure is crucial in understanding protein function. Therefore

computational methods have been used to accurately predict the secondary structure from the primary sequences of full length native-proteins. Nonetheless, structural prediction methods have been shown to accurately predict the partial structures of proteins encoded by sequences that contain approximately 50% or more of the full length sequence. Structural prediction methods might be useful for the prediction of proteins whose corresponding genes are mapped as expressed sequence tags (ESTs) that encode partial-length amino acid sequences (Laurenzi *et al.* 2013). Functional proteins basically have a relatively stable structure. Given an arbitrary protein sequence, it would be informative to accurately predict the probability that the partial protein sequence represents a foldable protein. This information would be valuable in genome annotation by supporting or rejecting hypothetical proteins stemming from unfamiliar regions of DNA (Laurenzi *et al.* 2013). Having an accurately predicted structure of an uncharacterized partial protein sequence is likely to provide information about function that a sequence alone cannot provide (Jones & Thornton 2004; Watson *et al.* 2007).

Homology modeling makes structure predictions based primarily on the sequence similarity of the query to one or more known structures. Comparative modeling comprises of the following steps (Jatav *et al.* 2014).

- a) Identifying evolutionary sequences of an already known structure. This is normally carried out using the Basic Local Alignment Tool-Protein (BLAST-P).
- b) Online protein modeling tools such as SWISS-MODEL and I-TASSER, will then align the query sequence to template structures.
- c) The protein structures are then constructed using conserved regions of known templates.
- d) Then the side chains and loops are modeled which are different to the templates.

### 3 RESEARCH DESIGN AND METHODOLOGY

#### 3.1 Research design

Field studies, laboratory and computational analysis were carried out in this study (Fig 18).

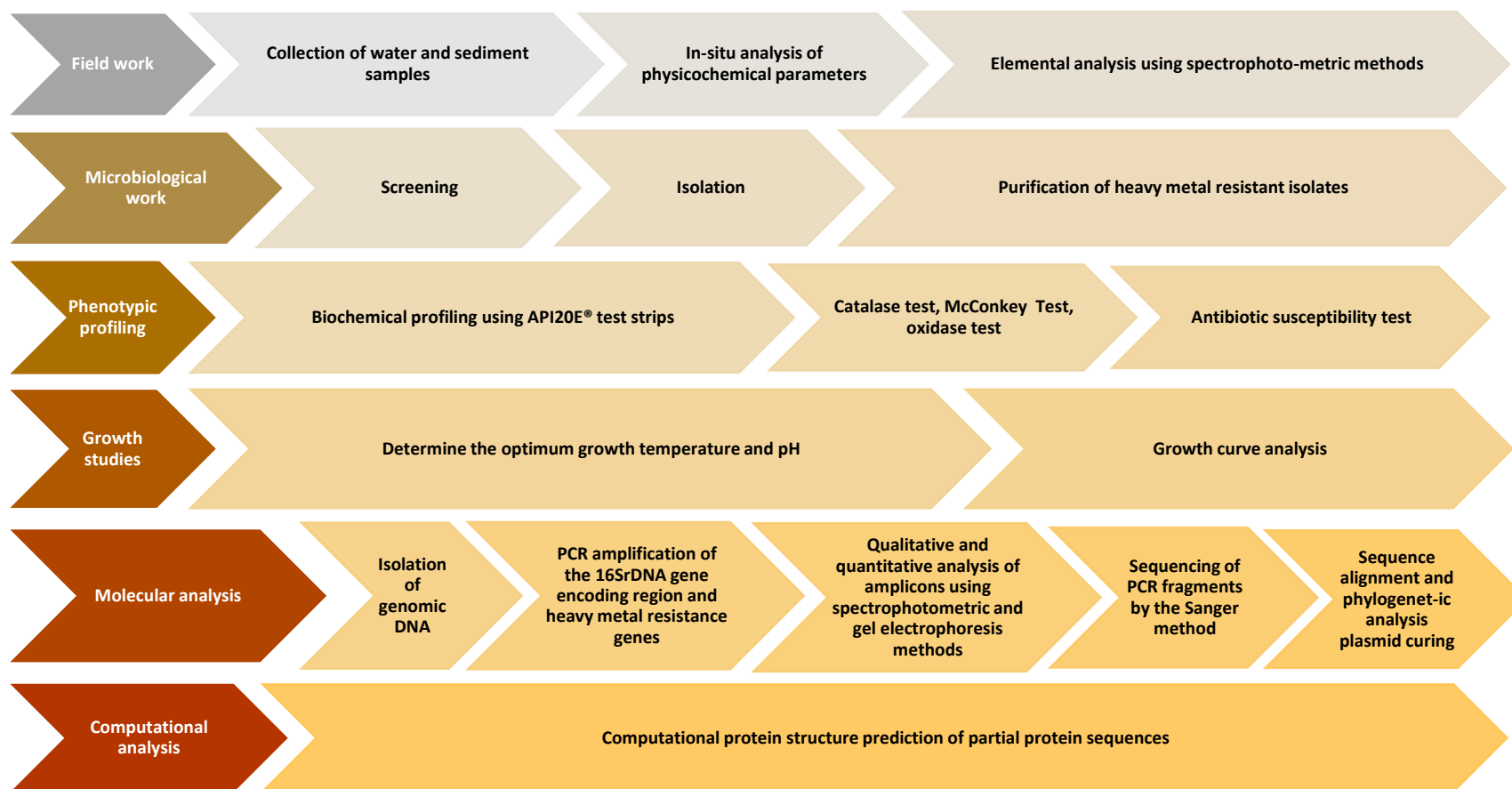


Figure 18: Research Design used in this study.



Water and sediment samples were collected along the course of the Klip River at designated sites. Heavy metal bacterial isolates were isolated and identified in the laboratory. The heavy metal resistant isolates were identified and characterized using biochemical, physiological and molecular methods. Genomic DNA of the isolates was isolated and amplified using primers for the 16SrDNA and the resulting DNA amplicons were sequenced. Sequences were matched with previously published bacterial 16SrDNA sequences in the NCBI databases using ADVANCED BLAST. The genes responsible for heavy metal resistance were amplified and analyzed using primers for the *pcoA*, *pcoR* genes (copper resistance genes), *czc* genes (zinc, cobalt and cadmium resistance genes), *cadA*, *cadC* (cadmium resistance genes), *pbrA*, *pbrB*, *pbrC* and *pbrD* (lead resistance genes) and *chrB* (chromate resistance genes). The plasmids were isolated and the molecular weights estimated. Plasmid curing was done to determine whether the heavy metal resistance genes are encoded on the plasmids or chromosome of the bacteria. The amplified fragments were translated and the resulting amino acid sequences were used to generate a phylogenetic tree. Finally, the physico-chemical properties as well as the 3D- structure of the proteins were predicted using computational methods.

### **3.2 Materials**

#### **3.2.1 Field data sheets**

All the data collected from the field work was recorded on field data sheets (APPENDIX I)

#### **3.2.2 Kits, reagents, and chemicals**

A variety of commercially available kits and reagents were used in this study, for a variety of applications. These are outlined in APPENDIX I.

#### **3.2.3 Buffers and stock solutions**

Analytical grade reagents were used for all buffers and solutions. Preparation of these solutions is outlined in APPENDIX III.

#### **3.2.4 Microbiological Media and Components**

The media used in this study are highlighted in APPENDIX IV.

#### **3.2.5 Sterilization of microbiological media, reagents, glassware, consumables and heavy metal stocks**

All items were sterilized by autoclaving at 121°C at 15psi for a minimum of 15 minutes.

#### **3.2.6 Pre-conditioning of plastic bottles**

The 1 litre plastic bottles used for collection of water samples required for heavy metal analysis were pre-conditioned before use. The procedure is outlined in APPENDIX V.

## Site Description

### 3.2.7 Samples and sampling sites

Water and sediment samples were obtained from the Klip River, South of Johannesburg.

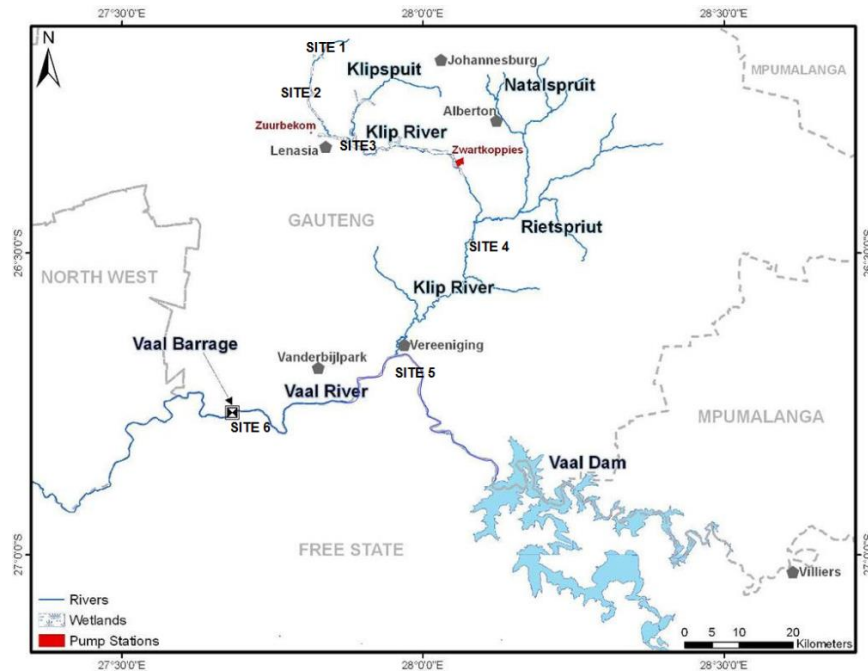


**Figure 19: Map showing sampling sites along the Klip River (Map adapted from Vermaak 2009)**

Samples were obtained from 6 different sites (Fig. 20-25) (Table 4) along the course of the Klip River. The sixth site was the Vaal Barrage that was used as a reference site for this study.



**Figure 20: Site 1- Located in Roodekrans, close to the source of the Klip River**



**Figure 21: Site 2- Klip River before it enters Lenasia Residential Area**



**Figure 22: Site 3-Located in Lenasia: this site is characterized by the presence of several informal settlements close to the Klip River**

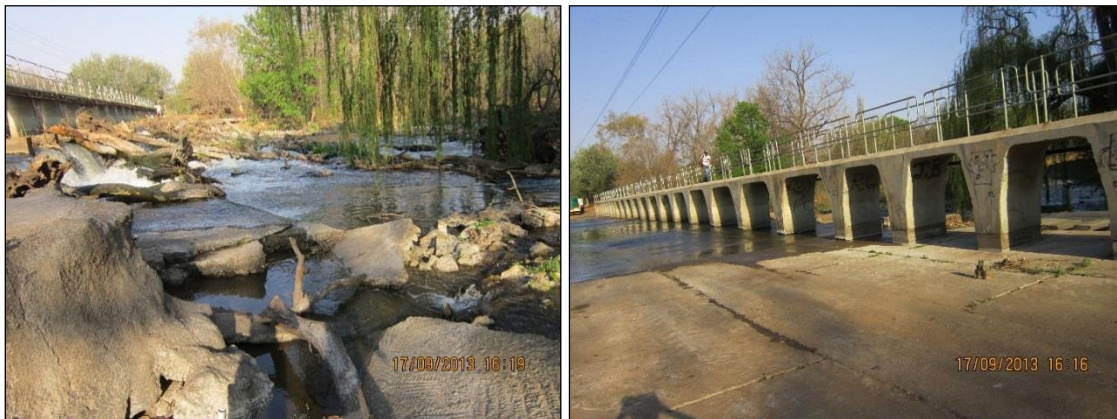


**Figure 23: Site 4- Henley on Klip Weir: this site is mainly a recreational area**





**Figure 24: Site 5- Klip River just upstream before the confluence of the Vaal River**



**Figure 25: Site 6- Vaal Barrage (Reference Site)**

**Table 4: Geographical coordinates of sampling sites**

Site no. and location	Geographical coordinates	
	Latitude N	Longitude E
1. (Source-Roodekraans)	26°08.428′	27°49.280′
2. Before Lenasia	26°10.558′	27°49.037′
3. (Lenasia)	26°17.668′	27°05.650′
4. (Henley on Klip Weir)	26°32.428′	27°03.8445′
5. (Confluence of the Klip and Vaal River)	26°39.879′	27°56.303′
6. (Vaal Barrage)	26°46.068′	27°40.498′

### 3.3 Sample Collection

Water and sediment samples were collected on the 17-18<sup>th</sup> September 2013 from 5 sites along the Klip River with site 6 (Vaal Barrage) selected as the reference. The Dissolved Oxygen (DO), temperature, conductivity, salinity and turbidity were measured in-situ by a multiparameter meter (HANNA Instrument Model 9828, Ann Arbor, MI). The pH was measured using an *in-situ* pH meter (HANNA Instrument Model 9025). All the data was recorded on field data sheets (APPENDIX I).

Sediment cores were obtained from depths of 10 cm by using a sediment corer. The corer consisted of a PVC pipe 4.8 cm in diameter and was graduated to collect a sediment sample of up to 10 cm in depth. The corer consisted of a removable cap on one end. The PVC pipe was pressed into the sediment to a depth of 10 cm and the cap was placed underneath the pipe. The sediment samples were transferred to a pre-sterilized wide mouth glass jar and kept on ice till they were transported to the lab for analysis.

Water samples for elemental analysis were collected using the grab method at depths of 20-30 cm from the river surface directly into pre-conditioned polyethylene bottles (APPENDIX V). The water samples were acidified with 1% nitric acid solution to keep the metal ions in a dissolved state. The water samples for bacteriological analysis were collected in autoclaved glass bottles.

### 3.4 Heavy Metal Analysis of water samples

Atomic Absorption Spectrophotometry was used to determine the amount of heavy metals in solution of the Klip River samples. Atomic Absorption Spectrophotometry is a highly sensitive method used to analyse and detect several trace elements. The main concept of AAS is measuring the radiation emitted by excited atoms after they return to the ground state. All the water samples were aspirated for a minimum time of 5 s before taking a reading (Pires 2010). When the measurement showed a high coefficient of variation, the system was re-calibrated. The following heavy metals (Cd, Cu, Zn, Cr, Fe and Ni) were quantified using flame atomic absorption spectrophotometer (Shimadzu-AA700, Kyoto Japan). The metals' standards were prepared from stock solutions of 1000 mg/l by successive dilutions (see APPENDIX III) the measurements were performed in triplicates (APPENDIX VII).

### 3.5 Preparation of heavy metal supplemented media

To isolate heavy metal resistant bacteria, Luria Bertani (LB) agar was supplemented with 5 mg/l of the following heavy metals; Cd, Cu, Cr, Fe, Ni, Pb and Zn. The stock solutions were prepared from  $CdCl_2$ ,  $CuSO_4 \cdot 5H_2O$ ,  $PbCl_2$ ,  $ZnCl_2$ ,  $FeSO_4 \cdot 7H_2O$ ,  $NiCl_2 \cdot 6H_2O$  and  $K_2Cr_2O_7$ . Stock solutions were autoclaved 121°C for 15 minutes. The metal stock solutions contained 5000 mg/l of Cd, Cu,

Cr, Fe, Ni, Pb and Zn, respectively (APPENDIX III). Appropriate volumes of the metal solutions were mixed with the media after being autoclaved.

### **3.6 Enumeration and Isolation of bacteria**

Water and core samples (0.1 ml) were plated and enumerated on LB agar plates supplemented with 5 mg/l concentration of the following metals: chromium, zinc, copper, cadmium, lead, iron and nickel, respectively, by the standard pour plate method (Raja *et al.* 2009). Plates were incubated at 30°C for 72 hr and colonies were selected based on their morphological differences. The colonies were further purified by the streak method on heavy metal constituted LB agar. Each bacterial culture was inoculated in nutrient broth, incubated overnight and glycerol stocks were prepared and frozen at -80°C (Maniatis *et al.* 1982).

### **3.7 Study of colonial morphology**

Purified strains were grown on solidified LB agar plates and colonial morphology data was recorded according to the following characteristics (chromogenesis, size, shape, margin, elevation, opacity and surface (Pelczar & Reid 1958).

### **3.8 Study of cellular morphology**

The Gram staining method was used to observe the staining reaction of the isolated strains. The Hucker protocol as described by Duguid (1989) was used. Pure colonies were fixed to a glass slide using the heat fixation method. Slides were then covered by crystal violet (Merck, Darmstadt, Germany) for one minute and gently rinsed with water. Gram iodine (Merck, Darmstadt, Germany) was then applied for one minute and again rinsed with water. Slides were then washed with acetone and rinsed with water. They were then covered by safranin (Merck, Darmstadt, Germany) for one minute and excess safranin was rinsed with distilled water. The slides were then observed under the light microscope (oil immersion, 100X). The shape, arrangement and Gram reaction was observed.

### **3.9 Determination of Minimum Inhibitory Concentration (MIC)**

Stock solutions (1 M) of  $CdCl_2$ ,  $PbCl_2$ ,  $ZnCl_2$ ,  $FeSO_4 \cdot 7H_2O$ ,  $NiCl_2 \cdot 6H_2O$  and  $K_2Cr_2O_7$  were prepared with deionized water and sterilized by autoclaving at 121°C for 15 minutes. The MIC of the selected isolates were determined against increasing concentrations of Cd, Cr, Cu, Fe, Ni, Pb and Zn on LB agar plates until no growth was observed. Starting with an initial concentration of 0.2 mM, further MIC tests were carried out with concentrations of 0.4 mM, 0.6 mM, 0.8 mM, 1 mM, 1.2 mM, 1.5 mM, 2 mM, 3mM and 4 mM. Cultures that showed growth at a particular

concentration were transferred to the next higher concentration. The MIC tests were determined at 30°C for 10 days (Raja *et al.* 2009).

### **3.10 Determination of antibiotic resistance**

Overnight cultures of 16 out of 48 bacterial isolates that exhibited high MICs were tested for antibiotic sensitivity towards nine different antibiotics (Bauer *et al.* 1966). Antibiotics used in this study included: Ampicillin (10 µg/ml), Amoxicillin (10 µg/ml), Cephalothin acid (30 µg/ml), Cotrimoxazole (25 µg/ml), Neomycin (30 µg/ml), Streptomycin (10 µg/ml), Tetracycline (30 µg/ml), Tobramycin (10 µg/ml) and Vancomycin (30 µg/ml).

For each antibiotic, 100 µl of a culture was transferred to a Muller-Hinton agar plate and spread evenly with a sterile swab. After 10-15 minutes the different antibiotic discs were placed on the medium then incubated at 37°C at pH 7 for 24 hours. Zones of inhibition, where applicable, were measured in millimeters (mm). Strains were considered to be susceptible when the inhibition zone was 12 mm or more in diameter (Raja *et al.* 2009). All antibiotic tests were performed in triplicate.

### **3.11 Biochemical characterization**

Biochemical phenotype profiles for the selected heavy metal resistant isolates were generated by using the API 20E® test strips and the isolates were tested for the presence of the following enzymes: beta-galactosidase, arginine dihydrolase, lysine decarboxylase, ornithine decarboxylase, deaminase and gelatinase. Additional biochemical tests included citrate utilization, urea hydrolysis, indole production and acetoin production. API 20E® test strips also included fermentation or oxidation tests for the following carbohydrates: glucose, mannitol, inositol, sorbitol, rhamnose, sucrose, melibiose, amygdalin, arabinose and nitrate reduction. Tests were performed according to the manufacturers' instructions (Biomerieux™, Marcy l'Etoile, France). Additional tests such as the catalase, oxidase tests and growth on MacConkey agar were also carried out. The number and types of positive tests were recorded and the results compared amongst isolates. A similarity dendrogram among the phenotypic profiles was created using NTSYSpc (Exeter Software, Setauket, NY). For the construction of the similarity dendrogram an input matrix was constructed with 20 API 20E® tests, the catalase and the McConkey tests. A total of 22 tests were used. If a bacterial isolate tested positive for a particular test, the matrix input was recorded as '1', and if the isolate tested negative the matrix input was recorded as '0'. Each isolate's profile was compared to other profiles and a Coefficient of Similarity on a scale of 0.00-1.00 with 1.00 being equal to 100% being reported (Phillips *et al.* 2012).

### **3.12 Catalase test**

Catalase was determined as described by Smibert and Krieg (1981). A drop of Hydrogen peroxide 3 % (v/v) was placed on a slide and bacterial cells were added. The presence of catalase was detected by the formation of oxygen bubbles.

### **3.13 Oxidase test**

A well grown colony was picked from the culture medium and applied to the reaction zone of a cytochrome oxidase test strip (Merck, Darmstadt, Germany). After 60 seconds the colour changes were compared with the colour scale provided by the manufacturer (Bactident® Oxydase, Merck, Darmstadt, Germany).

#### **3.13.1 Determination of optimal growth conditions**

The optimum pH and temperature conditions for growth of each of the 16 isolates were determined. For pH, three milliliters of LB broth was dispensed into different test tubes and the pH adjusted from 5 to 10 by using either 1M HCl or 1M NaOH. A 100 µl of overnight culture of each isolate was dispensed into the test tubes and incubated at 37°C for 24 hours. The tests were carried out in triplicate. The optical density (OD) of each culture was obtained at 600 nm with a UV spectrophotometer (Nanocolour UV/VIS Spectrophotometer Mahery-Nagel, Düren, Germany) (Giri 2011).

The optimal growth temperature was assessed as follows: three milliliters of LB broth was placed in different test tubes. A 100 µl of overnight culture of the pure culture of each isolate was dispensed into each of the test tubes. The tubes were incubated at four different temperatures i.e. 25°C, 30°C, 37°C and 40°C for 24 hours, respectively. The OD was measured at 600 nm using a UV/VIS Spectrophotometer (Nanocolour UV/VIS Spectrophotometer Mahery-Nagel) (Giri, 2011).

### **3.14 Growth studies**

Growth studies of the bacterial isolates was carried out in 250 ml flasks containing 50 ml LB medium supplemented with 0.2 mM concentration of  $CdCl_2$ ,  $PbCl_2$ ,  $ZnCl_2$ ,  $FeSO_4 \cdot 7H_2O$ ,  $NiCl_2 \cdot 6H_2O$  and  $K_2Cr_2O_7$ . Flasks were inoculated with 0.5 ml of overnight culture and incubated on a rotatory shaker (150 rev/min) at 30°C. The optical density was measured every four hours using a UV-spectrophotometer at 600 nm (Nanocolour UV/VIS Spectrophotometer Mahery-Nagel) (Raja *et al.* 2009).



The specific growth rate of the isolates was obtained by using the following formula:

$$\mu h^{-1} = \frac{\ln OD_t - \ln OD_0}{T_t - T_0}$$

### Equation 1 Specific growth rate

where  $\mu h^{-1}$  denotes specific growth rate of the initial bacterial concentration over a given period of time

$OD_t$  represents the optical density (600nm) of the cultures at time  $t$  and,

$OD_0$  represents the optical density (600nm) of the cultures at time  $0$  (Giri 2011).

## 3.15 MOLECULAR TECHNIQUES

### 3.16 DNA extraction

DNA was extracted from the bacterial isolates by using the ZR Fungal/Bacterial DNA Extraction Kit (ZYMO RESEARCH, Irvine, CA) according to the manufacturer's protocol. This method combines physical, chemical and silica gel column procedures. To determine the quality and quantification, both UV and electrophoresis techniques were used. Two millilitres of an overnight culture was centrifuged at 7000 x g for 2 minutes and the bacterial cells were resuspended in 200  $\mu$ l of water and transferred to a ZR BashingBead™ Lysis tube. Then, 750  $\mu$ l of Lysis solution was added to the tube. The tube was then vortexed at a maximum speed for 5 minutes. The ZR BashingBead™ Lysis tube was then centrifuged in a microcentrifuge at 10 000 xg for 1 minute. Then, up to 400  $\mu$ l of supernatant was transferred to a Zymo-Spin™IV Spin Filter (the base was snapped off before placing it in a collection tube). The Zymo-Spin™IV Spin Filter was then centrifuged at 7 000 x g for 1 minute. Next, 1200  $\mu$ l of Fungal/Bacterial DNA Binding Buffer was added to the filtrate in the Collection Tube and 800  $\mu$ l of the mixture was then transferred to Zymo-Spin™ IIC Column in a new collection tube and centrifuged at 10 000 x g for 1 minute. Subsequently 500  $\mu$ l of Fungal/Bacterial DNA Wash Buffer was added to the Zymo-Spin™ IIC Column and centrifuged at 10 000 x g for 1 minute. The Zymo-Spin™ IIC was transferred to a clean 1.5 ml microcentrifuge tube and 100  $\mu$ l of DNA Elution Buffer was added directly to the column matrix and centrifuged at 10 000 x g for 30 seconds to elute the DNA. The DNA was stored at -20 °C.

For UV procedures, 2  $\mu$ l of DNA samples were measured at absorbance of 260 and 280 nm using Nanodrop Spectrophotometer (Thermofischer Scientific, Waltham, MA). Moreover, the DNA concentration was calculated using standard  $1A_{260} = 50 \mu\text{g/ml}$  (Zhou *et al.* 1996). To confirm

successful DNA extraction the DNA samples were electrophoresed on a 1.0% (w/v) agarose gel stained with ethidium bromide.

### **3.17 Polymerase Chain Reaction (PCR)**

#### **3.17.1 16SrDNA Amplification**

The 16SrDNA fragments were amplified using the universal primer combination 27F (5'- AGA GTT TGA TCC TGG CTC AG-3') and 1,429R (5'-GGT TAC CTT GTT ACG ACT T-3') (Raja *et al.* 2009). The primers were synthesized by Inqaba Biotechnologies Industry, Pretoria, South Africa. Amplification was performed in a 50 µl reaction mixture containing 2x PCR Mastermix (Emerald Amp R MAX HS Master Mix, Otsu, Shiga Japan), 22 µl of PCR quality water, 1 µl of each forward and reverse primer (0.2 µM) and 1 µl DNA template. PCR was performed in a T100 Bio-Rad Thermocycler (Bio-Rad, Hercules, CA). Thermal cycling conditions were as follows: initial denaturation at 94°C for 5 minutes followed by 35 cycles consisting of denaturation 94°C for 1 minute, annealing at 55°C for 1 minute, extension at 72°C for 1 minute and a final extension at 72°C for 5 minutes. The amplicons were analysed in a Bio-Rad electrophoresis system for 1 hour at 90 V in 1xTBE buffer. The images of the gels were captured in a Bio-Rad Gel Doc™ EZ Imager (Bio-Rad, CA) using ImageLab™ Software version 5.0. Each gel contained 5 µl of KAPA Universal Ladder (KAPA Biosystems, Boston, MA) in the first well.

#### **3.17.2 Amplification of Heavy Metal resistant genes**

The following heavy metal resistance genes were amplified from the isolates; *pcoA*, *pcoR* (copper resistance), *czcA*, *czcB*, *czcD* (cadmium, zinc, cobalt resistance), *cadCA* (cadmium resistance) and *pbr* (Lead resistance). The genes were amplified using specific primers (Table 5). The PCR amplification of the target DNA was carried out in a T100 Biorad Thermocycler and all reaction mixtures were set up as in section 3.17.1. The following parameters were used to amplify the *pbr* and *cad* genes. Denaturation of DNA template at 95°C for 5 minutes, followed by 35 cycles of denaturation at 94°C for 90 seconds, annealing of template DNA for 1 minute at 57°C and an extension time of 3 minutes at 70°C for the primers. After the last cycle, a final extension was carried out at 70°C for 7 minutes to complete the synthesis of all strands after which the reaction was cooled to 4°C (Davis 2011).

To amplify the *pcoA*, *pcoR*, *czcA*, *czcB*, *czcD* and *chrB* genes the following PCR protocol was used: The reaction mixtures were set up as in Section 3.17.1. PCRs were run in T100 Biorad Thermocycler using the following parameters: Initial denaturation step at 95°C for 5 minutes, followed by 35 cycles of 94°C for 90 seconds (denaturation), 57°C for 90 seconds (annealing).

72°C for 2 minutes (elongation), followed by a final extension step of 72°C for 7 minutes. A cooling temperature of 4°C was applied (Nies *et al.* 1990).

**Table 5: Primers used to amplify heavy metal resistance gene in bacterial isolates**

Resistance determinant amplified	Sequence 5´–3´	Orientation	The corresponding target Microbes with heavy metal resis. Gene(s)	Exact length of amplified region (bp)	References
<i>Chromium reistance</i>					
<i>chrB</i>	GTCGTTAGCTTGCCAACATC	Forward	<i>A. eutrophus</i>	450	<b>Nies et al. 1990</b>
	CGGAAAGCAAGATGTCGATCG	Reverse	CH34		
<i>Zinc resistance</i>					
<i>czcA</i> gene of <i>czc</i> determinant of <i>A. eutrophus</i>	GTTTGAACGTATCATTAGTTTC	Forward	<i>A. eutrophus</i>	<b>1885</b>	<b>Nies et al. 1990</b>
	GTAGCCATCCGAAATATTCG	Reverse	CH34		
<i>czcB</i> gene of above	CTATTTCGAACAAACAAAAGG	Forward	<i>A. eutrophus</i>	<b>1520</b>	<b>Nies et al. 1990</b>
	CTTCAGAACAAAAGTGTGG	Reverse	CH34		
<i>czcD</i>	TTTAGATCTTTTACCACCATGGGCGCAGGT CACTCACACGACC	Forward	<i>A. eutrophus</i>  CH34	<b>1000</b>	<b>Nies et al. 1990</b>
	TTTCAGCTGAACATCATACCCTAGTTTCCT CTGCAGCAAGCGACTTC	Reverse			
<i>Cadmium resistance</i>					
Cad 1	GAATGAAGATGGGATGATAA	Forward	<i>S. aureus</i> gene encoded on the p1258 plasmid (P125CADA)	<b>625</b>	<b>Genbank ref:</b>  PI25CADA <b>Davis (2011)</b>
Cad 2	GATTGCTAGTTTTTTCAGGA	Reverse			
Cad 3	CAGCAACCAAGGCTACAA	Forward	<i>S. aureus</i> gene encoded on the p1258 plasmid (P125CADA)	<b>1049</b>	<b>Genbank ref:</b>  PI25CADA <b>Davis (2011)</b>
Cad 4	GCCCTAGCACATAAGAAAG	Reverse			

Cad 5	CGAAGTATTTGCAGGTACG	Forward	<i>S. aureus</i> gene encoded on the p1258 plasmid (P125CADA)	1289	Genbank ref:  PI25CADA Belinda (2011)
Cad 6	CCCATATCGGAAAGAATCG	Reverse			
Copper reistance					
<i>pcoR</i> gene of the <i>pco</i> operon	CAGGTCGTTACCTGCAGCAG CTCTGATCTCCAGGACATATC	Forward Reverse	<i>E.coli</i> ED8739 Plasmid- pPA87	636	Brown <i>et al.</i> 1992
<i>pcoA</i> gene of the <i>pco</i> operon	CGTCTCGACGAACTTTCCTG GGACTTCACGAAACATTCCC	Forward Reverse	<i>E.coli</i> ED8739 Plasmid- pPA87	1791	Brown <i>et al.</i> 1992
Lead resistance					
Pbr 8	ATCGGGGAGGCGCCAGAAT CGCCAGTCGCGAGATGA	Forward	<i>C.metallidurans</i> CH34	699	Genbank ref:  X71400 Davis (2011)
Pbr 9		Reverse			
Pbr 10	AGGACAGCTTCGCCTTCA CCTTGTTAGCCAGACCT	Forward	<i>C.metallidurans</i> CH34	740	Genbank ref:  X71400 Davis (2011)
Pbr 11		Reverse			
Pbr 12	TGAGGTACGCGGTCAGTT CTGCGTCTCCTTTTCGATT	Forward	<i>C.metallidurans</i> CH34	807	Genbank ref:  X71400 Davis (2011)
Pbr 13		Reverse			
Pbr 14	TTGTCTTGCGTGGCGAGA TGCCCGGTGGTGACCAT	Forward	<i>C.metallidurans</i> CH34	593	Genbank ref:  X71400 Davis (2011)
Pbr 15		Reverse			
Pbr 16	CAACAGCCCTTCTTGTTT GAGCCAGTACACGACCT	Forward	<i>C.metallidurans</i> CH34	766	Genbank ref:  X71400 Davis (2011)
Pbr 17		Reverse			
Pbr 18	AGTTCAATCTGGTGCAGC GATCCGCGCCAATGTTGA	Forward	<i>C.metallidurans</i>  CH34	769	Genbank ref:  X71400 Davis (2011)
Pbr 19		Reverse			

Primers manufactured by Inqaba Biotechnologies, Pretoria, South Africa

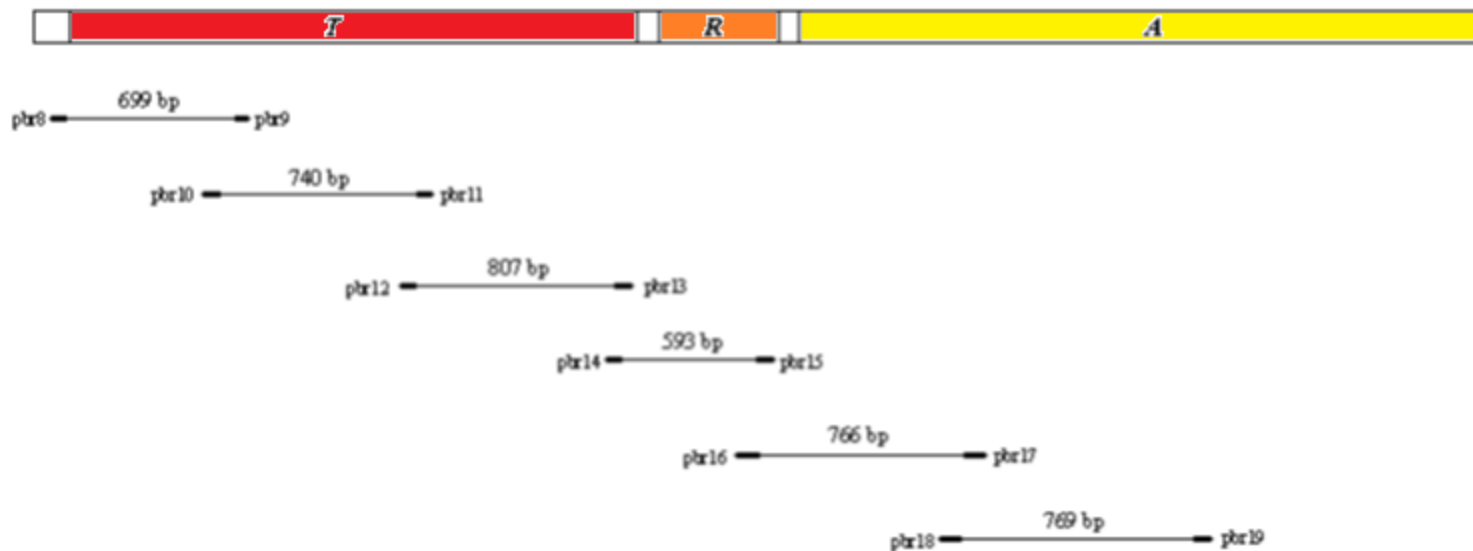


Figure 26: Location of primers designed to amplify the genes of the *pbr* operon. This figure indicates the location of and expected size of amplified products for each primer pair. These primers were designed based on the *pbr* operon of *C. metallidurans* CH34 (X71400) (Davis 2011)

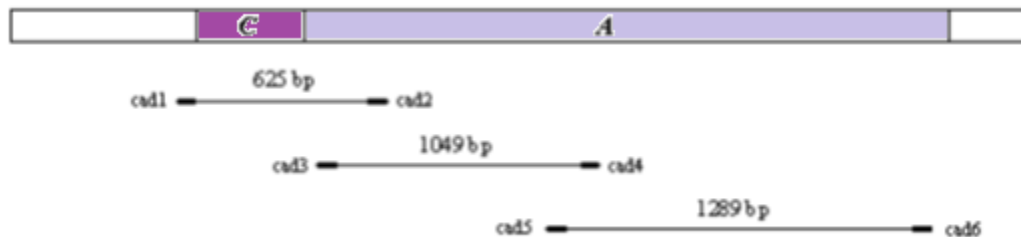


Figure 27: Location of primers designed to amplify the *cad* operon. This figure indicates the location of and expected size of amplified products for each primer pair. These primers were designed based on the *cadCA* genes of pI258 (PI25CADA) (Davis 2011)

### **3.18 Gel Electrophoresis**

Electrophoresis was carried out in a Biorad Electrophoresis System for 1 hour at 90V, using 1xTBE buffer. A Gel Doc™ EZ Imager was used to capture the image using ImageLab™ Software version 5.0. Each gel contained 5µl of KAPA Universal Ladder (KAPA Biosystems) in the first well. The image was analyzed using the ImageLab™ Software to determine the size of the bands produced in each lane.

### **3.19 PCR product purification and sequencing of 16SrDNA and heavy metal resistance genes**

The obtained PCR amplicons were purified using the GeneJET™ PCR Purification Kit (Fermentas, Hanover, Germany) according to the manufacturer's protocol. The binding buffer was added at a 1:1 volume to PCR mixtures and colour changes were noted. Since a 50 µl PCR volume was used, 50 µl of binding buffer was added to each reaction. A slight yellow colour change indicated that pH was optimum for DNA binding; however, if the colour of the solution changed to orange or violet, 10 µl of 3M sodium acetate, pH 5.2 was added to the mix.

Thereafter, 100 µl of the binding buffer and PCR products were added to the GeneJET™ purification column, centrifuged for 60 seconds and the flow-through was discarded. Then 700 µl of Wash Buffer was added to the GeneJET™ purification column, and centrifuged for 60 seconds and the flow-through discarded. The purification column was placed back into the collection tube and centrifuged again for an additional 1 minute to eliminate any residual Wash Buffer. The GeneJET™ purification column was then transferred to a clean 1.5 ml microcentrifuge tube and 50 µl of Elution Buffer was added to the center of the GeneJET™ purification column membrane and finally centrifuged for 1 minute. The GeneJET™ purification column was discarded and the purified DNA was stored at -20°C. The DNA was sent for sequencing at Inqaba Biotechnologies Industry. The 16SrDNA sequences were aligned and compared with other 16SrDNA genes in the Genbank (Benson & Karsch-Mizrachi 2000) by using the NCBI Basic Local Alignment Search Tools, BLAST*n* program (Altschul *et al.* 1997). Based on the scoring index, the most similar sequences were aligned with other bacterial 16SrDNA regions using MAFFT Multiple Sequence Alignment Software Version (Kato & Standley 2013). Phylogenetic analysis and similarity index was generated using the programme MEGA 6 (Tamura *et al.* 2013) and compared with other known species.

### **3.20 Isolation of plasmid DNA**

Plasmid DNA was isolated from the isolates, according to the Alkaline Lysis method (Birnboim & Doly1979). A single isolated colony was picked from a heavy metal constituted plate and inoculated in LB broth. The culture was grown overnight at 37°C with shaking. The overnight

cultures were centrifuged at 14 000 rpm for a minute in 1.5 ml eppendorf tubes. This procedure was repeated until all 5 ml of the overnight culture was centrifuged. The supernatant was discarded and the bacterial pellet was re-suspended in 200 µl of Solution I (50 mM Tris with HCl, 10 mM EDTA, 100 µg/ml of RNase A). The pellet was resuspended by pipetting up and down. Two hundred microliters of Solution II (200 mM, 1% SDS) was added and mixed by gently inverting the tube for 5-6 times, then 200 µl of Solution III (3M Potassium Acetate pH 5.5) was added and mixed by inverting the tube gently. A white precipitate was formed and the tube was further centrifuged for 10 minutes at 14 000 rpm. The supernatant was carefully transferred to a fresh tube ensuring that the white pellet was left undisturbed. Finally the DNA was precipitated by adding 900 µl of 100% ethanol to the supernatant. The solutions were mixed well by inverting the tube several times and the centrifuged at 14 000 rpm for 10 minutes. The supernatant was removed and discarded. The DNA pellet was washed by adding 100 µl of ice cold 75% ethanol and centrifuged again for 30 seconds. The supernatant was removed and discarded. The pellet was dried for 30 minutes. The pellet was then resuspended in sterile 50 µl TE buffer and was stored at -20°C.

An alternative method for plasmid isolation was also carried out using the Thermo Scientific GeneJET™ Plasmid Miniprep Kit since extraction of plasmids from the isolates proved to be difficult. A single colony was picked from a freshly streaked selective plate and inoculated in 5 ml LB medium. The medium was incubated for 12-16 hours at 37°C while shaking at 250 rpm. The bacterial culture was harvested by centrifugation at 6800 xg in a microcentrifuge for 2 minutes at room temperature. The supernatant was decanted. The pellet was resuspended in 250 µl of the resuspension solution that contains RNaseA. The cell suspension was transferred to a microcentrifuge tube and the bacteria were resuspended by pipetting up and down until no cell clumps were observed. Precisely 250 µl of the Lysis Solution was added and mixed thoroughly by gently inverting the tube 4-6 times until the solution became viscous and slightly clear. The solutions were incubated for not more than 5 minutes to avoid the denaturation of supercoiled plasmid DNA. Then, 350 µl of the neutralization solution was added and mixed thoroughly by gently inverting the tube 4-6 times. The solution was centrifuged for 5 minutes to pellet cell debris and chromosomal DNA. The supernatant was transferred to the GeneJET™ spin column by decanting. The spin columns were placed in a collection tube before transferring the supernatant. The collection tube was then centrifuged for 1 minute and the flow through discarded and the column was placed back in the collection tube. Then, 500 µl of Wash Solution was added to the GeneJET™ spin column, centrifuged for 60 seconds and the flow through was discarded and



placed back into the same collection tube. The wash step was repeated using 500 µl of the Wash Solution, the flowthrough was discarded and the column centrifuged for an additional 1 minute to remove residual Wash Solution. The GeneJET™ column was transferred to a fresh 1.5 ml microcentrifuge tube and 50 µl of Elution buffer was added to the centre of the GeneJET™ spin column membrane to elute the plasmid DNA. The columns were incubated at room temperature for 2 minutes and then centrifuged for 2 minutes. The column was discarded and the plasmid DNA was stored -20°C.

Plasmid DNA was electrophoresed and separated on 0.8% agarose gel. The gel was then visualized under UV after staining with ethidium bromide. The molecular weight of the plasmids was estimated from calibration curves constructed by using the Lambda DNA *EcoR1+HindIII* Marker (Ozer *et al.* 2013).

### **3.21 Plasmid curing**

To determine if the resistance gene is encoded by a plasmid, ethidium bromide was used to eliminate the plasmids from the strains and heat treatment was applied as a control. Ethidium bromide is the most commonly used curing method because it was found to be effective against plasmids in a wide variety of genera (Grinsted & Bennet 1988). The strains were grown with ethidium bromide (100 µg/ml) and then spread on Nutrient Agar (NA) plates each containing the metals, Zn, Pb, Cr, Cd, Cr, Ni and Cu while the control plates did not contain any of the heavy metals. The experiment was replicated and the plates were incubated at 30°C. Plasmids were considered to be eliminated from those that grew on metal free medium only (Malik & Jaiswal 2000). For heat treatment the strains were grown at 45°C and sub-cultured into fresh medium. The cultures were plated onto NA containing its respective metals and its metal free form (Ginns *et al.* 2000).

The plasmids of the cured derivatives were isolated using the protocol outlined in section 3.20. The antibiotic susceptibility tests of the cured isolates were then tested using the Kirby Bauer (1996) method outlined in section 3.10.

### **3.22 Homologous analysis of amplified genes**

The partial gene sequences obtained in this study (*pcoA*, *pcoR* and *chrB* genes) were translated using the JustBio Translator Tool ([www.justbio.com](http://www.justbio.com)). The protein sequences were then aligned and compared with other proteins in the Genbank (Benson & Karsch-Mizrachi 2000) by using the NCBI Basic Local Alignment Search Tools (BLASTp) programme (Altschul *et al.* 1997). The phylogenetic trees were constructed using the Phylogeny:fr programme (Dereeper *et al.* 2008).

The protein sequences were first aligned using MUSCLE version 3.7 (Edgar 2004). After alignment ambiguous regions were removed by G-blocks version 0.196. A phylogenetic tree was constructed using the Maximum Likelihood Method carried out by PhyML program version 3.0aLRT. A graphical representation of the tree was produced with TreeDyn version 198.3. The physico-chemical properties of the partial protein sequences were predicted using the Expasy's Prot Param Tool (Gasteiger *et al.* 2005). The secondary structure prediction of the protein sequences was obtained using SOPMA (Geourjon & Deleage 1995) and the 3D structures of the partial proteins were constructed I-TASSER (Zhang 2008). Function prediction analysis was carried out by Cofactor (Marhcler-Bauer *et al.* 2011). The modeled structure was then analysed using Molprobit (Davis *et al.* 2007). This programme checks the stereochemical quality of a protein structure, producing a number of PostScript plots assessing its overall and residue-by-residue geometry.

## 4. RESULTS

### 4.1 Diversity of bacterial isolates from study sites

A total of 48 different bacterial isolates were obtained from both the water and sediment samples and were distributed as follows; Site 1-the source (6), site 2- before Lenasia (11), site 3-Lenasia (7), site 4- Henley on Klip Weir (9), site 5- Confluence of the Klip River and Vaal River (13) and site 6- Vaal Barrage-(2) (Fig. 28).

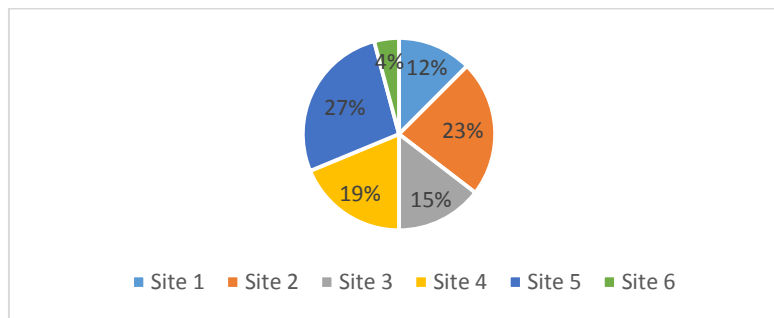


**Figure 28: Diversity of isolates from study sites along the Klip River**

### 4.2 Physico-chemical results

Turbidity, salinity and dissolved oxygen were not measured at site 1, therefore the results for these parameters are shown in Fig. 30-31. The graph for temperature, pH and dissolved oxygen is shown in Fig. 29. These values were compared with those provided in the Klip River Instream Guidelines (2003). The pH of the sites ranged from 5.9 to 7.9 and were within the compliance range ( $<6.0 > 9.0$ ) except for site 1, where a slightly lower pH of 5.9 was recorded. The Dissolved Oxygen (DO) values of 4.23 and 4.32 mg/l at sites 3 (Lenasia) and 5 (confluence of Klip River and Vaal River), respectively, were below the required range of  $>5$  mg/l. The temperature range was from 16.7 to 21.1, units with the lowest temperatures being recorded at the confluence of the Klip and Vaal River (site 5).

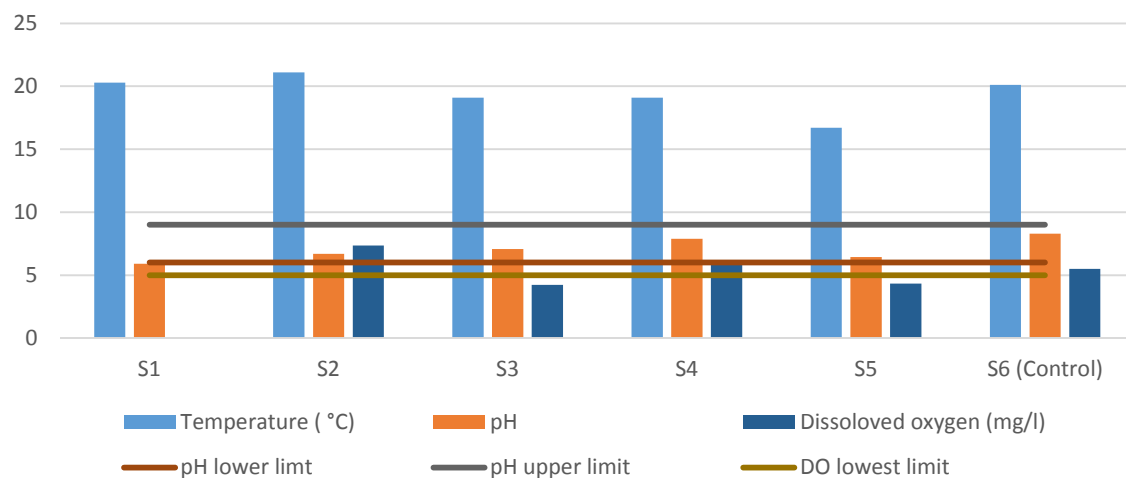


**Figure 29: In situ measurements of temperature, pH and dissolved oxygen at various sites along the Klip River.**

The turbidity, conductivity (Fig. 30) and salinity (Fig. 31) almost doubled at site 4, (Henley on Klip Weir), and a slight decrease was recorded at sites 5 (Confluence of the Klip and Vaal River) and 6 (Vaal Barrage).

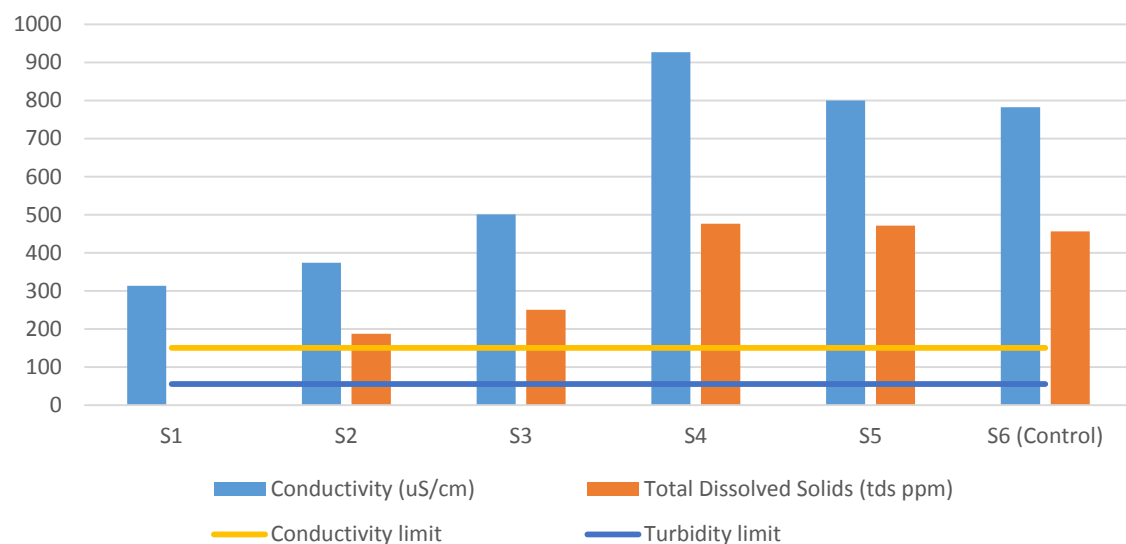


**Figure 30: In situ measurements of conductivity and total dissolved solids at different sites along the Klip River.**

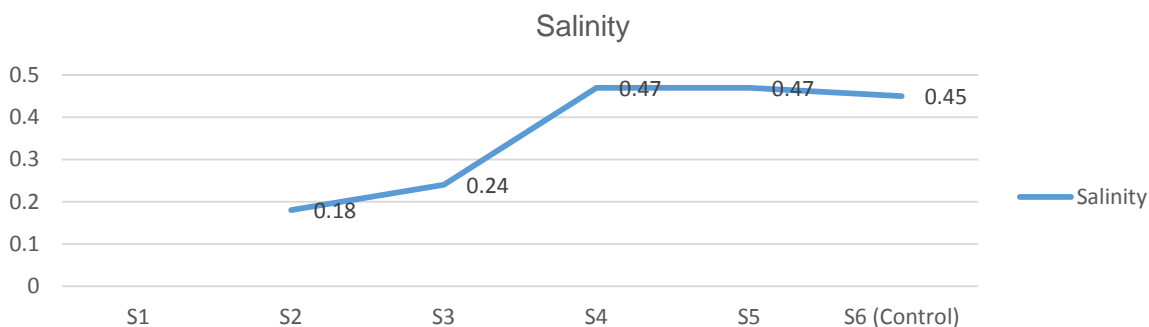


**Figure 31: Salinity trends at the different sites along the Klip River**

### 4.3 Heavy metal analysis of water samples

The highest concentrations of zinc, copper and cadmium were found at the source of the Klip River. The concentration of the heavy metals decreased downstream and remained more or less constant. Nickel concentrations were below detectable limits for all the sites except for site 5. Cadmium concentration was exceptionally high at site 1 where a concentration of 1 mg/l was detected; however it was not detected in the other sites. Copper and zinc was detected in all the water samples. The concentrations for zinc ranged from  $\pm 0.05$  to  $\pm 0.43$  mg/l, and for copper from  $\pm 0.31$  to  $\pm 0.86$  mg/l (Fig. 32).

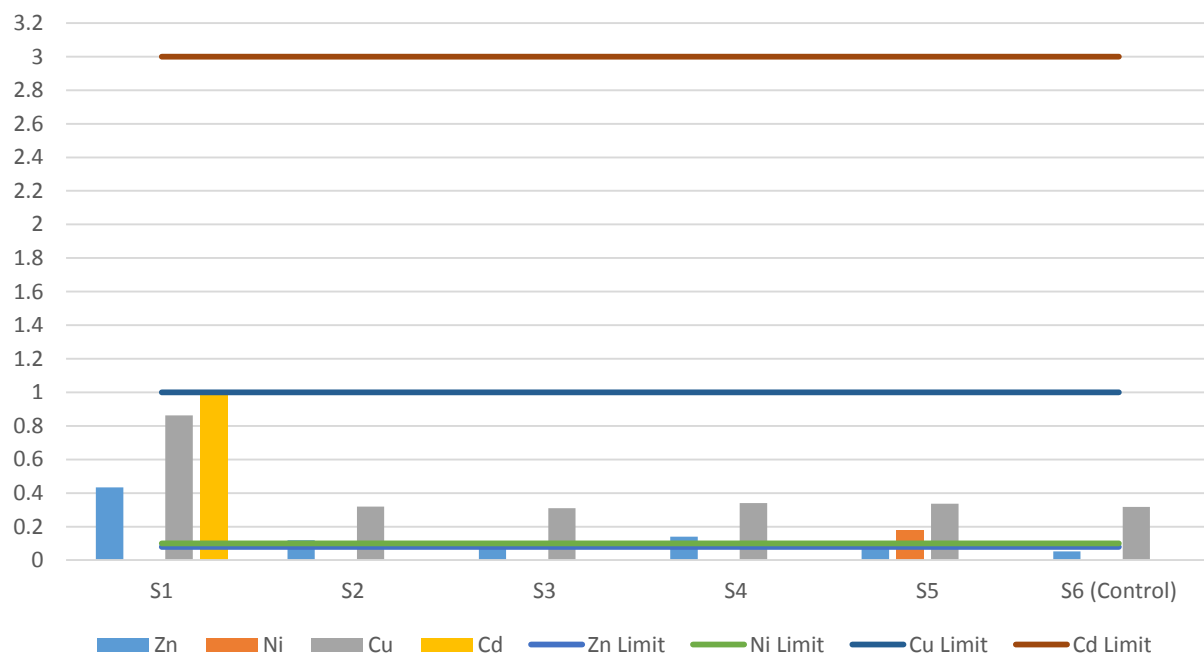


**Figure 32: Histograms showing concentrations of the heavy metals zinc, nickel, copper and cadmium at different sites along the Klip River**

The highest concentration of lead and zinc was detected at site 1. The concentration of both metals also decreased along the course of the Klip River (Fig. 33). High levels of lead were detected at site 1 (9.52 mg/l). The lowest concentration of lead was detected at site 3 ( $\pm 0.73$  mg/l). The iron concentrations ranged from  $\pm 0.23$  mg/l to  $\pm 2.23$  mg/l, with the lowest level being detected at site 3.

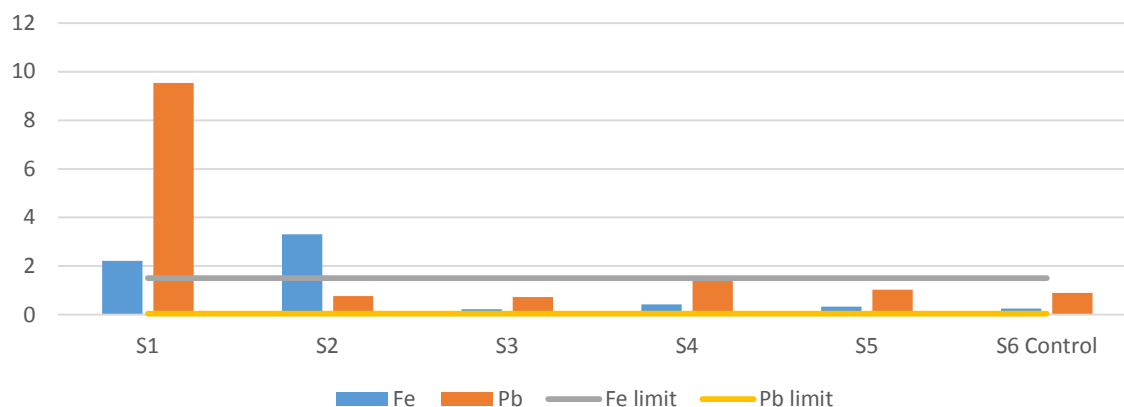


**Figure 33: Histogram of concentrations for lead and iron at various sites along the Klip River.**

#### 4.4 Statistical analysis of physicochemical parameters

The data for the following parameters were analysed: pH, temperature, DO, EC, salinity, turbidity, zinc, lead, nickel, iron, copper and cadmium. The data were analysed using Principle Component Analysis (XLSTAT 2014 Version).

The pH of 83% of the water samples were within the range stipulated by the by the Klip River Instream Guidelines (2003) (Table 6). The pH showed a negative correlation with the heavy metal concentrations and a positive correlation with all the other parameters (Table 7). Thirty three percent of the sites were under the optimum limit of dissolved oxygen stipulated by the Klip River In-stream Guidelines (2003) (Table 6). All the sites were found to be within the limit for electrical conductivity, and a relatively strong correlation was noted between salinity and turbidity ( $r=1$ ). All the sites were above the stipulated limit of 55 tds ppm. Sixty six percent of the sites were above the limit for zinc concentrations. There was a very strong correlation between zinc and iron ( $r=0.966$ ). Sixty-six percent of the sites were within the limit for iron concentrations. All of the sampling sites were higher than the permissible limit for lead concentrations. There was a very strong correlation among lead and copper ( $r=0.999$ ) and between cadmium and copper ( $r=0.998$ ). Cadmium concentrations were higher than the permissible limit in 17% of the sites.

**Table 6: Summary of the average measured parameters from the different sites and percentages that fall within permissible limits from the Instream Klip River Guidelines (2003)**

Parameter	Permissible	Summary			Sites (%)		
		Mean	Min.	Max.	Below	Optimum	Higher
pH	<6.0;>9.0	7.058	5.9	8.33	17%	83%	
Temp. (°C)	No range	19.4	16.7	21.1	-	-	-
DO	<5 mg/l	5.5	4.23	7.36	33%	-	67%
EC	>150 ms/m	616	313	927	100%	-	-
Salinity	No range	0.362	0.18	0.47	-	-	-
Turbidity	>55 tds ppm	368	187	476	-	-	100%
Zinc	>0.08 mg/l	0.207	0.052	0.453	17%	17%	66%
Lead	>0.05 mg/l	2.393	0.730	9.510	-	-	100%
Nickel	>0.1mg/l	0.000	0.000	0.000	100%	-	-
Iron	>1.5 mg/l	1.131	0.234	3.315	66%		34%
Copper	>1 mg/l	0.413	0.310	0.863	100%	-	-
Cadmium	>3 mg/l	0.167	0.000	1.003	100%	-	-

EC-electric conductivity, DO- dissolved oxygen

**Table 7: Correlation coefficients among the physico-chemical parameters along the course of the Klip River (average values of all the sites)**

Variables	pH	Temp.	DO	EC (uS/cm)	Salinity	Turbidity	Zn	Pb	Ni	Fe	Cu	Cd
pH	<b>1</b>	0.093	0.086	0.685	0.345	0.356	-0.621	-0.601		-0.545	-0.620	-0.621
Temp.	0.093	<b>1</b>	0.748	-0.580	-0.557	-0.551	0.654	0.263		0.668	0.251	0.289
DO	0.086	0.748	<b>1</b>	-0.257	-0.363	-0.364	0.677	0.002		0.763	-0.011	0.000
EC (uS/cm)	0.685	-0.580	-0.257	<b>1</b>	0.791	0.793	-0.791	-0.536		-0.758	-0.546	-0.585
Salinity	0.345	-0.557	-0.363	0.791	<b>1</b>	<b>1.000</b>	-0.565	0.052		-0.637	0.045	0.000
Turbidity	0.356	-0.551	-0.364	0.793	<b>1.000</b>	<b>1</b>	-0.570	0.052		-0.643	0.045	0.000
Zn	-0.621	0.654	0.677	-0.791	-0.565	-0.570	<b>1</b>	0.582		<b>0.966</b>	0.582	0.598
Pb	-0.601	0.263	0.002	-0.536	0.052	0.052	0.582	<b>1</b>		0.382	<b>0.999</b>	<b>0.997</b>
Ni												
Fe	-0.545	0.668	0.763	-0.758	-0.637	-0.643	<b>0.966</b>	0.382		<b>1</b>	0.384	0.405
Cu	-0.620	0.251	-0.011	-0.546	0.045	0.045	0.582	<b>0.999</b>		0.384	<b>1</b>	<b>0.998</b>
Cd	-0.621	0.289	0.000	-0.585	0.000	0.000	0.598	<b>0.997</b>		0.405	<b>0.998</b>	<b>1</b>

Values in bold are different from 0 with a significance level  $\alpha=0.05$

A scree plot (Fig. 34) was constructed based on the eigenvalues (Table 8). The 12 physicochemical parameters were reduced to two main factors (Factors 1 and 2) from the leveling off point (s) in the scree plot (Cattell & Jaspers 1967). The first factor corresponding to the largest eigenvalue (5.943) accounts for approximately 54.024% of the total variance. The second factor corresponding to the second eigen value (2.984) accounts for approximately 27.123% of the total variance. The remaining 10 factors have eigenvalues less than 1. A factor with eigenvalue greater than 1 is considered significant (Cattell & Jaspers 1967). The scree plot illustrates the eigenvalues sorted from large to small as a function of the principal components number (Praus 2007).

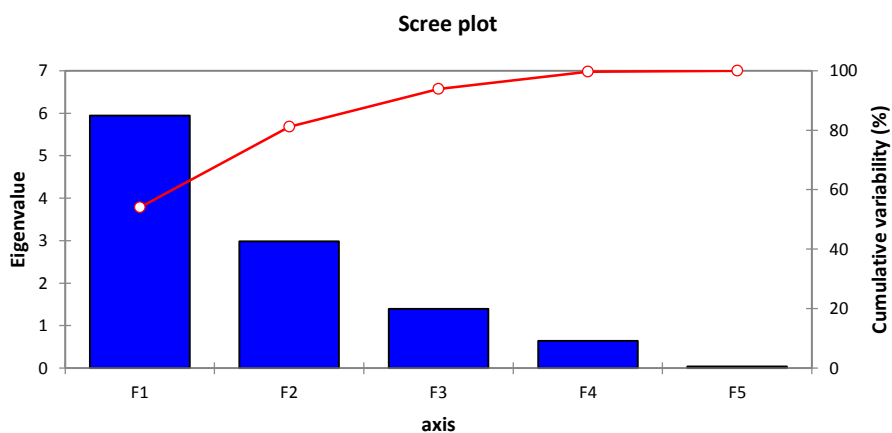


**Figure 34: Scree plot of the eigenvalues versus factor components along with % cumulative variance**

**Table 8: Explained total variance**

	F1	F2	F3	F4	F5
Eigenvalue	5.943	2.984	1.396	0.642	0.035
Variability (%)	54.024	27.123	12.691	5.841	0.321
Cumulative %	54.024	81.147	93.838	99.679	100.000

For factor 1, iron and zinc contributed the highest factor loading value ( $\geq 0.9$ ) (Table 9) and (Fig. 35) showing that these are the most influential variables for the first factor. For factor 2, Pb, Cu, and Cd have the highest factor loading values ( $> 0.7$ ) (Table 9), suggesting that Pb, Cu and Cd are major environmental pollutants in the Klip River. Factor loadings can be interpreted as the relationship between the factors and the variable, i.e. the physicochemical parameters (Bhat *et al.* 2014).



The factor loadings of the 12 experimental variables were used to construct histogram shown in Fig. 35. This diagram illustrates the correlation between the variables and the factors.

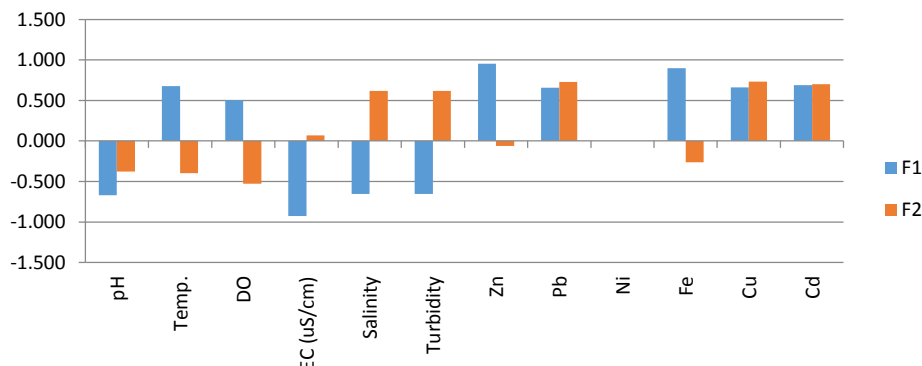


**Figure 35: Correlations between variables and factors**

To assess which sampling parameters were closely related a plot of factor coordinates for all significant observations was constructed using the factors attained from the factor loading analysis (Fig. 36).

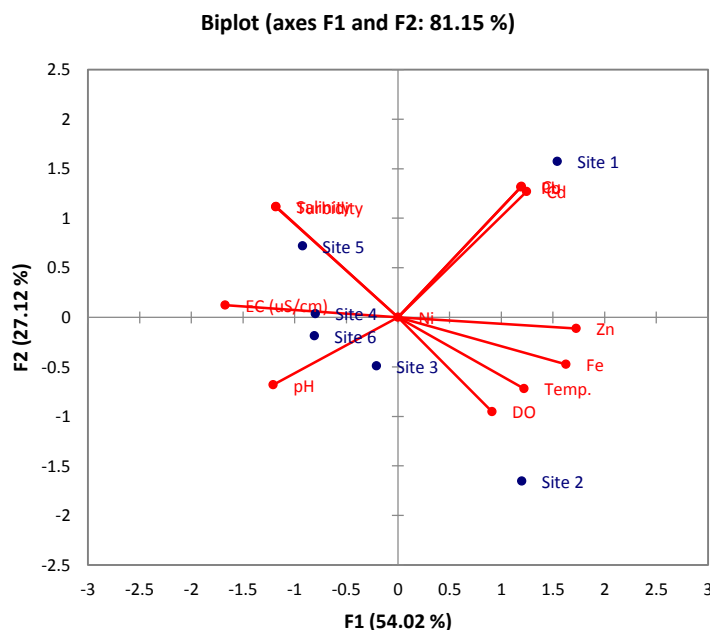


**Figure 36: Bi plots for principal component analysis 1 + 2 of water quality parameters**

#### 4.5 Enumeration of heavy metal resistant bacteria in sediment and water samples

The number of colony forming units (CFUs) on LB agar supplemented with 5 mg/l of each heavy metal (Cd, Cr, Cu, Fe, Ni, Pb and Zn) for the water samples is shown in Fig. 37. The CFUs for the sediment samples are shown in Fig. 38. The number of CFU's for the water samples were

considerably lower compared to those obtained for the sediment samples. The water sample at Site 3 recorded the highest CFUs for all the heavy metals whereas site 2 showed the lowest CFUs. For the sediment samples the highest CFUs for all the heavy metals was recorded at site 4, whereas the Vaal Barrage exhibited slightly lower CFUs for all the heavy metals. The controls for all the sites for both the water and sediment samples had higher CFUs than those of the heavy metals constituted agar plates.

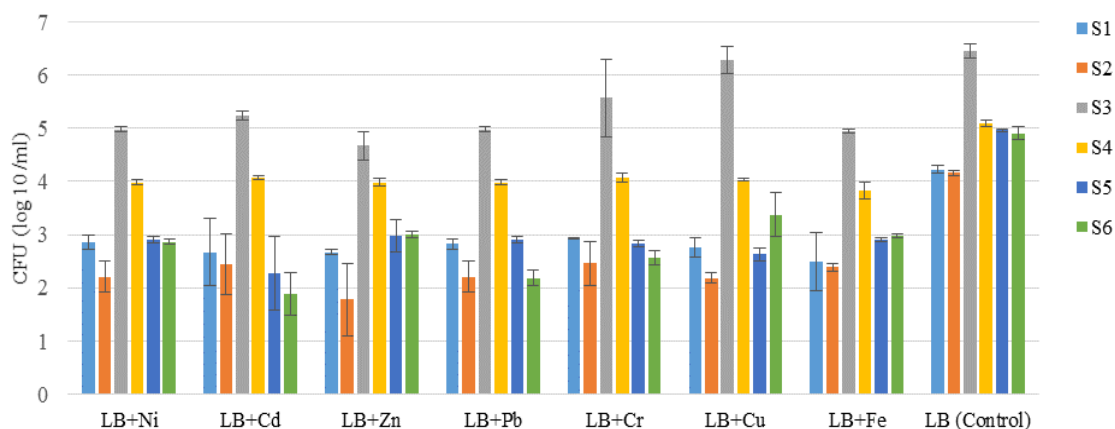


**Figure 37: Enumeration of heavy metal resistant bacteria in water samples**

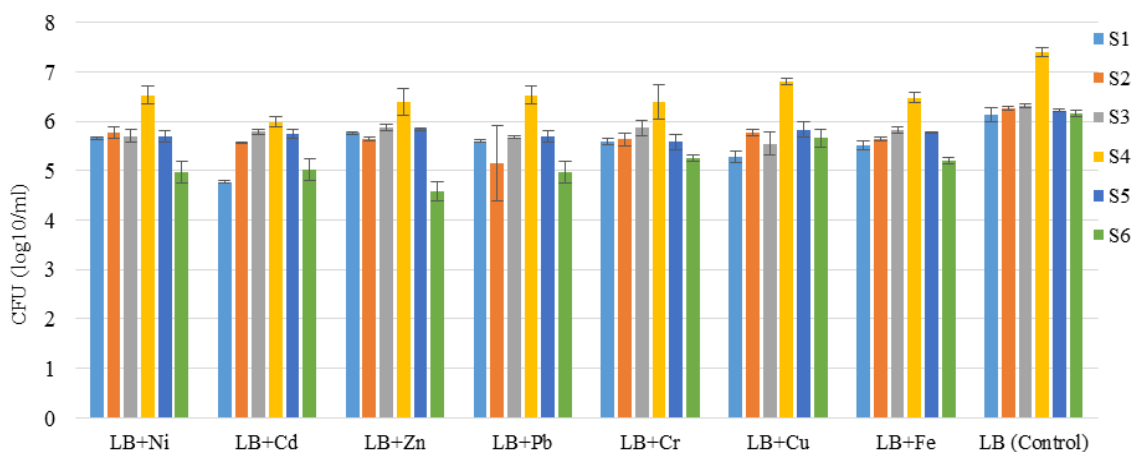


**Figure 38: Enumeration of heavy metal resistant bacteria in sediment samples**

#### 4.6 Colony Morphology of isolates

A total of 48 bacterial strains were isolated from both water and sediment samples based on their colony morphology. These were designated as KR01-KR48 (Table 9).

**Table 9: Colony morphology of bacterial isolates**

Strain codes	Initial strain code	Colour	Size	Shape	Margin	Elevation	Opacity	Surface
KR01	SS2PB006	Light brown	2mm	Round	Entire	Umbonate	Opaque	Smooth
KR02	WS1ZN001	White	5mm	Irregular	Undulate	Flat	Opaque	Rough
KR03	SS1PB005	White	7mm	Filament- uous	Filament- uous	Flat	Opaque	Rough
KR04	SS1CU002	Cream	5mm	Round	Undulate	Umbonate	Opaque	Rough
KR05	SS2PB007	Orange	2mm	Round	Entire	Flat	Opaque	Smooth
KR06	SS2CU001	White	4mm	Round	Undulate	Flat	Opaque	Rugose
KR07	SS4PB002	Cream	2mm	Round	Entire	Flat	Opaque	Smooth
KR08	SS4PB002	White	1mm	Round	Entire	Convex	Opaque	Smooth
KR09	WS5CR002	Orange	2mm	Round	Entire	Umbonate	Opaque	Smooth
KR10	WS2FE002	Light yellow	1mm	Round	Entire	Convex	Opaque	Smooth
KR11	WS2CU002	Yellow	3mm	Irregular	Lobate	Raised	Opaque	Rugose
KR12	WS2CR004	Deep yellow	4mm	Round	Entire	Umbonate	Opaque	Smooth
KR13	SS4CU001	Orange	5mm	Round	Undulate	Flat	Opaque	Smooth
KR14	SS2CU001	Cream	4mm	Round	Entire	Flat	Opaque	Smooth
KR15	WS2FE002	Cream	2mm	Round	Entire	Flat	Opaque	Smooth
KR16	SS2FE002	Light yellow	2mm	Round	Entire	Flat	Translu- scent	Smooth
KR17	WS5FE001	Light brown	1mm	Irregular	Irregular	Flat	Opaque	Rough
KR18	WS5PB001	Light pink	3mm	Round	Entire	Flat	Translu- scent	Smooth
KR19	WS5FE008	Cream	2mm	Round	Entire	Raised	Opaque	Smooth
KR20	WS5FE003	Yellow	2mm	Round	Entire	Flat	Opaque	Smooth
KR21	WS5FE005	Tan	2mm	Round	Entire	Umbonate	Opaque	Smooth
KR22	WS5FE006	Cream	1mm	Round	Entire	Raised	Opaque	Smooth
KR23	WS4CU005	Cream	2mm	Round	Entire	Convex	Opaque	Smooth
KR24	SS4CD001	Cream	4mm	Round	Entire	Convex	Opaque	Smooth
KR25	WS4PB004	White	3mm	Round	Entire	Flat	Opaque	Smooth
KR26	WS4FE004	Cream	2mm	Round	Entire	Umbonate	Opaque	Smooth
KR27	WS1CD002	Yellow	Punctifo rm	Round	Entire	Convex	Opaque	Smooth
KR28	WS4CR002	Light yellow	7mm	Round	Lobate	Flat	Opaque	Rugose
KR29	WS4CD005	White	5mm	Irregular	Lobate	Flat	Opaque	Rough
KR30	WS6CR002	White	1mm	Irregular	Irregular	Flat	Opaque	Rough

KR31	WS5FE001	Dark Orange	2mm	Round	Entire	Convex	Opaque	Smooth
KR32	WS5FE010	Dark brown	Punctiform	Round	Entire	Umbonate	Opaque	Smooth
KR33	WS2PB002	Yellow	Punctiform	Round	Entire	Convex	Opaque	Smooth
KR34	WS3CU002	Neon yellow	1mm	Round	Entire	Convex	Opaque	Smooth
KR35	WS3CU003	White	Punctiform	Round	Entire	Convex	Opaque	Smooth
KR36	SS3CU004	White	2mm	Round	Entire	Flat	Opaque	Smooth
KR37	WS3ZN002	Yellow	2mm	Round	Entire	Convex	Opaque	Smooth
KR38	WS5NI009	White	Punctiform	Round	Entire	Convex	Opaque	Smooth
KR39	WS5NI010	Deep pink	2mm	Round	Entire	Flat	Opaque	Smooth
KR40	WS3CU004	Yellow	2mm	Round	Entire	Convex	Opaque	Smooth
KR41	WS5ZN001	Cream	2mm	Round	Entire	Umbonate	Opaque	Smooth
KR42	WS5ZN002	Light yellow	3mm	Round	Entire	Flat	Opaque	Smooth
KR43	WS1ZN005	White	2mm	Round	Entire	Flat	Opaque	Smooth
KR44	WS2PB009	Pink	Punctiform	Round	Entire	Convex	Opaque	Smooth
KR45	WS6NI005	White	3mm	Round	Entire	Flat	Opaque	Smooth
KR46	SS3CU002	Cream	2mm	Round	Entire	Umbonate	Opaque	Smooth
KR47	SS1PB003	Cream	10mm	Round	Entire	Convex	Opaque	Smooth
KR48	WS3CR001	Neon yellow	2mm	Round	Entire	Flat	Opaque	Smooth

#### 4.7 Cellular Morphology of isolates

The cellular morphology of the 48 isolates was studied and observations are shown in Table 10.

**Table 9: Cellular morphology of bacterial isolates**

Strain codes	Shape	Arrangement	Type	Colour	Gram reaction
KR01	Rod	Scattered	Bacillus	Pink	-
KR02	Rod	Clustered	Bacillus	Blue-black	+
KR03	Rod	Linear and pairs	Bacillus	Blue-black	+
KR04	Rod	Linear	Bacillus	Blue-black	+
KR05	N/A	N/A	N/A	N/A	N/A
KR06	Rod	Scattered	Bacillus	Blue-black	+
KR07	Rod	Scattered	Bacillus	Pink	-
KR08	Round	Clustered	Coccus	Pink	-
KR09	Round	Clustered	Coccus	Blue-black	+

KR10	Round	Clustered	Coccus	Blue-black	+
KR11	Rod	Scattered	Bacillus	Pink	-
KR12	Rod	Scattered	Bacillus	Pink	-
KR13	Round	Clustered	Coccus	Blue-black	+
KR14	N/A	N/A	N/A	N/A	N/A
KR15	Rod	Scattered	Bacillus	Pink	-
KR16	N/A	N/A	N/A	N/A	N/A
KR17	Rod	Scattered	Bacillus	Pink	-
KR18	Rod	Clustered	Bacillus	Pink	-
KR19	Rod	Scattered	Bacillus	Pink	-
KR20	Rod	Scattered	Bacillus	Pink	-
KR21	Rod	Paired	Bacillus	Blue-black	+
KR22	Rod	Scattered	Bacillus	Pink	-
KR23	Rod	Scattered	Bacillus	Pink	-
KR24	Rod	Linear	Bacillus	Blue-black	+
KR25	Rod	Scattered	Bacillus	Blue-black	+
KR26	Rod	Scattered	Bacillus	Pink	-
KR27	Rod	Scattered	Bacillus	Pink	-
KR28	Rod	Scattered	Bacillus	Pink	-
KR29	Rod	Scattered	Bacillus	Pink	-
KR30	Rod	Linear	Bacillus	Blue-black	+
KR31	Round	Clustered	Coccus	Blue-black	+
KR32	Rod	Scattered	Bacillus	Pink	-
KR33	Rod	Scattered	Bacillus	Pink	-
KR34	Round	Scattered	Coccus	Pink	-
KR35	Round	Scattered	Coccus	Pink	-
KR36	N/A	N/A	N/A	N/A	N/A
KR37	Rod	Scattered	Bacillus	Pink	-
KR38	Round	Paired	Coccus	Pink	-
KR39	Rod	Scattered	Bacillus	Blue-black	+
KR40	Rod	Scattered	Bacillus	Blue-black	+
KR41	Rod	Scattered	Bacillus	Pink	-
KR42	Round	Clustered	Coccus	Blue-black	+
KR43	Rod	Scattered	Bacillus	Blue-black	+
KR44	Round	Clustered	Coccus	Blue-black	+

KR45	Rod	Scattered	Bacillus	Blue-black	+
KR46	Round	Clustered	Coccus	Pink	-
KR47	Rod	Scattered	Bacillus	Blue-black	+
KR48	Round	Clustered	Coccus	Blue-black	+

The different morphologies of a few bacterial isolates that were studied further are shown in Fig. 39. Figure 39a shows KR01 which is a gram-negative rod shaped, scattered bacteria; Fig. 39b shows KR02 as a gram-positive, clustered rod shaped bacteria; Fig. 39c is a filamentous shaped gram positive bacteria; Fig. 39d are very large gram positive bacilli showing both linear and clustered arrangements; Fig. 39e are very minute gram-negative rod shaped bacteria exhibiting a scattered arrangement and Fig. 39f shows very large spherical shaped structures held by bonds and they appear to be gram positive.

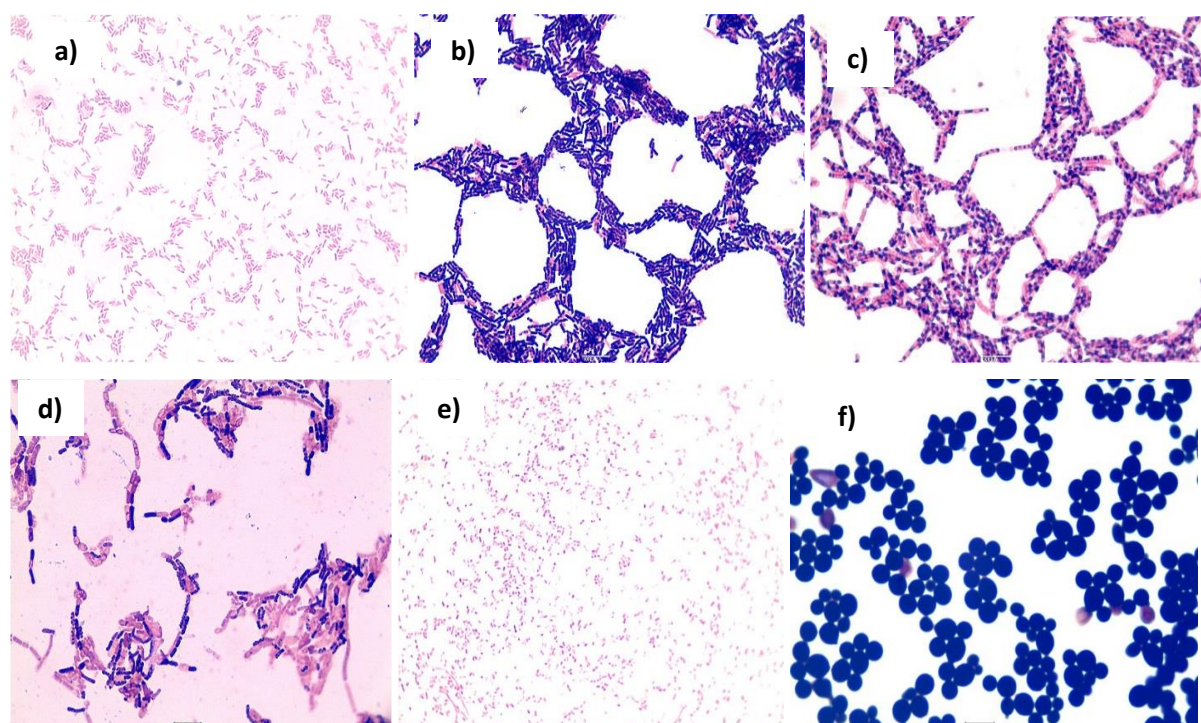


**Figure 39: Light microscope images (oil immersionx100) of bacterial strains a) KR01 b) KR02 c) KR03 d) KR04 e) KR29 f) KR44**

#### 4.8 Minimum Inhibitory Concentrations

Sixteen isolates were selected for further study based on their high MIC values. The Cd, Cr, Cu, Fe, Ni, Pb and Zn concentrations used during screening ranged from 0.2 - 4 mM. The MIC values for the 16 isolates are shown in Fig. 40. It was observed that 100% and 94% of the isolates were resistant to iron and lead, respectively. Lead was toxic to isolate KR22 as shown by an MIC value of 0 mM. Cadmium was toxic to 88% of the isolates. KR44 and KR48 exhibited very low MIC values of 0.2 mM. Chromium was moderately toxic to the isolates with the highest MIC value of 0.6 mM that was recorded for KR01 and KR04. KR01 and KR17 had MIC value of 4 mM for both lead and iron, while KR02, KR06, KR07, KR18 and KR23 showed an MIC value of 4 mM for lead and finally KR44 exhibited an MIC value of 4 mM for iron. Zinc was toxic to 94% of the isolates with the exception of KR08 which showed moderate zinc resistance with an MIC value of 0.8 mM.

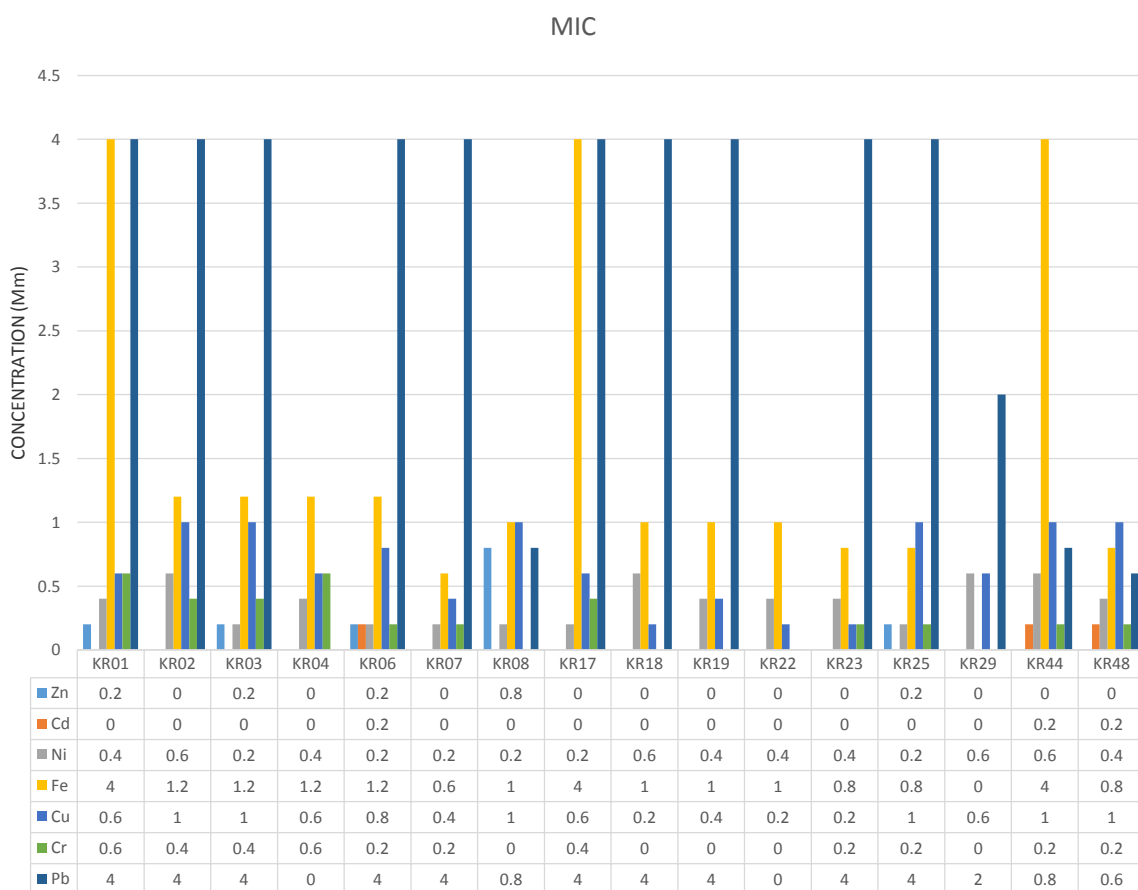


**Figure 40: Minimum Inhibitory Concentrations of heavy metal resistant isolates from the Klip River**

#### 4.9 Biochemical Tests

The isolates that were analysed exhibited a range of biochemical phenotypes when tested with the API 20E® test strips (Fig. 41). The test strips were designed for the rapid identification of enteric bacteria. However several tests on the strip are based on the traditional biochemical tests (Phillips *et al.* 2012). The strips were used in an ecological context in order to replace the traditional methods and rapidly construct a phenotypic profile of the isolates. The biochemical profiles of the isolates are shown in Table 11. Isolate KR17 showed positive results for most of the biochemical tests, while KR44 displayed negative results for all the tests except for catalase. Most of the isolates did not ferment glucose. A suite of 22 tests were used to construct a phenotypic profile for each isolate. The number of positives observed for each isolate ranged from 1 to 12. A comparison was made between each of the isolates and a similarity dendrogram was constructed. The similarity comparison analyzed both the number of positive tests and tests that were positive between the isolates. The phenotypic profiles of each of the 16 isolates were compared against each other. The similarity comparison is shown in Fig. 42. Most of the isolates did not ferment glucose in the carbohydrate fermentation tests.

The similarity dendrogram that resulted from the biochemical tests is shown in Fig. 42. Some isolates were highly similar or even 100% similar for instance KR03 and KR25. Eighty-eight percent (14/16) had a unique phenotype profile. All 16 isolates showed an API® profile similarity coefficient of at least 59%. Six of the sixteen isolates displayed greater than 90% similarity when profiled with API 20E® test strips.



**Figure 41: Biochemical test results for KR29 and KR22**



**Table 10: Biochemical characteristics of heavy metal resistant isolates from the Klip River**

Character	Bacterial Isolates															
	KR01	KR02	KR03	KR04	KR06	KR07	KR08	KR17	KR18	KR19	KR22	KR23	KR25	KR29	KR44	KR48
<b>Biochemical</b>																
Catalase	+	+	+	+	+	+	+	+	+	+	+	+	+	+	+	+
Oxidase	+	+	N/A	-	+	-	-	-	-	+	-	+	+	-	N/A	-
McC agar	+	-	-	-	-	-	-	-	-	+	-	+	-	-	-	-
ONPG	+	-	-	+	+	-	-	+	-	+	-	+	-	+	-	-
ADH	-	+	-	-	-	-	-	+	-	-	-	-	-	+	-	-
LDC	+	-	-	-	-	-	-	-	-	-	-	+	-	-	-	-
ODC	-	-	-	-	-	-	-	-	-	-	-	-	-	+	-	-
CIT	-	+	-	-	-	+	+	-	-	-	-	+	-	-	-	-
H <sub>2</sub> S	-	-	-	-	-	-	-	+	+	-	+	-	-	-	-	-
URE	-	-	-	-	-	-	-	+	-	-	+	-	-	-	-	-
TDA	-	-	-	-	-	-	-	-	-	-	+	-	-	+	-	-
IND	-	+	-	-	-	-	-	-	-	-	-	+	-	-	-	-
VP	+	-	-	-	-	+	+	+	-	+	-	+	-	-	-	-
GEL	+	+	+	+	+	-	-	+	+	+	+	+	+	-	-	+
Carbohydrate Fermentation or oxidation																
GLU	+	-	-	-	-	-	+	+	-	+	+	-	-	+	-	-
MAN	+	-	-	-	-	-	-	+	-	+	-	-	-	+	-	-
INO	-	-	-	-	-	-	-	-	-	-	-	-	-	-	-	-
SOR	-	-	-	-	-	-	-	-	-	+	-	-	-	+	-	-
RHA	-	-	-	-	-	-	-	-	-	-	-	-	-	+	-	+
SAC	+	-	-	-	-	-	-	+	-	+	+	-	-	+	-	-
MEL	-	-	-	-	-	-	+	-	-	-	-	-	-	-	-	-
AMY	-	-	-	-	-	-	-	-	-	+	-	-	-	-	-	-
ARA	+	-	-	-	-	-	+	+	-	+	-	-	-	+	-	-
NO <sub>2</sub>	+	-	-	+	-	-	-	+	-	+	+	+	-	+	-	+

**Tests:** McC, growth on MacConkey; ONPG,  $\alpha$ -galactosidase activity; ADH, Arginine Dihydrolase; LDC, Lysine Decarboxylase; ODC, Ornithine Decarboxylase; CIT, Citrate Utilization; H<sub>2</sub>S, Hydrogen Sulfide Production; URE, Urease; TDA, Tryptophan Deaminase; IND, Indole Production; VP, Acetoin Production (Voges-Proskaur); GEL, Gelatinase; GLU, Glucose; MAN, Mannitol; INO, Inositol; SOR, Sorbitol; RHA, Rhamnose; SAC, Sucrose; MEL, Melibiose; AMY, Amygdalin; ARA, Arabinose; NO<sub>2</sub>, Nitrate Reduction to Nitrite + Positive result; - negative result; N/A-not available

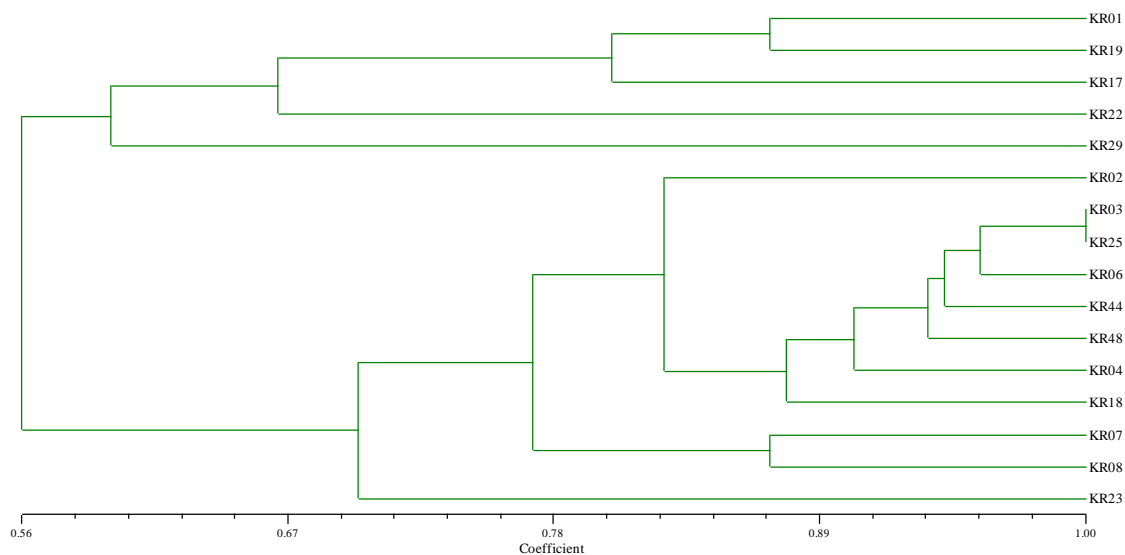


**Figure 42: Similarity dendrogram of cultured microorganisms isolated from the Klip River based on phenotypic profiles. A total of 23 different biochemical reactions were assayed using the API 20E®strips, catalase and McConkey Agar reactions (oxidase tests were excluded). Based on the number of positive tests, a phenotypic profile was constructed and compared to the profile of all other isolates. The similarity coefficient is shown at the bottom.**

#### 4.10 Antibiotic susceptibility tests

Vancomycin inhibited the growth of all the Gram positive bacteria (Table 12). Cephalothinic acid was effective against 69% of the isolates. However, KR04 (Fig. 43a), KR06, KR25 (Fig. 43c), KR29 and KR48 were resistant to this drug. The following isolates were resistant to streptomycin: KR01, KR06, KR17 (Fig. 43b), KR18, KR22 and KR25 (Fig. 43c). Several isolates showed resistance towards the  $\beta$ -lactam antibiotics, except for KR04, KR18, KR25 and KR48. Tetracycline was effective against 94% of the isolates with the exception of KR17 which was resistant to this antibiotic. The following isolates showed resistance to the sulphonamide, Cotrimoxazole: KR01, KR02, KR07, KR08, KR17 and KR44. Eighty-eight percent of the isolates were susceptible to the drug Tobramycin, with the exception of KR22 and KR48. KR17 (Fig. 43a) showed resistance to all antibiotics except for Tobramycin, while KR04 in contrast was susceptible to all 9 antibiotics (Fig. 43a.)

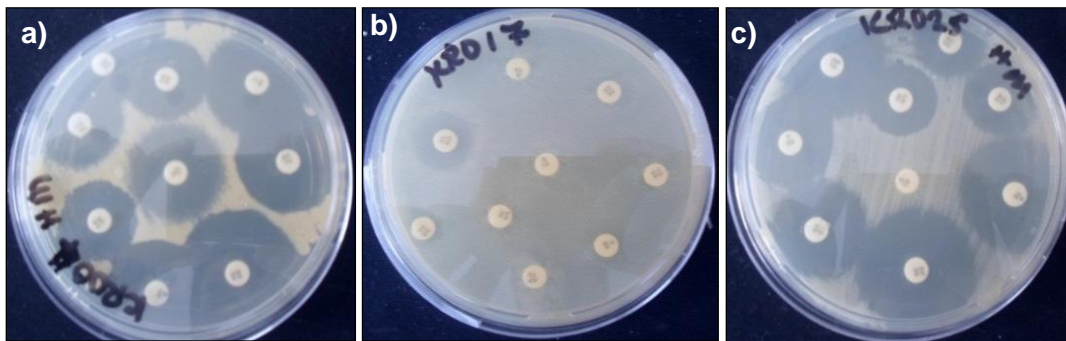


Figure 43: Antibiotic resistance profiles of a) KR04, b) KR17 and c) KR25

**Table 12: Antibiotic resistance profiles of heavy metal resistant isolates**

	Antibiotic Disc								
	Neomycin	Vancomycin	Cephalothin acid	Streptomycin	Ampicillin	Amoxycillin	Tetracycline	Cotrimoxazole	Tobramycin
KR01	19(S)	9(R)	NZ	7(R)	NZ	NZ	18(S)	NZ	15(S)
KR02	21(S)	18(S)	8(R)	24(S)	NZ	NZ	18(S)	NZ	18(S)
KR03	18(S)	16(S)	NZ	21(S)	NZ	NZ	22(S)	13(S)	16(S)
KR04	22(S)	20(S)	31(S)	26(S)	27(S)	29(S)	29(S)	24(S)	24(S)
KR06	20(S)	20(S)	34(S)	11(R)	11(R)	NZ	29(S)	24(S)	24(S)
KR07	18(S)	NZ	NZ	13(S)	NZ	NZ	19(S)	NZ	18(S)
KR08	16(S)	NZ	NZ	18(S)	NZ	NZ	18(S)	12(R)	17(S)
KR17	7(R)	NZ	NZ	NZ	NZ	NZ	NZ	NZ	13(S)
KR18	18(S)	14(S)	NZ	8(R)	17(S)	13(S)	17(S)	23(S)	17(S)
KR19	17(S)	NZ	NZ	16(S)	NZ	NZ	24(S)	17(S)	16(S)
KR22	NZ	NZ	NZ	NZ	NZ	NZ	15(S)	20(S)	11(R)
KR23	20(S)	7(R)	NZ	16(S)	NZ	NZ	23(S)	28(S)	21(S)
KR25	17(S)	18(S)	27(S)	NZ	27(S)	30(S)	21(S)	22(S)	18(S)
KR29	15(S)	NZ	13(S)	16(S)	14(S)	12(R)	19(S)	22(S)	13(S)
KR44	22(S)	16(S)	11(R)	24(S)	8(R)	8(R)	22(S)	NZ	13(S)
KR48	16(S)	21(S)	40(S)	18(S)	35(S)	29(S)	28(S)	23(S)	8(R)

Letters in parenthesis indicates the sensitivity of the isolate to the antibiotic  
R-Resistant; S-Sensitive; NZ-No Zone

#### 4.11 Optimal growth studies

The effect of pH was observed by exposing the bacterial cultures to different pH conditions ranging from 5 to 10. The pH trend for the isolates was recorded in Fig. 44.

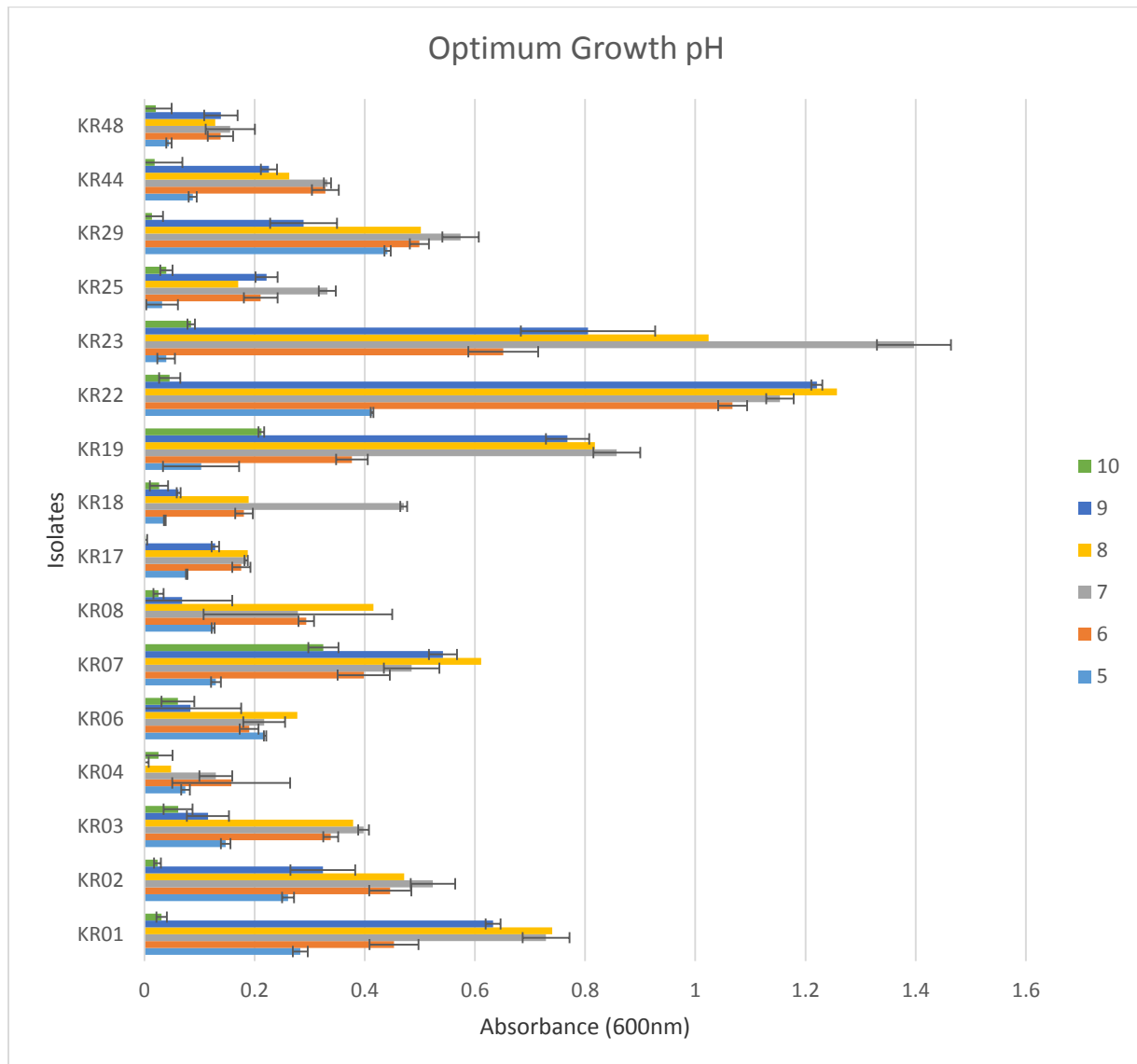


**Figure 44: Optimum pH determination of isolates. Experiments were performed in triplicate as described in Section 3.13.1. Cultures were inoculated with 100µl of parent culture and absorbance measured at an OD600.**

Sixty-nine percent of the isolates exhibited optimum growth at pH 7, except for KR04 and KR06 which grew in acidic conditions (pH 5) and KR07 and KR08 which grew under slightly alkaline conditions (pH 8) (Fig. 44).

The optimum temperatures for 75% of the isolates was in the range of 30-37°C except for KR06 which was 40°C, while KR17 and KR19 had optimum temperatures of 25°C (Fig. 45).

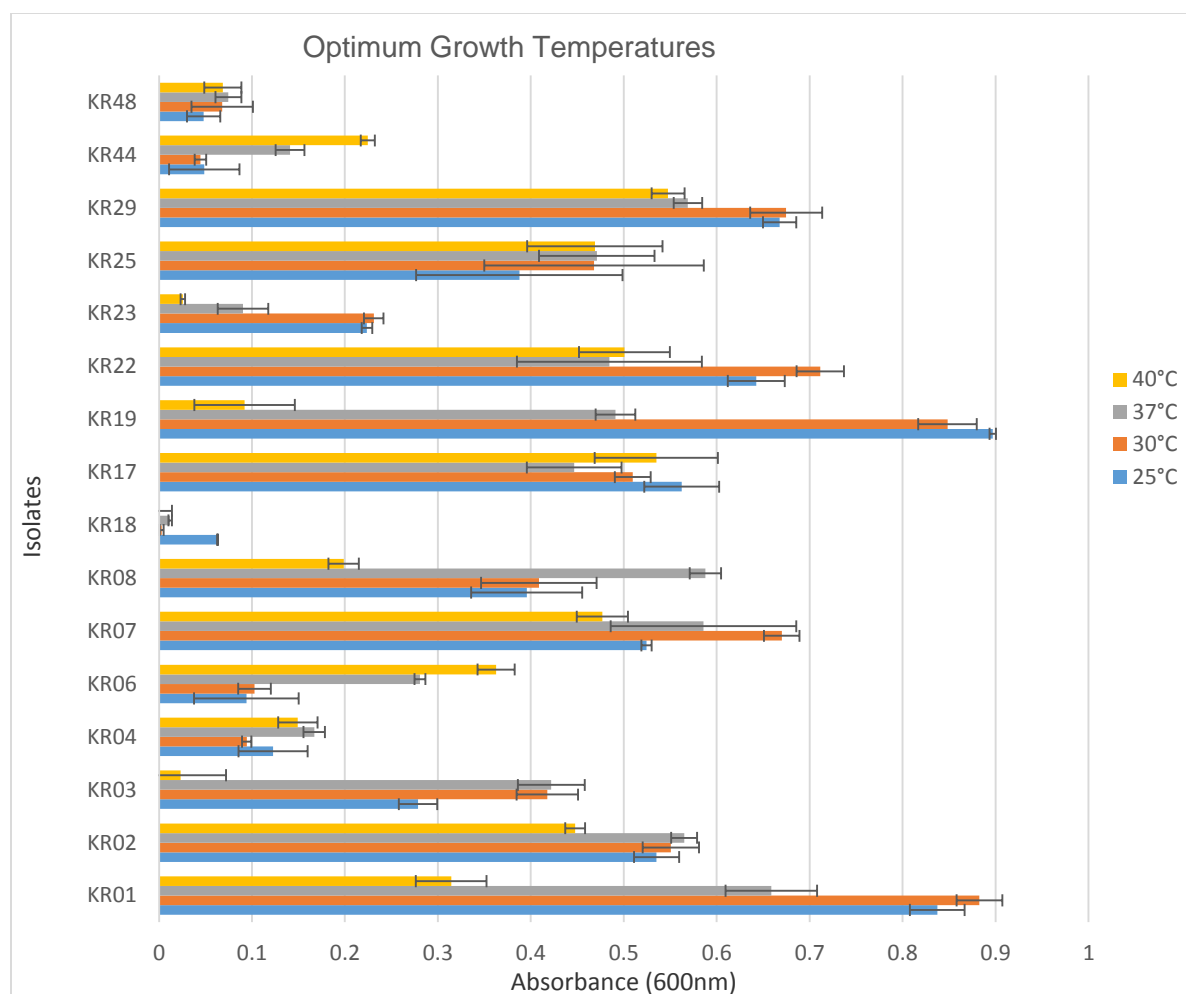
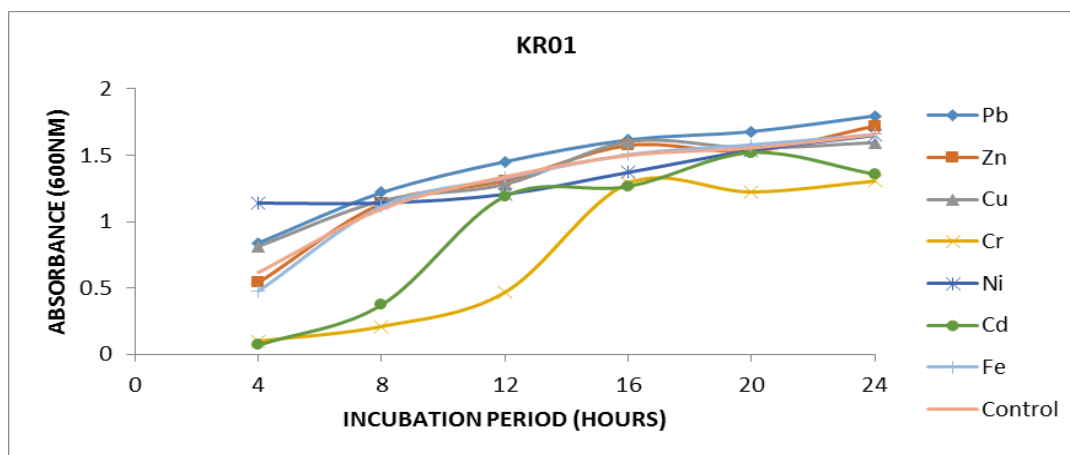


**Figure 45: Optimum temperature determination of isolates.** Experiments were performed in triplicate as described in Section 3.13.1. Cultures were inoculated with 100µl of parent culture and absorbance measured at an OD600.

#### 4.12 Influence of heavy metals on growth patterns of isolates

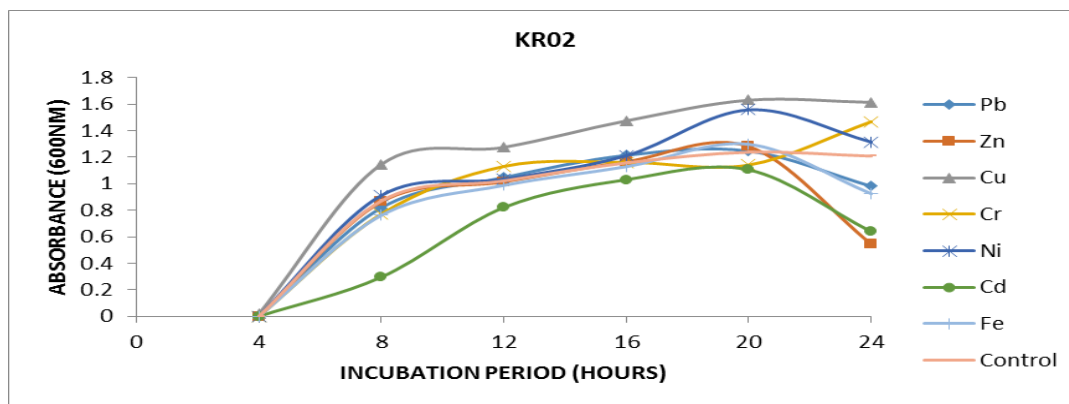
To analyse the influence of  $CdCl_2$ ,  $CuSO_4 \cdot 5H_2O$ ,  $PbCl_2$ ,  $ZnCl_2$ ,  $FeSO_4 \cdot 7H_2O$ ,  $NiCl_2 \cdot 6H_2O$  and  $K_2Cr_2O_7$  on cells in culture, a time course experiment was conducted in which the growth profiles of the 14 isolates were compared in the presence and absence of 0.2 mM of the above mentioned heavy metals. Growth patterns in the presence and absence of heavy metals were observed and the following curves for 14 isolates were observed (Fig. 46-59). The growth curve patterns of isolates KR03 and KR18 are not shown because the isolates stopped growing in the presence of heavy metals; therefore further studies on these isolates could no longer be carried out.

Figure 46 shows that the growth of KR01 was slightly affected by the presence of chromium and cadmium. However, the isolate exhibited significant growth in the presence of  $Pb^{2+}$  even higher than the control which had no heavy metals. By the 16<sup>th</sup> hour all cultures had reached an  $OD_{600}$  reading of >1.0 indicating the cells had entered the stationary phase. No significant lag phase was noted for all of the heavy metals. In the 20<sup>th</sup> hour cadmium caused a decline in the growth curve.



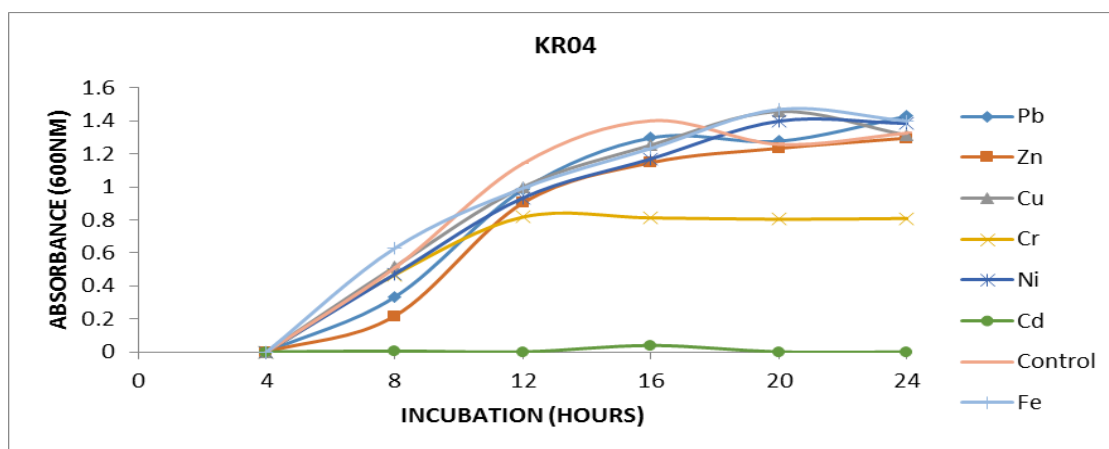
**Figure 46: Growth curves of KR01 in the absence and presence of heavy metals**

Figure 47 shows the growth curves for KR02. Between the 0 and the 4<sup>th</sup> hour there was no significant growth; however the isolate entered its exponential phase soon after the fourth hour, as noted by the steep gradient of the graphs. This isolate exhibited remarkable growth in the presence of copper. After the 20<sup>th</sup> hour the growth rate in the presence Cu, Ni, Fe, Zn, Cd and Pb began to decline, with the exception of Cr whereby an increase in the growth rate was noted. The presence of cadmium marginally decreased the growth rate of KR02.



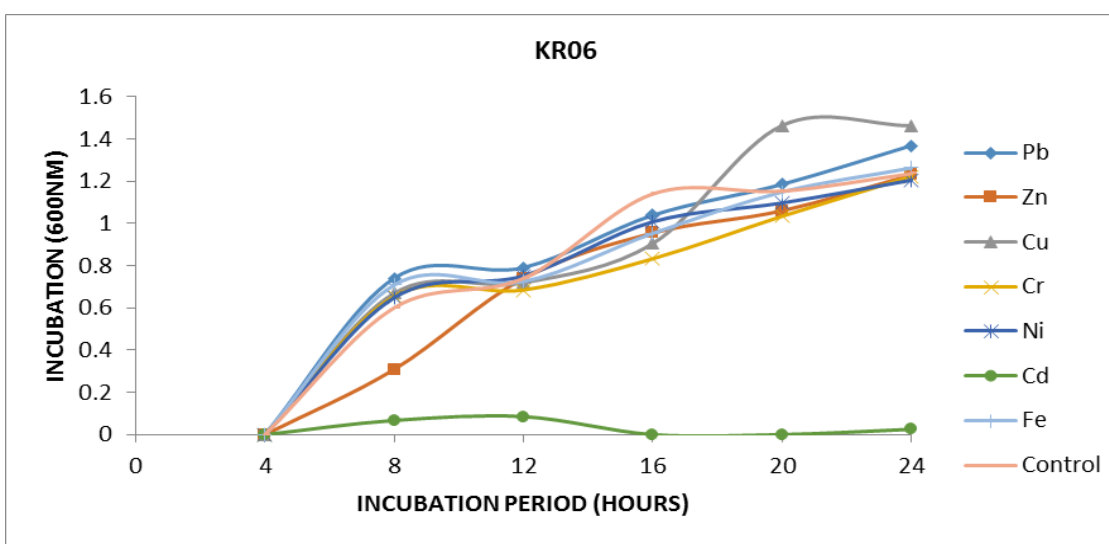
**Figure 47: Growth curves of KR02 in the absence and presence of heavy metals**

The growth rate of KR04 (Fig. 48) was inhibited in the presence of cadmium. In the presence of chromium the isolate entered its stationary phase in the 12<sup>th</sup> hour. The isolate seemed to be unaffected by the presence of lead, zinc, copper, nickel and iron since the isolate was displaying more or less similar growth rates as the control. However chromium, to some extent had a negative impact on cellular growth since the isolate entered its stationary phase early and the growth rate was slower as shown by the gradient of the graph.



**Figure 48: Growth curves of KR04 in the absence and presence of heavy metals**

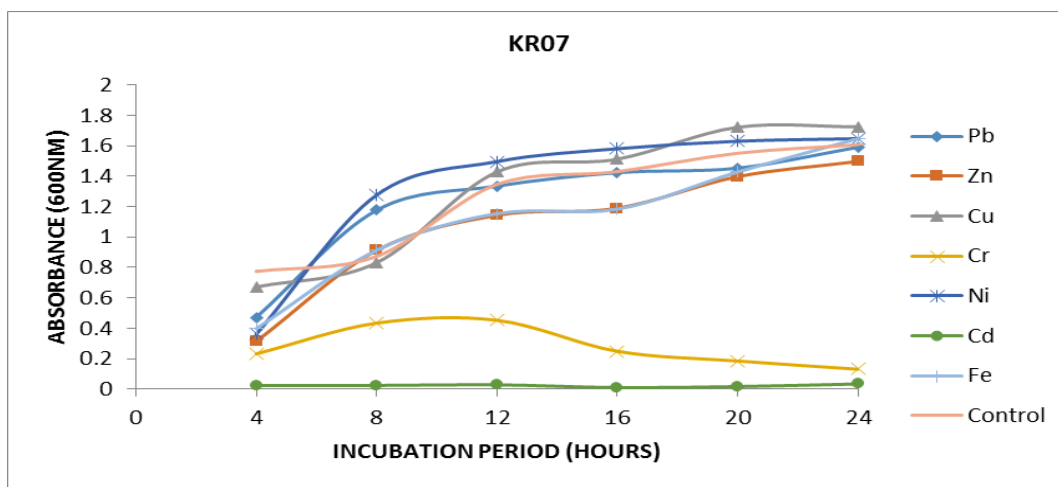
Figure 49 shows the growth curves of the isolate KR06. It appears that the cultures containing Pb, Cu, Cr, Ni, Fe and the control were growing at approximately equivalent rates and exhibiting similar growth patterns. The presence of these metals did not appear to have any influence on the growth of this isolate. However, the isolate's growth was adversely affected by the presence of cadmium.



**Figure 49: Growth curves of KR06 in the absence and presence of heavy metals**

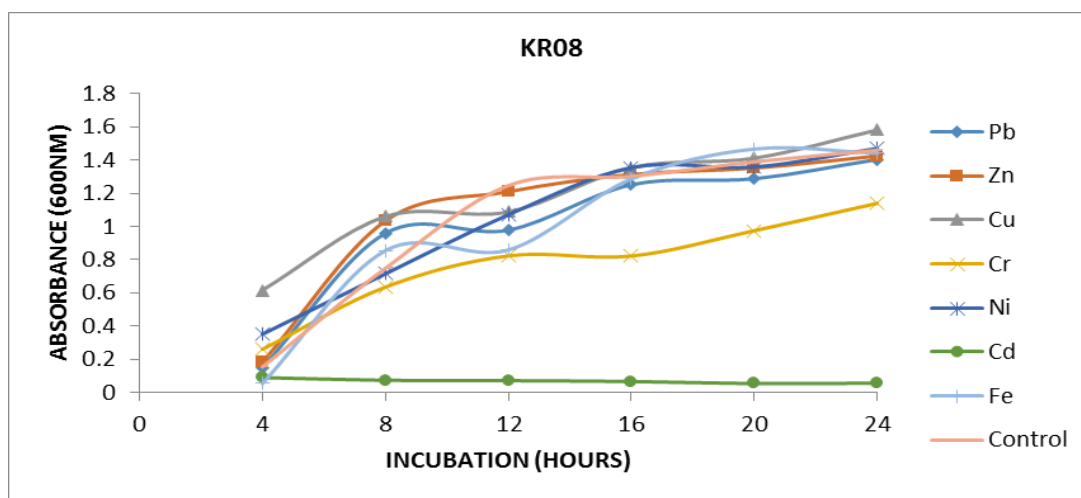


In the presence of chromium KR07 (Fig. 50) proliferated slowly and the biomass gradually increased between the 4<sup>th</sup> and 8<sup>th</sup> hour. The growth curve was marked by a short stationary phase and the optical density declined after the 12<sup>th</sup> hour. Cadmium was highly toxic to this isolate since biomass did not increase throughout the course of the study. However, the isolate showed exceptional growth in the presence of lead and nickel.



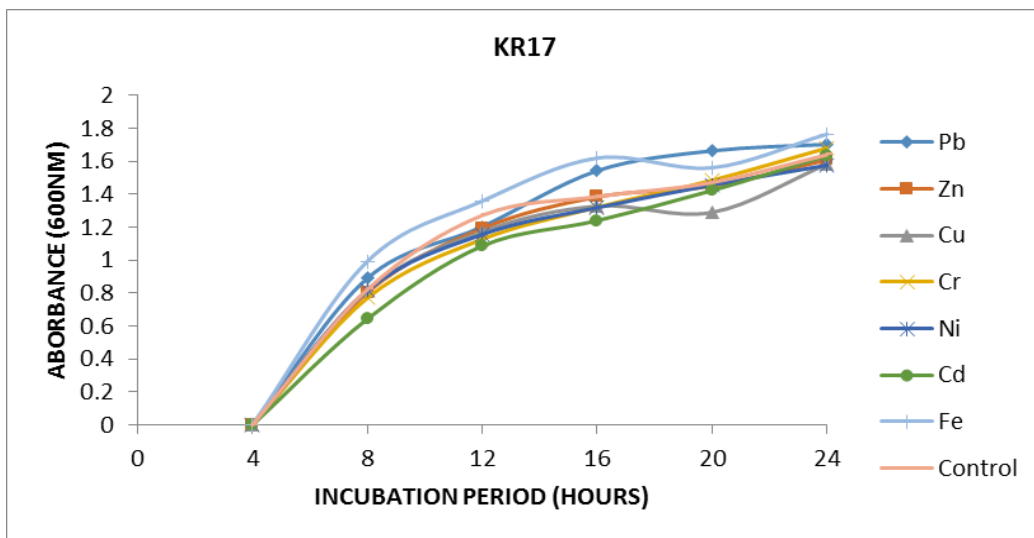
**Figure 50: Growth curves of KR07 in the absence and presence of heavy metals**

Figure 51 displays the growth pattern of KR08. The growth of this isolate was greatly repressed in the presence of cadmium; and the growth rate decreased in the presence chromium. However, the presence of Pb, Zn, Cu, Ni and Fe the other metals appeared to have little to no apparent effect on the growth rate of this isolate. The isolate entered its exponential phase early; as observed in the graph; no lag phase was noted and the stationary phase was reached in the 16<sup>th</sup> hour.



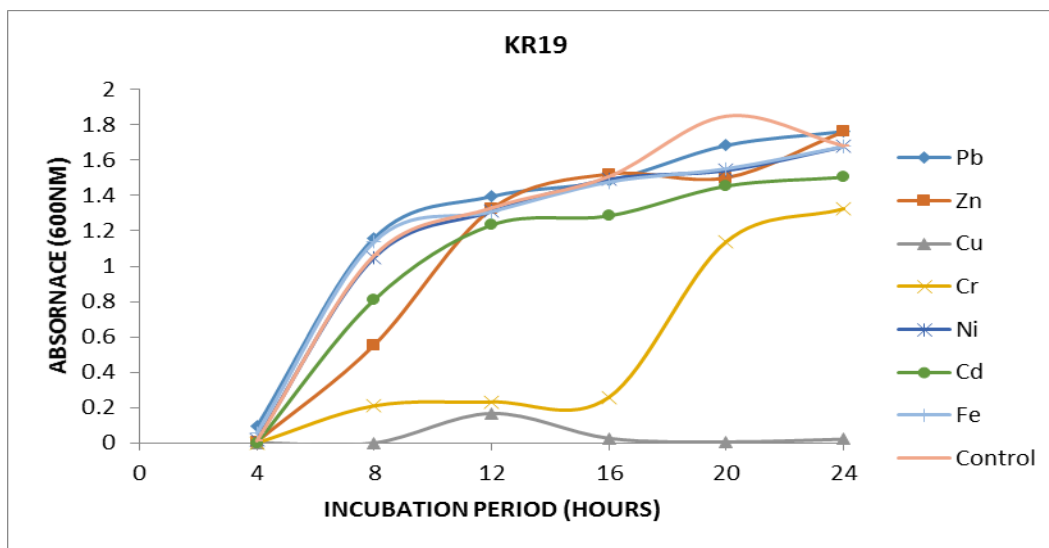
**Figure 51: Growth curves of KR08 in the absence and presence of heavy metals**

KR17 (Fig. 52) grew extremely well in the presence of all the heavy metals under study. The highest growth rates were observed for iron and lead. Conversely, growth was slightly repressed in the presence of chromium.



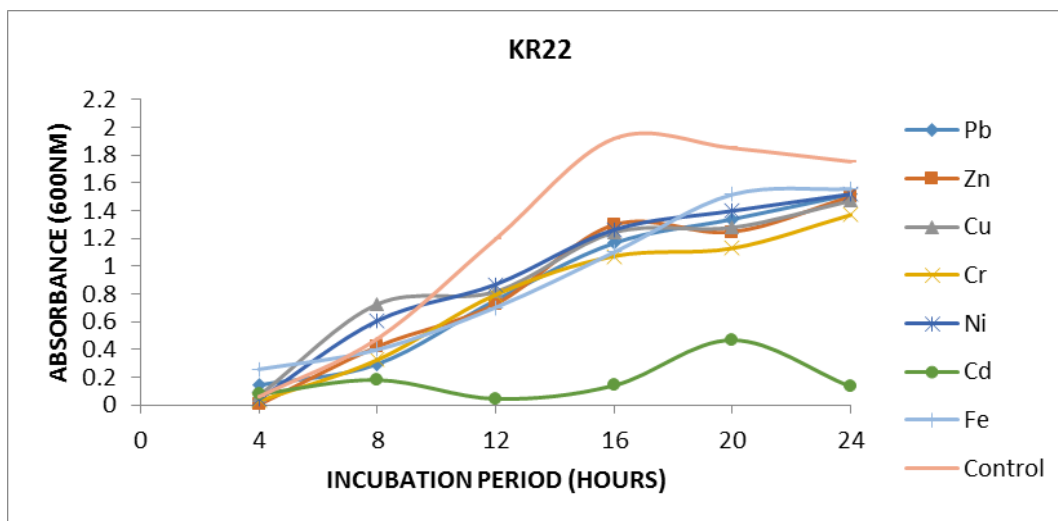
**Figure 52: Growth curves of KR17 in the absence and presence of heavy metals**

Figure 53 illustrates the growth pattern of KR19. Copper proved to be quite toxic to this isolate and a prolonged lag phase was noted in the presence of chromium; however the presence of cadmium, lead, iron, zinc and nickel did not influence the growth pattern of KR19.



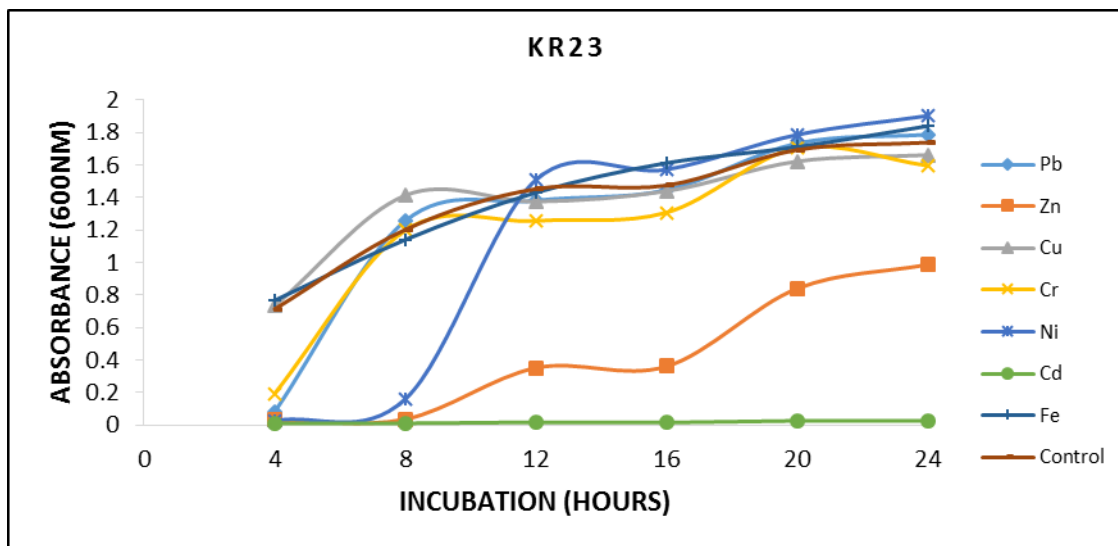
**Figure 53: Growth curves of KR19 in the absence and presence of heavy metals**

KR22 (Fig. 54) was inhibited in the presence of cadmium. A lag phase was noted for the control between the 4<sup>th</sup> and 8<sup>th</sup> hour. The isolate showed the highest growth rate in the absence of heavy metals; therefore this is an indication that the presence of heavy metal in the growth medium does inhibit the growth of this isolate.



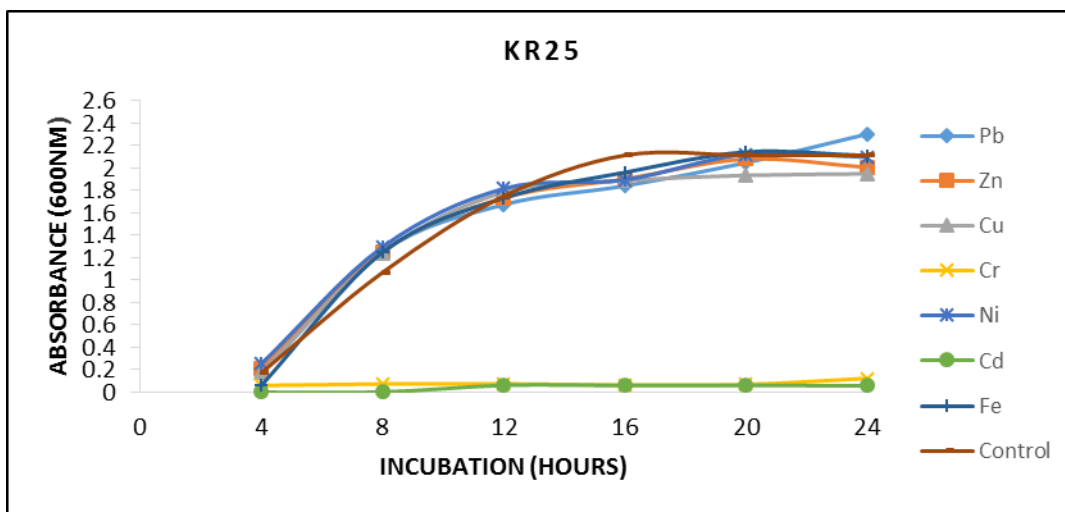
**Figure 54: Growth curves of KR22 in the absence and presence of heavy metals**

Figure 55 illustrates the growth curves of KR23. The growth of this isolate was hindered by the presence of cadmium since the absorbance remained close to zero throughout the experiment. The isolate experienced prolonged lag phases in the presence of zinc and nickel before the 8<sup>th</sup> hour. The growth curve in the presence of nickel was marked by a sharp increase and the growth rate decreased after the 12<sup>th</sup> hour as the isolate entered its stationary phase.



**Figure 55: Growth curves of KR23 in the absence and presence of heavy metals**

KR25 (Fig. 56) exhibited a typical growth curve pattern in the presence of lead, zinc, nickel, copper and iron. The growth rates of the isolate in the presence of previously mentioned metals were more or less identical to each other. However, the growth of this isolate was hindered in the presence of chromium and cadmium.



**Figure 56: Growth curves of KR25 in the absence and presence of heavy metals**

For KR29 (Fig. 57) the isolate was negatively affected by the presence of chromium and cadmium. The growth pattern in the presence of Pb, Zn, Ni, Cu and Fe was almost similar to the control, showing that this isolate is not affected by the presence of these metals.

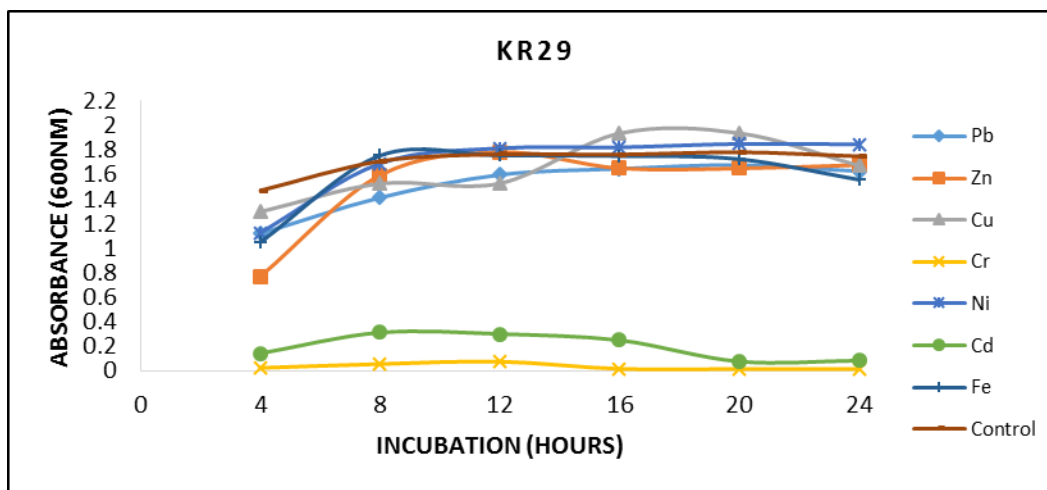


**Figure 57: Growth curves of KR29 in the absence and presence of heavy metals**

KR44 (Fig. 58) was the most adversely affected isolate as shown by the erratic growth patterns exhibited by the isolate. The isolate did not grow well in the absence of heavy metals as shown by the control. The control experienced a prolonged lag phase and exponential growth was noted after 20 hours. However, this isolate grew remarkably well in the presence of chromium.

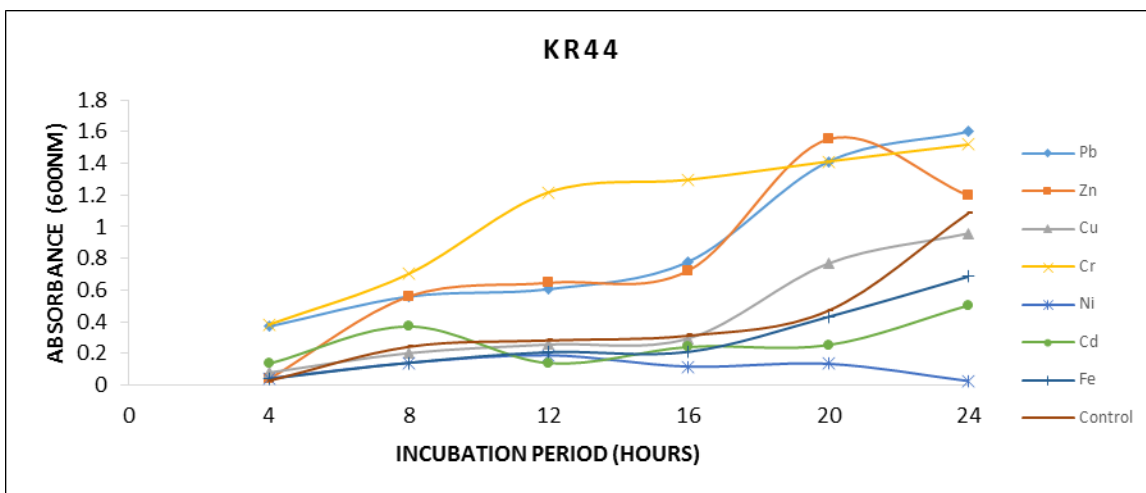


**Figure 58: Growth curves of KR44 in the absence and presence of heavy metals**

For KR48 (Fig. 59) the isolate was mostly affected by the presence of cadmium; however a slight increase was noted in the optical density in the 20<sup>th</sup> hour. A lag phase in the presence of zinc and iron was also observed between the 4<sup>th</sup> and 8<sup>th</sup> hour. The highest growth rate was recorded in the absence of heavy metals as shown by the control curve.

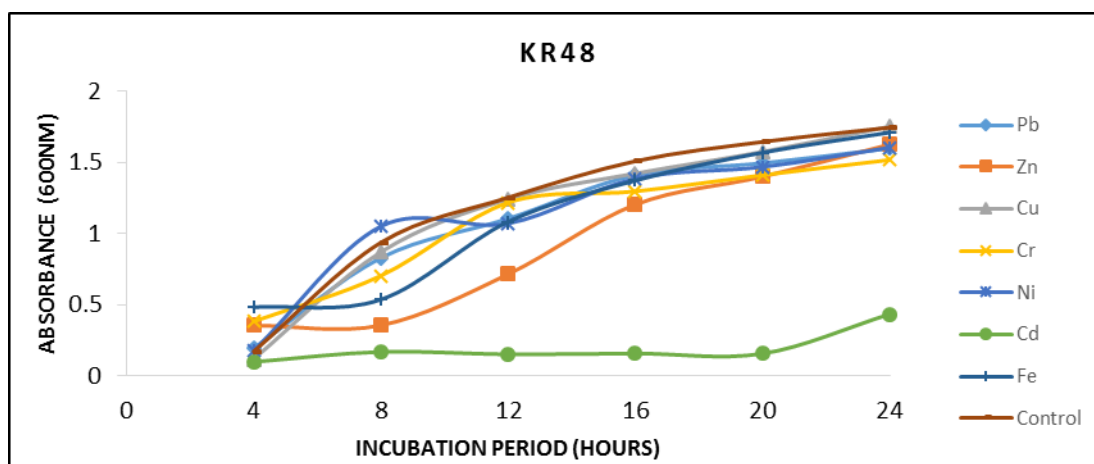


**Figure 59: Growth curves of KR48 in the absence and presence of heavy metals**

**Table 11: Specific and average growth rates of the bacterial isolates in the presence and absence of heavy metals**

The isolates KR01, KR17 and KR25 showed the highest mean specific growth rate, whereas KR44 exhibited the lowest (Table 13).

Strain	Phylogenteic group	Specific growth rate ( $\mu$ /h)							Control	Mean specific growth rate
		Pb (0.2mM)	Zn (0.2mM)	Cu (0.2mM)	Cr (0.2mM)	Ni (0.2mM)	Cd (0.2mM)	Fe (0.2mM)		
KR01	<i>Aeromonas hydrophila</i>	83.9	76.55	77.7	61.5	76.8	75.95	78.9	77.7	76.125
KR02	<i>Bacillus sp.</i>	62.3	64	81.5	57.05	77.85	55.2	64.85	61.85	65.575
KR04	<i>Bacillus megaterium</i>	63.8	61.65	72.8	40.5	69.9	-0.05	73.45	62.85	55.6125
KR06	<i>Bacillus subtilis</i>	59.2	52.95	73.15	51.65	54.8	-0.05	57.4	57.6	50.8375
KR07	<i>Pseudomonas</i>	72.65	69.85	86.1	9.1	81.5	0.8	71.4	77.5	58.6125
KR08	<i>Acinetobacter oleivorans</i>	64.35	67.55	70.55	48.7	67.9	2.6	73.3	69.45	58.05
KR17	<i>Proteus penneri</i>	83.15	72.45	64.45	74.2	72.75	71.1	78	73.5	73.7
KR19	<i>Aeromonas sp.</i>	84.15	75	.25	56.9	77.05	72.65	77.55	92.45	67
KR22	<i>Proteus sp.</i>	66.9	62.35	63.9	56.45	69.9	23.4	65.8	92.5	62.65
KR23	<i>Pseudomonas sp.</i>	86.6	41.9	81.05	85.1	89.25	1.2	85.5	84.6	69.4
KR25	<i>Lysinibacillus sp.</i>	102.3	103.95	96.7	3.7	106.15	3	107.15	105.7	78.5813
KR29	<i>Escherichia coli</i>	83.8	82.45	96.85	0.7	92.45	3.75	86.25	89.05	66.9125
KR44	<i>Bacillus licheniformis</i>	70.5	77.6	38.35	70.55	6.7	12.6	21.5	23.45	40.1563
KR48	<i>Arthrobacter sp.</i>	74.45	70	70.75	70.55	73.4	7.7	78.45	82.25	64.729

#### 4.13 16SrDNA Sequencing and Phylogentic analysis

PCR amplification of the 16SrDNA genes produced fragments of approximately 1500 base pairs in size (Fig. 60-61). Identification of the strains isolated in this study using comparative analysis of the 16SrDNA sequences (Appendix XIII) that were aligned with previously obtained sequences in the NCBI database is shown in Table 14. The sequences were used to construct a phylogenetic tree shown in Fig. 62. Figure 62 summarizes the phylogenetic relationships of the heavy metal resistant isolates. The isolates were grouped into three phyla; namely, *gamma-proteobacteria*, *firmicutes* and *actinobacteria*.

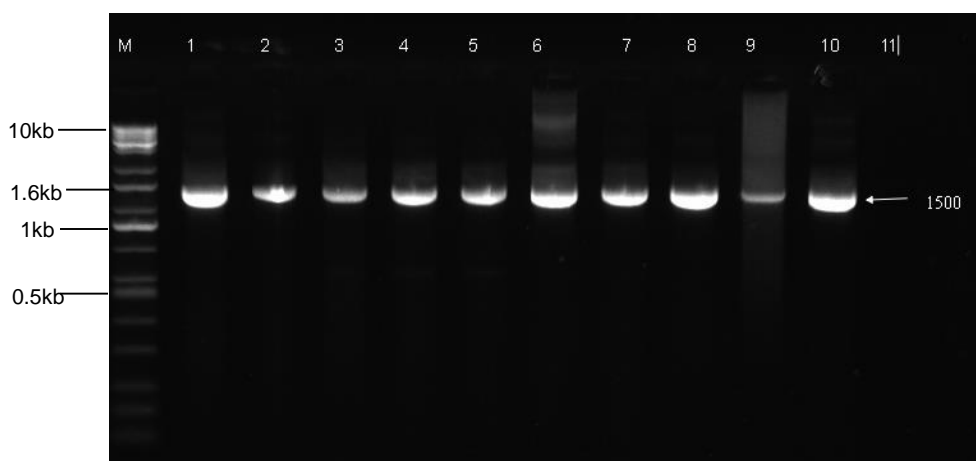


**Figure 60:** PCR amplification products of the 16SrDNA gene from the isolates separated on a 1% agarose gel and stained with ethidium bromide. Lanes represent the following: M. KAPA Universal Ladder, 1. KR44, 2. KR48, 3. KR33, 4. KR06, 5. KR08, 6. KR18, 7. KR25, 8. KR07, 9. KR01, 10. KR29 and 11. Negative control.

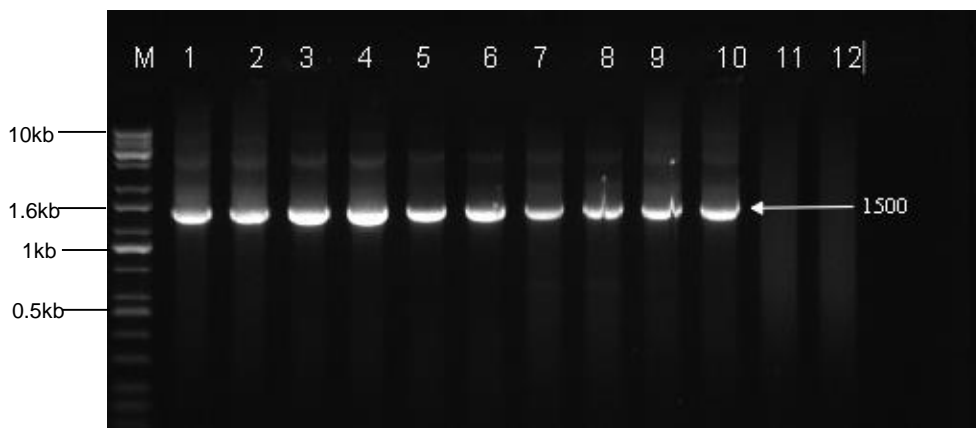


**Figure 61:** PCR amplification products of the 16SrDNA gene from the isolates separated on a 1% agarose gel and stained with ethidium bromide. Lanes represent the following: M. KAPA Universal Ladder, 1. KR19, 2. KR19, 3. KR22, 4. KR22, 5. KR23, 6. KR23, 7. KR04, 8. KR04, 9. KR17, 10. KR17 and 11. Negative control.

**Table 12: Comparative and phylogenetic analysis of 16SrDNA sequences of heavy metal resistant isolates from the Klip River using highly matched species available in NCBI**

Strains	Sequence Length	Accession no.	Highly matched bacteria/accession no.	% Similarity	Confidence level
KR01	1142	KJ935907	<i>Aeromonas hydrophila</i> strain M-1/HQ609947.1	99	Species
KR02	1155	KJ935908	<i>Bacillus</i> sp. hb91/KF8638801	99	Species
KR03			Not identified		
KR04	1157	KJ935909	<i>Bacillus megaterium</i> strain 1AR1-AN28	98	Genus
KR06	1146	KJ935910	<i>Bacillus subtilis</i> strain P38/JQ669676.1	99	Genus
KR07	1153	KJ935911	<i>Pseudomonas</i> F15/KF573430.1	97	Genus
KR08	1171		Not identified	84	No match
KR17	1136	KJ935912	<i>Proteus penneri</i> T202/KC764983.1	98	Genus
KR18	1152	KJ935913	<i>Shewanella</i> enriched culture clone AP-Enrich 20/JX82848.1	99	Species
KR19	1145	KJ935914	<i>Aeromonas</i> sp. IW-211/KF556692.1	98	Genus
KR22	1142	KJ935915	<i>Proteus</i> sp. W15 Dec34/JN106439.1	99	Species
KR23	1135	KJ935916	<i>Pseudomonas</i> sp. THG/KF532133.1	99	Species
KR25	1123	KJ935917	<i>Lysinibacillus</i> sp. C22 KF720925.1	99	Species
KR29	1139	KJ935918	<i>Escherichia coli</i> S5-6/ KC202264.1	98	Genus
KR44	1141	KJ935919	<i>Bacillus licheniformis</i> H37/KC441790.1	99	Species
KR48	1164	KJ935920	<i>Arthrobacter</i> sp. SMP5	98	Genus



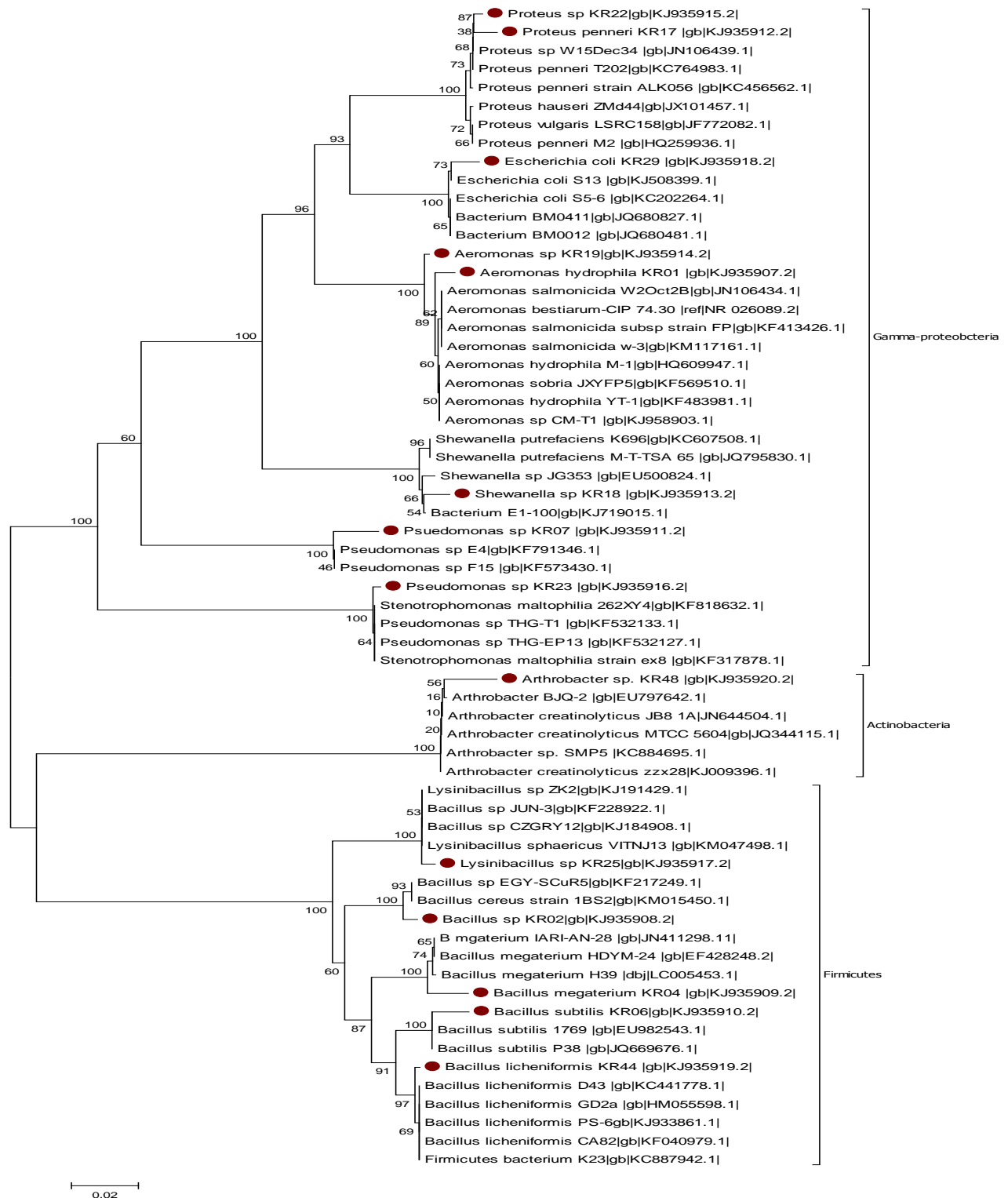


**Figure 62:** The evolutionary history was inferred using the Neighbour Joining Method (Saitou & Nei 1987). The optimal tree with the sum branch length 0.82472703 is shown. The percentage of the replicate trees in which the associated taxa clustered together in the bootstrap test (1000 replicates) are shown next to the branches (Felsenstein 1985). The evolutionary distances were computed using the Kimura 2-parameter model (Kimura 1980) and are in the units of the number of base substitutions per site. The analysis involved 63 nucleotide sequences. Evolutionary analysis was conducted using MEGA 6 (Tamura *et al.* 2013). The red markers indicate the bacterial strains identified in this study.

#### 4.14 PCR amplification of heavy metal resistance genes

No amplification products were obtained for the primers representing the *czcA*, *czcB*, *czcD* and *cadCA* genes (*Results not shown*).

For amplification of lead resistance genes, primers were designed based on the different genes found on the *pbr* operon of the pMOL30 mega plasmid of *C. metallidurans* CH34 (Borremans *et al.* 2001). The six primers targeting *pbrT*, *pbrR* and *pbrA* related genes were designed by Davis (2011). The amplification of *pbr* genes from the lead resistant isolates (Fig. 63-67, Table 15) led to amplified fragments which were not of expected sizes and multiple fragments were obtained in some cases.

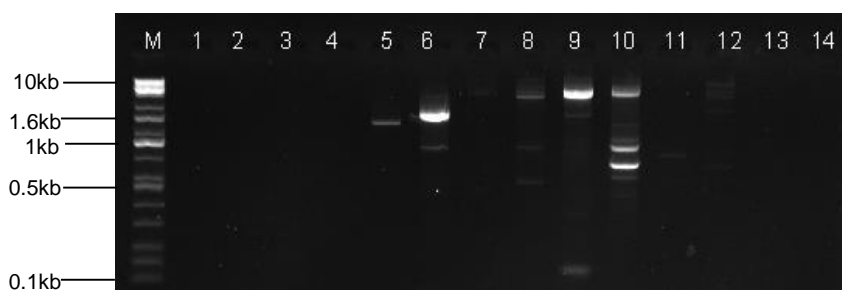


**Figure 63: PCR amplification products of the *pbrT* gene from isolates using pbr8-9 primers. PCR fragments were visualized on a 1% agarose gel stained with ethidium bromide. Lanes represent the following: M. KAPA Universal Ladder, 1. Negative control, 2. KR01, 3. KR02, 4. KR03, 5. KR06, 6. KR07, 7. KR08, 8. KR17, 9. KR18, 10. KR19, 11. KR23, 12. KR25, 13. KR44 and 14. KR48**

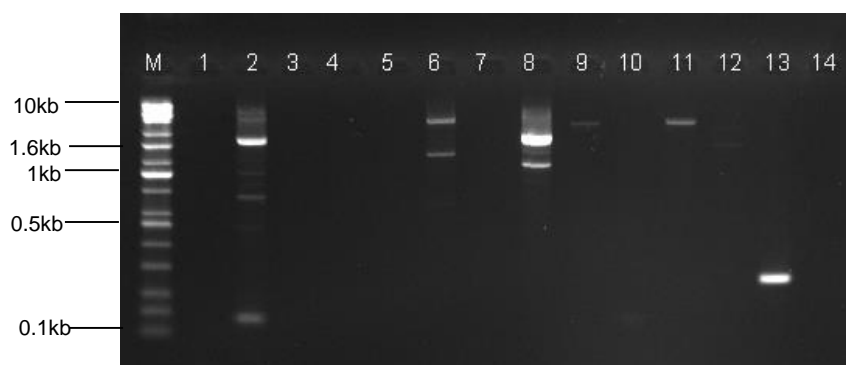


**Figure 64: PCR amplification products of the *pbrT* gene from isolates using pbr10-11 primers. PCR fragments were visualized on a 1% agarose gel stained with ethidium bromide. Lanes represent the following: M. KAPA Universal Ladder, 1. Negative control, 2. KR01, 3. KR02, 4. KR03, 5. KR06, 6. KR07, 7. KR08, 8. KR17, 9. KR18, 10. KR19, 11. KR23, 12. KR25, 13. KR44 and 14. KR48**

PCR amplification of *pbrT* gene sections from isolates using pbr12-13 primers. PCRs were set up as described in Section 3.17.2. However, there was no amplification observed.

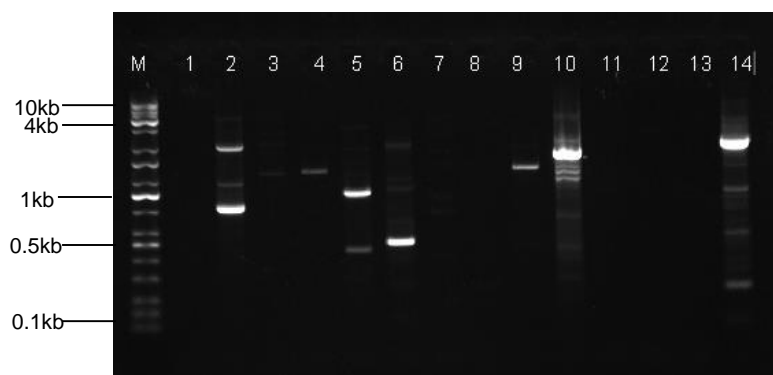


**Figure 65: PCR amplification of *pbrTR* gene from isolates using pbr14-15 primers. PCR fragments were visualized on a 1% agarose gel stained with ethidium bromide. Lanes represent the following: M. KAPA Universal Ladder, 1. Negative control, 2. KR48, 3. KR44, 4. KR25, 5. KR23, 6. KR19, 7. KR18, 8. KR17, 9. KR08, 10. KR07, 11. KR06, 12. KR03, 13. KR02 and 14. KR01.**

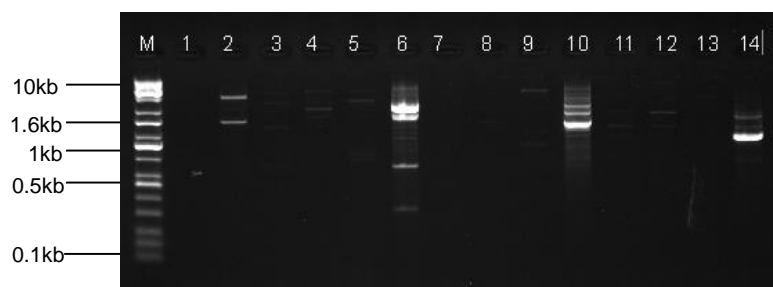


**Figure 66: PCR amplification of *pbrRA* gene from isolates using pbr16-17 primers. PCR fragments were visualized on a 1% agarose gel stained with ethidium bromide. Lanes represent the following: M. KAPA Universal Ladder, 1. Negative control, 2. KR48, 3. KR44, 4. KR25, 5. KR23, 6. KR19, 7. KR18, 8. KR17, 9. KR08, 10. KR07, 11. KR06, 12. KR03, 13. KR02 and 14. KR01.**

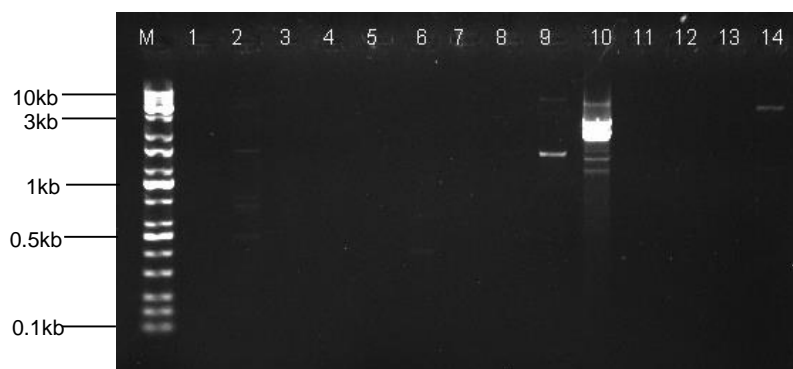


**Figure 67: PCR amplification of *pbrA* gene from isolates using pbr18-19 primers. PCR fragments were visualized on a 1% agarose gel stained with ethidium bromide. Lanes represent the following: M. KAPA Universal Ladder, 1. Negative control, 2. KR48, 3. KR44, 4. KR25, 5. KR23, 6. KR19, 7. KR18, 8. KR17, 9. KR08, 10. KR07, 11. KR06, 12. KR03, 13. KR02 and 14. KR01.**

**Table 13: Results obtained from the PCR analysis of the genomic DNA of the lead resistant isolates using pbr specific primers.**

Primer pair and gene targeted	Expected fragment size (bp)	Approximate fragment size obtained (bp)												
		KR01	KR02	KR03	KR06	KR07	KR08	KR17	KR18	KR19	KR23	KR25	KR44	KR48
Pbr8-9 <i>PbrT</i>	593	NA	NA	NA	1300	1600, 900	3000	2500, 600	3000, 1600, 125	3000, 1000, 700, 600	NA	>3000, 2000, 800	NA	NA
Pbr10-11 <i>PbrT</i>	740	>3000 1800, 1000, 700	NA	NA	NA	3000 1800	NA	1800 1200	3000	NA	3000	NA	250	NA
Pbr12-13 <i>pbrT</i>	807	NA	NA	NA	NA	NA	NA	NA	NA	NA	NA	NA	NA	NA
Pbr14-15 <i>pbrTR</i>	593	2000, 1000, 500, 200	NA	NA	NA	3000, 1400, 1300	1600	NA	NA	2200 1200, 1000, 700, 500	1000 450	1400	1400	>3000 2200, 1200, 850
Pbr16-17 <i>pbrRA</i>	766	2000, 1600, 1200	NA	2000	1600	2500, 2000, 1600	3000	NA	NA	2500, 2000, 1750, 1200, 700, 300	2500	3000, 2000	3000	3000, 1600
Pbr18-19 <i>pbrA</i>	769	3000	NA	NA	NA	3000, 2000, 1600, 1200	1600	NA	NA	NA	NA	NA	NA	NA

NA: No amplification

Fragments of approximately 1700 bp were obtained for *Lysinibacillus* strain KR25 and *E. coli* KR29 with the *pcoA* primers. Amplification was repeated for the microorganisms and the final results are shown in Fig. 71.

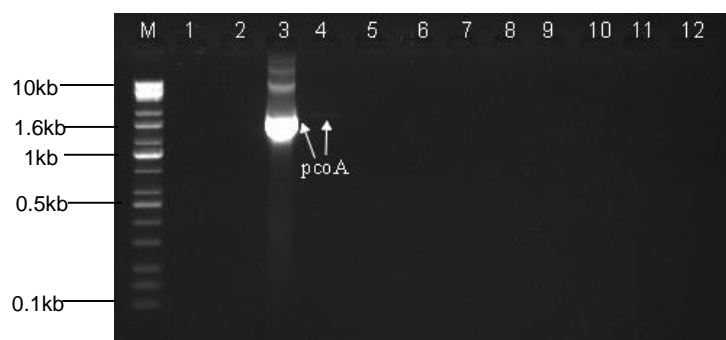


**Figure 68: PCR amplification of *pcoA* gene from the isolates. PCR fragments were visualized on a 1% agarose gel stained with ethidium bromide. Lanes represent the following: M. KAPA Universal Ladder, 1. Negative control, 2. KR44, 3. KR29, 4. KR25, 5. KR23, 6. KR19, 7. KR17, 8. KR06, 9. KR04, 10. KR03, 11. KR02 and 12. KR01**

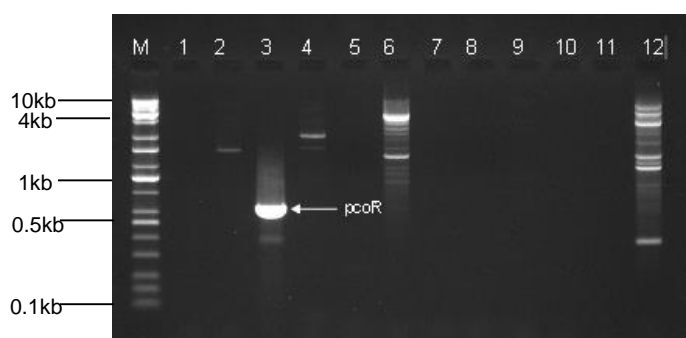


**Figure 69: PCR amplification of *pcoR* gene from isolates. PCR fragments were visualized on a 1% agarose gel stained with ethidium bromide. Lanes represent the following: M. KAPA Universal Ladder, 1. Negative control, 2. KR44, 3. KR29, 4. KR25, 5. KR23, 6. KR19, 7. KR17, 8. KR06, 9. KR04, 10. KR03, 11. KR02 and 12. KR01**

**Table 14: Results obtained from the PCR analysis of the genomic DNA from the PCR analysis of the genomic DNA from the copper resistant isolates using *pcoA* and *pcoR* specific primers**

Primer pair and gene targeted	Expected fragment size (bp)	Aproximate fragment size obtained (bp)										
		KR01	KR02	KR03	KR04	KR06	KR17	KR19	KR23	KR25	KR29	KR44
<i>pcoA</i>	1791	NA	NA	NA	NA	NA	NA	NA	NA	1800	1800	NA
<i>pcoA</i>												
<i>pcoR</i>	636	4000, 3500, 3000, 1600, 1500, 1200, 400	NA	NA	NA	NA	NA	4000, 3000, 1600	NA	2200, 1600	600	3000
<i>pcoR</i>												

Using chrB primers for amplifying the *chrB* gene from chromate resistant isolates, a fragment of estimated size, 400 bp was obtained for *Pseudomonas* sp. (KR23). Amplification was repeated for this isolate and the final results are shown in Fig. 71.



**Figure 70: PCR amplification of *chrB* gene from isolates. PCR fragments were visualized on a 1% agarose gel stained with ethidium bromide. Lanes represent the following: M. KAPA Universal Ladder, 1. KR01, 2. KR02, 3. KR04, 4. KR06, 5. KR07, 6. KR08, 7. KR17, 8. KR18, 9. KR22, 10. KR23, 11. KR25, 12. KR29, 13. KR44 and 14. KR48**

The chrB primers produced a fragment of approximately 400 bp (Fig. 71) in *Pseudomonas* sp. (KR23). This amplicon was designated chrB\_23. Amplification with the pcoA primers produced a fragment of 1.7 kb in the bacterial strains *Lysinibacillus* sp. (KR25) and *E. coli* (KR29) (Fig. 71). These amplicons were designated as pcoA\_25 and pcoA\_29, respectively. The pcoR primers produced a band of approximately 600 bp (Fig. 71) in *E.coli* (KR29) which was designated pcoR\_29.

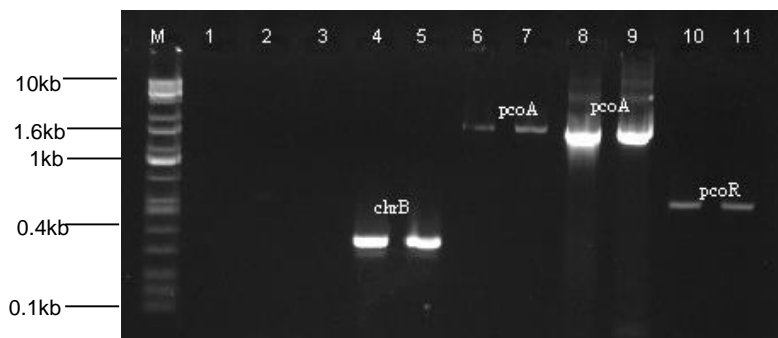


**Figure 71: PCR amplification of *chrB*, *pcoA* and *pcoR* genes from the isolates KR23, KR25 and KR29. The amplicons were visualized on a 1% agarose gel. Lanes represent the following: M 1. KAPA Universal Ladder, 2. Negative control for chrB primers, 2. Negative control for pcoA primers, 3. Negative control for pcoR primers, 4. chrB\_23; 5. chrB\_23, 6. pcoA\_25, 7. pcoA\_25, 8. pcoA\_29, 9. pcoA\_29, 10. pcoR\_29 and 11. pcoR\_29.**

#### 4.15 Homology analysis of amplified genes

The putative protein sequences translated from the nucleotide sequences are shown in Fig. 72.

**(a)**

1 - ATCCGGCCGGCGACATCATGGGCGCGATGGGCTTTGAGCACCGCAGCGAAGAAGCCAGCT - 60  
1 - M G A M G F E H R S E E A S Y - 15

61 - ACACCCCGGACCTGATGGTGCAGAAGGGCCAGATCGCCGGCACCACCGGCCAGCCGACCC - 120  
16 - T P D L M V Q K G Q I A G T T G Q P T R - 35

121 - GTGGCGACTACTCGCTCAACGAGGTCTACCTGGAAATGCAGGTGCCGCTGCTGGCCGACA - 180  
36 - G D Y S L N E V Y L E M Q V P L L A D M - 55

181 - TGGCCTTCGCCCCGCGAGCTGTCTGCTGGACCTGGCCGGTCTGCTACACCGACTACAACACCT - 240  
56 - A F A R E L S L D L A G R Y T D Y N T F - 75

241 - TCGGTTTCGACCACCAACAGCAAGTTCGGCCTGAAGTGGAAGCCGATCGACATCTTGCTTT - 300  
76 - G S T T N S K F G L K W K P I D I L L S - 95

301 - CC - 302 96 - X

**(b)**

1 - GGGAACCCCGGGAAAGCTTCGGCGTATGGAGTTTCAATCCCGCGTTCCAGTCTGAGCCTG - 60  
1 - M E F Q S R V P V \* A C - 12

61 - CCAGTTGCCGACTCCTGCAGGTACTCAGTTTGACCTGACCATTGGTGAAACGGCCGTCAA - 120  
13 - Q L P T P A G T Q F D L T I G E T A V N - 32

121 - TATCACGGGCAGTGAGCGTCAGGCCAAAACAATCAATGGAGGCCTGCCGGGGCCCGTTCT - 180  
33 - I T G S E R Q A K T I N G G L P G P V L - 52

181 - TCGCTGGAAAGAAGGTGACACCATTACCCTGAAGGTCAAAAACCGTCTTAATGAACAGAC - 240  
53 - R W K E G D T I T L K V K N R L N E Q T - 72

241 - GTCCATTCACTGGCACGGCATTATTCTTCCGGCCAATATGGATGGTGTTCCGGGGCTGAG - 300  
73 - S I H W H G I I L P A N M D G V P G L S - 92

301 - TTTTATGGGCATAGAGCCTGATGATACCTACGTTTACACCTTTAAGGTTAAGCAGAACGG - 360  
93 - F M G I E P D D T Y V Y T F K V K Q N G - 112

361 - GACTTACTGGTACCACAGCCATTCCGGTCTGCAGGAACAGGAGGGGTATACGGTGCCAT - 420  
113 - T Y W Y H S H S G L Q E Q E G V Y G A I - 132

421 - TATCATCGATGCCAGGGAGCCAGAACCGTTTGCTTACGATCGTGAGCATGTGGTCATGTT - 480  
133 - I I D A R E P E P F A Y D R E H V V M L - 152

481 - GTCTGACTGGACCGATGAAAATCCTCACAGCCTGCTGAAAAAATTAAAAAACAGTCGGA - 540  
153 - S D W T D E N P H S L L K K L K K Q S D - 172

541 - TTACTACAATTTCAATAAACCAACCGTTGGCTCTTTTTTCCGCGACGTGAATACCAGGGG - 600  
173 - Y Y N F N K P T V G S F F R D V N T R G - 192

601 - GCTGTGACCCACCATTGCCGATCGGAAAATGTGGGCTGAAATGAAATGAATCCGACTGA - 660  
193 - L S A T I A D R K M W A E M K M N P T D - 212

661 - CCTCGCGGATGTCTAGTGGCTACACCTACACCTATCTCATGAACGGGCAGGCCCCGCTGAA - 720  
 213 - L A D V S G Y T Y T Y L M N G Q A P L K - 232

721 - AACTGGACCGGACTGTTCCCGTCCCGGTGAAAAGATACGCTTACGGTTTTATCAACGGCT - 780  
 233 - T G P D C S R P G E K I R L R F Y Q R L - 252

781 - CGGCAATGACCTATTTTCGATATCCGTATCCCCGGGGTGAAAATGACGGTCGTGGCTGCA - 840  
 253 - G N D L F S I S V S P G \* K \* R S W L Q - 272

841 - GATGGGCCAGTATGTAACCCGGTTACCGGTGACAATTCAGGATTGCCGTTGCCCCGAAACC - 900  
 273 - M G Q Y V T R L P V T I Q D C R C P K P - 292

901 - TAATGAGGTCATGGGGGAGCCTCGGGTGAAGGCCCATACAATCTTCCAC - 949  
 293 - N E V M G E P R V K A H T I F H X - 312

**(c)**

1 - CCCAGGCGTACCCGGAAGTCTTGGCGTATGGAGTTTCAATGCGCGTTCCAGTCTGAGCCT - 60  
 1 - M E F Q C A F Q S E P - 11

61 - GCCAGTTGCCGCATCCCTGCAGGGTACTCAGTTTGACCTGACCATTGGTGAAACGGCCGT - 120  
 12 - A S C R I P A G Y S V \* P D H W \* N G R - 31

121 - CAATATCACGGGCAGTGAGCGTCAGGCCAAAACAATCAATGGAGGCCTGCCGGGGCCCGT - 180  
 32 - Q Y H G Q \* A S G Q N N Q W R P A G A R - 51

181 - TCTTCGCTGGAAGAAGGTGACACCATTACCCTGAAGGTCAAAAACCGTCTTAATGAACA - 240  
 52 - S S L E R R \* H H Y P E G Q K P S \* \* T - 71

241 - GACGTCCATTCACTGGCACGGCATTATTCTTCCGGCCAATATGGATGGTGTTCGGGGCT - 300  
 72 - D V H S L A R H Y S S G Q Y G W C S G A - 91

301 - GAGTTTTATGGGCATAGAGCCTGATGATACCTACGTTTACACCTTTAAGGTTAAGCAGAA - 360  
 92 - E F Y G H R A \* \* Y L R L H L \* G \* A E - 111

361 - CGGGACTTACTGGTACCACAGCCATTCCGGTCTGCAGGAACAGGAGGGGGTATACGGTGC - 420  
 112 - R D L L V P Q P F R S A G T G G G I R C - 131

421 - CATTATCATCGATGCCAGGGAGCCAGAACCGTTTGCTTACGATCGTGAGCATGTGGTCAT - 480  
 132 - H Y H R C Q G A R T V C L R S \* A C G H - 151

481 - GTTGTCTGACTGGACCGATGAAAATCCTCACAGCCTGCTGAAAAAATTAAAAAACAGTC - 540  
 152 - V V \* L D R \* K S S Q P A E K I K K T V - 171

541 - GGATTACTACAATTTCAATAAACCAACCGTTGGCTCTTTTTTCCGCGACGTGAATACCAG - 600  
 172 - G L L Q F Q \* T N R W L F F P R R E Y Q - 191

601 - GGGGCTGTCAGCCACCATTGCCGATCGGAAAATGTGGGCTGAAATGAAAATGAATCCGAC - 660  
 192 - G A V S H H C R S E N V G \* N E N E S D - 211

661 - TGACCTCGCGGATGTCTAGTGGCTACACCTACACCTATCTCATGAACGGGCAGGCCCCGCT - 720  
 212 - \* P R G C Q W L H L H L S H E R A G P A - 231

721 - GAAAACTGGACCGGACTGTTCCCGTCCCGGTGAAAAGATACGCTTACGGTTTTATCAACGG - 780  
 232 - E K L D R T V P S R \* K D T L T V Y Q R - 251

781 - CTCGGCAATGACCTATTTTCGATATCCGTATCCCCGGGCTGAAAATGACGGTCGTGGCTGC - 840  
 252 - L G N D L F R Y P Y P R A E N D G R G C - 271



841 - AGATGGCCAGTATGTAAACCCGGTTACCGTTGACGAATTCAGGATTGCCGTTGCCGAAAC - 900  
 272 - R W P V C K P G Y R \* R I Q D C R C R N - 291  
  
 901 - CTATGATGTCATTGTGGAGCCTCAGGGTGAGGCCTATACCATCTTCGCACAATCCATGGA - 960  
 292 - L \* C H C G A S G \* G L Y H L R T I H G - 311  
  
 961 - CAGGACCGGTTACGCTCGAGGGACACTGGCCACGAGAGAGGGGTAAAGTGCTGCCGTTCC - 1020  
 312 - Q D R L R S R D T G H E R G V K C C R S - 331  
  
 1021 - CCCCTCGATCCCCGTCTCTGTGACCATGGAGATATGGGTATGGGGGGGAATGGGACATG - 1080  
 332 - P L D P R P L \* P W R Y G Y G G E W D M - 351  
  
 1081 - ATATGGCAGAATGGACCACAGCAGATGGAAGCATGGTATACAGCCGAGAAGATGATGTCT - 1140  
 352 - I W Q N G P Q Q M E A W Y T A E K M M S - 371  
  
 1141 - TATTGGGAAGGCGGT - 1155  
 372 - Y W E G G - 389

**(d)**

1 - ATAGAAGCTTCAGGCCGATCTCTTTATAATGGCCGCGATGGTCTCGGGGCCGCGTCGAAG - 60  
 1 - M A A M V S G P R R R - 11  
  
 61 - GGACAGTATGATTTGATAATACTGGACGTGATGCTGCCTTTCTCGACGGGTGGCAAATC - 120  
 12 - D S M I \* \* Y W T \* C C L S S T G G K S - 31  
  
 121 - ATCAGCGCACTGAGGGAGTCCGGGCACGAAGAACCGGTCCTGTTTTTAACCGCAAAGGAC - 180  
 32 - S A H \* G S P G T K N R S C F \* P Q R T - 51  
  
 181 - AACGTGCGGGACAAAGTGAAAGGACTGGAGCTTGGCGCAGATGACTACCTGATTAAGCCC - 240  
 52 - T C G T K \* K D W S L A Q M T T \* L S P - 71  
  
 241 - TTTGATTTTACGGAGCTGGTTGCACGTGTAAGAACCCTACTGCGCCGGGCACGCTCGCAG - 300  
 72 - L I L R S W L H V \* E P Y C A G H A R R - 91  
  
 301 - GCCGCAACAGTCTGCACCATCGCCGATATGACCGTTGATATGGTGCGCCGGACCGTGATC - 360  
 92 - P Q Q S A P S P I \* P L I W C A G P \* S - 111  
  
 361 - CGTTTCGGGGAAGAAGATCCATCTCACCGGTAAAGAATACGTTCTGCTTGAGTTGCTGCTG - 420  
 112 - V R G R R S I S P V K N T F C L S C C C - 131  
  
 421 - CAACGCACCGGAGAAGTGTTACCCAGGAGTCTTATCTCGTCCCTGGTCTGGAACATGAAT - 480  
 132 - N A P E K C Y P G V L S R P W S G T \* I - 151  
  
 481 - TTTGACAGTGATACGAATGTGATTGATGTGCGCGTGAGACGTCTGAGAAGTAAATTTGAT - 540  
 152 - L T V I R M \* L M S P \* D V \* E V K L M - 171  
  
 541 - GATGACTTTGAGCCAAAAGTATCCATACCGTTTCGCGGTGCCGGATATGTCCTGAAAAAA - 600  
 172 - M T L S Q N \* S I P F A V P D M S \* K N - 191  
  
 601 - TCAAAGGA - 608  
 192 - Q R X

**Figure 72: Translated partial protein sequences of (a) chrB\_23 (b) pcoA\_25, (c) pcoA\_29 and (d) pcoR\_29.**

The BLASTp analysis for chrB\_23 aligned with 100 protein sequences in the database. Ninety seven (97%) of the query sequence from the chrB\_23, showed a 99% homology to a vitamin B12 transporter btuB in *Stenotrophus* sp. RIT309 [EZP42970.1] and a TonB dependant receptor protein found in *S. maltophilia* (SBA-1-2) [EVT68491.1]. The sequences that were obtained in the blastp alignment search were used to construct a phylogenetic tree (Fig. 73).

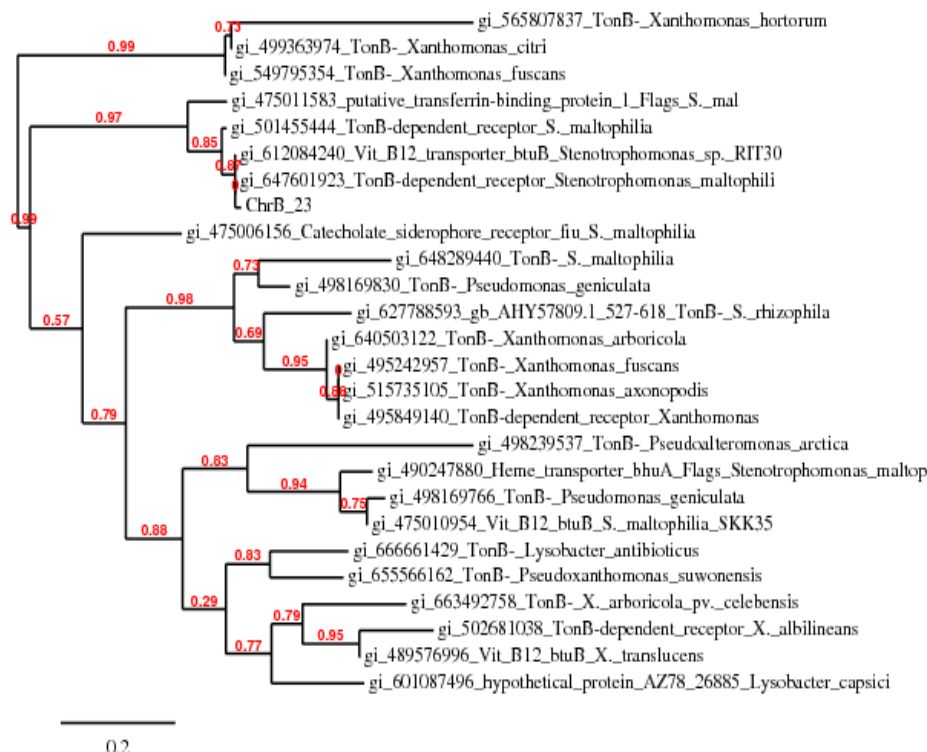


**Figure 73: Phylogenetic tree representing related protein sequences found in the Genbank database using chrB\_23 as the query. The tree was built using the Maximum Likelihood Method and the Approximate Likelihood –Ratio Test was used as statistical tests for branch support**

Sequence comparisons of the pcoA fragment amplified from *Lysinibacillus* sp. strain KR25 (pcoA\_25) showed high homology with copper resistance genes from other bacteria. For example, there was 82% homology with a copper resistant protein from both *Cronobacter turicensis* [YP003212800.1] and the copA protein in *E. coli* [WP\_001381484]. Two putative conserved domains belonging to the *cupredoxin* domain of copper resistance protein family were detected from the Conserved Domain Database (Marchler-Bauer *et al.* 2011) (APPENDIX XVI). Therefore several copA protein sequences were obtained from the Blastp programme. The pcoA\_25 protein was closely affiliated with orthologs from the following genera: *Klebsiella*, *Citrobacter*, *Escherichia*, *Cronobacter*, *Serratia*, *Leclercia* and *Salmonella* (Fig. 74).

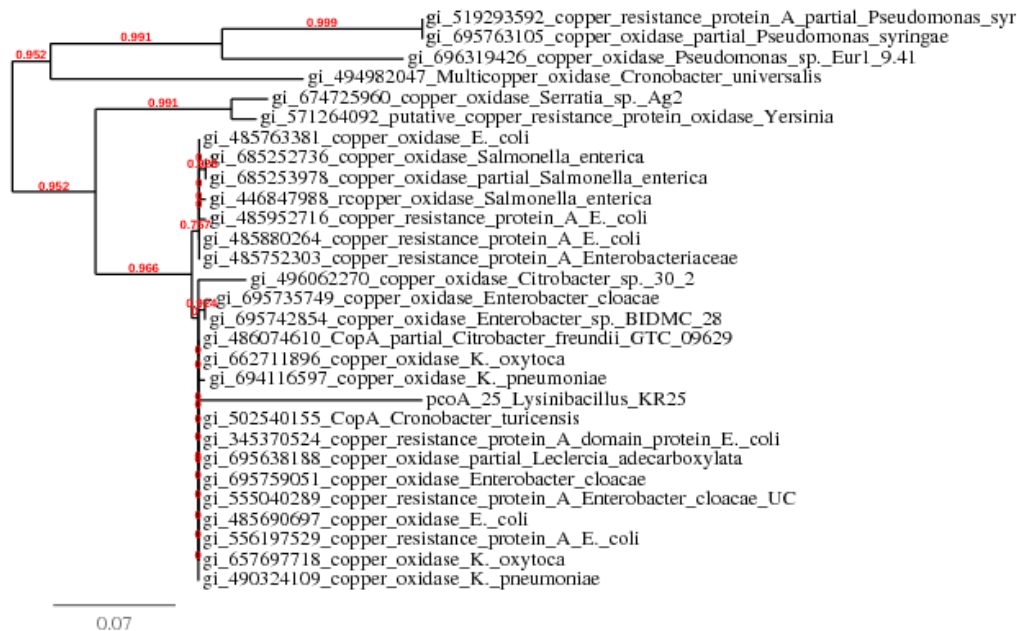


**Figure 74: Phylogenetic tree representing copA protein sequences found in the Genbank database using pcoA\_25 as the query. The tree was built using the Maximum Likelihood Method and the Approximate Likelihood –Ratio Test was used as statistical tests for branch support.**

Using the partial protein sequence of pcoA\_29 as query on the BLASTp programme, 13 orthologous sequences were retrieved. Twenty-nine amino acids (7%) of the query showed 97% similarity to 30 amino acids found in a hypothetical protein originating from *Cronobacter turicensis*. Nineteen amino acids (5%) of the pcoA\_29 query sequence also showed 100% similarity to 19 amino acids found in *Klebsiella pneumoniae*. The thirteen orthologous sequences obtained from the *blastp* search were used to construct the phylogenetic tree (Fig. 75)

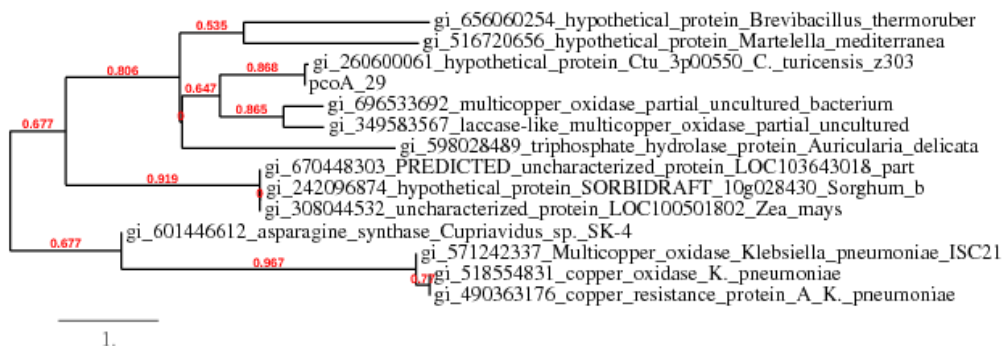


**Figure 75: Phylogenetic tree representing related protein sequences found in the Genbank database using pcoA\_29 as the query. The tree was built using the Maximum Likelihood Method and the Approximate Likelihood –Ratio Test was used as statistical tests for branch support.**

The partial protein sequence pcoR\_29, resulted in 3 hits using the BLASTp programme. Thirty-six amino acids (20% of the query cover) showed 100% similarity to 36 amino acids present in a transcriptional regulatory protein pcoR found in *E. coli* [WP014641166.1]. Forty-four percent of the query cover showed 26% similarity to 2-nitropropane dioxygenase found in *Crocinitomix catalasitica* [WP027418675.1] and 49 % of the query sequence showed 24% similarity to the 2-nitropropane dioxygenase present in *Flavobacterium frigidarium* [WP026709259.1]. The three sequences were used to construct a phylogenetic tree (Fig. 76)

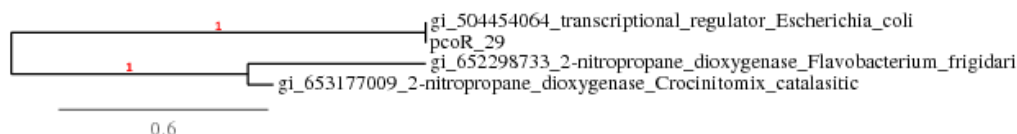


**Figure 76: Phylogenetic tree representing related protein sequences found in the Genbank database using pcoR\_29 as the query. The tree was built using the Maximum Likelihood Method and the Approximate Likelihood –Ratio Test was used as statistical tests for branch support.**

The partial primary structures of the proteins were used to predict their physico-chemical properties: the calculations were done using Expasy's Prot Param Tool (Table 17).

**Table 15: Physicochemical properties of partial protein sequences.**

Properties	ChrB_23	pcoA_25	pcoA_29	pcoR_29
Number of amino acids	96	306	357	178
Molecular weight (units)	10670.2	345634.6	41048	10670.2
Theoretical Pi	4.45	8.23	9.31	9.82
Total number of negatively charged residues (Asp+Glu)	12	33	33	7
Total number of negatively charged residues (Arg+Lys)	8	35	50	22
Extinction coefficient	12950	52620	88320	32595
Extinction coefficient*	-	52370	87320	31970
Instability Index	12.45	36.60	51.16	74.70
Aliphatic index	73.23	71.01	50.31	66.29
Grand average of hydropathicity	-0.320	-0.526	-0.931	-0.221

The first extinction coefficient is based on the assumption that all cysteine residues appear as half cystines, and the second extinction coefficient\* is based on assuming that no cysteine appears as half cystine

#### 4.16 Predictions of secondary structures using SOPMA

The predicted protein structures of ChrB\_23, pcoA\_25, pcoA\_29 and pcoR\_29 computed with the software program SOPMA (Self Optimized Prediction Method with Alignment (SOPMA) are

shown in Fig. 77. The secondary structures were constructed using the default settings (Window width: 7, similarity threshold: 8 and number of states 4).

(a)

```
MGAMGFEHRSEEASYTPDLMVQKGQIAGTTGQPTRGDYSLNEVYLEMQVPLLADMAFARELSLDLAGRYT
hhheeecccccccccccccheeettccccccccccccccccchhhhhhhhhhhhhhtcchhhhhhhhhhhccc
DYNTFGSTTNSKFGLKWKPIDILLSX
Ccccccccccccccccccccccheet
```

(b)

```

      10      20      30      40      50      60      70
      |      |      |      |      |      |      |
MEFQSRVPVACQLPTPAGTQFDLTIGETAVNITGSERQAKTINGGLPGPVLRWKEGDTITLKVKNRLNEQ
cccttccccccccccccccccceeeeeccccceetccccceeeettccccceeeettceeeeeehhtcccc
TSIHHWGIILPANMDGVPGLSFMGIEPDDTYVYTFKVKQNGTYWYHSHSGLQEQEGVYGAIIDAREPEP
ccceettteeecccccccccccccccccttceeeeeeeettceeeccccccchttccccceeecccccccc
FAYDREHVVLMSDWTDENPHSLKLLKKQSDYINFNKPTVGSFFRDVNTRGLSATIADRMWAEMKMNP
ccccceeeeeecccccccchhhhhhhhhhtccccccccchhhhhhhhhccttccchhhhhhhhhhhhhcccc
DLADVSGYTYTYLMNGQAPLKTGPDCSRPGEKIRLRFYQRLGNDLFSISVSPGKRSLQMGQYVTRLPVT
chhhhhhhheeeeeettccccccccceeccttceeeeeeeccccceeeettceeeeeettccccceee
IQDCRCPKPNEVMGEPRVKAHTIFHX
hhhhcccccheeeeeccccccccceeeeh
```

(c)

```

      10      20      30      40      50      60      70
      |      |      |      |      |      |      |
MEFQCAFQSEPASCRI PAGYSVPDHWNGRQYHGQASGQNNQWRPAGARSSLERRHHYPEGQKPDVHSL
ehhhhhhcccccccccccccccccttceeeccccccccccccccccchhhcccccttccccchhhh
ARHYSSGQYGWCSGAEFYGHAYLRLHLGAERDLLVPQPFPSAGTGGGIRCHYHRCQGARTVCLRSACGH
hhhhcttcccccttcheettchhhheeeetttttcecccccccttccccceeeettceeeecttte
VVLDRKSSQPAEKIKKTVGLLQFQTNRWLFFPREYQGA VSHHCRSENVGNENESDPRGCQWLHLHLSHE
eeettccccchhhhhhhheeeeeetceeecccttchhhheeeccccccccccccccccceeeecctt
RAGPAEKLDRTPVSRKDTLT VYQRLGNDLFRYPYPR AENDGRGCRWPVCKPGYRRIQDCRCRNLCHCGAS
ccccchhhhhhccccccccheeehhhhhtttecccccccccttcccccccccttccccccccceeeccct
GGLYHLRTIHGQDRLRSRDTGHERGVKCCRSPLDPRPLPWRYGYGGEWDMIWQNGPQQMEAWYTA EKMS
tteeeeeettccceccccccccccccceeeccccccccccccccccceeecccttchhhhhhhhhhhhh
YWEPGGX
Hhcttcc
```

(d)

```

      10      20      30      40      50      60      70
      |      |      |      |      |      |      |
MAAMVSGPRRRDSMIYWTCCLSSTGGKSSAHGSPGTKNRSCFPQRTTCGTKKDWSLAQM T T L S P L I L R S W
hheeeccccccccceeeeecccccccccccccttccccccccccccccccccccchhhhhcccchhhhhh
LHVEPYCAGHARRPQQSAPSPIPLIWCAGPSVRGRRSISPVKNTFCLSCCNAPKCYPGVLSRPWSGTI
ccccccccccccccccccccceeeccccccccccccccccctteeeccccccccccccceccccccc
LTVIRMLMSPDVEVKLMMT L S Q N S I P F A V P D M S K N Q R X
hhhhhhcttcheeeeeccccccccecccccccccc
```

**Figure 77: Shows the secondary structures of (a) chrB\_23 (b) pcoA\_25 (c) pcoA\_29 and (d) pcoR\_29 as predicted by SOPMA .**

The results of SOPMA are summarized in Table 18. The results showed a greater number of random coils in all the four proteins as compared to other secondary structural elements.

**Table 16: Secondary structure composition of chrB\_23, pcoA\_25, pcoA\_29 and pcoR\_29 partial proteins as derived using SOPMA (%).**

Properties	chrB_23	pcoA_25	pcoA_29	pcoR_29
Alpha helix (Hh)	32.29	14.71	16.25	12.36
3 <sub>10</sub> Helix (Gg)	0	0	0	0
P <sub>i</sub> Helix (Ii)	0	0	0	0
Beta bridge (Bb)	0	0	0	0
Extended strand (Ee)	14.58	30.07	20.17	17.98
Beta turn (Tt)	4.17	8.82	11.48	2.81
Bend region (Ss)	0	0	0	0
Random coil (Cc)	48.96	46.41	52.10	66.85
Ambiguous states (?)	0	0	0	0
Other states	0	0	0	0
Sequence length*	96	306	357	178

#### 4.17 I-TASSER structural prediction results

The 3D-models of chrB\_23, pcoA\_25, pcoA\_29 and pcoR\_29 were constructed using I-TASSER are shown in Fig. 78. The results of the C-score, TM-score and RMSD calculated in I-TASSER are shown in Table 20. The biological functions of the proteins were predicted using the Cofactor programme (Marchler-Bauer *et al.* 2011). The result obtained for chrB\_23 show that this protein might be responsible for vitamin transport with 42% probability. The partial protein pcoA\_25 and pcoA\_29 might be responsible for oxidation-reduction process, with probabilities of 81% and 57%, respectively. PcoR\_29 might be involved in rRNA processing with a probability of 7%.

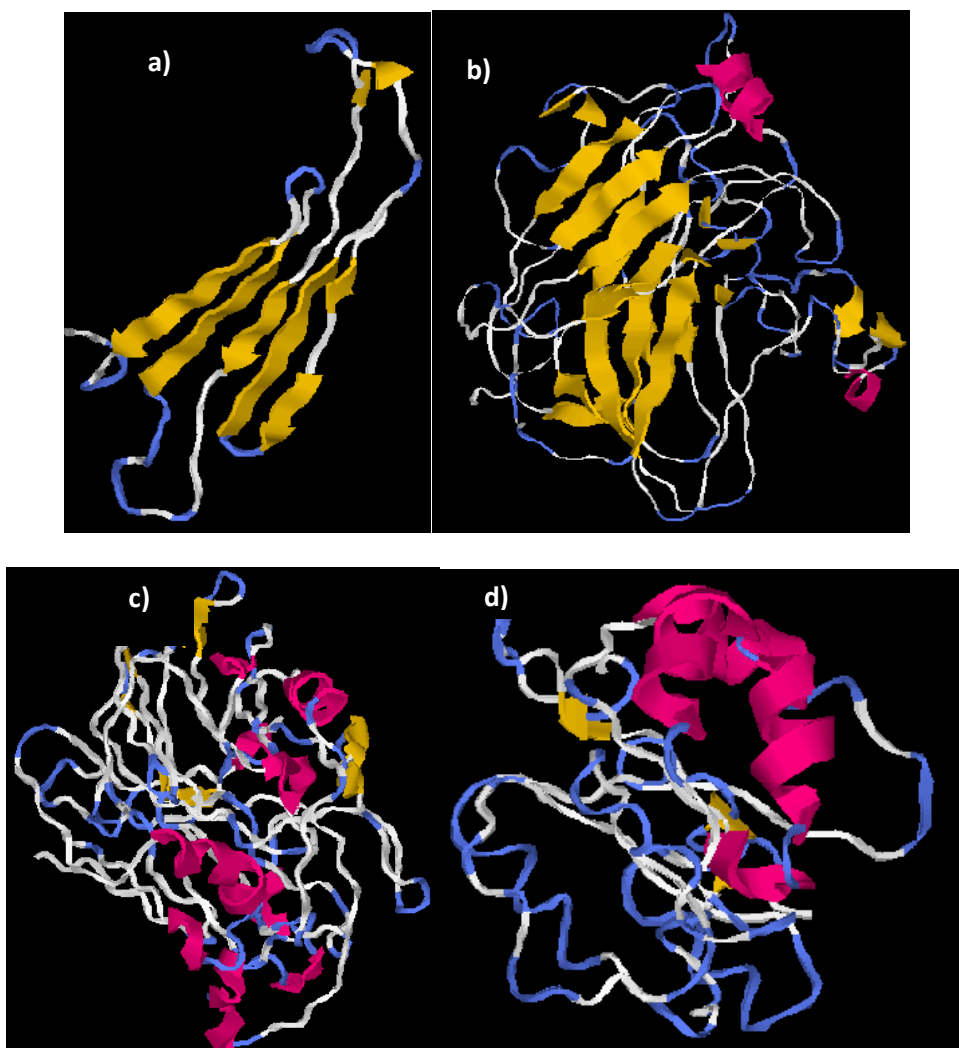


**Figure 78:** Shows the predicted structures of (a) chrB\_23 (b) pcoA\_25 (c) pcoA\_29 and (d) pcoR\_29 using I-TASSER

**Table 19:** Statistical analysis of predicted I-TASSER structures

Properties	chrB_23	pcoA_25	pcoA_29	pcoR_29
C-score	-1.35	-0.44	-3.84	-4.79
TM-score	0.55±0.15	0.66±0.13	0.30±0.1	0.22±0.06
Root Mean Square Deviation (Å)	6.5±3.9	7.2±4.2	16.2±3.1	16.9±2.8

#### 4.18 Ramachandran Plot Analysis

To investigate the accuracy and stereochemical quality of the predicted I-TASSER MODELS, the programme, MolProbity was used (Davis *et al.* 2007). The results obtained from Ramachandran plot analysis are shown in (Fig. 79a-d). The Ramachandran Plot for chrB\_23 (Fig. 79a) showed

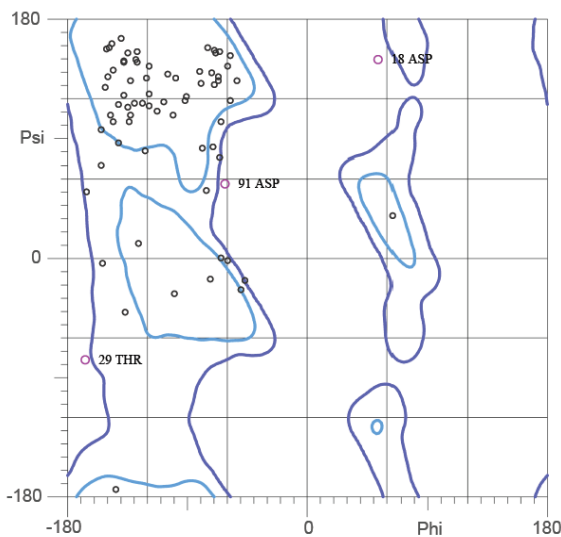
that 71.3% (67/94) of all the residues were in the most favoured regions. About 88.4% (88/94)% of the residues are in allowed regions. There were six outliers (phi, psi) as shown by the purple markers; residue 18 Asparagine (53.5, 150.2), 21 Valine (56.7,-166.7), 24 Glycine (-19.5, -56.0), 29 Threonine (-167.8, -77.3), 91 Asparagine (-62.8, 56.6) and 92 Isoleucine (-156.4,-26.4)

The Ramachandran plot for pcoA\_25 (Fig. 79b) shows that 64.55% (196/304) of the residues were in the most favoured regions and 84.9% (258/304) of all the residues were in the allowed regions. A total of 46 outliers were noted, as shown by the purple markers on the Ramchandran Plot.

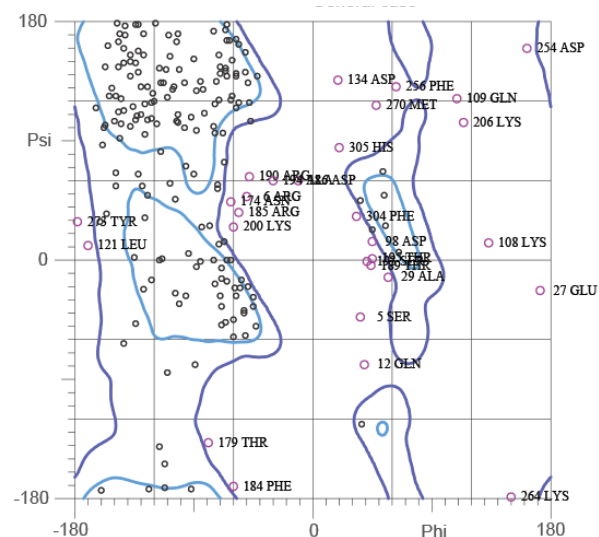
The Ramachandran plot of pcoA\_29 (Fig. 79c) indicates that 46.8% (166/355) of residues were in the most favoured regions. Approximately 79.4% of Residues are in allowed regions. There were 73 outliers that were detected.

For the pcoR\_29 protein translated from *E. coli* KR29 (Fig. 79d), some of the residues 44.3% (78/176) appeared in most favoured regions. Approximately 70.5% of Residues appeared in the allowed region. There were 52 outliers.

a)



b)





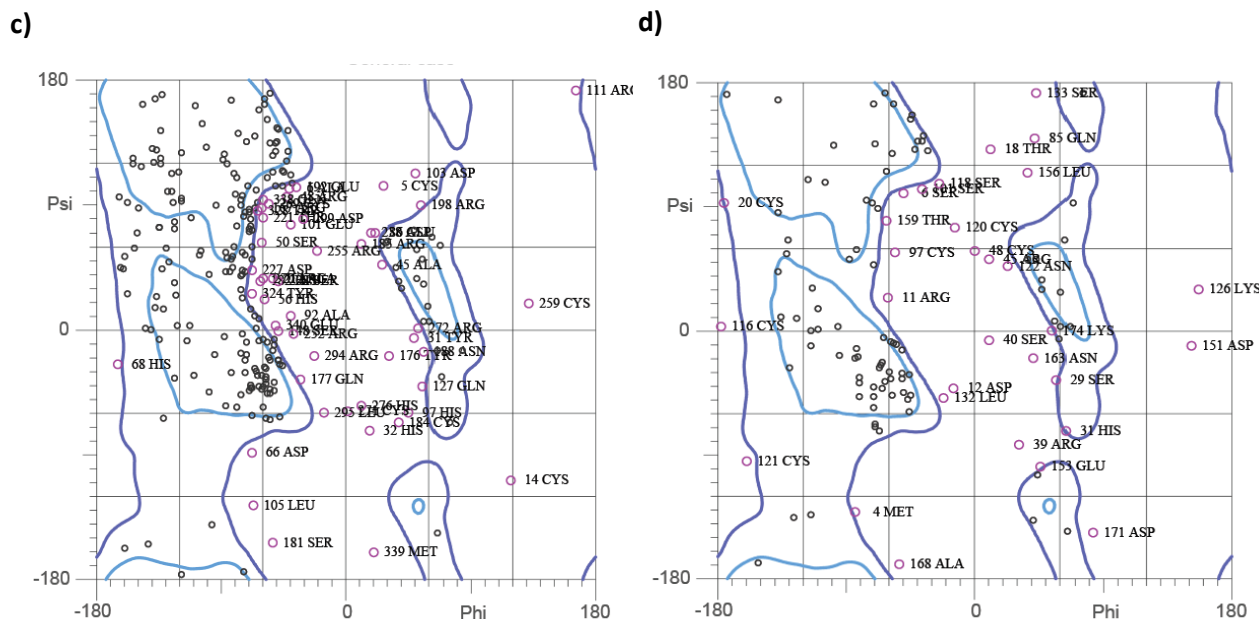


**Figure 79: Ramachandran Plot Analysis (Ramachandran of I-TASSER MODEL structures predicted for (a) chrB\_23 (b) pcoA\_25 (c) pcoA\_29 and (d) pcoR\_29**

#### 4.19 Plasmid profiles of wild type and cured strains

The plasmid profiles of 13 wild type strains and their cured derivatives are shown in Fig. 80-81. Three plasmids were detected in *A. hydrophila* (KR01). The largest plasmid was approximately 23.1 kb, followed by a 9.41 kb plasmid and the smallest was approximately 6.56 kb. No plasmids were detected in the cured derivative of *A. hydrophila* (KR01) (Fig. 80). A plasmid of approximately 21 kb was also detected in *E. coli* (KR29). However, the plasmid in *E. coli* (KR29) was eliminated after the curing process (Fig. 81). No plasmids were detected for the rest of the strains.

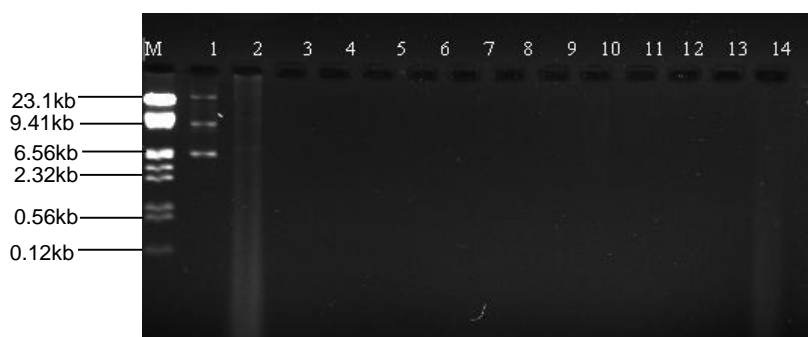


**Figure 80: Plasmid profiles of wild strains of heavy metal resistant isolates and their cured derivatives. 1. Lambda DNA+HindIII/EcoRI Marker, 2. *Aeromonas hydrophila* (KR01) WT, 3. *Aeromonas hydrophila* (KR01) C, 4. *Bacillus* sp. (KR02) WT, 5. *Bacillus* sp. (KR02) C, 6. *Bacillus megaterium* (KR04) WT, 7. *Bacillus megaterium* (KR04) C, 8. *Bacillus subtilis* (KR06) WT, 9. *Bacillus subtilis* (KR06) C, 10. *Pseudomonas* sp. (KR07) WT, 11. *Pseudomonas* sp. (KR07) C; 12. *Acinetobacter oleivorans* (KR08) WT, 13. *Acinetobacter oleivorans* (KR08) C, 14. *Proteus penneri* (KR17) WT and 15. *Proteus penneri* (KR17) C.**

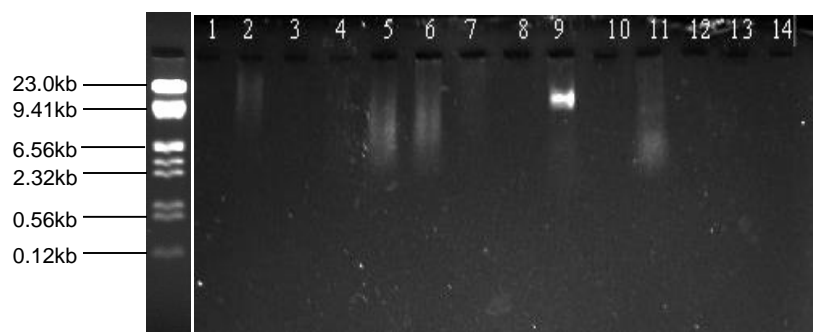


**Figure 81: Plasmid profiles of wild strains of heavy metal resistant isolates and their cured derivatives.** M. Lambda DNA+HindIII/EcoRI Marker; 1. *Aeromonas* sp. (KR19) WT, 2. *Aeromonas* sp. (KR19) C, 3. *Proteus* sp. (KR22) WT, 4 *Proteus* sp. (KR22) C, 5. *Pseudomonas* sp. (KR23) WT, 6. *Pseudomonas* sp. (KR23) C, 7. *Lyisnibacillus* sp. (KR25) WT, 8. *Lyisnibacillus* sp. (KR25) C, 9. *Escherichia coli* (KR29) WT, 10. *Escheriachia coli* (KR29) C, 11. *Arthrobacter* sp. (KR48) WT and 12. *Arthrobacter* sp. (KR48) C.

WT= wild type strain; C= cured derivative

#### 4.20 Plasmid curing

Fourteen strains were cured using 100 µg/ml of ethidium bromide. *Aeromonas hydrophila* (KR01) still exhibited metal resistance characteristics to the following heavy metals; Ni, Cu, Zn and Pb and the antibiotic profile of the cured derivative was similar to the antibiotic profile of the wild type strain. *Bacillus* sp. (KR02) showed resistance to Ni, Cr, Cu and Pb (Table 21); however the antibiotic profile of the cured derivative was different from that of the wild type strain (Fig. 82a-b). The cured strain became susceptible to Cephalothin acid, Amoxicillin, Cotrimoxazole and Ampicillin. *Bacillus megaterium* (KR04) displayed heavy metal resistance towards Ni, Cr and Cu (Table 21). The wild strain was susceptible to all the antibiotics; therefore, the cured derivative showed no resistance to any of the antibiotics under study (Fig. 82c-d). *Bacillus subtilis* KR06 was successfully cured of its antibiotic resistance to Streptomycin, Ampicillin and Amoxicillin; moreover, it lost resistance to Cd, Cu and Pb. *Pseudomonas* (KR07) retained its heavy metalresistance against Pb and also retained its resistance to Cephalothin acid, cotrimoxazole, Vancomycin, Ampicillin and Amoxicillin. KR08 still showed heavy metal resistance after curing against Zn and Pb; however the isolate lost its antibiotic resistance to Vancomycin, Cephalothin acid, Ampicillin, Amoxicillin and Cotrimoxazole (Fig. 82e-f). *Proteus penneri* (KR17) still retained its heavy metal resistance against Cr, Cu, and Pb and showed a similar profile to its wild type strain. It did not lose any of its antibiotic properties after the curing process. *Shewanella* (KR18), did not grow in the presence or absence of heavy metals. However, antibiotic susceptibility tests were carried out after curing. The isolate still retained its resistance against Cephalothin acid and Streptomycin. *Aeromonas* KR19 still retained its heavy metal and antibiotic resistance abilities

after curing. The curing of *Proteus* sp. (KR22) was unsuccessful, since it retained both its heavy metal resistance to iron and antibiotic resistance to Streptomycin, Cephalothin acid, Neomycin, Tetracycline, Cotrimoxazole, Vancomycin and Amoxicillin (Fig. 82g-h). Likewise, *Pseudomonas* sp. (KR23) retained its heavy metal resistance against Cr, Cu and Pb, and its antibiotic resistance to Streptomycin, Cephalothin acid, Vancomycin, Ampicillin and Amoxicillin even after curing. *Lysinibacillus* sp. (KR25) lost its resistance to Cu and Cd resistance but retained its resistance to Zn and Pb after curing. Moreover, the isolate was successfully cured of its Streptomycin resistance. *Escherichia coli* (KR29) exhibited resistance against Cu and Pb, and its antibiotic profile was almost similar to that of its wild type strain. *Bacillus licheniformis* (KR44) lost its Cd resistance abilities and *Arthrobacter* (KR48) lost its lead resistance and its resistance against the drug Tobramycin (Table 20-21).

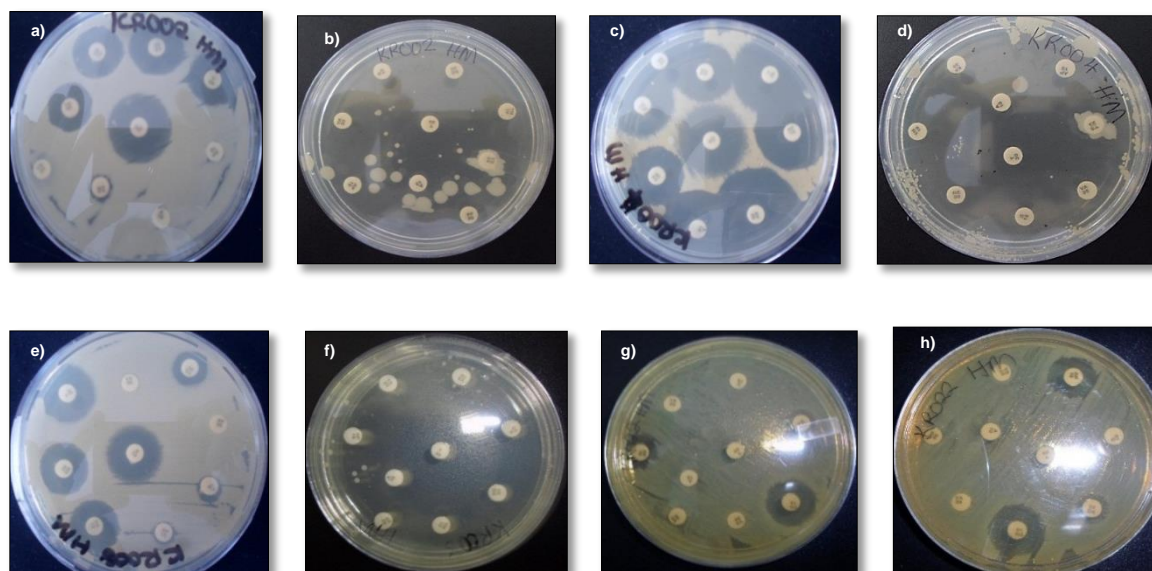


**Figure 82: Before and after curing antibiotic resistance profiles of isolates a) KR02-WT, b) KR02-C, c) KR04-WT, d) KR04- C, e) KR08- WT, f) KR08-C, g) KR22-WT and h) KR22-C.**

WT= wild type strain; C= cured derivative

**Table 17: Heavy metal resistance profiles after curing**

Isolate	Control	Ni (0.2mM)	Cr (0.2mM)	Cu (0.6mM)	Cd (0.2 mM)	Zn (0.2mM)	Pb (0.2 mM)
KR01	++	+	NT	+	NT	+	+
KR02	++	+	+	+	NT	NT	+
KR03	NT	NT	NT	NT	NT	NT	NT
KR04	++	+	+	+	NT	NT	+
KR06	+++	+++	++	-	-	+	-
KR07	++	NT	NT	NT	NT	NT	+
KR08	++	NT	NT	NT	NT	+	+
KR17	++	NT	+	+	NT	NT	+
KR18	-	NT	NT	NT	NT	NT	-
KR19	++	+	NT	+	NT	NT	+
KR22	++	NT	NT	NT	NT	NT	+
KR23	++	NT	+	+	NT	NT	+
KR25	++	NT	-	-	-	+	+
KR29	++	NT	-	+	NT	NT	+
KR44	++	+	NT	+	-	NT	+
KR48	++	NT	NT	NT	NT	NT	-

+++ Extensive growth; ++ moderate growth; +- minimal growth; NT- not tested

**Table 18: Antibiotic resistance profiles of cured isolates**

	Antibiotic Disc								
	Neomycin	Vancomycin	Cephalothin acid	Streptomycin	Ampicillin	Amoxycillin	Tetracycline	Cotrimoxazole	Tobramycin
KR01	19(S)	9(R)	NZ	7(R)	NZ	NZ	18(S)	NZ	15(S)
KR02	NG	NG	NG	NG	NG	NG	NG	NG	NG
KR03	18(S)	16(S)	NZ	21(S)	NZ	NZ	22(S)	13(S)	16(S)
KR04	NG	NG	NG	NG	NG	NG	NG	NG	NG
KR06	20(S)	20(S)	34(S)	11(R)	11(R)	NZ	29(S)	24(S)	24(S)
KR07	18(S)	NZ	NZ	13(S)	NZ	NZ	19(S)	NZ	18(S)
KR08	NG	NG	NG	NG	NG	NG	NG	NG	NG
KR17	7(R)	NZ	NZ	NZ	NZ	NZ	NZ	NZ	13(S)
KR18	18(S)	14(S)	NZ	8(R)	17(S)	13(S)	17(S)	23(S)	17(S)
KR19	17(S)	NZ	NZ	16(S)	NZ	NZ	24(S)	17(S)	16(S)
KR22	NZ	NZ	NZ	NZ	NZ	NZ	15(S)	20(S)	11(R)
KR23	20(S)	7(R)	NZ	16(S)	NZ	NZ	23(S)	28(S)	21(S)
KR25	NG	NG	NG	NG	NG	NG	NG	NG	NG
KR29	15(S)	NZ	13(S)	16(S)	14(S)	12(R)	19(S)	22(S)	13(S)
KR44	22(S)	16(S)	11(R)	24(S)	8(R)	8(R)	22(S)	NZ	13(S)

KR48	16(S)	21(S)	40(S)	18(S)	35(S)	29(S)	28(S)	23(S)	8(R)
------	-------	-------	-------	-------	-------	-------	-------	-------	------

Letters in parenthesis indicates the sensitivity of the isolate to the antibiotic  
R-Resistant; S-Sensitive; NZ-No Zone

## 5. DISCUSSION

### 5.1 Physico-chemical properties of water

The pH of a water sample is an important variable when assessing the concentrations of heavy metals in solution since it affects their removal as hydroxides in water (De La Torre *et al.* 2010) (Fig. 29). With the exception of nickel, all the metals (Cd, Cu, Fe, Pb and Zn) remained in solution at site 1 (Fig. 32-33). The pH of this site was 5.9. The low pH at this site could be attributed to mining and industrial activities (Muruven 2011), since the source is close to industrial areas such as Chamdor. The concentrations of heavy metals decreased downstream along the course of the Kip River as the pH of the water samples generally increased downstream from site 1 (Fig. 29). The decreasing concentrations of the heavy metals with an increasing pH may be due to the formation of metal hydroxides which are precipitated out of solution, consequently decreasing the amount of heavy metal concentration in the water (De La Torre *et al.* 2010). Neutralization of the water along the course of the Klip River is accredited to prolonged exposure to the Malmani Dolomites and the presence of wetlands in the area (Davidson 2003). The dissolved oxygen (DO) at sites 3 and 5 were considerably lower than 5 mg/l, the limit set by the Klip River Instream Guidelines (2003) (Fig. 29). DO can be used to evaluate the ecological health of a river. Unpolluted water bodies are normally characterized by elevated dissolved oxygen values, whereas low DOs indicate higher pollution levels (Rajkumar *et al.* 2012). The low DO at site 3 could perhaps be attributed to the close proximity of this site to an informal settlement in Lenasia (Fig. 29). Pollution of the river may be due to runoff from the informal settlement (personal observation) (Fig. 3). Evidence for this comes from the high microbial load at this site as shown by the high CFUs (Fig. 37). The DO was also low at site 5. This could be due to the relatively high CFUs (Fig. 37) and the high salt content as shown by the salinity value of 0.47 ppt (Fig. 31). Water with high concentrations of dissolved minerals such as salt can reduce the amount of DO concentration in water (Minnesota Pollution Control 2009) and this could have been a contributing factor to the decrease in DO at site 5. One interesting aspect of this study was the almost doubling of the turbidity, salinity and conductivity at site 4 (Fig. 30-31). This is perhaps due to AMD. AMD is a major contributor to high levels of salinity, conductivity and Total Dissolved Salts (TDS) (McCarthy 2011). Site 4 is situated after the Klip River's confluence with the Rietspruit which is greatly influenced by AMD. It is known that AMD is discharged into the Elsburgspruit, which flows into the Natalspruit and Rietspruit before joining the Klip River (Vermaak 2009; McCarthy 2011).

## 5.2 Interpretation of the principal components

Multivariate statistical analysis is applied to large and complex data sets in order to obtain better information and interpretation concerning surface water quality. Principal component analysis assisted in the identification of the major factors responsible for the variation in properties of Klip River's surface water in the 6 selected sites. The variation in factor 1 and 2 loadings indicate that inorganic matter such as the heavy metal concentrations of zinc, iron, copper, lead and cadmium could greatly influence the quality of the Klip River's surface water. Apparently, F1 is mainly saturated with zinc and iron (Fig. 35) and these two elements have a strong relationship, as shown by the high correlation coefficients (Table 7). The second principal component F2 is associated with lead, copper and cadmium (Fig. 35). The correlation coefficients of copper, lead and cadmium are very high, therefore a strong relationship exists between these three elements (Table 7). The negative correlation coefficients shown between pH and elemental concentrations does confirm that there is an inverse relationship that exists between the two variables (Table 7).

A biplot (Fig. 36) derived from the first and second factors, demonstrates the variable lines obtained from the factor loadings of the original variables. They represent the contribution of the variables to the samples. The closer the two variable lines the stronger the mutual correlation (Qu & Kelderman 2001). The sampling sites that are clustered in close proximity to each other have similar characteristics with respect to the factors (Bhat *et al.* 2014). In this study site 4, 5 and 6 were relatively close together, suggesting a similarity in their physico-chemical characteristics. The variable lines for Cu, Cd and Pb were very close together suggesting a very strong relationship between the three variables. Moreover, the variable lines for salinity and turbidity indicate a very strong correlation between the two variables.

## 5.3 Enumeration of bacteria

The presence of heavy metal resistant bacteria (MRB) in both the water and sediment samples is an indication that the Klip River is indeed polluted by the heavy metals examined in this study (Fig. 37, 38). However, nickel and cadmium were undetectable in some of the sites. The heterotrophic plate counts (HPC) in the controls (plates without heavy metals) for both the water and sediments samples were relatively higher than those obtained in the presence of heavy metals (Fig. 37, 38). This suggests that growth of some of the microorganisms were inhibited by the presence of heavy metals. The highest HPC at site 3 (Lenasia) was possibly due to its proximity to an informal settlement in Lenasia. The heterotrophic plate counts were highest in the sediment at site 4 (Henley on Klip Weir). This could be an indication of the extent to which the sediment at this site is polluted, possibly due to AMD (Vermaak 2009; McCarthy 2011).

#### 5.4 Morphological and physiological characteristics of isolates

Most of the isolates grew optimally at pH of 7 suggesting that they are neutrophilic. This characteristic could be attributed to the fact that they were isolated from an environment which was more or less neutral as shown by the pH values (Fig. 29). Microorganisms tend to respond to external pH changes by using certain mechanisms to maintain a constant internal environment. For neutrophilic bacteria, it has been suggested that they appear to exchange potassium for protons using an antiport transport system (Willey *et al.* 2009). Acidophilic bacteria (0 - 5.5) use a variety of measures to maintain a neutral internal pH. For example, the transportation of cations such as potassium into the cells decreases the movement of  $H^+$  into the cell (Willey *et al.* 2009). Another mechanism involves proton transporters that pump  $H^+$  out of the cell and highly impermeable membranes (Willey *et al.* 2009).

#### 5.5 Minimum Inhibitory Concentrations

The 16 isolates showed wide variability in the MIC for the different metals except for Zn, Cd and Cr to a lesser extent (Fig. 40). This suggests that the latter metals are relatively toxic to the bacterial isolates. Each isolate also differed in their MIC values for the different metals. Of all the metals, the isolates were most resistant to Pb and Fe and were able to grow in concentrations of up to 4 mM. The high levels of lead and iron in the Klip River (Fig. 33) appears to have given the indigenous microbial strains some level of tolerance to these metals. Micro-organisms have developed a variety of protective mechanisms to thrive in very high levels of lead and iron. Among the various adaptative mechanisms adopted by lead resistant microorganisms include: P -type ATPase mediated efflux of lead (Nies & Silver 1994) and metallothioneins (BmtA). It is known that metallothioneins play a crucial role in the immobilization of lead within the cell. In *Bacillus megaterium*, lead was sequestered by proteins which were almost similar to metallothioneins (Roane 1999). Lead resistance in *Proteus penneri* GM10 is due to the gene *SmtA* which encodes metal binding metallothioneins. Other methods of lead resistance includes its sequestration by exopolysaccharides (EPS) (Bramachari *et al.* 2007), cell surface adsorption and biosorption involving ion exchange, and adsorption and diffusion through cells and membranes (Chang *et al.* 1997). *Bacillus subtilis* has been shown to biosorb high amounts of lead ions, up to 97.68% under acidic conditions (Hossain & Anatharam 2006). Heavy metal resistant microorganisms with resistance mechanisms may serve as potential biotechnological agents for bioremediation of lead contaminated sites (Naik & Dubey 2013). Further research with some of the heavy metal resistant bacteria isolated in his study may be necessary to verify this potential.



## 5.6 Phenotypic profiles

The sixteen isolates display some diverse characteristics with regards to their biochemical profiles and carbohydrate fermentation (Fig. 42). Eighty-eight percent of the isolates had distinct profiles when assessed with the API 20E® test strips. Phenotypic profiling used in combination with 16SrDNA may aid in the identification of isolates and may be used to differentiate between isolates that have been identified up to genus level using 16SrDNA sequencing. For instance KR07 and KR23 have been identified by 16SrDNA sequencing up to genus level and one is most likely to assume that they are similar isolates; however, their phenotypic profiles are not similar. KR01 and KR19 belong to the genera *Aeromonas*, and these two isolates exhibit 88% similarity in their phenotypic profile.

## 5.7 Antibiotic susceptibility

Antibiotic resistance of the isolates used in this study may be due to the presence of antibiotics in the Klip River. Antibiotic resistant microorganisms are normally selected in environments contaminated with antibiotics and they are also found in natural environments in the presence of some non-antibiotic substances, especially heavy metals (mercury, arsenic, lead, cadmium etc.) (Chattopadhyay & Grossart 2011).

Streptomycin (Schantz & Kee-Woei 2004), Amoxicillin (Brogden *et al.* 1979), Ampicillin (Sharma *et al.* 2013) and Tetracycline (Zakeri & Wright 2008) are broad spectrum antibiotics which inhibit both Gram- positive and negative bacteria. However, some isolates identified in this study were resistant to these drugs (Fig. 43b). Isolate KR17 (Fig. 43b) which was identified as *Proteus penneri* showed antibiotic resistance to all the antibiotics except Tobramycin (Table 11; Fig. 43b). In a previous study *Proteus penneri* was tested against 71 antibiotics and found to be naturally resistant to several antibiotics such as penicillin G, oxacillin, all tested macrolides, streptogramins, lincosamides, rifampicin, glycopeptides, rifampicin and fusidic acid (Stock 2003). Tobramycin is active against Gram-negative bacteria especially *Pseudomonas* spp, *Enterobacteriaceae* and *Acinetobacter* spp. (Reyes *et al.* 2014). In this study KR22 (*Proteus* sp.) and KR48 (*Arthrobacter* spp.) were resistant to Tobramycin, and to all the  $\beta$ -lactam antibiotics. *Aeromonas* spp. were shown to be resistant to Cotrimoxazole (Kuijper *et al.* 1989); however, both of the *Aeromonas* sp (KR01 and KR19) in this study were resistant to this drug. Vancomycin is effective against Gram positive bacteria such as *Streptococci*, *Corynebacteria*, *Clostridia*, *Bacillus* and *Listeria* species (Wilhem & Estes 1999). In the current study all the Gram positive bacteria were susceptible to Vancomycin (Table 9 and 12)

## 5.8 Growth Patterns of selected isolates

Growth patterns of 14 isolates in the presence of cadmium, chromium, copper, nickel, lead, iron and zinc indicated difference levels of toxicity to the bacteria (Fig. 46-59). Two of the isolates under study (KR18 and KR03) stopped growing in the presence and absence of heavy metals, therefore their growth patterns were not assessed. The growth rate of the isolates in the presence of some heavy metals was generally faster than the control contrary to previous findings by Raja *et al.* (2009). Bacteria that are exposed to high levels of heavy metals in their environment have adapted to these stresses by developing several resistance or coping mechanisms (Raja *et al.* 2009)

The presence of cadmium slowed down the growth rates of 12 isolates, except for KR01 (Fig. 46) and KR19 (Fig. 53) (both of which are *Aeromonas* species). The *Aeromonas* spp. showed a certain level of tolerance to cadmium in solution. The MIC values for cadmium for most of the isolates was 0 mM, but managed to grow at a concentration of 0.2 mM LB broth, because of the type of media used. The growth of KR01 and KR19 in the presence of cadmium could have been attributed to the non-uniform availability of metals in the culture medium due to metals affinity for precipitation in rich media (Kumar *et al.* 2013). The presence of chromium showed a reduction in biomass production, however to a lesser extent when compared to cadmium. Isolates KR01, KR19 and KR29 were apparently more sensitive to chromium than cadmium. For KR25 chromium was equally toxic to the isolate as cadmium. The low MIC values for chromium and cadmium coincide with the decrease in growth rate of these isolates in the presence of these heavy metals. The decline in biomass observed whenever heavy metals were present, is possibly caused by a decrease in substrate utilization efficiency due to a higher energy cost of microorganisms subjected to heavy metal stress (Giller *et al.* 2009).

### **5.9 Comparative analysis of 16SrDNA sequences**

A comparative analysis of the 16SrDNA sequences of the 14 isolates identified 8 bacterial genera (Table 14) in this study. Eight (57%) of the 14 identified isolates belonged to the phylum *Gamma proteobacteria* (Fig. 62). The isolates were closely related to *Aeromonas*, *Pseudomonas*, *Proteus*, *Shewanella* and *Escherichia* (Fig. 62). Members of the *Y-proteobacteria* are all Gram negative, rod shaped bacteria and have been isolated from various heavy metal polluted habitats (Raja *et al.* 2009; Odeyemi *et al.* 2012; Abskharon *et al.* 2008). Isolate KR01 was identified as *Aeromonas hydrophila* while KR19 was similar to *Aeromonas* sp IW-211. Members of the genus *Aeromonas* are Gram-negative, rod shaped (Bhowmik *et al.* 2009), catalase positive and facultative anaerobic bacteria (Alperi *et al.* 2010). These morphological and biochemical characteristics corresponded with those of KR01 (Fig. 39a) and KR19 (Table 11) in this study. *Aeromonas* spp. isolated was

previously isolated from water and sediment contaminated with heavy metals and the isolates showed both, heavy metal and antibiotic resistant characteristics (Odeyemi *et al.* 2012). KR07 was similar to *Pseudomonas* F15, while KR23 was similar to *Pseudomonas* sp. THG-T1. *Pseudomonas* are Gram negative aerobic bacteria that are known to be resistant to heavy metals and antibiotics (Raja *et al.* 2009, Virender *et al.* 2010). KR18 was identified as *Shewanella* sp. which is a ubiquitous organism isolated from food, sewage, and both from fresh and salt water. Earlier it was termed *Pseudomonas putrefaciens* or *Shewanella putrefaciens* (Sharma & Kalawat 2010). Several reports have arisen stating that this organism causes human infections such as cellulitis, abscesses, bacteremia, and wound infection (Sharma & Kalawat 2010). It is oxidase and catalase-positive non-fermenter Gram-negative rod that produces hydrogen sulfide (Table 11) (Sharma & Kalawat 2010). *Shewanella* species were shown to mobilize copper (Toes *et al.* 2008). KR29 was identified as *E.coli* (Table 14). It is rod shaped, Gram-negative, able to ferment glucose, and was susceptible to almost all the antibiotics except for Vancomycin and Amoxicillin. *E. coli* is an accurate indicator of faecal contamination in drinking water and other matrices (Odonkor & Ampofo 2012). Several strains of *E. coli* were isolated from wastewater of El-Mahah in Egypt and were analysed for heavy metal resistance. One particular isolate showed multiple resistance to Cu, Co, Ni, Zn, Cr, Cd and Pb (Abskharon *et al.* 2008). Different MICs of several heavy metals were determined for *E. coli*: silver, gold, chromium and palladium proved to be the most toxic metals to *E. coli*.

Thirty-six percent of the isolates were grouped with low-G+C Gram-positive bacteria in the *Firmicutes* and were most closely related to *Bacillus* and *Lysinibacillus* (Fig. 62). *Firmicutes* are Gram positive bacteria and have been known for formation of endospores, namely; *Bacilli*, *Clostridia* and *Negativicutes*. This enables the bacteria to withstand a variety of environmental challenges, such as heat, solvents, UV irradiation and lysozyme (Setlow 2007). The Gram positive isolate KR02 was identified as *Bacillus* sp. In a previous study, *Bacillus* sp. was shown to have exceptional metal resistance against lead and arsenate (Panaday *et al.* 2011). KR04 was identified as *Bacillus megaterium*. This is a rod-like, Gram-positive, spore forming bacteria. This is one of the largest known bacteria that occur in pairs and chains (Fig. 39d) with an optimum growth temperature of 37°C. The optimum temperature for sporulation for *B. megaterium* is 40°C (Lüders *et al.* 2011). KR06 was identified as *Bacillus subtilis*. This was confirmed by its rugose colony appearance and Gram positive staining. *Bacillus subtilis* was isolated from agricultural and industrial areas in Mauritius, and was shown to be resistant to Cu, Ag, P, Zn and Hg (Hookoom & Puchooa 2013). KR25 was recognized as *Lysinibacillus* sp, which is a potential bioremediation

agent. Several isolates have been obtained from heavy metal polluted environments; for instance *L. sphaericus* strain OT4b.31 is a native Columbian strain widely applied in the bioremediation of heavy metals (Peña-Montenegro & Dussan 2013). In this study, KR44 could possibly be a *Bacillus* sp. which has sporulated (Fig. 39f). The bacterial isolate was not metabolically active in this state as elucidated by its metabolic profile (Table 11).

One of the 14 isolates belonged to the high-G+C Gram-positive bacteria in the *Actinobacteria* and was most closely related to *Arthrobacter* (Fig. 62). KR48 was ascertained to be *Arthrobacter* sp. that is known to display heavy metal resistance. For example, *Arthrobacter* sp. isolated from heavily polluted industrial areas showed remarkable resistance to nickel (up to 20mM) (Margesin & Schiner 2007).

All the sixteen isolates were resistant to lead except for KR22 (*Proteus* sp.). Lead resistant bacteria exhibiting multiple drug resistance is a disturbing signal for medical microbiologists since lead pollution can lead to the occurrence of bacterial pathogens resistant to all known antibacterial drugs (superbugs) (Naik & Dubey 2013).

### **5.10 Heavy metal resistance genes**

Due to the presence of heavy metals in the Klip River, bacteria inhabiting this environment have improved their heavy metal resistance mechanisms. Products encoded by heavy metal resistance genes have the potential to eliminate or reduce heavy metal toxicity (Wei *et al.* 2009). Several primers have been developed by other scientists to detect and amplify the heavy metal resistance genes in microbes. PCR amplification, gel electrophoresis and sequence analysis showed that the following isolates contained the following genes; KR23 (*Pseudomonas* sp.) contained the chromate resistance gene *chrB* gene, *Lysinibacillus* sp. KR25 contained the copper resistance gene *pcoA*, and *Escherichia coli* KR29 contained the copper resistance genes *pcoA* and *pcoR*. However other heavy metal resistance genes namely *pbrT*, *pbrRA*, *pbrA*, *czcA*, *czcB*, *czcD* and *cadCA* were not found in any of the organisms under study. It is likely that the primers used to amplify the previously mentioned genes were inappropriate or the genes were not present in the microorganisms.

#### **5.10.1 Chromate resistance genes**

*Pseudomonas* KR23 is resistant to chromate, and showed a minimum inhibitory concentration (MIC) value of 0.2mM to chromium (Fig. 40). Therefore, it was suspected that this isolate may be harbouring chromate resistance genes. The *chrB* gene is purported to play a regulatory role in the expression of the *ChrA* transporter (Nies *et al.* 1990) for the regulation of chromate resistance.

The primers for the *chrB* gene amplified a single fragment of about 400 bp in *Pseudomonas* KR23 in this study (Fig. 71). The fragment size is similar to the target gene in *C. metallidurans* CH34 (Nies *et al.* 1990). However, after sequence analysis of the protein and phylogenetic analysis with similar sequences from the NCBI database it was found that the *chrB\_23* protein was not associated with chromate resistance. However, the *chrB\_23* protein sequence was closely related mainly to the TonB dependent receptor protein and to a lesser extent to the vitamin B12 transporter *btuB* and to a single putative transferrin binding protein. The phylogenetic tree derived from the protein sequences (Fig. 73) shows that the TonB and vitamin B12 transporter *btuB* are found in variety of bacterial genera. Cofactor analysis infers that the *chrB\_23* gene amplified from *Pseudomonas* KR23 could possibly be a vitamin transport protein and not the targeted regulatory gene for chromate resistance.

#### 5.10.2 Copper resistance genes

The main genetic determinants responsible for copper resistance in bacteria are the *pcoA* gene that encodes for a multi-copper oxidase (MCO) (Djoko *et al.* 2008) and the *pcoR* gene that codes for the DNA binding repressor protein (Brown *et al.* 1992; Silver *et al.* 1993). Out of the 3 isolates that were amplified with primers for the *pcoA* and *pcoR* genes, the *pcoA* gene was present in 2 isolates, namely, *Lysinibacillus* sp. KR25 [KJ935917] and *E. coli* KR29 [KJ935918] (Fig. 71). These two isolates exhibited copper resistance and had (MIC) values of 1 mM and 0.6 mM, (Fig. 40) (Chihomvu *et al.* 2014). The phylogenetic tree (Fig. 74) shows that the *pcoA\_25* protein from *Lysinibacillus* KR25 is closely associated with *copA* proteins from *Klebsiella*, *Salmonella*, *Citrobacter*, *Enterobacter*, *Escherichia*, *Serratia* and *Cronobacter* strains, respectively. All of the bacterial genera in Fig. 74 are in the phylum *Gammaproteobacteria*. However, *Lysinibacillus* sp. KR25 from which the query sequence (*pcoA\_25*) was obtained, belongs to the phylum *Firmicutes*. The putative conserved domains detected in *pcoA\_25* are part of the *cupredoxin* domain of the *copA* copper resistance family of genes. *CopA* is related to the enzymes laccase and L-ascorbate oxidase, both of which are copper containing enzymes. It forms part of the regulatory protein *Cue* operon, which utilizes a cytosolic metalloregulatory protein *CueR* that induces the expression of *copA* and *CueO* in the presence of high concentrations of copper (Marchler-Bauer *et al.* 2011).

The blast search of the Genbank revealed that while one sequence (*pcoA\_25*) from *Lysinibacillus* sp. KR25, showed a relatively high level of similarity (82%) to the *copA* family, *pcoA\_29* from *E. coli* KR29 showed too low level of similarity (5%) to known proteins encoded by *copA/pcoA* genes. Therefore this gene product is thought to form a new heavy metal protein, involved in oxidation reduction function as elucidated by the Cofactor analysis.

The *pcoA*\_29 protein from *E. coli* KR29 is closely associated with *copA* proteins from *Cronobacter* and *Klebsiella* and a hypothetical protein, Ctu present in *Cronobacter turicensis* (Fig. 75). The *pcoA* genes of the two isolates *Lysinibacillus* KR25 and *E. coli* KR29 encodes a multicopper oxidase which oxidizes the toxic Cu(I) to its non-toxic form Cu(II) (Huffman *et al.* 2002; Djoko *et al.* 2008). The *pcoA* (*copA*) genes encoding multicopper oxidases has been described in the following plasmids pPT23D, pRJ1004 and pMOL30 from the following microorganisms; *E. coli* RJ92, *Pseudomonas syringae* pv. *tomato* PT23 and *Cupravidus metallidurans*, respectively (Tetaz & Luke 1983, Mellano & Cooksey 1988 and Monchy *et al.* 2007). Genes identical to the copper-resistant genes, *pcoR* and *pcoA* from *E. coli*, were amplified by PCR from a 1.4-Mb megaplasmid detected in a root nodule bacterium, *Sinorhizobium meliloti* CCNWSX0020 (Fan *et al.* 2011).

The partial protein sequence *pcoR*\_29, resulted in 3 hits using the BLASTp and showed 20% to a transcriptional regulatory protein *pcoR* found in *E. coli* [WP\_001381484]. This gene product is also assumed to form a novel heavy metal regulatory protein. Cofactor analysis elucidated that this protein may be involved in rRNA processing, however the confidence level for this function was very low (7%).

### 5.11 Physico-chemical properties

The predicted physico-chemical properties of protein sequences can give valuable insights to the characteristics of protein. For instance, protein with an instability index smaller than 40 are considered to be stable while those with an instability factor above 40 are predicted to be unstable (Jatav *et al.* 2014). In this study the ProtParam Tool was used to characterize the predicted physicochemical properties of the partial protein sequences that were obtained in this study (Table 18). The *pcoA* proteins from *Lysinibacillus* sp. KR25, the *chrB* protein from *Pseudomonas* sp. KR23 can be considered stable since their instability indices were 36.60 and 12.45, respectively.. The high instability index for *pcoA*\_29 and *pcoR*\_29 from *E.coli* KR29 predicts that these proteins are unstable. The high extinction coefficient of *pcoA*\_29 indicates the presence of high concentrations of Cysteine (Cys), Tryptophan (Trp) and Tyrosine (Tyr) residues, while the low extinction coefficient shown by the *chrB*\_23 indicates low concentrations of these amino acids in the proteins. The high aliphatic indices shown by the four partial proteins are indicators that the proteins may be stable over a wide temperature range (Jatav *et al.* 2014). The Grand Average of Hydropathicity Value (GRAVY) predicts the hydrophobic and hydrophilic nature of the protein. A negative value indicates that the protein is hydrophilic and a positive value indicates that the protein could be hydrophobic (Kyte & Doolittle 1982). The GRAVY values for all four proteins are negative suggesting that they are most likely hydrophilic.

### 5.12 Protein structures

The tool that was used in this study to predict the protein structures of the partial proteins was I-TASSER since it was reported to reliably predict partial structures of a source protein (Laurenzi *et al.* 2013). I-TASSER initiates the structure prediction process by performing threading to identify template Protein Database Structures that are similar to the query sequence. Structural fragments that are cut from the chosen templates are then used to construct the protein models (Laurenzi *et al.* 2013). The C-score output of I-TASSER were used to distinguish the foldable and non-foldable sequences because it is founded on the probability that the sequence is homologous to known structures at the subsequence level rather than globally. Structure predictions with a TM score greater than 0.6 was defined as “good”, “decent” (TM-score between 0.3 and 0.6) or “bad” (TM-scores less than 0.3) (Laurenzi *et al.* 2013).

The structure predicted for chrB\_23 was decent taking into account its high TM-score of 0.55. This structure is most likely to fold as depicted by the moderately high C-score value of -1.35. The Ramachandran plot for chrB\_23 confirms the good stereo-chemical structure of chrB\_23, since 93.6% of all the residues lie in the allowed regions and only six outliers were noted.

The highest C-score (-0.44) was obtained for the pcoA\_25 protein structure suggesting that the partial protein is most likely to fold into a stable structure that is considered to be of good quality as shown by the high TM-score of 0.66. The Ramachandran Plot for pcoA\_25 shows that the structure is of reasonable quality with 84.9% percent of all the residues lying in the allowed region.

The structure predicted for pcoA\_29, is unlikely to fold considering the low C-score value of -3.84 and it is considered to be “decent” considering the TM-value of 0.31 and the Ramachandran plot.

For pcoR\_29, the predicted structure is not likely to fold because its C-score value was very low (-4.79) and the quality of the prediction was bad, considering the low TM-score of 0.22 and the low quality of the structure was confirmed by the Ramachandran Plot which shows 52 outliers.

Computational methods aid in the prediction of protein structure rapidly and economically (Jatav *et al.* 2014). The results of this analysis indicated that the predicted structures are ready to be verified *in vitro* and will enable further research to be carried out on heavy metal resistance proteins. I-TASSER is a superior computational method compared to other protein prediction programme, since it takes into account the full length of the sequence and it uses several templates in the PDB database to construct the full structure. Through the threading method used by I-TASSER complete structures were constructed and predicting the foldability of a protein the C-score analysis is accurate since it considers the subsequence level (Laurenzi *et al.* 2013).

### 5.13 Plasmid isolation and curing

Although none of the heavy metal genes were detected in several isolates, plasmid curing was carried out to determine the location of the antibiotic and heavy metal determinants.

Plasmid isolation and curing was successful for *Aeromonas hydrophila* KR01 as shown in Fig. 80. Despite the loss of its plasmids the isolate still retained its antibiotic and heavy metal resistance properties. Therefore, it can be deduced that the antibiotic and heavy metal resistance determinants are present on the chromosome of the isolate.

Plasmid isolation for both *Bacillus* sp. KR02 and *Bacillus megaterium* KR04 was unsuccessful. However, the antibiotic profiles of the cured derivatives showed a large difference from their wild strains as shown in Fig. 82a-d. Therefore it can be inferred that the antibiotic determinants of these isolate are not harboured on the chromosome, but rather on plasmids/ mobile genetic elements. Both the isolates did not lose their heavy metal resistant characteristics after curing. Consequently the heavy metal determinants are situated on the chromosome of the isolates.

For *Bacillus subtilis* KR06, *Pseudomonas* sp. KR07, *Proteus penneri* KR17, *Shewanella* KR18, *Aeromonas* sp. KR19, *Proteus* sp. KR22, *Bacillus licheniformis* KR44 and *Arthrobacter* KR48, plasmid isolation was unsuccessful and these isolates still retained their antibiotic resistance patterns. The heavy metal resistance patterns for *B. licheniformis* KR44 changed since it lost its cadmium resistance. Similarly, *Arthrobacter* sp. KR48 lost its lead resistance. These results suggest that that the heavy metal resistance genes for cadmium and lead are probably present on the plasmid/ mobile genetic elements.

Most of the studies involving copper resistance in bacteria have shown that the *pco* system is well characterized in *E. coli* strains where the genes are harboured in plasmids (Brown *et al.* 1997, Rouche & Brown 1997). In this study, it appears that in *E. coli* KR29, the *pcoA* and *pcoR* genes are located on the chromosome since the isolate still retained its antibiotic and copper resistance after the plasmids were successfully eliminated (Fig. 81).

This study showed that the *pcoA* gene was present in *Lysinibacillus* sp. KR25. After curing the isolate lost both its antibiotic and copper resistance properties (Table 20-21). The strain lost its antibiotic resistance against Streptomycin; therefore it can be concluded that the resistance determinant for this drug is present on a plasmid. However, following plasmid isolation no DNA band/s were observed on ethidium bromide stained gels. It has been noted that plasmid isolation can be difficult in some bacterial strains (Altimara *et al.* 2012).



Environmental bacteria have been shown to be a great source of heavy metal resistance genes and a potential source of novel heavy metal genes. Bacteria can acquire genes for heavy metal and antibiotic resistance in several ways such as horizontal gene transfer that could arise from the presence of genetic mobile elements in bacteria such as plasmids, transposons, integrons, genomic islands and bacteriophages (Frost *et al.* 2005). The occurrence of the copper resistance gene in *Lyisnibacillus* KR25 and *E. coli* KR29 is most probably due to this mechanism.

Antibiotic resistance may be due to enzyme inactivation, lack of target sites for drugs, intracellular drug accrual, or the presence of genes that enable microorganisms to acquire antibiotic resistance (Schwarz & Chaslus-Dancla 2001). Antibiotic resistance genes tend to reside either on the plasmid (Fraser *et al.* 2000) or on the chromosome of the bacteria (Clermont & Horaud 1990). In this study, the strain *Pseudomonas* KR23 retained its antibiotic resistance to Streptomycin, Cephalothin acid, Vancomycin, Ampicillin and Amoxicillin after curing. Since plasmid isolation was unsuccessful for this strain it is difficult to deduce whether the resistance determinants are present on the plasmid or on the chromosome.

#### **5.14 CONCLUSION**

There was wide variation in the heavy metal concentration in the different sites. Sampling for heavy metals at one site may not provide a true reflection of the heavy metal pollutants in the Klip River. The concentration of iron and lead was highest at the source of the river perhaps due to the industrial and mining activity in the area. The high number of metal resistant bacteria is an indicator of the extent to which the Klip River is polluted. This situation can be rectified by bioremediative methods. The heavy metal resistant bacterial isolates obtained from this study are autochthonous to the Klip River. Their uniqueness and characteristics could be used as potential bioremediation agents to remove heavy metals from the environment. The heavy metal resistant isolates obtained belong to the phyla, *Y-Proteobacteria*, *Firmicutes* and *Actinobacteria*. A detailed analysis indicated that two isolates possess the *pcoA* gene (*Lyisnibacillus* sp. KR25 and *Escherichia coli* KR29) and a *pcoR* gene was detected in *E. coli* KR29. These genes are most likely responsible for their copper resistances. However, the genetic mechanisms behind their copper tolerances remains to be determined. A suspected *chrB* gene was detected in *Pseudomonas* sp. KR23, however after analysis the gene was shown not to be related to chromate resistance. Computational methods aided in understanding the structure and function of the copper resistance genes obtained in this study.

Further studies are necessary to evaluate the heavy metal removal abilities of these isolates. Investigations into the presence of heavy metal resistance genes in these isolates may lead to

the development of biosensors. The summation of all the information attained from this study will prove to be valuable when setting up bioremediation projects of the Klip River.

### **5.15 RECOMMENDATIONS**

This dissertation presents some valuable information on the characterization of heavy metal resistant bacteria at the physiological, biochemical and molecular level; these results raise a number of issues or questions about these isolates that need to be addressed in further studies.

Therefore further studies can be carried out to evaluate the heavy metal removal abilities of these isolates. The isolates can then be used in the bioremediation of water by the construction of bioreactors to treat industrial effluent and polluted water bodies. The isolates showing very high mean specific growth rates should be continued to be examined in detail. The heavy metal uptake and saturation rates should be determined and the kinetics modeled. The research must include the determination of the ratio of active transport vs passive binding to live biomass and comparison with dead biomass. It would also be noteworthy to evaluate the potential of the bacterial isolates in the promotion of plant growth in the presence of heavy metals (bioaugmentation). These isolates may be screened for their plant growth promotion abilities, indole acetic acid assessment and presence of siderophores. Plant growth assessment is not only important in agricultural applications, but can also play a vital role in the bioremediation of heavy metal contaminated soils.

An investigation into the formation of biofilms using microtitre plates can be performed. Biofilm formation can be investigated on different types of surfaces and larger cultures.

The heavy metal resistant genes isolated isolates can be used in the development of biosensors, whereby the isolated genes may be joined with reporter genes such as *luc*, *lacZ*, *lux* and *gfp* to detect heavy metal contaminants in environmental samples. The location of the identified genes could be determined by using the sequence which has already been obtained in PCR to isolate the flanking regions. Methods such as Real-Time PCR can be used to assess the level of gene expression of the identified genes. A proteomic approach involving two-dimensional polyacrylamide gel electrophoresis (2D PAGE) and mass spectrometry (MS) could be used to identify differentially expressed proteins under heavy metal stress.

Since some of the isolates did not lose their heavy metal and antibiotic resistance after curing with ethidium bromide, several other curing agents can be used to improve curing rates.

Another recommendation is that enumeration of MRB on a regular basis should be carried out along with microbiological analysis on environmental samples suspected to be polluted to assess

the health status of the environment. The higher the abundance of MRB the more likely is the concentrations of heavy metals to be elevated in the environment.

## REFERENCES

- ABSKHARON, R. N. N., HASSAN, S. H. A., GAD EL-RAB, S. M. F. & SHOREIT, A. A. M. 2008. Heavy Metal Resistant of *E. coli* Isolated from wastewater sites in Assiut City, Egypt. *Bulletin of Environmental and Contamination Toxicology*, **81**:309-315.
- AGUILAR-BARAJAS, E., PALUSCIO, E., CERVANTES, C. & RENSING, C. 2008. Expression of chromate resistance genes from *Shewanella* sp. strain ANA-3 in *Escherichia coli*. *FEMS Microbiology Letters*, **285**(1):97-100.
- AHEMAD, M. 2014. Bacterial mechanisms for Cr(VI) resistance and reduction: an overview and recent advances. *Folia Microbiology*, **59**(4):321-332.
- AISEN, P., ENNS, C. & WESSLING-RENSICK, M. 2001. Chemistry and Biology of eukaryotic iron metabolism. *International Journal of Biochemistry and Cell Biology*, **33**:940-959.
- AKTAN, T., TAN, S. & ICGEN, B. 2013. Characterization of lead-resistant river isolate *Enterococcus faecalis* and assessment of its multiple metal and antibiotic resistance. *Environmental Monitoring and Assessment*, **185**:5285-5293.
- ALPERI, A., MARTINEZ-MURCIA, A. J., WECHIEN, K. O., ARTURO. M., MARIA J. S. & MARIA J. F. 2010. *International Journal of Systematic and Evolutional Microbiology*, **60**:2048-2055.
- ALTIMIRA, F., YÁÑEZ, C., BRAVO, G., GONZÁLEZ, M., ROJAS, L. & SEEGER, M. 2012. Characterization of copper-resistant bacteria and bacterial communities from copper-polluted agricultural soils of central Chile. *BMC Microbiology*, **12**(1):193.
- ALTSCHUL, S. F., MADDAN, T. L., SCHAFFER, A. A., ZANG, J., ZANG, Z., MILLER, W. & LIPMAN, D. J. 1997. Gapped BLAST and PSI-BLAST a generation of protein database search programmes. *Nucleic Acids Research*, **25**:3389-3402.
- ALVAREZ, A. H., MORENO-SANCHEZ, R. & CERVANTES, C. 1999. Chromate Efflux by Means of the ChrA Chromate Resistance Protein from *Pseudomonas aeruginosa*. *Journal of Bacteriology*, **181**(23):7398-7400.
- ANDREWS, J. M. 2001a. Determination of minimum inhibitory concentrations. *Journal of Antimicrobial Chemotherapy*, **48**:5-16.
- ANDREWS, J. M. 2001b. The development of the BSAC standardized method of disc diffusion testing. *Journal of Antimicrobial Chemotherapy*, **1**:29-42.

- ANDREWS, S. C., ROBINS, A. K. & RODRIGUEZ-QUINONES, F. 2003. Bacterial Iron homeostasis. *FEMS Microbiology Reviews*, **27**:215-237.
- ASHISH, B., KAPPOR, N. & KHAJURIA, H. 2013. Copper Toxicity. *Research Journal of Recent Sciences*, **2**(ISC-2012):58-67.
- ASSEM, L. & ZHU, H. 2007. *Chromium toxicological overview*. Version 1. United Kingdom: Health Protection Agency.
- AYRES, R. U., AYRES, L. W. & RADE, I. 2001. *The Life Cycle of Copper, its Co-products and By-products*. 2188452. England: International Institute for Environment and Development (IIED) and World Business Council for Sustainable Development (WBCSD).
- BADAR, U., AHMED, N., SHOEB, E. & GADD, G. 2014. Identification of the pco operon in *Enterobacter* species isolated from contaminated soil. *International Journal of Advanced Reseach*, **2**(3):227-233.
- BAQUERO, F., MARTINEZ, J. & COUTON, R. 2008. Antibiotics and antibiotic resistance in water environment. *Current Opinion in Biotechnology*, **19**:260-265.
- BARAKAT, M. 2011. New trends in removing heavy metals from industrial wastewater. *Arabian Journal of Chemistry*, **4**(4):361-377.
- BARNHART, J. 1997. Occurrences, Uses, and Properties of Chromium. *Regulatory Toxicology and Pharmacology*, **26**(1):S3-S7.
- BAUER, A. W., KIRBY, W. M., SHERRIS, J. C. & TURCK, M. 1966. Antibiotic Susceptibility Testing by a standardized single disc method. *American Journal of Clinical Pathology*, **36**:493-496.
- BCS INCORPORATED, 2002. *Energy and environmental profile of the US Mining Industry*. USA: US Department of Energy Office of Energy Efficiency and Renewable Energy.
- BEARD, S. J., HASHIM, R., MEMBRILLO-HERNANDEZ, J., HUGHES, M. N. & POOLE, R. K. 1997. Zinc (II) tolerance in *Escherichia coli* K-12: evidence that the *ZntA* gene (o732) encodes a cation transport ATPase. *Molecular Microbiology*, **25**(5):883-891.
- BENSON, D. A. & KARSCH-MIZRACHI, I. 2000. Genbank. *Nucleic Acids Research*, **28**:15-18.
- BERTIN, G. & AVERBECK, D. 2006. Cadmium: Cellular effects, modifications of biomolecules, modulation of DNA repairs and genotoxic consequences (a review). *Biochimie*, **88**(11):1549-1559.

- BHAGAT, R. & SRIVASTAVA, S. 1993. Growth response of *Pseudomonas stutzeri* RS34 to the ethylenediaminetetraacetic acid (EDTA) and its interaction with zinc. *Indian Journal of Experimental Biology*, **31**:590–594.
- BHOWMIK, P., BAG, P. K., HAJRA, T. K., RITUPAMA, P. S. & RAMAMURTHY, T. 2009. Pathogenic potential of *Aeromonas hydrophila* isolated from surface waters in Kolkata, India. *Journal of Medical Microbiology*, **58**:1549-1558.
- BIRNBOIM, H. & DOLY, J. 1979. A rapid alkaline procedure for screening recombinant plasmid DNA. *Nucleic Acid Research*, **7**:1513-1523.
- BLAUDEZ, D., JACOB, C., & TURNAN, K. 2000. Differential responses to ectomycorrhizal fungi to heavy metals in vitro. *Mycological Research*, **104**(11):1366-1371.
- BLINDAUER, C. A., HARRISON, M. D., ROBINSON, A. K., PARKINSON, J. A., BOWNESS, P. W., SADLER, P. J. & ROBINSON, N. J. 2002. Multiple bacteria encode metallothioneins and SmtA-like fingers. *Molecular Microbiology*, **45**:1421-1432.
- BOPP, L. H., CHAKRABARTY, A. M. & EHRLICH, H. L. 1983. Chromate resistance plasmid in *Pseudomonas fluorescens*. *Journal of Bacteriology*, **155**:1105-1109.
- BORREMANS, B., HOBMAN, J. L., PROVOOST, A., BROWN, N. L. & VAN DER LELIE, D. 2001. Cloning and Functional Analysis of the *Pbr* Lead Resistance Determinant of *Ralstonia metallidurans* CH34. *Journal of Bacteriology*, **183**:5651-5658.
- BOUANCHAUD, D., SCAVIZZI, M. & CHABBERT, Y. 1968. Elimination by ethidium bromide of antibiotic resistance in *enterobacteria* and *staphylococci*. *Journal of General Microbiology*, **54**(3):417-425.
- BRAMACHARI, P. V., KAVI KISHOR, P. B., RAMADEVI, R., KUMAR, R., RAO, B. R. & DUBEY, S. K. 2007. Isolation and characterization of mucous exopolysaccharide produced by *Vibrio furnissii* VB0s3. *Journal of Microbiology and Biotechnology*, **17**:44-51.
- BRANCO, ACHUNG, A. P., JOHNSTON, T., GUREL, V., MORAIS, P. & ZHITKOVICH, A. 2008. The chromate inducible *chrBACF* Operon from the Transposable Element Tn Ot Chr confers resistance to Chromium (IV) superoxide. *Journal of Bacteriology*, **190**(21): 6996-7003.
- BRANCO, R. & MORAIS, P. V. 2013. Identification and Characterization of the Transcriptional Regulator ChrB in the Chromate Resistance Determinant of *Ochrobactrum tritici* 5bvl1. *Plos One*, **8**(11):1-12.

- BRAYMER, J. & GIEDROC, D. 2014. Recent developments in copper and zinc homeostasis in bacterial pathogens. *Current Opinion in Chemical Biology*, **19**:59-66.
- BROGDEN, R. N., HEEL, R. C., SEIGHT, T. M. & AVERY, G. S. 1979. Amoxicillin injectable: a review of its antibacterial spectrum, pharmacokinetics and therapeutic use. *Drugs*, **18**(3):169-184.
- BROWN, N. L., BARRET, S. R., CAMAKARIS, J., LEE, B. T. O. & ROUCH, D. A. 1997. Molecular genetics and transport analysis of the copper resistance determinant (pco) form *Escherichia coli* plasmid pRJ1004. *Molecular Biology*, **17**(6):1153-1166.
- BROWN, D. & KOTHARI, D. 1975. Comparison of tablets and paper discs for antibiotic sensitivity testing. *Journal of Clinical Pathology*, **28**(12):983-988.
- BROWN, N. L., ROUCH, D. A. & LEE, B. T. O. 1992. Copper resistance systems in bacteria. *Plasmid*, **27**:41-51.
- BUTTERMAN, W. C. & PLACHY, J. 2002. Mineral Commodity Profiles Cadmium. [Online]. Available at: <http://pubs.usgs.gov/of/2002/of02-238/of02-238.pdf>. Date accessed on 02/03/2014.
- CATTELL, R. B. & JASPERS, J. 1967. A general plasmode (No. 30-10-5-2) for factor analytic exercises and research. *Multivariate Behavioral Research Monographs*.
- CERVANTES, C., OHTAKE, H., CHU, L., MISRA, T. K. & SILVER, S. 1990. Cloning, nucleotide sequence and expression of the chromate resistance determinant of *Pseudomonas aeruginosa* plasmid pUM505. *Journal of Bacteriology*, **172**:287-291.
- CHANG, J. S., LAW, R. & CHANG, C. C. 1997. Biosorption of lead, copper and cadmium by biomass of *Pseudomonas aeruginosa* PU21. *WaterResearch*, **31**:1651-1658.
- CHATTOPADHYAY, M. K & GROSSART, H. P. 2011. Antibiotic and heavy metal resistance of bacterial isolates obtained from some lakes in northern Germany. *Journal of Pharmacy and Healthcare Management*, **2**:74-75.
- CHIHOMVU, P., STEGMANN, P. & PILLAY, M. 2014. Identification and Characterization of Heavy Metal Resistant Bacteria from the Klip River. *International Conference on Ecological, Environmental and Biological Sciences, WASET*, Cape Town, **8**(11):166-174.
- CHOUDHURY, R. & SRIVASTAVA, S. 2001a. Mechanism of zinc resistance in *Pseudomonas Putida* strain S4. *World Journal of Microbiology*, **17**:149-153.
- CHOUDHURY, R. & SRIVASTAVA, S. 2001b. Zinc resistance mechanisms in bacteria. *Current Science*, **81**(7):768-775.

- CLERMONT, D. & HORAUD, T. 1990. Identification of chromosomal antibiotic resistance genes in *Streptococcus anginosus* (" *S. milleri*"). *Antimicrobial agents and chemotherapy*, **34**(9):1685-1690.
- CLOWERS, R. C. 1972. Molecular structure of bacterial plasmids. *Bacterial Revolution*, **36**:361-405.
- ÇOLAK, F., ATAR, N., YAZICIOĞLU, D. & OLGUN, A. 2011. Biosorption of lead from aqueous solutions by *Bacillus* strains possessing heavy-metal resistance. *Chemical Engineering Journal*, **173**(2):422-428.
- COOKSEY, D.A. 1990. Genetics of bactericide resistance in plant pathogenic bacteria. *Annual Review of Phytopathology*, **28**:201-219.
- DALLAS, H. F. & DAY, J. A. 2004. *The effect of water quality variables on aquatic water systems: a review*. TT 224/04. Pretoria, South Africa: Water Research Commission.
- DAVIDSON, C. 2003. *Catchment Diagnostic Framework for the Klip River Catchment, Vaal Barrage*. MSc Dissertation, University of Witwatersrand, Johannesburg.
- DAVIS, B. 2011. *Identification and characterization of bacterial genes associated with resistance to and/or degradation of environmental pollutants*. DPhil. Thesis, School of Engineering and Science, Victoria University, Melbourne, Victoria, Australia.
- DAVIS, I. W., LEAVER-FAY, A., CHEN, V. B., BLOCK, J. N., KAPRA, G. J., WANG, X. *et al.* 2007. MolProbity: all-atom contacts and structure validation for proteins and nucleic acids. *Nucleic Acids Research*, **35**:W375-W383.
- DE LA TORRE, M. L., SANCHEZ RHODAS, D., GRANDE, J. A. & GOMEZ, T. 2010. Relationships between pH, colour and heavy metal concentrations in the Tinto and Odiel Rivers (Southwest Spain). *Hydrology Research*, **41**(5):406-413.
- DEB, S., AHMED, S. F. & BASU, M. 2013. Metal accumulation in cell wall: A possible mechanism of cadmium resistance *Pseudomonas stutzeri*. *Bull Environmental Contamination and Toxicology*, **90**:323-328.
- DEFOREST, D. K., BRIX, K. V. & ADAMS W, J. 2007. Assessing metal bioaccumulation in Aquatic environments. The inverse relationship between bioaccumulation factors, trophic transfer factors and exposure concentration. *Aquatic toxicology*, **84**:236-246.
- DENKHAUS, E. & SALNIKOW, K. 2002. Nickel essentiality, toxicity, and carcinogenicity. *Critical Reviews in Oncology/Hematology*, **42**(1):35-56.



- DEPARTMENT OF WATER AFFAIRS AND FORESTRY (DWAF), 1999. *Development of Water Quality Management Plan for the Klip River Catchment. Phase 1: situation analysis. Draft Final Report*. Pretoria, South Africa.
- DEREEPER, A., GUIGNON, V., BLANC, G., AUDIC, S., BUFFET, S., CHEVENET, F. *et al.* 2008. Phylogeny. fr: robust phylogenetic analysis for the non-specialist. *Nucleic Acids Research*, **36**(2):465-469.
- DI´AZ-PE´REZ, C., CERVANTEZ, C., CAMPOS-GARCIA´A, J., JULIAN´N-SA´NCHEZ, A. & RIVEROS-ROSAS, H. 2007. Phylogenetic analysis of the chromate ion transporter (CHR) superfamily. *FEBS Journal*, **274**:6215-6227.
- DIELS, L., DONG, Q., VAN DER LELIE, D., BAEYENS, W. & MERGEAY, M. 1995. The *czc* operon of *Alcaligenes eutrophus* CH34: from resistance mechanism to the removal of heavy metals. *Journal of Industrial Microbiology*, **14**:142-153.
- DJOKO, K., CHONG L., WEDD, A. & XIAO, Z. 2010. Reaction mechanisms of the multicopper oxidase CueO from *Escherichia coli* support its functional role as a cuprous oxidase. *Journal of the American Chemical Society*, **132**(6):2005-2015.
- DUGUID, J. P. 1989. *Staining methods*. In MACKIE, T. J. & MCCARTNEY, J. E. (eds.). Practical Medical Microbiology. Churchill Livingstone. New York. pp 41-51.
- EDGAR, R. C. 2004. MUSCLE: multiple sequence alignment with high accuracy and high throughput. *Nucleic acids research*, **32**(5):1792-1797.
- EFSTATHIOU, J. D. & MCKAY, L. L. 1977. Inorganic salts resistance associated with a lactose-fermenting plasmid in *Streptococcus lactis*. *Journal of Bacteriology*, **13**:257-265.
- ESPINOZA, E. L., BAINES, A. L. D. & LOWE, K. L. 2013. Biochemical, Nutrient and Inhibitory Characteristics of *Streptomyces* Cultured from a Hypersaline Estuary, The Laguna Madre (Texas). *OnLine Journal of Biological Sciences*, **13**(1):18-27.
- FAN, L., MA, Z., LIANG, J., LI, H., WANG, E. & WEI, G. 2011. Characterization of a copper-resistant symbiotic bacterium isolated from *Medicago lupulina* growing in mine tailings. *Bioresource Technology*, **102**(2):703-709.
- FELSENSTEIN, J. 1985. Confidence limits on phylogenies: an approach using the bootstrap. *Evolution*: 783-791.
- FLORA, G., GUPTA, D. & TIWARI, A. 2012. Toxicity of lead: A review with recent updates. *Interdisciplinary Toxicology*, **5**(2):7-58.

- FRAGA, C. G. & OTEIZA, P. I. 2002. Iron toxicity and anti-oxidant nutrients. *Toxicology*, **180**: 23-32.
- FROST, L. S., LEPLACE, R., SUMMERS, A. O. & TOUSSAINT, A. 2005. Mobile genetic elements: the agents of open source evolution. *Nature Reviews Microbiology*, **3**:722-732.
- GADD, G. 1990. Heavy metal accumulation by bacteria and other microorganisms. *Experientia*, **46**(8):834-840.
- GADD, G. M. 1993. Interactions of fungi with toxic metals. *New Phytologist*, **24**(1):25-60.
- GARCIA-DOMINGUEZ, M., LOPEZ-MAURY, L., FLORENCIO, F. J. & REYES, J. C. 2000. A gene cluster involved in metal homeostasis in the cyanobacterium *Synechocystis* sp. strain PCC 6803. *Journal of Bacteriology*, **182**:1507-1514.
- GASTEIGER, E., HOOGLAND, C., GATTIKER, A., DUVAUD, S., WILKINS, M. R., APPEL, R. D. & BAIROCH, A. 2005. *Protein identification and analysis tools on the ExPASy server*. In WALKER, J. M. (ed.). The proteomics protocols handbook. Humana Press. New Jersey. pp 571-607.
- GEOURJON, C. & DELEAGE, G. 1995. SOPMA: significant improvements in protein secondary structure prediction by consensus prediction from multiple alignments. *Computer Applications in the Biosciences: CABIOS*, **11**(6), 681-684.
- GILLER, K. E., WITTER, E., & MCGRATH, S. P. 2009. Heavy metals and soil microbes. *Soil Biology and Biochemistry*, **41**(10):2031-2037.
- GINNS, C., BENHAM, M., ADAMS, L., WHITHEAR, K., BETTELHEIM, K., CRABB, B. *et al.* 2000. Colonization of the respiratory tract by a virulent strain of avian *Escherichia coli* requires carriage of a conjugative plasmid. *Infection and Immunity*, **68**(3):1535-1541.
- GIRI, S. 2011. *Isolation and biochemical characterization of Mercury Resistant Bacteria (MRB) from soil samples of industrially contaminated areas of Rourkela, Orissa*. MSc. Dissertation, National Institute of Technology Rourkela, Orissa.
- GLINDE, H. & JOHAL, I. 2011. Zinc and its uses: Protective for Humans and steel. Hot Dip Galvanizing magazine. *Galvanizers Association*:3-4.
- GOWRI, P. & SRIVASTAVA, S. 1996. Encapsulation as a response of *Azospirillum brasilense* sp7 to zinc stress. *World Journal of Microbiology & Biotechnology*, **12**(4):319-322.

- GRASS, G., FAN, B., ROSEN, B., LEMKE, K., SCHLEGEL, H. & RENSING, C. 2001. NreB from *Achromobacter xylosoxidans* 31A is a Nickel-Induced Transporter Conferring Nickel Resistance. *Journal of Bacteriology*, **183**(9):2803-2807.
- GRINSTED, J. & BENNET, P. M. 1988. (eds.). *Methods in Microbiology Volume 21, Plasmid Technology*. 2nd Edition. Academic Press. London.
- GROßE, C., ANTON, C., HOFFMAN, T., FRANKE, S., SCHLEUDER, G. & NIES, D. H. 2004. Identification of a regulatory pathway that controls the heavy-metal resistance system Czc via promoter *czcNp* in *Ralstonia metallidurans*. *Archives of Microbiology* **182**:109-118.
- HALLIWELL, B. & GUTTERIDGE, J. M. C. 1990. The role of free radicals and catalytic metal ions in human disease: an overview. *Methods in Enzymology*, **186**:1-85.
- HANTKE, K. & BRAUN, V. 2000. The art of keeping low and high iron concentrations in balance. In STORZ, G. & HENGGE-ARONIS, R. (eds.). *Bacterial Stress Responses*. ASM Press. Washington, DC. pp. 275-288.
- HARISPRASAD, N. V. & DAYANADA, H. S. 2013. Environmental Impact due to Agricultural runoff containing Heavy Metals -A Review. *International Journal of Scientific and Research Publications*, **3**(5):672-677.
- HARITHA, A., SAGAR, K. P., TIWARI, A., KIRANMAYI, P., RODRIGUE, A., MOHAN, P. M. & SINGH, S. S. 2009. *MrdH*, a novel metal resistance determinant of *Pseudomonas putida* KT2440, is flanked by metal inducible mobile genetic elements. *Journal of Bacteriology*, **191**:5976-5987.
- HAU, H. & GRALNICK, J. 2007. Ecology and Biotechnology of the Genus *Shewanella*. *Annual Review of Microbiology*, **61**(1):237-258.
- HE, M., LI, X., GUO, L., MILLER, S. J., RENSING, C. & WANG, G. 2010. Characterization and genomic analysis of chromate resistant and reducing *Bacillus cereus* strain SJ1. *BMC Microbiology*, **10**(221):1-10.
- HENDERSON, R., DURANDO, J., OLLER, A., MERKEL, D., MARONE, P. & BATES, H. 2012. Acute oral toxicity of nickel compounds. *Regulatory Toxicology and Pharmacology*, **62**(3):425-432.
- HENNE, K. L., NAKATSU, C. H, THOMPSON, D. K. & KONOPOKA, A. K. 2009. High-level chromate resistance in *Arthrobacter* sp. strain FB24 requires previously uncharacterized accessory genes. *BMC Microbiology*, **9**:199-213.

- HOOKOOM, M. & PUCHOOA, D. 2013. Isolation and identification of Heavy Metal Tolerant Bacteria from Industrial and Agricultural Areas in Mauritius. *Current Research in Microbiology and Biotechnology*, **1**(3):119-123.
- HOSSAIN, S. M. & ANATHARAM, N. 2006. Studies on bacterial growth and lead biosorption using *Bacillus subtilis*. *Indian Journal of Chemical Technology*, **13**:591–596.
- HUFFMAN, D., HUYETT, J., OUTTEN, F., DOAN, P., FINNEY, L., HOFFMAN, B. *et al.* 2002. Spectroscopy of Cu (II)-PcoC and the multicopper oxidase function of PcoA, two essential components of *Escherichia coli* pco copper resistance operon. *Biochemistry*, **41**(31):10046-10055.
- HYNNINEN, A. 2010. *Zinc, cadmium and lead resistance mechanisms in bacteria and their contribution to biosensing*. MSc dissertation, Department of Food and Environmental Sciences Faculty of Agriculture and Forestry, University of Helsinki, Finland.
- HYNNINEN, A., TOUZE, T., PITKANEN, L., MENGIN-LECREUX, D. & VIRTÄ, M. 2009. An efflux transporter PbrA and a phosphatase PbrB cooperate in Lead Resistance mechanisms in bacteria. *Molecular Biology*, **74**(2):384-394.
- INTORNE, A. C., OLIVEIRA, M. C. V., PEREIRA, L. & DE SOUZA FILHO, G. 2012. Essential Role of the *czc* determinant for cadmium, cobalt and zinc resistance in *Gluconobacter diazotrophus* PAI 5. *International Microbiology*, **15**:69-78.
- JATAV, V. K., LOVEKESH, P., ANKIT, R. & SMARADDHI, T. 2014. Homology modelling and analysis of structure predictions of KLF8 protein from *Homo Sapiens*. *International Journal of Pharmaceutical Sciences and Research*, **5**(3):1045-1050.
- JACOBSEN, F. E., KASMIERCZAK, K. M., LISHER, J. P., WINKLER, M. E. & GIEDROC, D. P. 2011. Interplay between manganese and zinc homeostasis in the human pathogen *Streptococcus pneumoniae*. *Metallomics*, **3**:38-41.
- JONES, S. & THORNTON, J. 2004. Searching for functional sites in protein structures. *Current Opinion in Chemical Biology*, **8**(1): 3-7.
- JUSTBIO. [Online]. Available at: <http://www.justbio.com/index.php?page=translator>. Date accessed on 13/05/2014.
- IN-STREAM WATER QUALITY GUIDELINES FOR THE KLIP RIVER CATCHMENT. 2003. [Online]. Available at: [www.reservoir.co.za](http://www.reservoir.co.za). Date accessed on 4/10/2013.

- KAMIKA, I. & MOMBA, M. 2013. Assessing the resistance and bioremediation ability of selected bacterial and protozoan species to heavy metals in metal-rich industrial wastewater. *BMC Microbiology*, **13**(1):28.
- KATOH, K. & STANDLEY, D. 2013. MAFFT Multiple Sequence Alignment Software Version 7: Improvements in Performance and Usability. *Molecular Biology and Evolution*, **30**(4):772-780.
- KASPRZAK, K. S., SUNDERMAN, F. W. J. R. & SALNIKOW, K. 2003. Nickel carcinogenesis. *Mutation Research*, **533**:67-97.
- KIMURA, M. 1980. A simple method for estimating evolutionary rates of base substitutions through comparative studies of nucleotide sequences. *Journal of Molecular Evolution*, **16**(2):111-120.
- KOTZE, P. J. 2008. The Klip River Catchment (Gauteng) and Study Area. Chapter 2. [Online]. Available at: [http://ujdigisapce.uj.ac.za:8080/dsapce/bitstream/102101/1144/22/CHAPTER 2 Catchment\\_.pdf](http://ujdigisapce.uj.ac.za:8080/dsapce/bitstream/102101/1144/22/CHAPTER_2_Catchment_.pdf). Date accessed on 02/04/2014.
- KUIJPER, E., J., PEETERS, M. F., SCHOENMAKERS, B. S. & ZANEN, H. C. 1989. Antimicrobial susceptibility of sixty human fecal isolates of *Aeromonas* species. *European Journal of Clinical Microbiology & Infectious Diseases*, **8**:248-250.
- KUMAR, R., NONGKHILAW, M., ACHARYA, C. & JOSHI, S.R. 2013. Growth media composition and heavy metal tolerance behaviour of bacteria characterized from the Sub-surface soil of uranium rich ore bearing site of Domiastat in Meghalaya. *Indian Journal of Biotechnology*, **12**:115-119.
- KYTE, J. & DOLITTLE, R. F. 1982. A simple method for displaying the hydropathic character of a protein. *Journal of Molecular Biology*, **157**(1):105-132.
- LAURENZI, A., HUNG, L. & SAMUDRALA, R. 2013. Structure Prediction of Partial-Length Protein Sequences. *International Journal of Molecular Sciences*. **14**(7):14892-14907.
- LAWSON, E. O. 2011. Physicochemical parameters and Heavy Metal contents of water from the Mangrove Swamps of Lagos Lagoon, Lagos Nigeria. *Advances in Biological Research*, **5**(1):8-21.
- LEVY, S. B. 1998. The challenge of antibiotic resistance. *Scientific American*, **278**(3):46-53.
- LOTTERMOSTER, B. 2010. *Mine Wastes: Characterization, Treatment and Environmental Impacts*. London New York: Springer Heidelberg Dordrecht.

- LÜDERS, S., DAVID, F., STEINWAND, M., JORDAN, E., HUST, M., DÜBEL, S. & FRANCO-LARA, E. 2011. Influence of the hydromechanical stress and temperature on growth and antibody fragment production with *Bacillus megaterium*. *Applied Microbiology and Biotechnology*, **91**:81-90.
- MACOMBER, L. & IMLAY, J. 2009. The iron-sulfur clusters of dehydratases are primary intracellular targets of copper toxicity. *Proceedings of the National Academy of Sciences*, **106**(20):8344-8349.
- MALIK, A. & JAISWAL, R. 2000. Metal resistance in *Pseudomonas* strains isolated from soil treated with industrial wastewater. *World Journal of Microbiology and Biotechnology*, **16**(2):177-182.
- MANIATIS, T., FRITISCH, E. F. & SAMBROOK, J. 1982. *Molecular cloning a laboratory manual*. Cold Spring Harbor, New York, USA: Cold Spring Harbor, Laboratory.
- MARCHLER-BAUER, A., LU, S., ANDERSON, J., CHITSAZ, F., DERBYSHIRE, M., DEWEESE-SCOTT, C. *et al.* 2011. CDD: a Conserved Domain Database for the functional annotation of proteins. *Nucleic Acids Research*, **39**(1):225-229.
- MARGESIN, R. & SCHINER, F. 2007. Bacterial heavy metal-tolerance- extreme resistance to nickel in *Arthrobacter* spp. strains. *Journal of Basic Microbiology*, **36**(4):269-282.
- MARTINS, V., PITONDO-SILVA, A., DE MELO MANÇO, L., FALCÃO, J., FREITAS, S., DA SILVEIRA, W. & STEHLING, E. 2013. Pathogenic potential and genetic diversity of environmental and clinical isolates of *Pseudomonas aeruginosa*. *APMIS*, **122**(2):92-100.
- MCCARTHY, T. S. & VENTER J. S. 2006. Increasing pollution levels in the Witwatersrand recorded in the peat deposits of the Klip River Wetland. *South African Journal of Science*, **102**: 27-34.
- MCCARTHY, T. S., ARNOLD, V., VENTER, J. S. & ELLERY, W. N. 2007. The collapse of the Johannesburg Klip River Wetland. *South African Journal of Science*, **103**(9-10):391-397.
- MCCARTHY, T.S. 2011. The impact of Acid mine Drainage in South Africa. *South African Journal of Science*, **107**(6/7):1-8.
- MEISSNER, R. 2010. Panoramio. [Online]. Available at: <http://www.panoramio.com/user/796092>. Date accessed on 03/02/2014.
- MELLANO, M. & COOKSEY, D. 1988. Induction of the copper resistance operon from *Pseudomonas syringae*. *Journal of Bacteriology*, **170**(9), 4399-4401.

- MINNESOTA POLLUTION CONTROL, 2009. *Low Dissolved Oxygen in water*. Water Quality/Impaired Waters 3.24. Minnesota. USA
- MISTRY, P. 2013. *Salmonella in companion animals*. DPhil. Thesis, Aston University, Birmingham, England.
- MONCHY, S., BENOTMANE, M., JANSSEN, P., VALLAEYS, T., TAGHAVI, S, VAN DER LELIE, D. *et al.* 2007. Plasmids pMOL28 and pMOL30 of *Cupriavidus metallidurans* are specialized in the maximal viable response to heavy metals. *Journal of Bacteriology*, **189**(20): 7417-7425.
- MURUVEN, D. N. 2011. *An Evaluation of the cumulative surface water pollution within the consolidated Main Reef Area, Roodeport, South Africa*, University of South Africa.
- NAIK, M. M. & DUBEY, S. K. 2013. Lead resistant bacteria: Lead resistance mechanisms, their applications in lead bioremediation and biomonitoring. *Ecotoxicology and Environmental Safety*, **98**:1-7.
- NICKEL INSTITUTE, 2011. [Online]. Available at: [www.nickelinstitute.org](http://www.nickelinstitute.org), Date accessed on 08/04/2014.
- NIES, A., NIES, D. H. & SILVER, S. 1989. Cloning and expression of plasmid genes encoding resistances to chromate and cobalt in *Alcaligenes eutrophus*. *Journal of Bacteriology*, **171**:5065-5070.
- NIES, D. 1999. Microbial heavy-metal resistance. *Applied Microbiology and Biotechnology*, **51**(6):730-750.
- NIES, A., NIES, D. H. & SILVER, S. 1990. Nucleotide sequence and expression of a plasmid-encoded chromate resistance determinant from *Alcaligenes eutrophus*. *Journal of Biological Chemistry*, **265**:5648–5653.
- NIES, D. H. 2003. Efflux mediated heavy metal resistance in prokaryotes. *FEMS Microbiology Reviews*, **27**:313-339.
- NIES, D. H. 1992. *Czc R* and *CzcD*, gene products Affecting Regulation of resistance to cobalt, zinc, and cadmium (*czc* system) in *Alcaligenes eutrophus*. *Journal of Bacteriology*, **174**(24):8102-8110.
- NIES, D. H. & SILVER, S. 1995. Ion efflux systems involved in bacterial metal resistance. *Journal of Industrial Microbiology*, **14**:186-199.
- NRIAGU, J. 2007. *Zinc Toxicity in humans*. Michigan, United States: Elsevier.

- NUCIFORA, G., CHU, L., MISRA, T. & SILVER, S. 1989. Cadmium resistance from *Staphylococcus aureus* plasmid pI258 *cadA* gene results from a cadmium-efflux ATPase. *Proceedings of the National Academy of Sciences*, **86**(10):3544-3548.
- ODEYEMI, A. O., ASMAT, A. & USUP, G. 2012. Antibiotic resistance and putative virulence factors of *Aeromonas hydrophila* isolated from estuary. *Journal of Microbiology, Biotechnology and Food sciences*, **1**(6):1339-1357.
- ODONKOR, S. T. & AMPOFO, J. K. 2013. *E. coli* as an indicator of bacteriological quality of water: an overview. *Microbiology Research*, **4**(e2):5-11.
- OLAFSON, R. W., MCCUBBIN, W. D. & KAY, C. M. 1988. Primary and secondary structural analysis of a unique prokaryotic metallothionein from a *Synechococcus* sp. cyanobacterium. *Biochemical Journal*, **251**:691-699.
- OZER, G., ERGENE, A. & ICGEN, B. 2013. Biochemical and molecular characterization of strontium resistant environment isolates of *Pseudomonas fluorescens* and *Sphingomonas paucimobilis*. *Geomicrobiology Journal*, **30**(5):381-390.
- PANADAY, S., SAHA, P., BISWAS, S. & MAITI, T. 2011. Characterization of two metal resistant *Bacillus* strains isolated from slag disposal site at Burnpur, India. *Journal of Environmental Biology*, **32**:773-779.
- PATZER, S. & HANTKE, K. 1998. The ZnuABC high-affinity zinc uptake system and its regulator Zur in *Escherichia coli*. *Molecular Microbiology*, **28**(6):1199-1210.
- PELCZAR, M. J. J. & REID, R. D. 1958. Pure cultures and growth characteristics. In *Microbiology*. McGraw Hill Book Company. New York. pp 76-84.
- PEÑA-MONTENEGRO, T. D. & DUSSAN, J. 2013. Genome sequence and description of the heavy metal tolerant bacterium *Lysinibacillus sphaericus* strain OT4b.31. *Standards in Genomic Sciences*, **9**(1):42-56.
- PHILLIPS, K., ZAIDAN, F., ELIZONDO, O. & LOWE, K. 2012. Phenotypic characterization and 16S rDNA identification of culturable non-obligate halophilic bacterial communities from a hypersaline lake, La Sal del Rey, in extreme South Texas (USA). *Aquatic Biosystems*, **8**(5):1-11.
- PIRES, C. 2010. *Bacteria in heavy metals contaminated soil, diversity, tolerance and use in remediation system*. PhD Thesis, Cranfield University, Cranfield, United Kingdom.



- PRAUS, P. 2007. Urban water quality evaluation using multivariate analysis. *Acta Montanistica Slovaca*, **12**(2):150-158.
- RAJA, E. C., SELVAM, G. S. & OMNIE, K. 2009. *Isolation, identification and characterization of heavy metal resistant bacteria from sewage*. International Joint Symposium on Geodisaster Prevention and Geoenvironment in Asia:205-2011
- RAJA. E. C. & SELVAM, G. S. 2009. Plasmid profile and curing analysis of *Pseudomonas aeruginosa* as metal resistant. *International Journal of Environmental Science and technology*, **6**(2):259-266.
- RAJKUMAR, B., SHARMA, G. D. & PAUL, A. K. 2012. Isolation and characterization of heavy metal resistant bacteria from Barak River contaminated with pulp paper mill effluent, South Assam. *Bull Environmental Contamination and Toxicology*, **89**:263-268.
- RAMÍREZ-DÍAZ, M., DÍAZ-PÉREZ, C., VARGAS, E., RIVEROS-ROSAS, H., CAMPOS-GARCÍA, J. & CERVANTES, C. 2007. Mechanisms of bacterial resistance to chromium compounds. *Biometals*, **21**(3):321-332.
- RAND WATER. [Online]. Available at:  
<http://www.randwater.co.za/corporateresponsibility/www/pages/waterpollution.aspx>. Date accessed on 25/04/2014.
- RENSING, C., MITRA, B. & ROSEN, B. P. 1997. The *zntA* gene of *Escherichia coli* encodes a Zn (II)-translocating P-type ATPase. *Proceedings of the National Academy of Sciences*, **94**(26): 14326-14331.
- REYES, M. P., ZHAO, J. J. & BUENSALIDO, J. A. L. 2014. Current Perspectives: Therapeutic Uses of Tobramycin. *Pharmacovigilance*, **2**(2):1-5.
- ROANE, T. 1999. Lead resistance in two bacterial isolates from heavy metal contaminated soils. *Microbial Ecology*, **37**:218-224.
- RODRIGUE, A., EFFANTIN, G., & MANDRAND-BERTHELOT, M. A. 2005. Identification of *rcnA* (yohM), a nickel and cobalt resistance gene in *Escherichia coli*. *Journal of Bacteriology*, **187**:2912-2916.
- ROUCH, D. A. & BROWN, N. L. 1997. Copper inducible transcriptional regulation in two promoters in the *Escherichia coli* copper resistance determinant *pco*. *Microbiology*, **143**:1191-1202.

- SAITOU, N. & NEI, M. 1987. The neighbor-joining method: a new method for reconstructing phylogenetic trees. *Molecular Biology and Evolution*, **4**(4):406-425.
- SARMA, B., AXHARYA, C. & JOSHI, S. R. 2010. Pseudomonads: a versatile bacterial group exhibiting dual resistance to metals and antibiotics. *African Journal of Microbiology Research*, **4**:2828-2835.
- SCHANTZ, J. T. & KEE-WOEI, N. 2004. A manual for primary cell culture. *World Scientific*, pp. 89.
- SCHWARZ, S. & CHASLUS-DANCLA, E. 2001. Use of antimicrobials in veterinary medicine and mechanisms of resistance. *Veterinary Research*, **32**(3-4):201-225.
- SETLOW, P. 2007. I will survive: DNA protection in bacterial spores. *Trends in Microbiology*, **15**: 172–180.
- SHARMA, K. K. & KALAWAT, U. 2010. Emerging infections: *Shewanella*, A series of Five Cases. *Journal of Laboratory Physicians*, **2**(2):61-65.
- SHARMA, S. K., SINGH, L. & SINGH, S. 2013. Comparative Study between Penicillin and Ampicillin. *Scholars Journal of Applied Medical Sciences*, **1**(4):291-294.
- SILVER, S., LEE, B. T. O., BROWN, N. L. & COOKSEY, D.A. 1993. Bacterial plasmid resistances to copper, cadmium and zinc. In WELCH, A. J. (ed.). *Chemistry of Copper and Zinc Triads*. The Royal Society of Chemistry. London. pp 33-53.
- SILVER, S. & PHUNG, L. T. 2009. Heavy metals, bacterial resistance. In SCHAECHTER, M. (ed.). *Encyclopedia of Microbiology*. Elsevier. Oxford, UK. pp 220-227.
- SILVER, S. 1992. Plasmid determined metal resistance mechanisms: Range and Overview. *Plasmid*, **27**(1):1-3.
- SMIBERT, R. M. & KRIEG, N. R. 1981. General characterization. In GERDhardt, P., MURRAY, R. G. E., COSTILOW, R. N., NESTER, E. W., WOOD, W. A., KRIEG N. R. & PHILLIPS, G. B (eds.). *Manual of Methods for General Bacteriology*. American Society for Microbiology. Washington, DC. pp. 409–443.
- SPENGLER, G., MOLNAR, A., SCHELZ, Z., AMARA, L., SHARPLES, D. & MOLNAR, J. 2006. The Mechanism of Plasmid Curing in Bacteria. *Current Drug Targets*, **7**(7):1-18.
- SRIVASTA, P. & KOWSHIK, M. 2013. Mechanisms of metal resistance and homeostasis in Haloearchaea. *Archaea*, **2013**:1-16.


- STÄHLER, F. N., ODENBREIT, S., HAAS, R., WILRICH, J., VAN VLIET, A. H. M., KUSTERS, J. G., KIST, M. & BERESWILL, S. 2006. The novel *Helicobacter pylori* CznABC metal efflux pump is required for cadmium, zinc, and nickel resistance, urease modulation, and gastric colonization. *Infection and Immunity*, **74**:3845-3852.
- STOCK, I. 2003. Natural Antibiotic Susceptibility of *Proteus spp.* with special reference to *P. mirabilis* and *P. penneri* strains. *Journal of Chemotherapy*, **15**(1):12-26.
- TAGHAVI, S., LESAULNIER, C., MONCHY, S., WATTIEZ, R., MERGEAY, M. & VAN DER LELIE, D. 2009. Lead (II) resistance in *Cupriavidus metallidurans* CH34: interplay between plasmid and chromosomally-located functions. *Antonie van Leeuwenhoek*, **96**:171-182.
- TAMURA, K., STECHER G., PETERSON, D., FILIPSKI, A. & KUMAR, S. 2013. MEGA6: Molecular Evolutionary Genetics Analysis version 6.0. *Molecular Biology and Evolution*, **30**(12): 2725-2729.
- TETAZ, T. & LUKE, R. 1983. Plasmid-controlled resistance to copper in *Escherichia coli*. *Journal of Bacteriology*, **154**(3):1263-1268.
- TIAN, J., WU, N., LI, J., LIU, Y., GUO, J., YAO, B. & FAN, Y. 2007. Nickel-resistant determinant from *Leptospirillum ferriphilum*. *Applied and Environmental Microbiology*, **73**:2364-2368.
- TOES, A., GEELHOED, J., KUENEN, J. & MUYZER, G. 2008. Characterization of Heavy Metal Resistance of Metal-Reducing *Shewanella* Isolates from Marine Sediments. *Geomicrobiology Journal*, **25**(6):304-314.
- TREVORS, J. T. 1985. Plasmid curing in bacteria. *FEMS Microbiology Letters*, **32**(3-4):149-157.
- VENKATESHARAJU, K., RAVIKUMAR, P., SOMASHEKAR, R. K. & PRAKASH, K. L. 2010. Physico-chemical and bacteriological investigation on the River Cauvery of Kollegal Stretch in Karnataka. *Kathmandu University of Science, Engineering and Technology*, **6**(1):50-59.
- VERMAAK, V. 2009. *A geomorphological Investigation of the Klip River Wetland, South of Johannesburg*. MSc. Dissertation, University of Witwatersrand, Johannesburg.
- VIRENDER, S., CHAUCHAN, P. K., KANTA, R., PHEWA, T. & KUMAR, V. 2010. Isolation and characterization of *Pseudomonas* resistant to heavy metal contaminants. *International Journal of Pharmaceutical Sciences Review and Research*, **3**(2):164-167.
- WARING, M. 1966. Cross-linking and interaction in nucleic acids. *A symposium of the Society in General Microbiology*, **16**:235-265.


- WATSON, J., SANDERSON, S., EZERSKY, A., SAVCHENKO, A., EDWARDS, A., ORENGO, C. *et al.* 2007. Towards fully automated structure-based function prediction in structural genomics: a case study. *Journal of Molecular Biology*, **367**(5):1511-1522.
- WEI, G., FAN, L., ZHU, W., FU, Y. & TANG, M. 2009. Isolation and characterization of the heavy metal resistant bacteria CCNWS33-2 isolated from root nodule of *Lespedeza cuneata* in gold mine tailings in China. *Journal of Hazardous Materials*, **162**:50-56.
- WILHEM, M. P. & ESTES, L. 1999. Vancomycin. *Mayo Clinic Proceedings*, **74**(9):928-935.
- WILLEY, J., SHERWOOD, L. & WOOLVERTON, C. 2009. Microbial Growth. In WILLEY, J., SHERWOOD, L. & WOOLVERTON, C. (eds.). *Prescotts's Microbiology*. 1st edn. McGraw-Hill Custom Publishing. New York. pp. 126-151.
- XIANG, Z. 2006. Advances in Homology Protein Structure Modeling. *Current Protein and Peptide Science*, **7**(3):217-227.
- XIONG, J., LI, D., LI, H., HE, M., MILLER, S. J., YU, L. & WANG, G. 2011. Genome analysis and characterization of zinc efflux systems of a highly zinc resistant bacterium, *Comamonas testosteroni* S44. *Research in Microbiology*, **162**:671-679.
- ZAKERI, B. & WRIGHT, G. D. 2008. Chemical biology of Tetracycline antibiotics *Biochemistry and Cell Biology*, **86**(2):124-136.
- ZAMAN, M. A., PASHA, M. H. & AKHTER M. Z. 2010. Plasmid Curing of *Escherichia coli* Cells with Ethidium Bromide, Sodium Dodecyl Sulfate and Acridine Orange. *Bangladesh Journal of Microbiology*, **27**(1):28-31.
- ZAREE, N. N., NASSIRABADY N. N. & AMIR, T. 2014. Antimicrobial Susceptibility Profiles of Environmental *Enterobacteriaceae* Isolates From Karun River, Iran. *International Journal of Enteric Pathogens*, **2**(2):1-5.
- ZHANG, Y. 2008. I-TASSER server for protein 3D structure prediction. *BMC Bioinformatics*, **9**(1):40.
- ZHITKOVICH, A. 2005. Importance of chromium-DNA adducts in mutagenicity and toxicity of chromium (VI). *Chemical Research in Toxicology*, **18**:3-11.
- ZHOU, J., BRUNS, M. A. & TIEDJE, J. M. 1996. DNA recovery from Soils of Diverse Composition. *Applied and Environmental Microbiology*, **62**(2):316-322.

## **APPENDICES**

### **APPENDIX I: FIELD SHEETS**

This appendix indicates the forms that were used to collect data physic-chemical data at each site for both the water and sediment samples.

SWAMP Field Data Sheet (Sediment Chemistry) - EventType=WQ										Entered in d-base (initial/date)		Pg      of      Pgs	
*StationID: _____			*Date (mm/dd/yyyy):      /      /		*Group: _____			VUT					
*Funding: _____			ArrivalTime: _____		DepartureTime: _____		*SampleTime (1st sample): _____			*Protocol: _____			
*ProjectCode: _____			*Personnel: _____			*Purpose (circle applicable): SedChem SedTox Habitat Benthic			*PurposeFailure: _____				
*Location: Bank Thalweg Midchannel OpenWater			*GPS/DGPS		Lat (dd.ddddd)		Long (ddd.ddddd)		OCCUPATION METHOD: Walk-in Bridge R/V _____ Other				
GPS Device: _____			*Target: _____		-		STARTING BANK (facing downstream): LB / RB / NA						
			*Actual: _____		-		Point of Sample (if Integrated, then -88 in dbase)						
Datum: NAD83		Accuracy (ft / m): _____		Same as Water/Probe Collection? YES NO					DISTANCE		STREAM WIDTH (m):		
Habitat Observations (CollectionMethod = Habitat generic ) **Only complete Sed Observations (bolded) if WQ Observations are already recorded				WADEABILITY: Y / N / Unk		BEAUFORT SCALE see Attachment		FROM BANK (m):		WATER DEPTH (m):			
SITE ODOR: _____		None, Sulfides, Sew age, Petroleum, Smoke, Other _____		WIND DIRECTION (from):				HYDROMODIFICATION: None, Bridge, Pipes, ConcreteChannel, GradeControl, Culvert, AerialZipline, Other		LOCATION (to sample): US / DS / WI / NA			
OTHERPRESENCE: _____		Vascular, Nonvascular, Oily Sheen, Foam, Trash, Other _____		DOMINANTSUBSTRATE: _____		Bedrock, Concrete, Cobble, Boulder, Gravel, Sand, Mud, Unk, Other _____		PHOTOS (RB & LB assigned when facing downstream; RENAME to StationCode_yyyy_mm_dd_uniquecode):		1: (RB / LB / BB / US / DS / ##)			
SEDODOR: _____		None, Sulfides, Sew age, Petroleum, Mixed, Other _____		PRECIPITATION: _____		None, Fog, Drizzle, Rain, Snow		2: (RB / LB / BB / US / DS / ##)					
SEDCOLOR: _____		Colorless, Green, Yellow, Brown		PRECIPITATION (last 24 hrs): _____		Unknown, <1", >1", None		3: (RB / LB / BB / US / DS / ##)					
SEDCOMPOSITION: _____		Silt/Clay, FineSand, CoarseSand, Gravel, Cobble, Mixed, HardPanC		EVIDENCE OF FIRES: _____		No, <1 years, <5 years							
OBSERVED FLOW: NA, Dry Waterbody Bed, No Obs Flow, Isolated Pool, Trickle (<0.1cfs), 0.1-1cfs, 1-5cfs, 5-20cfs, 20-50cfs, 50-200cfs.													
Samples Taken (# of containers filled) - Method=Sed_Grab										Field Dup YES / NO: (SampleType = Grab / Integrated; LABEL_ID = FieldQA; create collection record upon data entry)			
COLLECTION DEVICE:			Scoop (SS / PC / PE, Core (SS / PC / PE), Grab (Van Veen / Eckman / Petite Ponar)							COLLECTION DEVICE AREA (m2): _____			
Sample Type:	Depth Collec (cm)	Equipment Used	Sediment Only (Y / N)	Grain Size/TOC	Organics	Metals/HgT	Selenium	Toxicity	SWI	Archive Chemistry	Benthic Infauna	Benthic Coll. Area (m²)	Sieve Size (mm)
Integrated Grab													
Integrated Grab													
Integrated Grab													
Integrated Grab													
COMMENTS:													

SWAMP Field Data Sheet (Water Chemistry & Discrete Probe) - EventType=WQ										Entered in d-base (initial/date)		Pg of Pgs	
*StationID: _____			*Date (mm/dd/yyyy): ____/____/____		*Group: _____		VUT						
*Funding: _____			ArrivalTime: _____		DepartureTime: _____		*SampleTime (1st sample): _____		*Protocol: _____				
*ProjectCode: _____			*Personnel: _____		*Purpose (circle applicable): WaterChem WaterToxHabitat FieldMeas				*PurposeFailure: _____				
*Location: Bank Thalweg Midchannel OpenWater			*GPS/DGPS	Lat (dd.ddddd)	Long (ddd.ddddd)	OCCUPATION METHOD: Walk-in Bridge R/V _____ Other							
GPS Device: _____			Target: _____	-	-	STARTING BANK (facing downstream): LB / RB / NA							
Datum: NAD83		Accuracy ( ft / m ):	*Actual: _____	-	-	Point of Sample (if Integrated, then -88 in dbase)							
Habitat Observations (CollectionMethod = Habitat_generic )				WADEABILITY: Y / N / Unk	BEAUFORT SCALE (see attachment)		DISTANCE FROM BANK (m):	STREAM WIDTH (m):					
SITE ODOR: _____		None, Sulfides, Sew age, Petroleum, Smoke, Other						WATER DEPTH (m):					
SKY CODE: _____		Clear, Partly Cloudy, Overcast, Fog, Smoky, Hazy		WIND DIRECTION (from):				HYDROMODIFICATION: None, Bridge, Pipes, ConcreteChannel, GradeControl, Culvert, AerialZipline, Other					
OTHER PRESENCE: _____		Vascular, Nonvascular, Oily Sheen, Foam, Trash, Other									LOCATION (to sample): US / DS / WI / NA		
DOMINANT SUBSTRATE: _____				Bedrock, Concrete, Cobble, Boulder, Gravel, Sand, Mud, Unk, Other							1: (RB / LB / BB / US / DS / ##)		
WATERCLARITY: _____		Clear (see bottom), Cloudy (>4" vis), Murky (<4" vis)		PRECIPITATION: _____		None, Fog, Drizzle, Rain, Snow					2: (RB / LB / BB / US / DS / ##)		
WATERODOR: _____		None, Sulfides, Sew age, Petroleum, Mixed, Other		PRECIPITATION (last 24 hrs): _____		Unknown, <1", >1", None					3: (RB / LB / BB / US / DS / ##)		
WATERCOLOR: _____		Colorless, Green, Yellow, Brown		EVIDENCE OF FIRES: _____		No, <1 year, <5 years							
OVERLAND RUNOFF (Last 24 hrs): _____				none, light, moderate / heavy, unknown									
OBSERVED FLOW: _____				NA, Dry Waterbody Bed, No Obs Flow, Isolated Pool, Trickle (<0.1cfs), 0.1-1cfs, 1-5cfs, 5-20cfs, 20-50cfs, 50-200cfs, >200cfs									
Field Measurements (SampleType = FieldMeasure; Method = Field)													
	Depth Collec (m)	Velocity (fps)	Air Temp (°C)	Water Temp (°C)	pH	O <sub>2</sub> (mg/L)	O <sub>2</sub> (%)	Specific Conductivity (µS/cm)	Salinity (ppt)	Turbidity (ntu)			
SUBSURF/MID / BOTTOM/REP													
SUBSURF/MID / BOTTOM/REP													
SUBSURF/MID / BOTTOM/REP													
Instrument:													
Calib. Date:													
Samples Taken (# of containers filled) - Method=Water_Grab						Field Dup YES / NO: (SampleType = Grab / Integrated; LABEL_ID = FieldQA; create collection record upon data entry)							
SAMPLE TYPE: Grab / Integrated		COLLECTION DEVICE: _____				Indiv bottle (by hand, by pole, by bucket); Teflon tubing; Kemmer; Pole & Beaker; Other							
	Depth Collec (m)	Inorganics	Bacteria	Chl a	TSS / SSC	TOC / DOC	Total Hg	Dissolved Mercury	Total Metals	Dissolved Metals	Organics	Toxicity	VOAs
Sub/Surface													
Sub/Surface													
COMMENTS:													

## APPENDIX II: KITS, REAGENTS AND CHEMICALS

### Chemicals used in this investigation

This table shows all chemicals used in the preparation of buffers, solutions and reagents used in this dissertation. Supplier details are provided.

Chemicals	Supplier
Absolute Ethanol	Sigma-Aldrich, USA
Agarose	Conda, SA
Cadmium chloride	NT Laboratory Supplies, SA
Copper Sulphate	Merck, Germany
Crystal violet	Minema, SA
Ethylenediamine tetra-acetic acid (EDTA)	Sigma, LifeScience, USA
Glacial Acetic Acid	Rochelle Chemicals, SA
Glycerol	Sigma-Aldrich, USA
Glycerol (87%)	Saarchem, SA
Hydrochloric acid (37%)	Sigma Aldrich, USA
Iodine crystals	Thomas Baker, India
Iron sulphate	Merck, Germany
Lead chloride	Merck, Germany
Mineral oil	Sigma, Life Sciences, USA
Nickel chloride	Merck, Germany
Nitric Acid (69%)	Sigma-Aldrich, USA
Potassium acetate	Saarchem, Merck Germany
Potassium dichromate	Merck, Germany
RNAse A	Sigma-Aldrich, USA
Safranin	Merck, Germany
Sodium dodecyl sulphate (SDS)	Sigma-Aldrich, USA
Sodium hydroxide	Rochelle Chemicals, SA
Tris(2-amino-2-hydroxymethyl-1,3-propanediol) (Tris)	Sigma, Life Science, USA
Zinc chloride	Thomas, Baker

### Commercial Reagents and Kits

Reagent	Supplier	Application
API 20E®	BioMerieux, France	Biochemical Analysis
ZR Fungal/ Bacterial DNA Extraction Kit	ZYMORESEARCH, USA	DNA extraction
Primers	Inqaba Biotechnologies, SA	PCR
Emerald Amp R MAX HS Master Mix	Takara, JAPAN	PCR
Lambda (λ Hind III DNA Marker)	Thermo Scientific, USA	Agarase Gel Electrophoresis
KAPA Universal Ladder	KAPA Biosystems, USA	Agarase Gel Electrophoresis
Genejet Purification Kit	Fermentas	PCR product purification
GeneJET™ Plasmid Miniprep Kit	Thermo Scientific, USA	Plasmid isolation
Antibiotic Discs		
Ampicillin (10 µg/ml)	Mast Diagnostics, UK	Kirby Bauer Test
Amoxicillin (10 µg/ml)	Mast Diagnostics, UK	Kirby Bauer Test
Cephalothin acid (30 µg/ml)	Mast Diagnostics, UK	Kirby Bauer Test
Cotrimoxazole (25 µg/ml)	Mast Diagnostics, UK	Kirby Bauer Test
Neomycin (30 µg/ml)	Mast Diagnostics, UK	Kirby Bauer Test



Streptomycin (10 µg/ml)	Mast Diagnostics, UK	Kirby Bauer Test
Tetracycline (30 µg/ml)	Mast Diagnostics, UK	Kirby Bauer Test
Tobramycin (10 µg/ml)	Mast Diagnostics, UK	Kirby Bauer Test
Vancomycin (30 µg/ml)	Mast Diagnostics, UK	Kirby Bauer Test

### APPENDIX III: BUFFERS AND STOCK SOLUTIONS

#### Preparation of heavy metal stock solutions for elemental analysis

The calibration standards were prepared by multiple dilutions of the stock metal solutions. A reagent blank was prepared and 5 calibration standards ranging from 1 mg/l to 5 mg/l were prepared. The following amounts of heavy metal salts were dissolved in 1000 l to prepare a 1000 mg/ml stock solution.

Name of salt	Mr	Amount of salt to be dissolved in 1000L (g)
Copper sulphate ( $CuSO_4 \cdot 5H_2O$ )	249.69	3.9321
Cadmium chloride ( $CdCl_2$ )	228.34	2.0313
Lead chloride ( $PbCl_2$ )	278.12	1.3422
Zinc chloride ( $Zn Cl_2$ )	136.29	2.0843
Iron (II)Sulphate ( $FeSO_4 \cdot 7H_2O$ )	278.03	4.9784
Nickel chloride ( $NiCl_2 \cdot 6H_2O$ )	237.72	4.0502

#### Preparation of heavy metal stock solution for bacterial screening

The 5 g/l stock solutions used for the screening of heavy metal resistant bacteria were prepared in 1000 l deionized water and these solutions were autoclaved at 121 °C at 15 psi for a minimum of 15 minutes. The table below shows the amounts of heavy metal salts that were dissolved in 1000 l to make a stock solution of 5 g/l.

Name of salt	Mr	Amount of salt to be dissolved in 1000 l (g)
Copper sulphate ( $CuSO_4 \cdot 5H_2O$ )	249.69	19.6609
Cadmium chloride ( $CdCl_2$ )	228.34	10.1565
Lead chloride ( $PbCl_2$ )	278.12	6.7109
Zinc chloride ( $Zn Cl_2$ )	136.29	10.4213
Iron (II)Sulphate ( $FeSO_4 \cdot 7H_2O$ )	278.03	24.8921
Nickel chloride ( $NiCl_2 \cdot 6H_2O$ )	237.72	20.251
Potassium dichromate ( $K_2Cr_2O_7$ )	254.22	12.223

**10% SDS:** 50 g SDS was dissolved in 500 ml dH<sub>2</sub>O.

5M Sodium chloride was prepared by dissolving 73.05 g in 500 ml dH<sub>2</sub>O.

10N Sodium hydroxide stock solution was prepared by dissolving 400 g NaOH pellets were dissolved in 1000 ml dH<sub>2</sub>O.

**Solution I:** 50 mM Tris pH 8.0 with HCl, 10 mM EDTA, 100 µg/ml RNase A

For the preparation of 1 litre of solution I, 6.06 g of Tris base, 3.72 g EDTA 2H<sub>2</sub>O was dissolved in water in 800 ml H<sub>2</sub>O and the pH was adjusted to 8.0 with HCl (aq). Deionized distilled water was added to make 1 litre.

**Solution II:** 200 mM NaOH, 1% SDS

For the preparation of solution II, 8.0 g NaOH pellets were dissolved in 950 ml of ddH<sub>2</sub>O, 50 ml of 20% SDS solution was added. Then final ddH<sub>2</sub>O was added to make 1 litre

**Solution III:** 3.0 M Potassium Acetate, pH5.5

For the preparation of solution III, 294.5 g of potassium acetate was dissolved in 500 ml of H<sub>2</sub>O, and the pH was adjusted to 5.5 with glacial acetic acid (~110 ml). The volume was then adjusted to 1 liter with ddH<sub>2</sub>O.

**TE 10mM Tris pH 8.0 with HCl, 1mM EDTA**

TE buffere was prepared by dissolving 1.21 g Tris base and 0.37 g EDTA. 2H<sub>2</sub>O in 800 ml of ddH<sub>2</sub>O and the volume was adjusted to 1 litre with ddH<sub>2</sub>O.

**APPENDIX IV: MICROBIOLOGICAL MEDIA AND COMPONENTS**

Chemicals	Supplier
Luria Bertani agar	Neogen, USA
Luria Bertani broth	Neogen, USA
Nutrient agar	Neogen, USA
Nutrient Broth	Neogen, USA
Muller-Hinton agar	Neogen, USA

**APPENDIX V: PRECONDITIONING OF PLASTIC BOTTLES**

The high density polyethylene (HDPE) bottles were washed with detergent and designated a clean chemistry scrubber. The bottles were filled to capacity with the detergent, shaken, labelled and left to sit in cable tied bags for 24 hours. The bottles were emptied of the detergent and rinsed with deionized water. The bottles were then filled to capacity with 50% nitric acid solution. The procedure was carried out under a vent hood and capped tightly. The bottles were left to sit for two days. The bottles were emptied of the nitric solution. The bottles were rinsed with deionized water. The bottles were then filled to capacity with 10% hydrochloric acid solution under the vent hood. The bottles were capped tightly and left to sit for 48 hours. The bottles were then rinsed with deionized water and dried with the lid on.

## APPENDIX VI: RAW DATA FOR WATER QUALITY PARAMETERS

The water parameters, temperature, pH, dissolved oxygen, specific conductivity, salinity and turbidity were measured for the water samples collected from the Klip River Catchment.

Site no. and location	Geographical coordinates		pH	Temp. (°C)	DO (ppm)	EC (uS/cm)	Salinity (ppt)	Turbidity (ppm)
	Latitude N	Longitude E						
1 (Source- Roodekraans)	26°08.428'	27°49.280'	5.9	20.3		313		
2 (Before Lenasia)	26°10.558'	27°49.037'	6.7	21.1	7.36	374	0.18	187
3 (Lenasia)	26°17.668'	27°05.650'	7.08	19.1	4.23	501	0.24	250
4 (Henley on Klip Weir)	26°32.428'	27°03.8445'	7.9	19.1	5.93	927	0.47	476
5 (Confluence of the Klip and Vaal River)	26°39.879'	27°56.303'	6.44	16.7	4.32	800	0.47	471
6 (Vaal Barrage)	26°46.068'	27°40.498'	8.33	20.1	5.52	782	0.45	456

## LOADINGS OF THE 12 EXPERIMENTAL VARIABLES ON PRINCIPAL COMPONENTS FOR THE KLIP RIVER

	F1	F2
pH	-0.669	-0.378
Temp.	0.676	-0.399
DO	0.504	-0.528
EC (uS/cm)	-0.925	0.067
Salinity	-0.653	0.619
Turbidity	-0.656	0.618
Zn	0.956	-0.062
Pb	0.659	0.729
Ni	0.000	0.000
Fe	0.900	-0.263
Cu	0.662	0.732
Cd	0.689	0.703

**APPENDIX VII: RAW DATA FOR HEAVY METAL CONCENTRATIONS OF WATER SAMPLES**

Zinc	Reading 1	Reading 2	Reading 3	Average	Std. deviation
1	1.1326	0.0511	0.115	0.4329	0.6068
2	1.1317	0.1075	0.119	0.452733	0.58803
3	0.0746	0.1009	0.0962	0.090567	0.014026
4	0.0897	0.1539	0.1746	0.1394	0.044268
5	0.0939	0.0547	0.0766	0.075067	0.019645
6	0.055	0.0547	0.0456	0.051767	0.005343
Lead					
1	26.9099	1.07	0.55	9.509967	15.07103
2	0.9013	0.8584	0.5579	0.772533	0.187111
3	0.8584	0.6867	0.6438	0.729633	0.113559
4	1.2446	1.4163	1.588	1.4163	0.1717
5	0.9871	1.1159	1.03	1.044333	0.065585
6	1.1159	0.8155	0.7296	0.887	0.202833
Nickel					
1	0	0	0	0	0
2	0	0	0	0	0
3	0	0	0	0	0
4	0	0	0	0	0
5	0	0	0	0	0
6	0	0	0	0	0
Iron					
1	2.4248	2.1542	2.0805	2.219833	0.181291
2	3.2343	3.3269	3.3824	3.31453	0.07482
3	0.249	0.2332	0.2192	0.2338	0.014909
4	0.4252	0.4319	0.4302	0.4291	0.003483
5	0.335	0.3359	0.3383	0.3364	0.001706
6	0.2564	0.2498	0.2581	0.25476	0.004384
Copper					
1	1.7758	0.44	0.372	0.8626	0.791585
2	0.322	0.3082	0.3065	0.312233	0.008501
3	0.3074	0.3115	0.3123	0.3104	0.002629
4	0.3289	0.3438	0.3455	0.3394	0.009133
5	0.3405	0.3422	0.3297	0.337467	0.00678
6	0.2883	0.3289	0.3331	0.316767	0.024742
Cadmium					
1	1.7431	0.6534	0.611	1.0025	0.641729
2	0	0	0	0	0
3	0	0	0	0	0
4	0	0	0	0	0
5	0	0	0	0	0
6	0	0	0	0	0

## APPENDIX VIII: RAW DATA FOR PLATE COUNTS

Raw data for sediment plate counts (*CFU log<sub>10</sub>/g*)

SITE 1	Plate 1	Plate 2	Average	Std. Deviation
LB+Ni	5.672098	5.643453	5.657775	0.020255
LB+Cd	4.78533	4.763428	4.774379	0.015487
LB+Zn	5.748188	5.770852	5.75952	0.016026
LB+Pb	5.579784	5.612784	5.596284	0.023335
LB+Cr	5.633468	5.544068	5.588768	0.063216
LB+Cu	5.193125	5.369216	5.28117	0.124515
LB+Fe	5.447158	5.579784	5.513471	0.09378
Control	6.30103	6.064457	6.182744	0.12146
Site 2				
LB+Ni	5.681241	5.857332	5.769287	0.124515
LB+Cd	5.579784	5.556303	5.568043	0.016604
LB+Zn	5.662758	5.623249	5.643004	0.027937
LB+Pb	5.690196	4.60206	5.146128	0.769428
LB+Cr	5.724276	5.544068	5.634172	0.127426
LB+Cu	5.819544	5.724276	5.77191	0.067365
LB+Fe	5.681241	5.623249	5.652245	0.041006
Control	6.47712	6.30535	6.391235	0.12146
Site 3				
LB+Ni	5.612784	5.799341	5.706062	0.131916
LB+Cd	5.819544	5.748188	5.783866	0.050456
LB+Zn	5.832509	5.924279	5.878394	0.064891
LB+Pb	5.690196	5.653213	5.671704	0.026151
LB+Cr	5.755875	5.982271	5.869073	0.160086
LB+Cu	5.716003	5.380211	5.548107	0.237441
LB+Fe	5.863323	5.778151	5.820737	0.060225
Control	6.60205	6.6354	6.61872	0.023582
Site 4				
LB+Ni	6.39794	6.653213	6.525576	0.180505
LB+Cd	5.908485	6.071882	5.990184	0.115539
LB+Zn	6.20412	6.579784	6.391952	0.265634
LB+Pb	6.39794	6.653213	6.525576	0.180505
LB+Cr	6.146128	6.643453	6.39479	0.351662
LB+Cu	6.845098	6.763428	6.804263	0.057749
LB+Fe	6.556303	6.39794	6.477121	0.111979
Control	7.39794	7.18184	7.28989	0.152806
Site 5				
LB+Ni	5.612784	5.778151	5.695468	0.116932
LB+Cd	5.672098	5.799341	5.735719	0.089974
LB+Zn	5.857332	5.826075	5.841704	0.022103

LB+Pb	5.612784	5.778151	5.695468	0.116932
LB+Cr	5.477121	5.690196	5.583659	0.150667
LB+Cu	5.724276	5.934498	5.829387	0.14865
LB+Fe	5.755875	5.778151	5.767013	0.015752
Control	6.30102	6.25527	6.278145	0.03235
Site 6				
LB+Ni	5.120574	4.812913	4.966744	0.217549
LB+Cd	5.184691	4.869232	5.026962	0.223064
LB+Zn	4.716003	4.447158	4.581581	0.190102
LB+Pb	5.120574	4.812913	4.966744	0.217549
LB+Cr	5.303196	5.212188	5.257692	0.064353
LB+Cu	5.78533	5.531479	5.658404	0.1795
LB+Fe	5.25042	5.155336	5.202878	0.067235
Control	6.25527	6.13354	6.1944505	0.086076

#### Raw data for plate counts of water samples (*CFU log<sub>10</sub>/ml*)

SITE 1	Plate 1	Plate 2	Average	Std. Deviation
LB+Ni	2.755875	2.959041	2.857458	0.14366
LB+Cd	2.230449	3.113943	2.672196	0.624725
LB+Zn	2.716003	2.633468	2.674736	0.058361
LB+Pb	2.763428	2.897627	2.830528	0.094893
LB+Cr	2.919078	2.939519	2.929299	0.014454
LB+Cu	2.886491	2.633468	2.75998	0.178914
LB+Fe	2.886491	2.113943	2.500217	0.546273
Control	4.14612	4.255272	4.200695	0.077181
Site 2				
LB+Ni	2.414973	2	2.207487	0.29343
LB+Cd	2.845098	2.041393	2.443245	0.568306
LB+Zn	1.30103	2.255273	1.778151	0.674751
LB+Pb	2.414973	2	2.207487	0.29343
LB+Cr	2.755875	2.176091	2.465983	0.409969
LB+Cu	2.113943	2.255273	2.184608	0.099935
LB+Fe	2.447158	2.342423	2.39479	0.074059
Control	4.20411	4.1932	4.19861	0.007771
Site 3				
LB+Ni	5.0086	4.944483	4.976541	0.045338
LB+Cd	5.178977	5.305351	5.242164	0.08936
LB+Zn	4.857332	4.477121	4.667227	0.26885
LB+Pb	5.0086	4.944483	4.976541	0.045338
LB+Cr	5.053078	6.08636	5.569719	0.73064
LB+Cu	6.089905	6.450249	6.270077	0.254802

LB+Fe	4.963788	4.919078	4.941433	0.031615
Control	6.25527	6.34242	6.298845	0.0961624
Site 4				
LB+Ni	4.017033	3.944483	3.980758	0.051301
LB+Cd	4.045323	4.103804	4.074563	0.041352
LB+Zn	3.934498	4.029384	3.981941	0.067094
LB+Pb	4.017033	3.944483	3.980758	0.051301
LB+Cr	4.0086	4.127105	4.067852	0.083795
LB+Cu	4.012837	4.049218	4.031028	0.025725
LB+Fe	3.944483	3.716003	3.830243	0.161559
Site 5				
LB+Ni	2.857332	2.944483	2.900908	0.061624
LB+Cd	1.778151	2.770852	2.274502	0.701945
LB+Zn	3.193125	2.763428	2.978276	0.303841
LB+Pb	2.857332	2.944483	2.900908	0.061624
LB+Cr	2.880814	2.792392	2.836603	0.062524
LB+Cu	2.544068	2.716003	2.630036	0.121577
LB+Fe	2.929419	2.875061	2.90224	0.038437
Control	4.84509	5.11394	4.97951	0.190106
Site 6				
LB+Ni	2.832509	2.90309	2.867799	0.049908
LB+Cd	2.176091	1.60206	1.889076	0.405901
LB+Zn	2.954243	3.049218	3.00173	0.067158
LB+Pb	2.079181	2.30103	2.190106	0.156871
LB+Cr	2.653213	2.477121	2.565167	0.124515
LB+Cu	3.662758	3.079181	3.37097	0.412651
LB+Fe	2.944483	3.0086	2.976541	0.045338
Control	4.8510	4.74818	4.79959	0.072705

**APPENDIX IX: MINIMUM INHIBITORY CONCENTRATION ASSAY**

Strain	Zn	Cd	Ni	Fe	Cu	Cr	Pb
KR01	0.2	0	0.4	4	0.6	0.6	4
KR02	0	0	0.6	1.2	1	0.4	4
KR03	0.2	0	0.2	1.2	1	0.4	4
KR04	0	0	0.4	1.2	0.6	0.6	0
KR05	0.2	0.2	0.2	1.2	0.8	0.2	4
KR06	0	0	0.2	0.6	0.4	0.2	4
KR07	0	0	0.2	0.6	0.4	0.2	3
KR08	0.8	0	0.2	1	1	0	0.8
KR17	0	0	0.2	4	0.6	0.4	4
KR18	0	0	0.6	1	0.2	0	4
KR19	0	0	0.4	1	0.4	0	4
KR22	0	0	0.4	2	0.2	0	0
KR23	0	0	0.4	0.8	0.2	0	4
KR25	0.2	0	0.2	0.8	1	0.2	4
KR29	0	0	0.6	0	0.6	0	2
KR44	0	0.2	0.6	4	1	0.2	0.8
KR48	0	0.2	0.4	0.8	1	0.2	0.6



**APPENDIX X: RAW DATA FOR OPTIMAL GROWTH STUDIES DATA**  
***OD*<sub>600</sub> Readings for the 16 cultures exposed to different pH conditions**

	Reading 1	Reading 2	Reading 3	Average	Std. deviation
<b>KR01</b>					
5	0.288	0.272	0.289	0.283	0.009539
6	0.44	0.452	0.467	0.453	0.013528
7	0.705	0.774	0.708	0.729	0.039
8	0.77	0.71		0.74	0.042426
9	0.636	0.587	0.676	0.633	0.044576
10	0.017	0.044	0.032	0.031	0.013528
<b>KR02</b>					
5	0.256	0.265		0.2605	0.006364
6	0.47	0.489	0.379	0.446	0.058796
7	0.528	0.521	0.522	0.523667	0.003786
8	0.492	0.425	0.498	0.471667	0.040526
9	0.351		0.297	0.324	0.038184
10	0.016	0.019	0.036	0.023667	0.010786
<b>KR03</b>					
5	0.162	0.163	0.117	0.147333	0.026274
6	0.357	0.363	0.294	0.338	0.038223
7	0.42	0.36	0.413	0.397667	0.032808
8	0.37	0.378	0.389	0.379	0.009539
9	0.131	0.107	0.108	0.115333	0.013577
10	0.051	0.067	0.065	0.061	0.008718
<b>KR04</b>					
5	0.074	0.049	0.1	0.074333	0.025502
6	0.152	0.163		0.1575	0.007778
7	0.132	0.129	0.127	0.129333	0.002517
8	0.08	0.021	0.043	0.048	0.029816
9	0.11	0.03	0.242	0	0.107058
10	0.031	0.02		0.0255	0.007778
<b>KR06</b>					
5	0.185	0.231	0.241	0.219	0.029866
6	0.287	0.179	0.104	0.19	0.091995
7	0.219	0.183	0.25	0.217333	0.033531
8	0.239	0.315	0.278	0.277333	0.038004
9	0.078	0.07	0.103	0.083667	0.017214
10	0.059	0.062		0.0605	0.002121
<b>KR07</b>					
5	0.154	0.1	0.135	0.129667	0.027392
6	0.416	0.38		0.398	0.025456
7	0.475	0.487	0.493	0.485	0.009165
8	0.669	0.58	0.584	0.611	0.050269
9	0.589	0.494	0.543	0.542	0.047508
10	0.315	0.326	0.333	0.324667	0.009074
<b>KR08</b>					
5	0.129	0.114	0.131	0.124667	0.009292
6	0.358	0.229		0.2935	0.091217
7	0.21	0.201	0.425	0.278667	0.126808
8	0.551	0.223	0.472	0.415333	0.171185
9	0.058	0.084	0.062	0.068	0.014
10	0.026	0.0225	0.028	0.0255	0.002784
<b>KR17</b>					
5	0.074	0.078	0.078	0.076667	0.002309
6	0.17	0.174	0.183	0.175667	0.006658
7	0.176	0.177	0.201	0.184667	0.014154
8	0.19	0.184	0.188	0.187333	0.003055
9	0.11	0.135	0.141	0.128667	0.016442
10	0.001	0.002	0.004	0.002333	0.001528
<b>KR18</b>					

5	0.018	0.049	0.044	0.037	0.016643
6	0.178	0.183		0.1805	0.003536
7	0.456	0.502	0.454	0.470667	0.027154
8	0.194	0.192	0.182	0.189333	0.006429
9	0.046	0.078	0.062	0.062	0.016
10	0.026	0.025	0.028	0.026333	0.001528
KR19					
5	0.104	0.097	0.107	0.102667	0.005132
6	0.351	0.357	0.422	0.376667	0.039374
7	0.869	0.882	0.821	0.857333	0.03213
8	0.828	0.771	0.854	0.817667	0.042454
9	0.754	0.749	0.801	0.768	0.028688
10	0.29	0.189	0.158	0.212333	0.069024
KR22					
5	0.391	0.426	0.422	0.413	0.019157
6	1.073	1.056	1.074	1.067667	0.010116
7	1.202	1.137	1.122	1.153667	0.042525
8	1.277	1.266	1.229	1.257333	0.025146
9	1.197	1.249	1.216	1.220667	0.026312
10	0.043	0.048	0.046	0.045667	0.002517
KR23					
5	0.032	0.041	0.045	0.039333	0.006658
6	0.522	0.764	0.668	0.651333	0.121858
7	1.304	1.432	1.455	1.397	0.081357
8	1.102	0.983	0.988	1.024333	0.067308
9	0.876	0.786	0.754	0.805333	0.063256
10	0.067	0.089	0.098	0.084667	0.015948
KR25					
5	0.02	0.034	0.042	0.032	0.011136
6	0.188	0.224	0.221	0.211	0.019975
7	0.355	0.306	0.335	0.332	0.024637
8	0.162	0.161	0.188	0.170333	0.015308
9	0.2	0.243		0.2215	0.030406
10	0.021	0.073	0.025	0.039667	0.028937
KR29					
5	0.429	0.43	0.465	0.441333	0.020502
6	0.429	0.534	0.534	0.499	0.060622
7	0.531	0.621	0.569	0.573667	0.045181
8	0.519	0.464	0.523	0.502	0.03297
9	0.307	0.272	0.287	0.288667	0.017559
10	0.007	0.018	0.015	0.013333	0.005686
KR44					
5	0.098	0.033	0.132	0.087667	0.050302
6	0.341	0.332	0.312	0.328333	0.014844
7	0.339	0.284	0.373	0.332	0.044911
8	0.27	0.258	0.26	0.262667	0.006429
9	0.238	0.198	0.242	0.226	0.024331
10	0.016	0.013	0.027	0.018667	0.007371
KR48					
5	0.034	0.077	0.022	0.044333	0.028919
6	0.103	0.154	0.157	0.138	0.030348
7	0.182	0.172	0.113	0.155667	0.037287
8	0.16	0.097		0.1285	0.044548
9	0.153	0.151	0.112	0.138667	0.023116
10	0.024	0.022	0.015	0.020333	0.004726

**OD<sub>600</sub> Readings for the 16 cultures exposed to different temperature conditions**

	1 <sup>st</sup> Reading	2 <sup>nd</sup> Reading	3 <sup>rd</sup> Reading	Average	Std. Deviation
KR01					
25°C	0.798	0.874	0.84	0.837333	0.03807
30°C	0.934	0.836	0.878	0.882667	0.049166
37°C	0.644	0.687	0.645	0.658667	0.024542
40°C	0.284	0.316	0.343	0.314333	0.029535
KR02					
25°C	0.54	0.543	0.523	0.535333	0.010786
30°C	0.564	0.536	0.552	0.550667	0.014048
37°C	0.58	0.585	0.53	0.565	0.030414
40°C	0.443	0.426	0.474	0.447667	0.024338
KR03					
25°C	0.273	0.33	0.233	0.278667	0.048748
30°C	0.382	0.454	0.417	0.417667	0.036005
37°C	0.389	0.455	0.422	0.422	0.033
40°C	0.01	0.047	0.013	0.023333	0.020551
KR04					
25°C	0.147	0.108	0.113	0.122667	0.021221
30°C	0.106	0.083	0.094	0.094333	0.011504
37°C	0.167	0.162	0.172	0.167	0.005
40°C	0.115	0.189	0.144	0.149333	0.037287
KR06					
25°C	0.089	0.116	0.077	0.094	0.019975
30°C	0.106	0.096	0.106	0.102667	0.005774
37°C	0.295	0.261	0.286	0.280667	0.017616
40°C	0.373	0.413	0.302	0.362667	0.056217
KR07					
25°C	0.505	0.544		0.5245	0.027577
30°C	0.605	0.785	0.62	0.67	0.099875
37°C	0.583	0.568	0.606	0.585667	0.01914
40°C	0.481	0.473		0.477	0.005657
KR08					
25°C	0.377	0.403	0.407	0.395667	0.016289
30°C	0.428	0.397	0.401	0.408667	0.016862
37°C	0.544		0.632	0.588	0.062225
40°C	0.255	0.136	0.205	0.198667	0.059752
KR17					
25°C	0.515	0.638	0.534	0.562333	0.066214
30°C	0.543	0.451	0.535	0.509667	0.050964
37°C	0.444	0.467	0.429	0.446667	0.01914
40°C	0.529	0.498	0.578	0.535	0.040336

KR18	No growth				
KR19					
25°C	0.912	0.837	0.942	0.897	0.054083
30°C	0.837	0.873	0.835	0.848333	0.021385
37°C	0.455	0.513	0.505	0.491	0.031432
40°C	0.095	0.088	0.093	0.092	0.003606
KR22					
25°C	0.608	0.677		0.6425	0.04879
30°C	0.647	0.661	0.826	0.711333	0.099551
37°C	0.457	0.507	0.49	0.484667	0.025423
40°C	0.533	0.472	0.497	0.500667	0.030665
KR23					
25°C	0.221	0.224	0.226	0.223667	0.002517
30°C	0.254	0.201	0.238	0.231	0.027185
37°C	0.101	0.09	0.08	0.090333	0.010504
40°C	0.032	0.024	0.021	0.025667	0.005686
KR25					
25°C	0.446	0.411	0.306	0.387667	0.072858
30°C	0.424	0.539	0.441	0.468	0.062073
37°C	0.477	0.35	0.586	0.471	0.118114
40°C	0.349	0.568	0.49	0.469	0.111
KR29					
25°C	0.688	0.66	0.655	0.667667	0.017786
30°C	0.678	0.658	0.688	0.674667	0.015275
37°C	0.533	0.564	0.61	0.569	0.038743
40°C	0.528	0.563	0.552	0.547667	0.017898
KR44					
25°C	0.04	0.052	0.054	0.048667	0.007572
30°C	0.051	0.027	0.056	0.044667	0.015503
37°C	0.134	0.143	0.146	0.141	0.006245
40°C	0.268	0.208	0.198	0.224667	0.037859

# APPENDIX XI: RAW DATA FOR ANTIBIOTIC SUSCEPTIBILITY TESTS (WILD TYPE STRAINS)

	Neomycin	Vancomycin	Cephalothin acid	Streptomycin	Ampicillin	Amoxycillin	Tetracycline	Cotrimoxazole	Tobramycin
KR001	18	10	0	7	0	0	20	0	11
	20	7	0	7	0	0	17	0	18
	18	9	0	7	0	0	18	0	16
Average	19	9	0	7	0	0	18	0	15
StD. Deviation	1.154701	1.527525	0	0	0	0	1.527525	0	3.605551
KR003	19	16	0	21	0	0	24	13	16
	20	17	0	23	0	0	23	12	18
	16	16	0	18	0	0	20		15
Average	18	16	0	20	0	0	22	13	16
StD. Deviation	2.081666	0.57735	0	2.516611	0	0	2.081666	0.707107	1.527525
KR004	22	19	30	25	28	28	30	24	24
	22	22	30	28		30	30	24	24
	21	20	32	25	26	28	28		
Average	22	20	31	26	27	29	29	24	24
StD. Deviation	0.57735	1.527525	1.154701	1.732051	1.414214	1.154701	1.154701	0	0
KR007	18	0	0	9	0	0	19	0	18
	18	0	0	14	0	0	18	0	18
	19	0	0	16	0	0	20	0	18
Average	18	0	0	13	0	0	19	0	18
StD. Deviation	0.57735	0	0	3.605551	0	0	1	0	0
KR008	16	0	0	18	0	0	16	12	17
	15	0	0	18	0	0	20		15
	18	0	0	19	0	0	18	12	18
Average	16	0	0	18	0	0	18	12	17
StD. Deviation	1.527525	0	0	0.57735	0	0	2	0	1.527525
KR017	7	0	0	0	0	0	0	0	11
	8	0	0	0	0	0	0	0	15

	7	0	0	0	0	0	0	0	14
Average	7	0	0	0	0	0	0	0	13
StD. Deviation	0.57735	0	0	0	0	0	0	0	2.081666
KR018	18	0	14	8	16	12	17	24	18
	18	0	14	8	17	14	17	22	16
	18	0	13	8	18	14	17	24	16
Average	18	0	14	8	17	13	17	23	17
StD. Deviation	0	0	0.509175	0	0.57735	0.3849	0	1.01835	0.3849
KR019	18	0	0	17	0	0	22	18	18
	18	0	0	17	0	0	25	17	16
	16	0	0	15	0	0	26	16	14
Average	17	0	0	16	0	0	24	17	16
StD. Deviation	1.154701	0	0	1.154701	0	0	2.081666	1	2
KR022	0	0	0	0	0	0	16	19	11
	0	0	0	0	0	0	13	22	10
	0	0	0	0	0	0	15	18	12
Average	0	0	0	0	0	0	14.66667	19.66667	11
StD. Deviation	0	0	0	0	0	0	1.527525	2.081666	1
KR025	16	17	28	0	28	30	21	22	17
	18	18	28	0	28	30	21	22	18
	16	20	26	0	26	30	21	23	
Average	16.66667	18.33333	27.33333	0	27.33333	30	21	22.33333	17.5
StD. Deviation	1.154701	1.527525	1.154701	0	1.154701	0	0	0.57735	0.707107
KR029	15	0	13	15	14	14	20	20	14
	16	0	14	19	16	13	20	24	14
Average	13	0	13	13	13	10	18	21	10
StD. Deviation	14.66667	0	13.33333	15.66667	14.33333	12.33333	19.33333	21.66667	12.66667
KR044	23	18	14	24	8	9	22	0	12
	20	13	10	24	10	8	22	0	11
	22	18	10	24	7	8	22	0	15
	21.66667	16.33333	11.33333	24	8.333333	8.333333	22	0	12.66667

KR048	15	22	40	18	36	28	24	20	8
	16	20	40	18	34	30	29	26	9
	17	22		18	36	30	30	24	8
Average	16	21.33333	40	18	35.33333	29.33333	27.66667	23.33333	8.333333
StD. Deviation	1	1.154701	0	0	1.154701	1.154701	3.21455	3.05505	0.57735
KR002	21	18	8	24	0	0	18	0	20
	20	16	7	24	0	0	18	0	17
	21	19	9	24	0	0	17	0	18
Average	20.66667	17.66667	8	24	0	0	17.66667	0	18.33333
StD. Deviation									

**APPENDIX XII: RAW GROWTH CURVE DATA (MEAN VALUES)**

Hours	Pb	Zn	Cu	Cr	Ni	Cd	Fe	Control
KR01								
4	0.84	0.541	0.816	0.101	1.14	0.07	0.477	0.618
8	1.219	1.135	1.157	0.211	1.141	0.374	1.115	1.096
12	1.452	1.309	1.282	0.468	1.206	1.191	1.328	1.338
16	1.616	1.574	1.602	1.288	1.371	1.265	1.505	1.499
20	1.679	1.532	1.555	1.224	1.537	1.52	1.579	1.555
24	1.797	1.72	1.596	1.306	1.65	1.358	1.656	1.656
KR02								
4	0	0	0.018	0	0	0	0	0
8	0.819	0.864	1.147	0.772	0.912	0.296	0.762	0.871
12	1.047	1.015	1.275	1.131	1.035	0.821	0.988	1.022
16	1.215	1.167	1.475	1.162	1.212	1.031	1.129	1.158
20	1.247	1.281	1.631	1.142	1.558	1.105	1.298	1.238
24	0.981	0.545	1.614	1.469	1.315	0.638	0.925	1.209
KR04								
4	0	0	0	0	0	0	0	0
8	0.332	0.217	0.516	0.467	0.471	0.005	0.628	0.509
12	0.983	0.902	0.999	0.817	0.933	0	0.992	1.141
16	1.297	1.147	1.253	0.812	1.17	0.039	1.233	1.401
20	1.277	1.234	1.457	0.804	1.399	0	1.47	1.258
24	1.428	1.296	1.313	0.809	1.385	0	1.399	1.326
KR06								
4	0	0	0	0	0	0	0	0
8	0.741	0.309	0.67	0.655	0.649	0.067	0.709	0.601
12	0.791	0.74	0.719	0.685	0.752	0.085	0.725	0.74
16	1.039	0.955	0.905	0.833	1.008	0	0.953	1.14
20	1.185	1.06	1.464	1.034	1.097	0	1.149	1.153
24	1.369	1.23	1.463	1.223	1.205	0.025	1.263	1.236
KR07								
4	0.472	0.314	0.672	0.232	0.362	0.023	0.398	0.774
8	1.177	0.913	0.832	0.434	1.277	0.024	0.914	0.874
12	1.336	1.144	1.429	0.453	1.497	0.028	1.155	1.347
16	1.424	1.19	1.513	0.249	1.582	0.01	1.184	1.431
20	1.454	1.398	1.723	0.185	1.631	0.017	1.429	1.552
24	1.592	1.498	1.726	0.131	1.648	0.034	1.648	1.608
KR08								
4	0.149	0.181	0.616	0.26	0.351	0.089	0.053	0.153
8	0.959	1.034	1.06	0.635	0.715	0.073	0.855	0.748
12	0.978	1.21	1.088	0.823	1.071	0.071	0.859	1.247
16	1.252	1.314	1.355	0.822	1.355	0.066	1.287	1.302



20	1.288	1.352	1.412	0.975	1.359	0.053	1.467	1.39
24	1.404	1.425	1.582	1.14	1.471	0.056	1.442	1.46
KR17								
4	0	0	0	0	0	0	0	0
8	0.89	0.804	0.816	0.77	0.816	0.643	0.993	0.822
12	1.203	1.192	1.173	1.127	1.156	1.086	1.359	1.272
16	1.543	1.384	1.328	1.321	1.319	1.24	1.62	1.386
20	1.664	1.45	1.29	1.485	1.456	1.423	1.561	1.471
24	1.703	1.609	1.583	1.681	1.576	1.634	1.765	1.64
KR19								
4	0.093	0.007	0	0	0.02	0	0.056	0.012
8	1.16	0.554	0	0.21	1.05	0.81	1.139	1.061
12	1.395	1.324	0.167	0.232	1.31	1.233	1.309	1.33
16	1.484	1.522	0.026	0.258	1.492	1.285	1.477	1.508
20	1.684	1.501	0.006	1.139	1.542	1.454	1.552	1.85
24	1.763	1.762	0.021	1.326	1.677	1.504	1.678	1.682
KR22								
4	0.145	0.004	0.069	0.031	0.043	0.08	0.259	0.062
8	0.296	0.422	0.727	0.326	0.608	0.182	0.4	0.478
12	0.756	0.728	0.818	0.796	0.87	0.046	0.704	1.197
16	1.167	1.299	1.244	1.073	1.263	0.142	1.101	1.92
20	1.339	1.248	1.279	1.13	1.399	0.469	1.517	1.851
24	1.518	1.501	1.472	1.37	1.52	0.133	1.557	1.754
KR23								
4	0.08	0.029	0.732	0.193	0.026	0.01	0.766	0.713
8	1.256	0.035	1.413	1.198	0.159	0.01	1.14	1.202
12	1.381	0.351	1.375	1.256	1.508	0.016	1.43	1.453
16	1.446	0.36	1.439	1.307	1.572	0.014	1.612	1.474
20	1.733	0.839	1.622	1.703	1.786	0.025	1.711	1.693
24	1.787	0.987	1.661	1.596	1.903	0.025	1.84	1.738
KR25								
4	0.168	0.208	0.18	0.06	0.251	0	0.057	0.171
8	1.254	1.254	1.244	0.073	1.295	0.001	1.247	1.067
12	1.673	1.733	1.784	0.075	1.817	0.061	1.732	1.748
16	1.841	1.902	1.887	0.063	1.895	0.06	1.961	2.114
20	2.047	2.08	1.935	0.069	2.124	0.061	2.144	2.115
24	2.304	2.007	1.949	0.124	2.098	0.057	2.111	2.116
KR29								
4	1.119	0.77	1.297	0.024	1.126	0.142	1.05	1.47
8	1.412	1.594	1.526	0.055	1.691	0.312	1.755	1.709
12	1.598	1.783	1.528	0.075	1.814	0.3	1.756	1.765
16	1.647	1.651	1.936	0.016	1.822	0.249	1.751	1.763

20	1.677	1.65	1.938	0.015	1.85	0.076	1.726	1.782
24	1.627	1.678	1.674	0.014	1.846	0.083	1.558	1.749
KR44								
4	0.37	0.038	0.079	0.382	0.043	0.135	0.039	0.027
8	0.559	0.559	0.202	0.703	0.141	0.37	0.141	0.242
12	0.606	0.646	0.256	1.218	0.189	0.139	0.208	0.282
16	0.78	0.723	0.295	1.297	0.117	0.241	0.21	0.312
20	1.411	1.553	0.768	1.412	0.135	0.253	0.431	0.47
24	1.6	1.197	0.958	1.519	0.026	0.503	0.685	1.085
KR48								
4	0.193	0.353	0.117	0.382	0.174	0.097	0.482	0.17
8	0.829	0.354	0.87	0.703	1.051	0.168	0.536	0.937
12	1.105	0.714	1.243	1.218	1.071	0.15	1.083	1.253
16	1.412	1.204	1.423	1.297	1.387	0.156	1.374	1.51
20	1.496	1.401	1.576	1.412	1.469	0.155	1.57	1.646
24	1.6	1.627	1.754	1.519	1.606	0.433	1.712	1.747

### APPENDIX XIII: 16SRDNA NUCLEOTIDE SEQUENCES AND ACCESSION NUMBERS OF HEAVY METAL RESISTANT ISOLATES

>gi|700289016|gb|KJ935907.2| *Aeromonas hydrophila* strain KR01 16S ribosomal RNA gene, partial sequence

CGGAAGTCAGGCAGTGGGGGATACTGCACATTGGGGGAATCTGATGCAGGCATGCCGCGTGTGTGAGGAAGG  
CTTTCGGGTGTAAAGCACTTTCAGCGAGGGAGGAAAGGTGATGCTATACGTATCARCTGTGACGTTACTCGCAG  
AAGAAGCACCGGCTAACTCCGTGCCAGCAGCCGCGTAATACGGAGGGTGCAAGCGTTAATCGGAATTACTGG  
GCGTAAAGCGCACGCAGGCGGTTGGATAAGTTAGATGTGAAAGCCCCGGGCTCAACCTGGGAATTGCATTTAA  
ACTGTCCAGCTAGAGTCTTGTAGAGGGGGGTAGAATTCCAGGTGTAGCGGTGAAATGCGTAGAGATCTGGAGG  
AATACCGGTGGCGAAGGCGGCCCCCTGGACAAAGACTGACGCTCAGGTGCGAAAGCGTGGGGAGCAAACAGG  
ATTAGATACCCTGGTAGTCCACGCCGTAAACGATGTCGATTTGGAGGCTGTGTCTTGAGACGTGGCTTCCGGA  
GCTAACGCGTTAAATCGACCGCCTGGGGAGTACGGCCGCAAGGTTAAACTCAAATGAATTGACGGGGGCCCG  
CACAAGCGGTGGAGCATGTGGTTAATTGATGCAACGCGAAGAACCCTTACCTGGCCTTGACATGTCTGGAATC  
CTGCAGAGATGCGGGAGTGCCTTCGGGAATCAGAACACAGGTGCTGCATGGCTGTCTCGTCAGCTCGTGTCTGA  
GATGTTGGGTAAAGTCCCGCAACGAGCGCAACCCCTGTCTTTGTTGCCAGCACGTAATGGTGGGAACCTCAAGG  
GAGACTGCCGGTGATAAACCGGAGGAAGGTGGGGATGACGTCAAGTCATCATGGCCCTTACGGCCAGGGCTAC  
ACACGTGCTACAATGGCGCGTACAGAGGGCTGCAAGCTAGCGATAGTGAGCGAATCCAAAAAGCGCGTCGTA  
GTCCGGATCGGAGTCTGCAACTCGACTCCGTGAAGTCGGAATCGCTAGTAATCGCAAATCAGAATGTTGCGGTG  
AATACGTTCCCGGGCCTTGACACACCGCCCGTCACACCATGGGAGTGGGTTGCACCAGAAGTAGATAGCTTAA  
CCTCGGGAGGGCG

>gi|700289017|gb|KJ935908.2| *Bacillus* sp. KR02 16S ribosomal RNA gene, partial sequence

CGGCCCAGACTCCTTACGGGAGGCAGCAGTAAGGATCTCGCATGGACGAAAGTCTGACGAGCACGCCGCGTGA  
GTGATGAAAGGCTTCGGTCGTAAACTCTGTTGTTAGGGAAAGAACAAGTGCTAGTTGAATAAGCTGGCACCTTG  
ACGGTACCTAACCAGAAAGCCACGGCTAACTACGTGCCAGCAGCCGCGTAATACGTAGGTGGCAAGCGTTAT  
CCGGAATTATTGGGCGTAAAGCGCGCGCAGGTGGTTTCTTAAGTCTGATGTGAAAGCCCACGGCTCAACCGTG  
GAGGGTCATTGGAAACTGGGAGACTTGAGTGCAGAAGAGGAAAGTGGAATTCCATGTGTAGCGGTGAAATGCG  
TAGAGATATGGAGGAACACCAAGTGGCGAAGGCGACTTTCTGGTCTGTAAGTACACTGAGGCGCGAAAGCGTG  
GGGAGCAAACAGGATTAGATACCCTGGTAGTCCACGCCGTAAACGATGAGTGCTAAGTGTTAGAGGGTTTCCGC  
CCTTTAGTGCTGAAGTTAACGCATTAAGCACTCCGCCTGGGGAGTACGGCCGCAAGGCTGAAACTCAAAGGAAT  
TGACGGGGGGCCGCACAAGCGGTGGAGCATGTGGTTTAATTCGAAGCAACGCGAAGAACCCTTACCAGGTCTTG  
ACATCCTCTGAAAACCTAGAGATAGGGCTTCTCCTTCGGGAGCAGAGTGACAGGTGGTGCATGGTTGTCGTCA  
GCTCGTGTCTGAGATGTTGGGTTAAGTCCCGCAACGAGCGCAACCCTTGATCTTAGTTGCCATCATTAAAGTTG  
GGCACTAAGGTGACCGGTGACAAACCGGAGGAAGGTGGGGATGACGTCAAATCATCATGCCCTTAAAGTTG  
ACCTGGGCTACACACGTGCTACAATGGACGGTACAAGAGCTGCAAGACCGCGAGGTGGAGCTAATCTCATAAA  
ACCGTTCTCAGTTTCGGATTGTAGGCTGCAACTCGCCTACATGAAGCTGGAATCGCTAGTAATCGCGGATCAGCA  
TGCCGCGGTGAATACGTTCCCGGGCCTTGACACACCGCCAGGGACACCACGAGAGTTTGTAAACCCGAAGT  
CGGTGGGG

>gi|700289018|gb|KJ935909.2| *Bacillus megaterium* strain KR04 16S ribosomal RNA gene, partial sequence

CGAGTGAAGTATAGCTACGCTTGCTTCTATGACGTTAGCGGCGGACGGGTGAGTAACACGTGGGCAACCTGC  
CTGTAAGACTGGGATAAATTCGGGAAACCGAAGCTAATACCGGATAGGATCTTCTCCTTCATGGGAGATGATTGA  
AAGATGGTTTTCGGCTATCACTTACAGATGGGCCCCGCGGTGCATTAGCTAGTTGGTGAGGTAACGGCTCACCAAG  
GCCACGATGCATAGCCGACCTGAGAGGGTGATCGGCCACACTGGGACTGAGACACGGCCCAGACTCCTACGG  
GAGGCAGCAGTAGGGAATCTTCCGCAATGGACGAAAGTCTGACGGAGCAACGCCGCGTGAGTGATGAAGGCTT  
TCGGGTCGTAAACTCTGTTGTTAGGGAAGAACAAGTACAAGAGTAAGTCTGTACCTTGACGGTACCTAACCA  
GAAAGCCACGGCTAACTACGTGCCAGCAGCCGCGGTAATACGTAGGTGGCAAGCGTTATCCGGAATTATTGGG  
CGTAAAGCGCGCGCAGGCGGTTTCTTAAGTCTGATGTGAAAGCCACGGCTCAACCGTGAGGGGTCATTGGAA  
ACTGGGGAACCTGAGTGCAGAAGAGAAAAGCGGAATTCCACGTGTAGCGGTGAAATGCGTAGAGATGTGGAGG  
AACACCAGTGGCGAAGGCGGCTTTTGGTCTGTAAGTACGCTGAGGCGCGAAAGCGTGGGGAGCAAACAGGA  
TTAGATACCCTGGTAGTCCACGCCGTAAACGATGAGTGCTAAGTGTTAGAGGGTTTCCGCCCTTTAGTGCTGCA  
GCTAACGCATTAAGCACTCCGCCTGGGGGAGTACGGTCGCAAGACTGAAACTCAAAGGAATTGACGGGGGGCC  
CGCACAAGCGGTGGAGCATGTGGTTAATTCGAAGCAACGCGAAGAACCCTTACCAGGTCTTGACATCCTCTGA  
CAACTCTAGAGATAGAGCGTTCCCTTCGGGGGACAGAGTGACAGGTGCTGCATGGTTGTCTGCAGCTCGTGTG  
GTGAGATGTTTGGTTTAAAGTCCCCGCACGAGCGCAACCCTTGAATCTTAGTTGCAGCATTACGTGGGCACTTCT  
AAGG

>gi|700289019|gb|KJ935910.2| *Bacillus subtilis* strain KR06 16S ribosomal RNA gene, partial sequence

TGCAAGTCGAGCGGACAGATGGGAGCTTGCTCCCTGATGTTAGCGGCGGACGGGTGACTAACACGTGGGTAAAC  
CTGCCTGTAAGACTGGGATAAATCCGGGAAACCGGGGCTAATACCGGATGGTTGTTTGAACCGCATGGTTCAAA  
CATAAAAGGTGGCTTCGGCTACCACTTACAGATGGACCCGCGCGCATTAGCTAGTTGGTGAGGTAACGGCTCA  
CCAAGGCAACGATGCGTAGCCGACCTGAGAGGGTGATCGGCCACACTGGGACTGAGACACGGCCCAGACTCC  
TACGGGAGGCAGCAGTAGGGAATCTTCCGCAATGGACGAAAGTCTGACGGAGCAACGCCGCGTGAGTGATGAA  
GGTTTTCGGATCGTAAAGCTCTGTTGTTAGGGAAGAACAAGTACCGTTCGAATAGGGCGGTACCTTGACGGTAC  
CTAACCAGAAAGCCACGGCTAACTACGTGCCAGCAGCCGCGTAATACGTAGGTGGCAAGCGTTGTCCGGAAT  
TATTGGGCGTAAAGGGCTCGCAGGCGGTTTTCTTAAGTCTGATGTGAAAGCCCCCGGCTCAACCGGGGAGGGTC  
ATTGAAACTGGGGAACCTTGAGTGCAGAAAGAGGAGAGTGGAATTCCACGTGTAGCGGTGAAATGCGTAGAGAT  
GTGGAGGAACACCAGTGGCGAAGGCGACTCTCTGGTCTGTAAGTACGCTGAGGAGCGAAAGCGTGGGGAGC  
GAACAGGATTAGATACCCTGGTAGTCCACGCCGTAAACGATGAGTGCTAAGTGTTAGGGGGTTTCCGCCCTTA  
GTGCTGCAGCTAACGCATTAAGCACTCCGCTGGGGAGTACGGTTCGAAGACTGAAACTCAAAGGAATTGACG  
GGGGCCCCGCACAAGCGGTGGAGCATGTGGTTTAATTCGAAGCAACGCGAAGAACCCTTACCAGTCTTGACATCCT  
CTGACAATCCTAGAGATAGGACGTCCCCTTTCCGGGGCAGAGTGACAGGTGGTGCATGATTGTCGTCAGCTCGT  
GTCGTGAAATGTGGGTTTAAGTCCCGCAACGGAGCGCAACCTGATCTAAGTTGCCAGCATTAGTTGGCACTCT  
AGTTGACTGGCCGTTGAACAAAACCGGAGGAAAGG

>gi|700369155|gb|KJ935911.2| *Pseudomonas* sp. KR07 16S ribosomal RNA gene, partial sequence

GGTCTCAGGACCTCCTACGGAAGGCCAGCAGTGGGAATACTGACATTGGACGAAAGCCTGATTCAGCATGCTG  
CGTGTGTGAAGAAGTCTCGGATTGTATAGCACTTAAGTTGGGAGGAAGGGCATTAACTAATACGTTAGTGTTTTG  
ACGTTACCGACAGAATAAAGCACCGGCTAACTTCGTGCCAGCAGCCGCGTAATACGAAGGGTGCAAGCGTTAA  
TCGGAATTACTGGGCGTAAAGCGCGCTAGGTGGTTCGTTAAGTTGGATGTGAAAGCCCCGGGCTCAACCTGG  
GAACTGCATCCAAAACCTGGCGAGCTAGAGTACGGTAGAGGGTGTTGGAATTTCTGTGTAGCGGTGAAATGCGT  
AGATATAGGAAGGAACACCAGTGGCGAAGGCGACCACTGGACTGATACTGACACTGAGGTGCGAAAGCGTGG  
GGAGCAAACAGGATTAGATACCCTGGTAGTCCACGCCGTAAACGATGTCAACTAGCCGTTGGGTTCTTGAGAA  
CTTAGTGGCGCAGCTAACGCATTAAGTTGACCGCTGGGGAGTACGGCCGCAAGGTTAAAACCTCAAATGAATTG  
ACGGGGGGCCGCACAAGCGGTGGAGCATGTGGTTTAATTCGAAGCAACGCGAAGAACCCTTACCTGGCCTTGAC  
ATGCTGAGAACTTTCCAGAGATGGATTGGTGCCTTCGGGAACCTCAGACACAGGTGCTGCATGGCTGTCGTCAGC  
TCGTGTCGTGAGATGTTGGGTTAAGTCCCGTAACGAGCGCAACCCTTGTCTTAGTTACCAGCACGTAATGGTG  
GGCACTCTAAGGAGACWGCCGGTGACAAACCGGAGGAAGGTGGGGATGACGTCAAGTCATCATGGCCCTTAC  
GTAGTAGGCGTACACACGTTAGTCAATGGTCCG

>gi|700289020|gb|KJ935912.2| *Proteus penneri* strain KR17 16S ribosomal RNA gene, partial sequence

GGACTGAGAACACGGCCAGACTCCTTACGGAAGCAGCAGTGGATATTGCACAATGGCGCATCTGATGCAGCCA  
TGCCGCGTGATTGAAGAAGTCTTAGGTTGTAAAGTACTTTAGCGGGGAGGAAGGTGATAAAGTTAATACCTTT  
ATCAATTGACGTTACCCGCAGAAGAAGCACCGGCTAACTCCGTGCCAGCAGCCGCGGTAATACGGAGGGTGCA  
AGCGTTAATCGGAATTACTGGGCGTAAAGCGCACGCAGGCGGTCAATTAAGTCAGATGTGAAAGCCCCGAGCTT  
AAGTTGGGAATTGCATCTGAAACTGGTTGGCTAGAGTCTTGTAGAGGGGGGTAGAATTCACGTGTAGCGGTGA  
AATGCGTAGAGATGTGGAGGAATACCGGTGGCGAAGGCGGCCCTTGACAAAGACTGACGCTCAGGTGCGA  
AAGCGTGGGGAGCAAACAGGATTAGATACCCTGGTAGTCCACGCTGTAACGATGTGATTTAGAGGTTGTGGT  
CTTGAACCGTGGCTTCTGGAGCTAACCGGTTAAATCGACCGCCTGGGGAGTACGGCCGCAAGGTTAAAACCTCAA  
ATGAATTGACGGGGGGCCGCACAAGCGGTGGAGCATGTGGTTTAATTCGATGCAACGCGAAGAACCCTTACCTAC  
TCTTGACATCCAGAGAATCCTTTAGAGATAGAGGAGTGCCTTCGGGAACCTCTGAGACAGGTGCTGCATGGCTGT  
CGTCAGCTCGTGTGTTGTAAATGTTGGGTTAAGTCCCGCAACGAGCGCAACCCTTATCCTTTGTTGCCAGCGCGT  
GATGGCGGGAACCTCAAAGGAGACTGCCGGTGATAAACCGGAGGAAGGTGGGGATGACGTCAAGTCATCATGGC  
CCTTACGAGTAGGGCTACACACGTGCTACAATGGCAGATACAAAGAGAAGCGACCTCGCGAGAGCAAGCGGAA  
CTCATAAAGTCTGTGCTAGTCCGGATTGGAGTCTGCAACTCGACTCCATGAAGTCGGAATCGCTAGTAATCGTAG  
ATCAGAATTATACGGTGAATACGTTCCCGGGCCTTGACACACCTCCCGTCACACCATAGATAGTGTTACAAAAG  
AAGTAGGTAGCTCAACCTCAGCAGAGGCAATC

>gi|700289021|gb|KJ935913.2| *Shewanella* sp. KR18 16S ribosomal RNA gene, partial sequence

ACACGGCCCCAGAATCTACGGGAGGCAGCCAGTGGGGATATGCACAATGGGGGAAACCTGATGCAGGCATG  
CCGCGTGGGTGAAGAAGGCCTTCGGTTGTAAAGCACTTCAGTAGGGAGGAAAGGGTGAGTCTAATACGGCTCA  
TCTGTGACGTTACCTACAGAAGAAGGACCGGCTAACTCCGTGCCAGCAGCCGCGGTAATACGGAGGGTCCGAG  
CGTTAATCGGAATTACTGGGCGTAAAGCGTGCGCAGGCGGTTTGTTAAGCGAGATGTGAAAGCCCAGGGCTCA

ACCTAGGAATAGCATTTCGAACTGGCGAACTAGAGTCTTGTAGAGGGGGGTAGAATTCCAGGTGTAGCGGTGAA  
ATGCGTAGAGATCTGGAGGAATACCGGTGGCGAAGGCGGCCCCCTGGACAAAGACTGACGCTCATGCACGAAA  
GCGTGGGGAGCAAACAGGATTAGATACCCTGGTAGTCCACGCCGTAAACGATGTCTACTCGGAGTTTGGTGTCT  
TGAACACTGGGCTCTCAAGCTAACGCATTAAGTAGACCGCCTGGGGAGTACGGCCGCAAGGTTAAAACTCAAAT  
GAATTGACGGGGGCCCCGCACAAGCGGTGGAGCATGTGGTTTAATTCGATGCAACGCGAAGAACCTTACCTACTC  
TTGACATCCACAGAAGACTGCAGAGATGCGGTTGTGCCTTCGGGAAGTGTGAGACAGGTGCTGCATGGCTGTC  
GTCAGCTCGTGTGTGAAATGTTGGGTTAAGTCCCACAACGAGCGCAACCCCTATCCTTATTTGCCAGCACGTAA  
TGGTGGGAAGTCTAGGGAGACTGCCGGTGATAAACCGGAGGAAGGTGGGGACGACGTCAAGTCATCATGGCCC  
TTACGAGTAGGGCTACACACGTGCTACAATGGCGAGTACAGAGGGTTGCAAAGCCGCGAGGTGGAGCTAATCT  
CACAAAGCTCGTCGTAGTCCGGATTGGAGTCTGCAACTCGACTCCATGAAGTCGGAATCGCTAGTAATCGTGGA  
TCAGAATGCCACGGTGAATACGTTCCCGGGCCTTGTACACACCGCCCGT

>gi|700289022|gb|KJ935914.2| *Aeromonas* sp. KR19 16S ribosomal RNA gene, partial sequence

CTATCGGGAGGCAGCAGTGGGGAAATATGCACAATGGGGAATCCTGATGCAGTCATGCCGCGTGTGTGAAGAA  
GGCCTTCGGGTGTAAAGCACTTTCAGCGGGGAGGAAAAGGTTGAAGCTAATACGTGTCAACTGTTGACGTTAC  
TCGCAGAAGAAGCACCGGCTAACTCCGTGCCAGCAGCCGCGGTAATACGGAGGGTGCAAGCGTTAATCGGAAT  
TACTGGGCGTAAAGCGCACGCAGGCGGTTGGATAAGTTAGATGTGAAAGCCCCGGGCTCAACCTGGGAATTGC  
ATTTAAACTGTCCAGCTAGAGTCTTGTAGAGGGGGGTAGAATTCAGGTGTAGCGGTGAAATGCGTAGAGATC  
TGGAGGAATACCGGTGGCGAAGGCGGCCCCCTGGACAAAGACTGACGCTCAGGTGCGAAAGCGTGGGGAGCA  
AACAGGATTAGATACCCTGGTAGTCCACGCCGTAAACGATGTCGATTTGGAGGCTGTGTCCTTGAGACGTGGCT  
TCCGGAGCTAACCGGTTAATCGACCGCCTGGGGAGTACGGCCGCAAGGTTAAACTCAAATGAATTGACGGG  
GGCCCGCACAAAGCGGTGGAGCATGTGGTTTAATTCGATGCAACGCGAAGAACCTTACCTGGCCTTGACATGTCT  
GGAATCCTGCAGAGATGCGGGAGTGCCTTCGGGAATCAGAACACAGGTGCTGCATGGCTGTGCTCAGCTCGTG  
TCGTGAGATGTTGGGTTAAGTCCCGCAACGAGCGCAACCCCTGTCTTTGTTGCCAGCACGTAATGGTGGGAAC  
TCAAGGGAGACTGCCGGTGATAAACCGGAGGAAGGTGGGGATGACGTCAAGTCATCATGGCCCTTACGGCCAG  
GGCTACACACGTGCTACAATGGCGCGTACAGAGGGGTGCAAGCTAGCGATAGTGAGCGAATCCCAAAAAGCGC  
GTCGTAGTCCGGATCGGAGTCTGCAACTCGACTCSTTGAAGTCGGAATCGCTGGTAATCGTGAATCAGAAGTCT  
CGGTGAATAATTAGTAGTACCTTCACACAACTCGTGGCACCCCATGC

>gi|700289023|gb|KJ935915.2| *Proteus* sp. KR22 16S ribosomal RNA gene, partial sequence

CCCAGACTCCTTACGGGAGCCAGCAGTGGGATATGCACATTGGCGCAAGCCTGATGCAGCCATGCCGCGTGTA  
TGAAGAAGCTTAGGGTTGTAAAGTACTTTCAGCGGGAGGAAAGGTGATAAAGTTAATACCTTTATCAATTGACGT  
TACCCGCAGAAGAAGCACCGGCTAACTCCGTGCCAGCAGCCGCGGTAATACGGAGGGTGCAAGCGTTAATCGG  
AATTACTGGGCGTAAAGCGCACGCAGGCGGTCAATTAAGTCAGATGTGAAAGCCCCGAGCTTAACTTGGGAATT  
GCATCTGAAACTGGTTGGCTAGAGTCTTGTAGAGGGGGGTAGAATTCCACGTGTAGCGGTGAAATGCGTAGA  
GATGTGGAGGAATACCGGTGGCGAAGGCGGCCCCCTGGACAAAGACTGACGCTCAGGTGCGAAAGCGTGGGG  
AGCAAAACAGGATTAGATACCCTGGTAGTCCACGCTGTAAACGATGTCGATTTAGAGGTTGTGGTCTTGAACCGT  
GGCTTCTGGAGCTAACCGGTTAATCGACCGCCTGGGGAGTACGGCCGCAAGGTTAAACTCAAATGAATTGAC  
GGGGGCCCGCACAAAGCGGTGGAGCATGTGGTTTAATTCGATGCAACGCGAAGAACCTTACCTACTCTTGACATC  
CAGAGAATCCTTTAGAGATAGAGGAGTGCCTTCGGGAAGTCTGAGACAGGTGCTGCATGGCTGTGCTCAGCTCG  
TGTGTGAAATGTTGGGTTAAGTCCCGCAACGAGCGCAACCCCTTATCCTTTGTTGCCAGCGCGTGATGGCGGGA  
ACTCAAAGGAGACTGCCGGTGATAAACCGGAGGAAGGTGGGGATGACGTCAAGTCATCATGGCCCTTACGAGT  
AGGGCTACACACGTGCTACAATGGCAGATACAAAGAGAAGCGACCTCGCGAGAGCAAGCGGAAGTCATAAAGT  
CTGTCGTAGTCCGGATTGGAGTCTGCAACTCGACTCCATGAAGTCGGAATCGCTAGTAATCGTAGATCAGAATG  
CTACGGTGAATACGTTCCCGGGCCTTGTACACACCGCCCGTCACACCATGGGAGTGGGTTGCAAAAGAAGTAG  
GTAGCTTAACCTCGG

>gi|700289024|gb|KJ935916.2| *Pseudomonas* sp. KR23 16S ribosomal RNA gene, partial sequence

GCAGTGGGGGATATTGATCAATTGGGCGCAAGCCTGATTCCCAGCCCATACCGCGTGGGTGAGAAGGCCTTCG  
GGTGTAAGCCTTTGTTGGGAAAGAATCCAGCCGGCTAATACCTGGTTGGGATGACGGTACCCAAAGAATAAGC  
ACCGGCTAACTTCGTGCCAGCAGCCGCGGTAATACGAAGGGTGCAAGCGTTACTCGGAATTACTGGGCGTAA  
GCGTGCGTAGGTGGTTGTTAAGTCTGTTGTGAAAGCCCTGGGCTCAACCTGGGAAGTGCAGTGGAACTGGAC  
AACTAGAGTGTGGTAGAGGGTAGCGGAATCCCGGTGTAGCAGTGAATGCGTAGAGATCGGGAGGAACATCC  
ATGGCGAAGGCAGCTACCTGGACCAACACTGACACTGAGGCACGAAAGCGTGGGGAGCAAACAGGATTAGATA  
CCCTGGTAGTCCACGCCCTAAACGATGCGAACTGGATGTTGGGTGCAATTTGGCACGCAGTATCGAAGCTAACG  
CGTTAAGTTCGCCGCTGGGGAGTACGGTGCAGACTGAAACTCAAAGGAATTGACGGGGGCCCGCACAAAGC

GGTGGAGTATGTGGTTTAATTCGATGCAACGCGAAGAACCTTACCTGGCCTTGACATGTCGAGAACTTTCCAGA  
GATGGATTGGTGCCTTCGGGAACCTCGAACACAGGTGCTGCATGGCTGTCGTGAGATGTTG  
GGTTAAGTCCCGCAACGAGCGCAACCCCTTGTCCTTAGTTGCCAGCACGTAATGGTGGGAACCTAAGGAGACCG  
CCGGTGACAAACCGGAGGAAGGTGGGGATGACGTCAAGTCATCATGGCCCTTACGGCCAGGGCTACACACGTA  
CTACAATGGTGGGGACAGAGGGCTGCAAGCCGGCGACGGTAAGCCAATCCCAGAAACCCCATCTCAGTCCGGA  
TTGGAGTCTGCAACTCGACTCCATGAAGTCGGAATCGCTAGTAATCGCAGATCAGCATTGCTGCGGTGAATACG  
TTCCCGGCCCTTGACACACCGCCCGTCACACCATGGGAGTGTGTTGCACCAGAAGCTGGTAGCTTAACCTCGG  
GAGTGCG

>gi|700289025|gb|KJ935917.2| *Lysinibacillus* sp. KR25 16S ribosomal RNA gene, partial sequence

GCAGTAGGGAATCTCACAGTGGCGAAGCCTGATGAAGCAACCGCGCGTGAGTGAGGACGATTTCCGTTTCGTAA  
AACTCTGTGTAAGGGAAGAACAAGTACAGTAGTAAGTGGCTGTACCTTGACGGTACCTTATTAGAAAGCCACGG  
CTAACTACGTGCCAGCAGCCGCGGTAATACGTAGGTGGCAAGCGTTGTCCGGAATTATTGGGCGTAAAGCGCG  
CGCAGGTGGTTTTCTTAAGTCTGATGTGAAAGCCACGGCTCAACCGTGGAGGGTCATTGGAAACTGGGAGACTT  
GAGTGCAAGAAGAGGATAGTGGAAATCCAAGTGTAGCGGTGAAATGCGTAGAGATTTGGAGGAACACCAAGTGGC  
GAAGGCGACTATCTGGTCTGTAAGTACACTGAGGCGCGAAAGCGTGGGGAGCAAACAGGATTAGATACCCTG  
GTAGTCCACGCCGTAAACGATGAGTGCTAAGTGTTAGGGGGTTTTCCGCCCTTAGTGCTGCAGCTAACGCATTA  
AGCACTCCGCCTGGGGAGTACGGTCGCAAGACTGAAACTCAAAGGAATTGACGGGGGCCCCGCACAAGCGGTG  
GAGCATGTGGTTTAATTCGAAGCAACGCGAAGAACCTTACCAGGTCTTGACATCCCCTTGACCACTGTAGAGATA  
TGTTTTCCCTTCGGGGGCAACGGTGACAGGTGGTGCATGGTTGTCGTGAGCTCGTGTGCTGAGATGTTGGGT  
TAAGTCCCGCAACGAGCGCAACCCCTTGATCTTAGTTGCCATCATTTAGTTGGGCACTCTAAGGTGACTGCCGGT  
GACAAACCGGAGGAAGGTGGGGATGACGTCAAATCATCATGCCCTTATGACCTGGGCTACACACGTGCTACAA  
TGGACGATACAAACGGTTGCCAACTCGCGAGAGGGAGCTAATCCGATAAAGTCGTTCTCAGTTCGGATTGTAGG  
CTGCAACTCGCCTACATGAAGCCGGAATCGCTAGTAATCGCGGATCAGCATGCCGCGGTGAATACGTTCCCGG  
GCCTTGACACACCGCCCGTCACACCACGAGAGTTTGTAAACCCGAAGTCGGTGAGGTAACCTTTTGGAGCCA  
GCCGCCGAA

>gi|700289026|gb|KJ935918.2| *Escherichia coli* strain KR29 16S ribosomal RNA gene, partial sequence

TCCAAGACTCCCTACCGGAGCAAGCACGTGGGGATATGCACATTGACGCAGCTGATGCAGCATGCGCGTGTAT  
GAGGAAGCTTCGGGGTGTAAGTACTTTTCAGCGGGGAGGAAGGGAGTAAAGTTAATACCTTTGCTCATTGACG  
TTACCCGCGAGAAGAAGCACCGGCTAACTCCGTGCCAGCAGCCGCGGTAATACGGAGGGTGCAAGCGTTAATCG  
GAATTACTGGGCGTAAAGCGCACGCAGGCGGTTTTGTTAAGTCAGATGTGAAATCCCCGGGCTCAACCTGGGAA  
CTGCATCTGATACTGGCAAGCTTGAGTCTCGTAGAGGGGGGTAGAATTCCAGGTGTAGCGGTGAAATGCGTAGA  
GATCTGGAGGAATACCGGTGGCGAAGGCGGCCCTTGACGAAGACTGACGCTCAGGTGCGAAAGCGTGGGG  
AGCAAACAGGATTAGATACCCTGGTAGTCCACGCCGTAAACGATGTCGACTTGAGGTTGTGCCCTTGAGGCGT  
GGCTTCGGGAGCTAACGCGTTAAGTCGACCGCCTGGGGAGTACGGCCGCAAGGTTAAACTCAAATGAATTGA  
CGGGGGCCCCGCACAAGCGGTGGAGCATGTGGTTTAATTCGATGCAACGCGAAGAACCTTACCTGGTCTTGACA  
TCCACGGAAGTTTTTCAGAGATGRRRAAGGTGCCTTCGGGAACCGTGAGACAGGTGCTGCATGGCTGTCGTGAGC  
TCGTGTTGTGAAATGTTGGGTAAAGTCCCGCAACGAGCGCAACCCCTTATCCTTTGTTGCCAGCGGTCCGGCCGG  
GAACTCAAAGGAGACTGCCAGTGATAAACTGGAGGAAGGTGGGGATGACGTCAAGTCATCATGGCCCTTACGA  
CCAGGGCTACACACGTGCTACAATGGCGCATACAAAGAGAAGCGACCTCGCGAGAGCAAGCGGACCTCATAAA  
GTGCGTCGTAGTCCGGATTGGAGTCTGCAACTCGACTCCATGAAGTCGGAATCGCTAGTAATCGTGGATCAGAA  
TGCCACGGTGAATACGTTCCCGGGCCTTGACACACCTCCCGTCACACCATGGGAGTGGGTTGCAAAAAGAAGTA  
GGTAGCTTAACCTCGGGAGGGCCGCTT

>gi|700289027|gb|KJ935919.2| *Bacillus licheniformis* strain KR44 16S ribosomal RNA gene, partial sequence

GGCCAGGACTCCTACGGGAGGCAAGCCAGTAGGGATCTCGCATGGACCGAAAGTCTGACCGAGCCACGCGC  
GTGAGTGATGAAGTTTTTCGGATCGTAAACTCTGTTGTAGGGAAGAACAAGTACCGTTTCGAATAGGCGGTACCTT  
GACGGTACCTAACCCAGAAAGCCACGGCTAACTACGTGCCAGCAGCCGCGGTAATACGTAGGTGGCAAGCGTT  
GTCCGGAATTATTGGCGTAAAGCGCGCGCAGGCGGTTTTCTTAAGTCTGATGTGAAAGCCCGGCTCAACCG  
GGGAGGGTCATTGGAACTGGGGAACCTTGAGTGCAAGAGGAGAGTGGAATTCCACGTGTAGCGGTGAAATG  
CGTAGAGATGTGGAGGAACACCAAGTGGCGAAGGCGACTCTCTGGTCTGTAAGTACGCTGAGGCGCGAAAGCG  
TGGGGAGCGAACAGGATTAGATACCCTGGTAGTCCACGCCGTAAACGATGAGTGCTAAGTGTTAGAGGGTTTCC  
GCCCTTAGTGCTGCAGCAAACGCATTAAGCACTCCGCCTGGGGAGTACGGTCGCAAGACTGAAACTCAAAGGA  
ATTGACGGGGGCCCGCACAAGCGGTGGAGCATGTGGTTTAATTCGAAGCAACGCGAAGAACCTTACCAGGTCT

TGACATCCTCTGACAACCCTAGAGATAGGGCTTCCCCTTCGGGGGCAGAGTGACAGGTGGTGCATGGTTGTCGT  
CAGCTCGTGTCTGTGAGATGTTGGGTAAAGTCCCGCAACGAGCGCAACCCTTGATCTTAGTTGCCAGCATTCACT  
TGGGCACTCTAAGGTGACTGCCGGTGACAAACCGGAGGAAGGTGGGGATGACGTCAAATCATCATGCCCCCTTA  
TGACCTGGGCTACACACGTGCTACAATGGGCAGAACAAAGGGCAGCGAAGCCGCGAGGCTAAGCCAATCCCAC  
AAATCTGTTCTCAGTTCGGATCGCAGTCTGCAACTCGACTGCGTGAAGCTGGAATCGCTAGTAATCGCGGATCA  
GCATGCCGCGGTGAATACGTTCCCGGGCCTTGACACACCGCCCGTCACACCACGAGAGTTTGTAAACACCCGA  
AGTCGGTGAGGTAACCTTTTGAGGC

>gi|700289028|gb|KJ935920.2| *Arthrobacter* sp. KR48 16S ribosomal RNA gene, partial sequence

CGGCCCAGAACTTCCTTACCGGGAGGCAGCAGTGGGATATTGCCCAATTGGGCGGAATGCTTGATGCAGCGAC  
GCCCCGCTGGAAGGGATGACGGCCTTCCGGTGTAACCTCCTTTTCAGTAAGGGAAGAAGCCCCCTTTTGGGGG  
TGACGGTACTTGCAAGAAGCGCCGGCTAACTACGTGCCAGCAGCCGCGGTAATACGTAGGGCGCAAGCGTT  
ATCCGGAATTATTGGGCGTAAAGAGCTCGTAGGCGGTTTGTGCGCTCTGCCGTGAAAGTCCGAGGCTCAACCTC  
GGATCTGCGGTGGGTACGGGCAGACTAGAGTGATGTAGGGGAGACTGGAATTCCTGGTGTAGCGGTGAAATGC  
GCAGATATCAGGAGGAACACCGATGGCGAAGGCAGGTCTCTGGGCATTTACTGACGCTGAGGAGCGAAAGCAT  
GGGAGCGAACAGGATTAGATACCCTGGTAGTCCATGCCGTAAACGTTGGGCACTAGGTGTGGGGGACATTCC  
ACGTTTTCCGCGCCGTAGCTAACGCATTAAGTGCCCCGCCTGGGGAGTACGGCCGCAAGGCTAAAACTCAAAG  
GAATTGACGGGGGCCCCGCACAAGCGGCGGAGCATGCGGATTAATTCGATGCAACGCGAAGAACCTTACCAAGG  
CTTGACATGTTCCAGACCGGGCCAGAGATGGTCTTTCCCCTTTTGGGGCTGGTTCACAGGTGGTGCATGGTTGT  
CGTCAGCTCGTGTCTGTGAGATGTTGGGTAAAGTCCCGCAACGAGCGCAACCCTCGTTCCATGTTGCCAGCGGG  
TTATGCCGGGGACTCATGGGAGACTGCCGGGGTCAACTCGGAGGAAGGTGGGGATGACGTCAAATCATCATGC  
CCCTTATGTCTTGGGCTTCACGCATGCTACAATGGCCGGTACAATGGGTTGCGATACTGTGAGGTGGAGCTAAT  
CCCTAAAAGCCGGTCTCAGTTCGGATTGGGGTCTGCAACTCGACCCCATGAAGTCGGAGTCGCTAGTAATCGCA  
GATCAGCAACGCTGCGGTGAATACGTTCCCGGGCCTTGACACACCGCCCGTCAAGTCACGAAAGTTAGTACAC

## APPENDIX XIV: NUCLEOTIDE SEQUENCES AND TRANSLATED AMINO ACID SEQUENCES

>KR23\_chrB

ATCCGGCCGGCGACATCATGGGCGCGATGGGCTTTGAGCACCGCAGCGAAGAAGCCAGCTACACCCCGGACC  
TGATGGTGCAGAAGGGCCAGATCGCCGGCACCACCGGCCAGCCGACCCGTGGCGACTACTCGCTCAACGAGG  
TCTACCTGGAAATGCAGGTGCCGCTGCTGGCCGACATGGCCTTCGCCCGCGAGCTGTCGCTGGACCTGGCCG  
GTCGCTACACCGACTACAACACCTTCGGTTTCGACCACCAACAGCAAGTTTCGGCCTGAAGTGAAGCCGATCGAC  
ATCTTGCTTTCC

>pcoA\_25

GGGAACCCCGGGAAAGCTTCGGCGTATGGAGTTTCAATCCCGCGTTCCAGTCTGAGCCTGCCAGTTGCCGACT  
CCTGCAGGTAAGTCAAGTTTGACCTGACCATTGGTGAAACGGCCGTCAATATCACGGGCAGTGAGCGTCAGGCCAA  
AACAATCAATGGAGGCCTGCCGGGGCCCGTTCTTCGCTGGAAAGAAGGTGACACCATTACCCTGAAGGTCAAAA  
ACCGTCTTAATGAACAGACGTCCATTCACTGGCACGGCATTATTCTTCCGGCCAATATGGATGGTGTTCGGGG  
CTGAGTTTTATGGGCATAGAGCCTGATGATACCTACGTTTACACCTTTAAGGTTAAGCAGAACGGGACTTACTGG  
TACCACAGCCATTCCGGTCTGCAGGAACAGGAGGGGGTATACGGTGCCATTATCATCGATGCCAGGGAGCCAG  
AACCGTTTGCTTACGATCGTGAGCATGTGGTCATGTTGTCTGACTGGACCGATGAAAATCCTCACAGCCTGCTGA  
AAAAATTAACAGTTCGATTACTACAATTTCAATAAACCAACCGTTGGCTCTTTTTCCGCGACGTGAATAC  
CAGGGGGCTGTCAGCCACCATTGCCGATCGGAAAATGTGGGCTGAAATGAAAATGAATCCGACTGACCTCGCG  
GATGTCAGTGGCTACACCTACACCTATCTCATGAACGGGCAGGCCCGCTGAAAATGGACCGGACTGTTCCC  
GTCCCGGTGAAAAGATACGCTTACGGTTTTATCAACGGCTCGGCAATGACCTATTTTCGATATCCGATCCCCG  
GGTGAAAATGACGGTCGTGGCTGCAGATGGGCCAGTATGTAACCCGGTTACCGGTGACAATTCAGGATTGCCG  
TTGCCCGAAACCTAATGAGGTCATGGGGGAGCCTCGGGTGAAGGCCCATACAATCTTCCAC

>pcoA\_29

CCCGGGCGTACCCGGAAGTCTTGGCGTATGGAGTTTCAATGCGCGTTCCAGTCTGAGCCTGCCAGTTGCCGCA  
TCCCTGCAGGTAAGTCAAGTTTGACCTGACCATTGGTGAAACGGCCGTCAATATCACGGGCAGTGAGCGTCAGG  
CCAAAACAATCAATGGAGGCCTGCCGGGGCCCGTTCTTCGCTGGAAAGAAGGTGACACCATTACCCTGAAGGT  
CAAAAACCGTCTTAATGAACAGACGTCCATTCACTGGCACGGCATTATTCTTCCGGCCAATATGGATGGTGTTC  
GGGGCTGAGTTTTATGGGCATAGAGCCTGATGATACCTACGTTTACACCTTTAAGGTTAAGCAGAACGGGACTTA  
CTGGTACCACAGCCATTCCGGTCTGCAGGAACAGGAGGGGGTATACGGTGCCATTATCATCGATGCCAGGGAG  
CCAGAACCCTTTGCTTACGATCGTGAGCATGTGGTCATGTTGTCTGACTGGACCGATGAAAATCCTCACAGCCT  
GCTGAAAAAATTAACAGTTCGATTACTACAATTTCAATAAACCAACCGTTGGCTCTTTTTCCGCGACGTG  
AATACCAGGGGGCTGTCAGCCACCATTGCCGATCGGAAAATGTGGGCTGAAATGAAAATGAATCCGACTGACCT  
CGCGGATGTCAGTGGCTACACCTACACCTATCTCATGAACGGGCAGGCCCGCTGAAAAATGGACCGGACTG  
TTCCGTCCCGGTGAAAAGATACGCTTACGGTTTTATCAACGGCTCGGCAATGACCTATTTTCGATATCCGATCCCC  
GGGCTGAAAATGACGGTCGTGGCTGCAGATGGCCAGTATGTAACCCGGTTACCGTTGACGAATTCAGGATTGC  
CGTTGCCGAAACCTATGATGTCATTGTGGAGCCTCAGGGTGAGGCCATACCATCTTCGCACAATCCATGGACA  
GGACCGGTTACGCTCGAGGGACACTGGCCACGAGAGAGGGGTTAAGTGCTGCCGTTCCCCCTCGATCCCCGT  
CCTCTGTGACCATGGAGATATGGGTATGGGGGGGAATGGGACATGATATGGCAGAATGGACCACAGCAGATGG  
AAGCATGGTATACAGCCGAGAAGATGATGTCTTATTGGGAAGGCGGT

>pcoR\_29

ATAGAAGCTTCAGGCCGATCTCTTTATAATGGCCGCGATGGTCTCGGGGCCGCGTGAAGGGACAGTATGATTT  
GATAATACTGGACGTGATGCTGCCTTTCCTCGACGGGTGGCAAATCATCAGCGCACTGAGGGAGTCCGGGCAC  
GAAGAACCGTCTCTGTTTTAACCGCAAAGGACAACGTGCGGGACAAAGTGAAGGACTGGAGCTTGCGCGAG  
ATGACTACCTGATTAAGCCCTTTGATTTTACGGAGCTGGTTGCACGTGTAAGAACCCTACTGCGCCGGGCACGC  
TCGACGGCCGCAACAGTCTGCACCATCGCCGATATGACCGTTGATATGGTGCGCCGGACCGTGATCCGTTCCGG  
GGAAGAAGATCCATCTCACCGGTAAGAATACGTTCTGCTTGAGTTGCTGCTGCAACGCACCGGAGAAGTGTTA  
CCCAGGAGTCTTATCTCGTCCCTGGTCTGGAACATGAATTTTGACAGTGATACGAATGTGATTGATGTCGCCGTG  
AGACGTCTGAGAAGTAAATTGATGATGACTTTGAGCCAAAATGATCCATACCGTTTCGCGGTGCCGGATATGTC  
CTGAAAAAATCAAAGGA



## APPENDIX XV TRANSLATED PROTEIN SEQUENCES OF HEAVY METAL RESISTANCE GENES

>ChrB\_23

MGAMGFEHRSEEASYTPDLMVQKGQIAGTTGQPTRGDYSLNEVYLEMQVPLLADMAFARELSLDLAGRYTDYNTFG  
STTNSKFGLKWKPIDILLSX

>pcoA\_25

MEFQSRVPV\*ACQLPTPAGTQFDLTIGETAVNITGSERQAKTINGGLPGPVLRWKEGDTITLKVKNRLNEQTSIHWHGII  
LPANMDGVPGLSFMGIEPDDTYVYTFKVKQNGTYWYHSHSGLQEQEGVYGAIIDAREPEPFAYDREHVVM LSDWTD  
ENPHSLLKKLKKQSDYYNFKPTVGSFFRDVNTRGLSATIADRKMWAEKMMNPTDLADVSGYTYTYLMNGQAPLKT  
GPDCSRPGEKIRLRFYQRLGNDLFSISVSPG\*K\*RSWLQMGQYVTRLPVTIQDCRCPKPNEVMGEPRVKAHTIFHX

>pcoA\_29

MEFQCAFQSEPASCRIPAGYSV\*PDHW\*NGRQYHGQ\*ASGQNNQWRPAGARSSLERR\*HHYPEGQKPS\*\*TDVHSL  
ARHYSSGQYWCSCGAEFYGHRA\*\*YLRHL\*L\*G\*AERDLLVPQPFRSAGTGGGIRCHYHRCQGARTVCLRS\*ACGHVV  
\*LDR\*KSSQPAEKIKKTVGLLQFQ\*TNRWLFFPRREYQGAVSHHCRSENVG\*NENESD\*PRGCQWLHLHLSHERAGPA  
EKLDRTVPSR\*KDTLTVYQRLGNDLFRYPYPRAENDGRGCRWPVCKPGYR\*RIQDCRCRNL\*CHCGASG\*GLYHLRTI  
HGQDRLRSRDTGHERGVKCCRSPLDPRPL\*PWRYGYGGEWDMIWQNGPQQMEAWYAEKMMSYWEGGX

>pcoR\_29

MAAMVSGPRRRDSMI\*\*YWT\*CCLSSTGGKSSAH\*GSPGTKNRSCF\*PQRTTCGTK\*KDWSLAQMTT\*LSPLILRSWL  
HV\*EPYCAGHARRPQQSAPSPI\*PLIWCAGP\*SVRGRRSISPVKNTFCLSCCCNAPEKCYPGVLSRPWSGT\*ILTVIRM\*  
LMSP\*DV\*EVKLMMLTSQN\*SIPFAVPDMS\*KNQRX

## APPENDIX XVI: PUTATIVE CONSERVED DOMAINS OF PCOA\_25 PARTIAL PROTEIN SEQUENCE

